SANDIA REPORT

SAND97–1763 • UC–721
Unlimited Release
Printed April 1998

Laboratory Column Experiments for Radionuclide Adsorption Studies of the Culebra Dolomite Member of the Rustler Formation

Daniel A. Lucero, Glenn O. Brown, Charles E. Heath

Prepared by
Sandia National Laboratories
Albuquerque, New Mexico 87185 and Livermore, California 94550

Sandia is a multiprogram laboratory operated by Sandia Corporation, a Lockheed Martin Company, for the United States Department of Energy under Contract DE-AC04-94AL85000.

Sandia National Laboratories

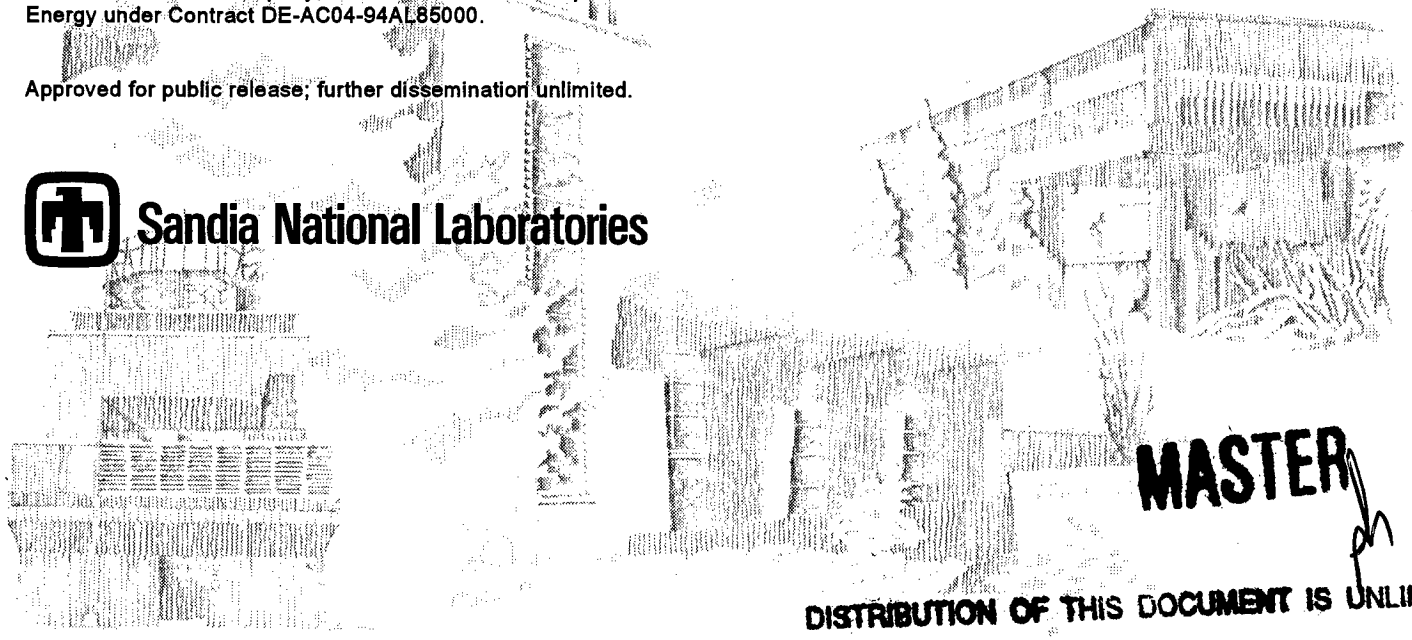

Issued by Sandia National Laboratories, operated for the United States Department of Energy by Sandia Corporation.

Available to DOE and DOE contractors from
Office of Scientific and Technical Information
P.O. Box 62
Oak Ridge, TN 37831

Prices available from (615) 576-8401, FTS 626-8401

Available to the public from
National Technical Information Service
U.S. Department of Commerce
5285 Port Royal Rd
Springfield, VA 22161

NTIS price codes
Printed copy: A16
Microfiche copy: A01

SAND97-1763
Unlimited Release
Printed April 1998

Distribution
Category UC-721

Waste Isolation Pilot Plant

Laboratory Column Experiments for Radionuclide Adsorption Studies of the Culebra Dolomite Member of the Rustler Formation

Daniel A. Lucero
WIPP Chemical and Disposal Room Processes Department
Sandia National Laboratories
P.O. Box 5800
Albuquerque, NM 87185-1320

Glenn O. Brown
Biosystems and Agricultural Engineering Department
Oklahoma State University
Stillwater, OK 74078

Charles E. Heath
WIPP Chemical and Disposal Room Processes Department
Sandia National Laboratories
P.O. Box 5800
Albuquerque, NM 87185-1320

ABSTRACT

Radionuclide transport experiments were carried out using intact cores obtained from the Culebra member of the Rustler Formation inside the Waste Isolation Pilot Plant, Air Intake Shaft. Twenty-seven separate tests are reported here and include experiments with ^{3}H, ^{22}Na, ^{241}Am, ^{239}Np, ^{228}Th, ^{232}U and ^{241}Pu, and two brine types, AIS and ERDA 6. The ^{3}H was bound as water and provides a measure of advection, dispersion, and water self-diffusion. The other tracers were injected as dissolved ions at concentrations below solubility limits, except for americium.

^{22}Na was transported similarly to ^{3}H, which shows it is a conservative tracer in the Culebra samples and can be used as a replacement for ^{3}H to eliminate interference with ^{241}Pu analysis.

Two tracers eluted but were moderately retarded, ^{239}Np and ^{232}U. Three tracers, ^{241}Am, ^{228}Th and ^{241}Pu, were not detected in column effluent.

Breakthrough curves for eluting species were fitted to single and dual porosity models. The single porosity model assumed a homogeneous porous medium and advection-dispersion transport. The dual porosity model is similar to the Performance Assessment transport model, SECO-TP. A macro or advective pore space transports solute by advection and dispersion, while a micro or matrix pore space is only accessible by diffusion. Diffusion geomtry is one-dimensional. Fitting ^{3}H and ^{22}Na data provided core porosity and solute dispersion coefficients. Fitted parameters for conservative solute showed little difference between single and dual porosity models indicating limited effective distinction between the two. In three cores, single porosity fits provided porosity only 1/2 to 1/6 of an independent estimate of the total porosity. In all cores the hydrodynamic dispersion coefficient was an order of magnitude greater than packed columns. This indicates significant preferential flow occurred in the columns and is consistent with dispersion in heterogeneous media.

No clear trend is apparent with regard to flow rate dependencies. Likewise, the Salado brine, ERDA 6 did not produced a significant change in retardation relative to AIS.

Fitted retardation factors, R for ^{239}Np ranged from to 30 to 78 and from 2 to 18 for ^{232}U, with the single porosity model. In general, good fits could be obtained with the dual porosity model only if the advective porosity was allowed to retard the solute. The dual porosity fit for ^{232}U and ^{239}Np yielded matrix retardation's one to two orders of magnitude greater than the single porosity model. Those higher values may be the best estimates of the dolomite retardation potential. However, since the overall fitting to the elution curve is not clearly better than the single porosity model, the higher retardation is considered unproven by these experiments.

Theoretical analysis using the minimum detection limits for ^{241}Am, ^{228}Th and ^{241}Pu and the single porosity model provided minimum retardation estimates for the non-eluting species. Minimum R values were 520 to 18,000 for ^{241}Am, 9.1 to 47 for ^{228}Th, and 800 to 38,000 for ^{241}Pu. The range of these minimum R values is a function of the individual test conditions and does not indicate data uncertainty.

ACKNOWLEDGMENTS

Many persons contributed to this project and several deserve special note. Fred Gelbard was the original Principal Investigator and provided the initial vision for its scope and objectives. Hans Papenguth and later Larry Brush were overall Principal Investigators for the retardation of dissolved actinide program. They have integrated the results of this work into the larger program. George Newton of ITRI provided sample spikes, Kent Budge wrote the data fitting program used, and Yugal Behl of SCIRES Corporation assisted in test planning. Robert Holt of New Mexico Technical University provided core logging of the Air Intake Shaft cores, and J. A. Romero assisted in the initial test plan and equipment setup. Finally, Fred Salis was instrumental in the collection of much of this data and George Perkins provided a detailed review.

TABLE OF CONTENTS

LIST OF TABLES

LIST OF FIGURES

LIST OF ACRONYMS

AIS	Air intake shaft
ASTM	American Society for Testing and Materials
BTC	Breakthrough curve
DOE	U.S. Department of Energy
EPA	U.S. Environmental Protection Agency
ITRI	Inhalation Toxicology Research Institute
LSC	Liquid scintillation counter
MDA	Minimum detection activity
NIST	National Institute of Standards and Technology
PA	Performance Assessment
PI	Principal Investigator
QA	Quality Assurance
RMS	Root mean squared error
SOP	Standard operating procedure
SNL	Sandia National Laboratories
SVD	Singular value decomposition
WIPP	Waste Isolation Pilot Plant
γ Spec	Gamma ray spectrometry

INTRODUCTION

Under the authorization of Public Law 96-164 (1979), the U.S. Department of Energy (DOE) has been developing a nuclear waste disposal facility, the Waste Isolation Pilot Plant (WIPP), located approximately 42 km east of Carlsbad, New Mexico. The WIPP is designed to demonstrate the safe disposal of transuranic wastes produced by the defense nuclear-weapons program. Transuranic waste is defined as waste contaminated with radionuclides having an atomic number greater than 92, a half-life greater than 20 years and a concentration greater than 100 nCi/g (U.S. EPA, 1993). This radioactive waste is regulated by U.S. Environmental Protection Agency regulations 40 CFR Part 191 (U.S. EPA, 1993). These regulations place limits on cumulative radioactive release to the accessible environment over 10,000 years and require that Performance Assessment (PA) analyses be performed to demonstrate the WIPP facility compliance with the regulations.

PA analyses of the WIPP repository are being performed by Sandia National Laboratories (SNL) to determine if the repository would meet regulatory requirements. Preliminary WIPP PA calculations have been iterative in nature and have been performed using the best data and models available at the time. Initial PA calculations and sensitivity analyses (Helton et al., 1991 and 1992; Bertram-Howery et al., 1990) have identified the radionuclide retardation factor (relative transport rate of radionuclides with respect to the ambient fluid flow velocity) in the Culebra Dolomite as a key parameter.

Chemical retardation is caused by various chemical reactions that may occur between the chemical species in the solution and at the mineral/water interface. The chemical retardation phenomenon has been observed both in laboratory and field tests associated with groundwater contaminant transport studies involving inorganic contaminants (Weber et al., 1991, and references therein) and organic contaminants (Mackay et al., 1986).

Chemical retardation can be quantified by the distribution coefficient, k_d, (Fetter, 1993; p. 117-118)

$$k_d = \frac{S}{C} \tag{1}$$

where k_d is the distribution coef., S is the mass of solute sorbed per mass of sorbate and C is the aqueous solute mass concentration. Use of k_d assumes local adsorption equilibrium and a linear relationship between S and C over the range of interest. Non-linear isotherm forms are available (Fetter, 1993), but WIPP-specific materials and solutions are not adequate to derive those isotherm's parameters (Dosch, 1980, 1981; Dosch and Lynch, 1978; Lynch and Dosch, 1980; Nowak, 1980; Novak, 1992; and Trauth et al., 1992). Previously conducted batch experiments also do not differentiate between mechanisms contained in the sorption term (absorption and ion exchange) or other potential mechanisms, such as precipitation of actinide-bearing solids. Partly for those reasons, the SNL PA group has relied on expert judgment to develop the probability distributions for k_d (Trauth et al., 1992). However, the final PA calculations in support of the application to the EPA for opening the WIPP repository, required that these probability distributions be based on experimental data. The Working Agreement of the Consultation and

Cooperation Agreement between the Department of Energy and the State of New Mexico on the Waste Isolation Pilot Plant (as modified, U.S. DOE and State of New Mexico, 1988, p. 8-9) stipulates:

> "DOE will select, after consultation with the State, a range of values to be conservative, but reasonable, based on the lowest reasonable values experimentally obtained. In the absence of experimentally justifiable values, k_d will equal zero, i.e., no credit for retardation will be taken in the performance assessment calculations."

Intact rock column experiments have been designed as one part of the Culebra retardation studies program to demonstrate retardation in the Culebra Dolomite. Semi-empirical batch sorption experiments have provided most of the sorption values submitted for performance assessment calculations. The strategy for batch experiments was to empirically identify combinations of geochemical parameters (brine composition, organic/inorganic ligands, rock composition, actinide concentration and oxidation state) that affect the value of k_d. Once those parameters were identified, a matrix of experiments was conducted to produce statistically valid k_d distributions. Results of the static sorption experiments were compared with results from the column flow experiments to provide the final k_d distributions submitted to PA (Brush, 1996b).

Column flow experiments with large diameter intact core provide information on the effects of advective fluid flow on sorption behavior in the Culebra Dolomite. A major value of the column experiments is that they simulate the subsurface environment, (albeit at an intermediate scale smaller than the field) and provide a means to quantify some effects of coupled transport processes under simulated flow conditions. However, recent multi-rate modeling of conservative tracer tests at the WIPP site (Meigs et al., 1997), combined with consideration of the effects of scale (Holt, 1997), indicate that the intact rock-column flow experiments may provide low values for retardation factors. It should be noted, therefore that inclusion of k_d values from the intact rock column experiments into the PA parameter set (Brush, 1996b) is conservative.

Additional column testing has been carried out by Lucero et al. (1995) with colloidal materials. Colloid experiments used the same procedures, materials and cores as reported here, with the exception of the introduction of humic compounds and bacteria. No increase in actinide transport over soluble rates were observed.

OBJECTIVE

The objective of the intact rock column flow experiments is to demonstrate and quantify transport retardation coefficients, (R) for the actinides Pu, Am, U, Th and Np, in intact core samples of the Culebra Dolomite. The measured R values are used to estimate partition coefficients, (k_d) for the solute species. Those k_d values may be compared to values obtained from empirical and mechanistic adsorption batch experiments, to provide predictions of actinide retardation in the Culebra.

Three parameters that may influence actinide R values were varied in the experiments; core, brine and flow rate. Testing five separate core samples from four different core borings provided an indication of sample variability. While most testing was performed with Culebra brine, limited tests were carried out with a Salado brine to evaluate the effect of intrusion of those lower waters. Varying flow rate provided an indication of rate dependent solute interactions such as sorption kinetics.

MATERIALS AND PROCEDURES

Detailed information on test materials, equipment and procedures are presented in Lucero et al. (1995), and WIPP Lab Notebooks (Lucero, 1995-1996). The following section summarizes the general procedures used and parameters specific to these tests.

Cores

CORE COLLECTION

Representative samples were needed from the Culebra Dolomite for the laboratory tests. The Culebra is a laterally extensive rock unit ranging in thickness from approximately 13 to 38 ft (Holt, 1997). Initially, vertical cores archived at the Westinghouse Core Library at the WIPP Site were examined to determine if any of them could be used for the retardation experiments. Most of the archived cores were 2 inches in diameter, and inadequate to capture the heterogeneity in the Culebra. No suitable larger diameter cores were available. Moreover, none of the cores had been preserved to prevent drying. Since drying may change mineral surface properties, experiments with these cores could be subject to criticism. Finally, and most importantly, the Culebra is confined above and below by relatively impermeable rock units, which restricts flow to a horizontal path. The best measure of Culebra transport would be achieved using horizontal core oriented parallel to the bedding. Therefore, it was decided to obtain new core at the WIPP site.

There are four shafts on the WIPP site where Culebra samples may be obtained: the exhaust shaft, the waste-handling shaft, the salt-handling shaft, and the air-intake shaft. Three shafts were rejected for horizontal coring for several reasons. The exhaust and waste shafts had been pressure-grouted and surrounding rock may be contaminated, while the waste-handling shaft does not have a suspended platform needed for drilling. Furthermore, the stratigraphy of the first three shafts has not been precisely mapped, so the location of the Culebra is not known accurately. Thus, the air intake shaft (AIS) was chosen for core drilling.

At the AIS the Culebra Dolomite is approximately 24 ft thick and has been mapped as three major units, with the lower Unit 3 having three subunits a, b and c. Selection of specific locations within the Culebra for drilling was based on the variability of flow within those units. Holt and Powers (1990) state Unit 3a is the most transmissive unit based on fluid production during the AIS geologic mapping. This suggests that the present day brine flow in the Culebra at the AIS is predominantly through that unit.

A 6-inch diameter core barrel was used for drilling which produced 5.7 inch diameter core. The scale of heterogeneity within the Culebra is on the order of one inch, and was a consideration in choosing the rock sample diameter. A 5.7 inch-diameter core is more likely to be removed intact and provides a representative sample with respect to heterogeneity. Smaller diameter cores would be less likely to capture the heterogeneity adequately. Larger samples (e.g., the next core barrel size available is 8 inch) would not provide any significant advantage at the expense of being much larger and therefore harder to manage.

Since the geologic properties of the Culebra Dolomite are not uniform, it was decided to collect samples from four different boreholes rather than extract all samples from one. Figure 1 shows the borehole positions in the AIS. Each borehole was drilled in a north-south direction, since that is the probable direction of flow in the Culebra at the site (Ramsey et al., 1996). "VPX" accompanied by a number follows the standard sample requisition numbering system established by SNL.

After removal from the core barrel, samples were sealed in PVC tubing, before being moved to surface and inspected for about 20 minutes. The cores were observed to have an abundance of horizontal and subhorizontal fractures, some along the bedding planes, and high-angle fractures. The orientation of some of the samples was marked on them, while for the remainder it can be determined by the analysis of geopetal features. A photograph album of the core is a part of the WIPP QA records. Practical constraints of transporting and storing cores limited the total length of cores to about 65 feet.

After inspection, cores were wrapped in heavy-duty plastic wrap and stored in capped PVC tubing to prevent drying. The cores were divided into two groups for safety, and stowed in secure areas. Storage temperature has been kept near 20° C and monitored continuously. Core temperature data are archived about every two months and provided to the WIPP QA Department. A copy of the data is also maintained in a Core Log Book kept in the laboratory.

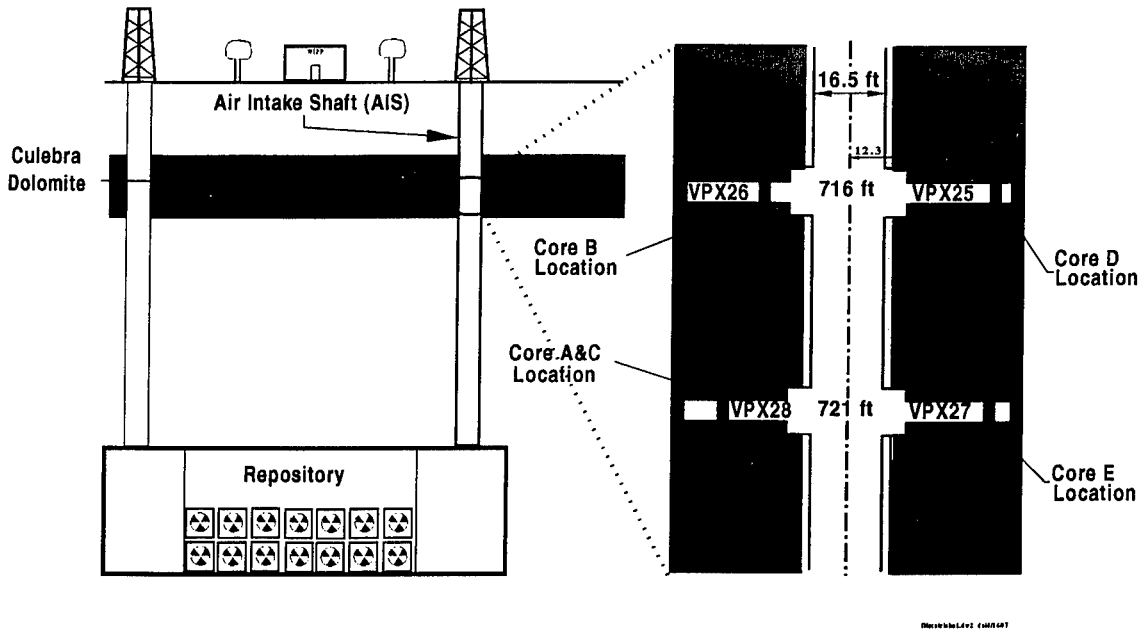

Figure 1. Borehole locations.

Liquid production rates were measured during the drilling and are also listed in Table 1. VPX 27 would most likely to be representative of rocks found along rapid flow paths, as demonstrated by its borehole flow, an order of magnitude greater than the others. Other measurements performed on site were the temperature and the pH of the brine samples collected at the coring locations.

Table 1. Borehole properties.

Borehole	VPX 25	VPX 26	VPX 27	VPX 28
Depth (m)	218.2	218.2	219.8	219.9
Side of AIS	North	South	North	South
Borehole flow (L/min)	0.34	0.16	3.0	0.16
pH	7.65	7.69	8.10	8.09
Temperature (^{o}C)	21.0	20.9	21.1	20.1

TEST SAMPLES

Tests used samples from all four boreholes to provide a range of core properties. Series A, B, C, D and E used cores VPX 28, 26, 28, 25 and 27 respectively, and are shown in Figures 2 through 6. Note that Figure 1 also shows the approximate position of the tested core sections. Core sections selected were relatively solid and intact, but demonstrated the fractures, gypsum infilling and vugs typical of WIPP Rustler cores. Core C had a fracture going almost entirely through the sample between 270^{0} and 100^{0}. That fracture is visible on both ends, but did not split the sample. It is not believed to be a drilling artifact, but may be a natural unloading fracture that is partly cemented. Table 2 lists dimensions, weights and density of the sample used in each Test.

Holt (1997) estimated core composition by visual inspection of Cores C, D and E photographs. He quantified solid dolomite, silty dolomite, gypsum, fractures and vugs. Core C showed the least evidence of macropores, (fractures, silty dolomite and vugs), Core E showed the most, while Core D was intermediate with respect to the other two.. Hsieh et al. (1997) used gamma ray tomography to measure core density inside a separate sample of VPX 26. He quantified compositional changes throughout the sample and found that while dolomite content was relatively constant, macorpores, (Hsieh's mixed voxels) increased by a factor of three in a distance of 6 cm along the length. Together, these studies indicate AIS Culebra cores are highly variable and should show measurable differences in transport properties.

ESTIMATED POROSITY

The total core porosity is an important parameter for interpretation of these results. Unfortunately, a direct measurement of the core porosity was not possible because of concerns that drying the samples would affect their chemical properties, and thus impact the latter retardation experiments. Measurements were made by Terra Tek (1996) and Brown (1995-1996, page 87) of separate end cuts from core VPX 26. Terra Tek reported an average porosity of 17.6% from three 1.5" diameter by 2" long sub-cores with only trace gypsum. Brown estimated a porosity of 15.5% from a slightly irregular 1.3" long by 5.7" diameter slice with

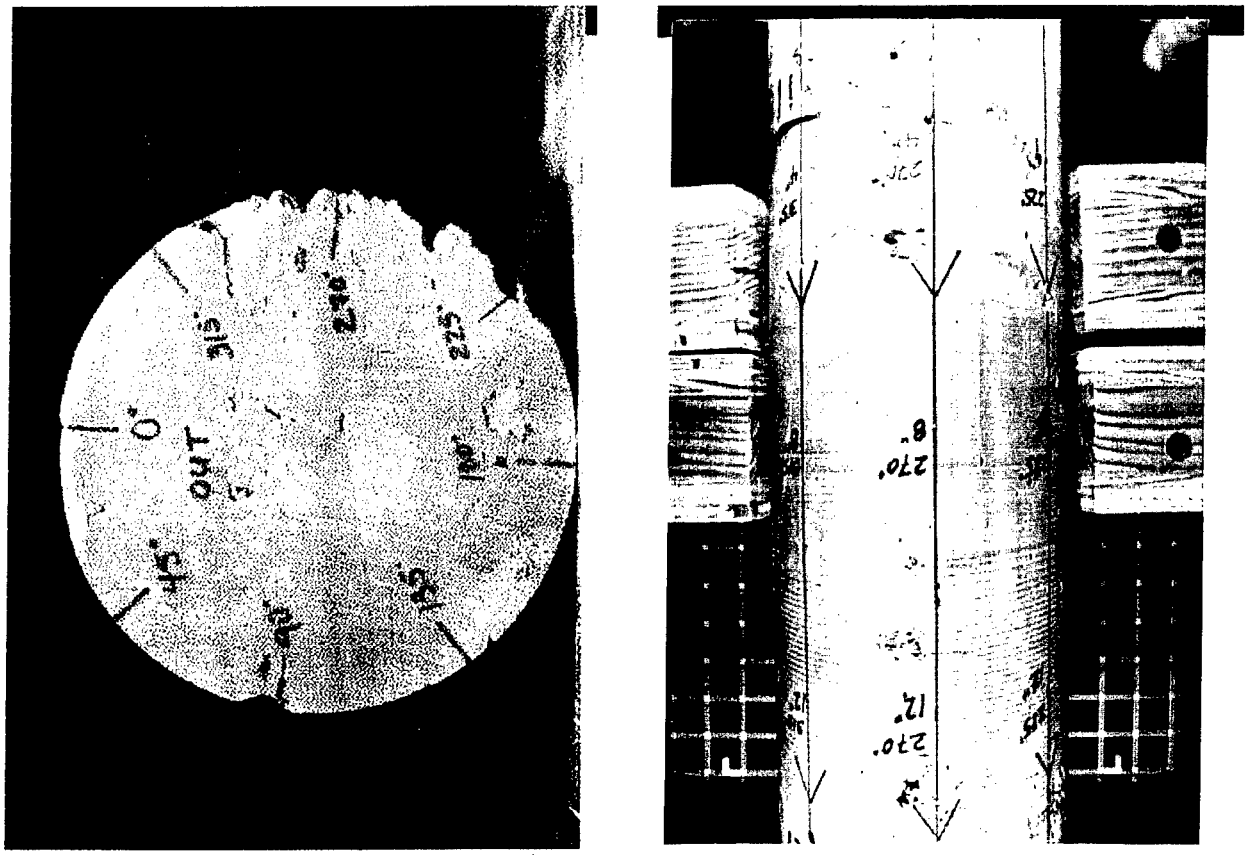

Figure 2. Photographs of Core VPX 28-6B, Test Series A.

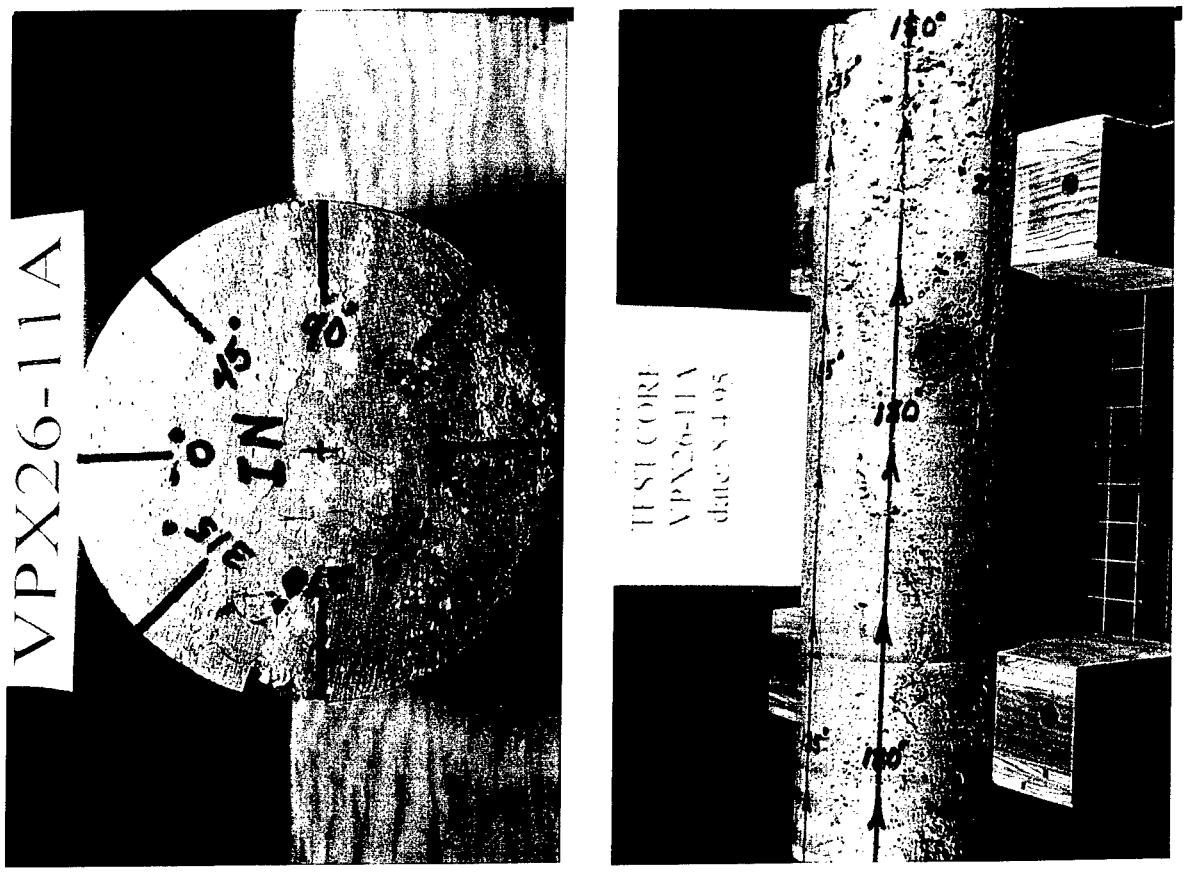

Figure 3. Photographs of Core VPX 26-11A, Test Series B.

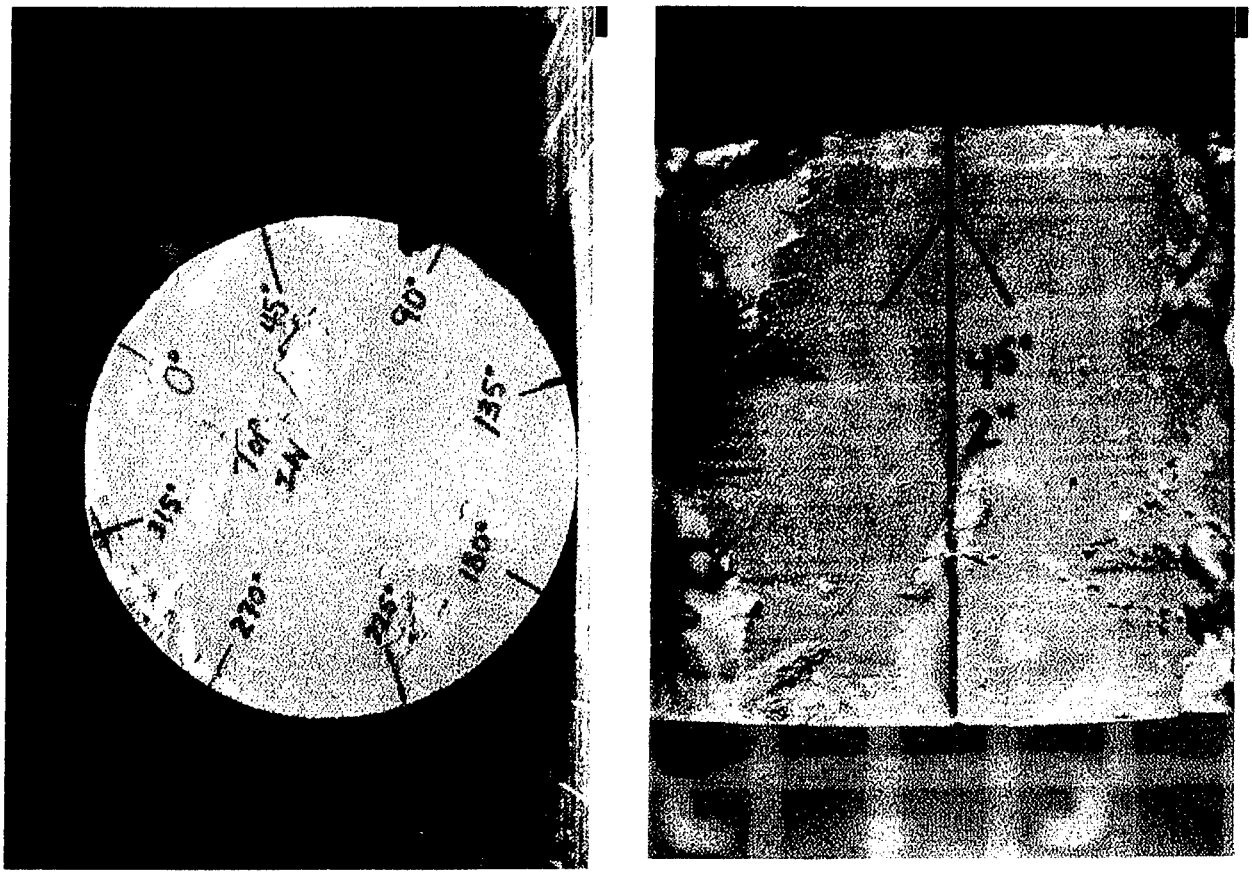

Figure 4. Photographs of Core VPX 28-6C, Test Series C.

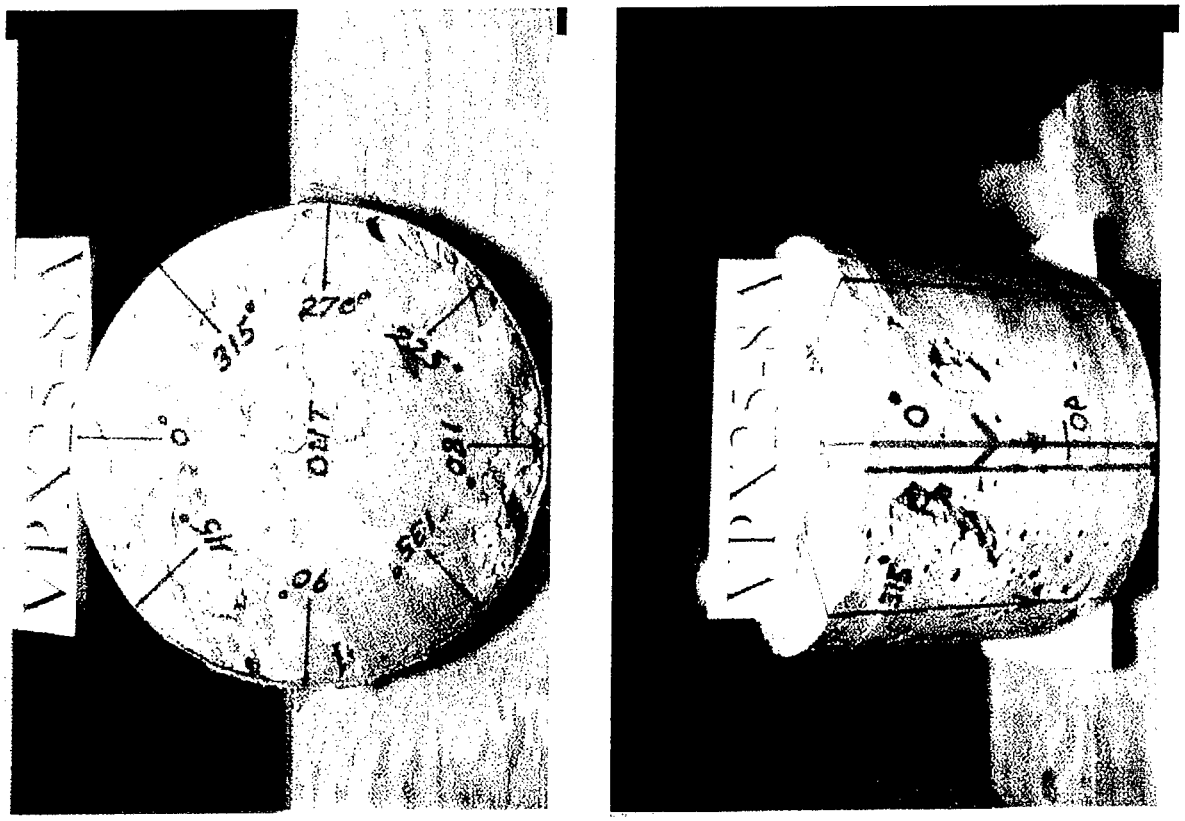

Figure 5. Photographs of Core VPX 25-8A, Test Series D.

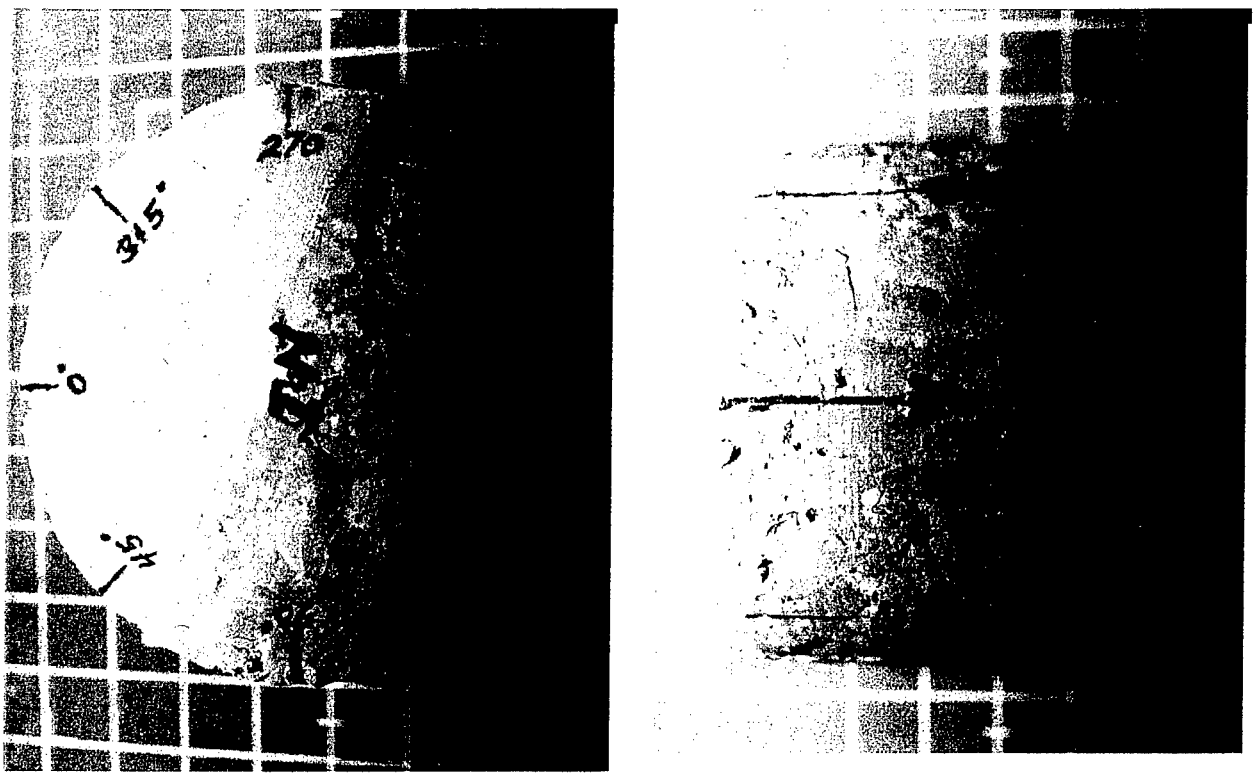

Figure 6. Photographs of Core VPX 27-7A, Test Series E.

Table 2. Test sample cores.

Series	A	B	C	D	E
Core: VPX	28-6B	26-11A	28-6C	25-8A	27-7A
Cut core measures					
Length (cm)	40.6	50.9	10.2	10.8	10.2
Diameter (cm)	14.5	14.5	14.5	14.5	14.5
Volume (cm^3)	6703	8404	1666	1773	1666
Wet weight (gm)	16582	20900	4146	4401	4102
Estimated Properties					
Dry bulk density (gm/cm^3)	2.38	2.40	2.40	2.40	2.38
Porosity	0.15	0.14	0.14	0.14	0.15

gypsum content. Both of those measurements are consistent with other WIPP cores studied by Kelley and Saulnier (1990).

As an alternative, estimates of total core porosity can be made by applying basic principles to the core volume and wet weight. First the dry sample weight, wt_d is given by,

$$wt_d = \frac{wt_w}{(1+\theta_w)} \tag{2}$$

where wt_w is the wet sample weight and θ_w is the sample water content by weight. Dry bulk density, ρ_b is given by,

$$\rho_b = \frac{wt_d}{V_s} = \frac{wt_w}{(1+\theta_w)V_s} \tag{3}$$

where V_s is the sample volume. With the bulk density defined, total porosity can then be calculated by,

$$\phi = 1 - \frac{\rho_b}{\rho_p} \tag{4}$$

where ρ_p is the bulk average mineral or particle density. Particle density will vary in these cores according to the gypsum content, which is again unknown without destructive sampling. Thus the particle density must be estimated with,

$$\rho_p = \frac{(1-x)\rho_d}{(1-x)+x\rho_d/\rho_g} + \frac{x\rho_g}{(1-x)\rho_g/\rho_d + x} \tag{5}$$

where ρ_d is dolomite's density, ρ_g is gypsum's density and x is the mass fraction of gypsum in the total solid minerals. Equation 5 follows from volume averaging the mineral densities. Substituting Eqs. 3 and 5 into Eq. 4 yields a direct expression for porosity,

$$\phi = 1 - \frac{wt_w}{(1+\theta_w)V_s\left[\frac{(1-x)\rho_d}{(1-x)+x\rho_d/\rho_g} + \frac{x\rho_g}{(1-x)\rho_g/\rho_d + x}\right]} \quad (6)$$

In Eq. 6 wt_w and V_s are measured, ρ_d and ρ_g are approximated at 2.83 and 2.32 gm/cm^3 respectively (Hsieh et al., 1997), and θ_w and x must be estimated from other measurements on AIS core samples. The cores were saturated when drilled and allowed to drain freely, but not dried, before storage. Thus, it can be assumed the dolomite intrinsic porosity is water filled, but the large pores are empty. With one exception, since the dolomite intrinsic porosity is relatively constant throughout the site, it is reasonable to assume that all the cores will have the same weight based water content regardless of their macroporosity. The exception results from the variable gypsum content in the cores. Gypsum will impact water contents and porosity estimates in two ways. Since it has no intrinsic porosity, increasing gypsum will reduce porosity and water content. However, because gypsum has a lower mineral density it reduces the net particle density, and will increase the porosity computed from bulk volumes (note Eq. 3). These two opposing factors tend to reduce the sensitivity of core porosity to estimated gypsum content.

Sewards et al. (1991) found gypsum ranging from 0 to 25% in the Culebra. Visual inspections of these cores indicate a similar range. A value of 10% is used here. Water content was measured on an end cut of VPX 26 at 3.6% by weight (Brown, 1995-1996, page 87), and will be assumed for these samples. Table 2 lists the estimated core porosity computed with those values. Surprisingly, the cores had equivalent porosity even though they appeared dissimilar.

CORE PREPARATION AND PRECONDITIONING

Cores were carefully removed from their storage tubes and cut to the desired length on a 10" dry diamond saw. A urethane rubber sleeve was poured around the core to form a liner using a custom form. Liner properties are listed in Table 3. After pouring, the liner was allowed to cure at room temperature a minimum of two days before mounting in a core holder. At no time during the core preparation was the sample heated above room temperature or allowed to dry.

Table 3. Liner properties.*

Brand	Devcon, Flexane 80 15800
Type	Two-part urethane rubber
Mix Ratio	3:1
Specific Volume	26.5 in^3/lb
Operating Temperature	120° F, maximum wet
Cured Hardness	87, Shore A
Tensile Strength	2100 psi, ASTM D412
Tear resistance	250 pli, ASTM D624
Additives used	None

* ITW Devcon, 30 Endicott Street, Danvers, Massachusetts, 01923.

After mounting in their holders, the cores where preconditioned by leaching with their matching air intake shaft (AIS) brine. Preconditioning insures that the core is in chemical equilibrium with the leachate solution before the sample spikes are injected. Conditioning was generally carried out at standard flow conditions of 0.1 ml/min over a period of two weeks. Depending on the core, that provided two to eight pore volumes of flow.

Brines

Synthetic solutions matching the measured composition of water taken from the bore holes were used in most of the test series. In two tests, a brine matching the composition of the deeper Salado Formation brine, ERDA 6, was used to determine if transport is influenced by intrusion of deeper waters. Table 4 lists the composition of each brine used. These compositions are the average ion values of all samples neglecting ions occurring at concentrations less than 10 mg/l (Geotech, 1992; Brush, 1990).

Table 4. Brine composition.

Brine	VPX 25	VPX 26	VPX 27	VPX 28	ERDA 6
Ions (gm/L)					
Boron	0.0258	0.0263	0.0266	0.0274	0.68
Bromine	0.054	0.0226	0.0243	0.0217	0.88
Calcium	0.8750	0.832	0.8580	0.8350	0.49
Carbon, inorganic	0.0113	0.0121	0.017	0.0120	0.19
Chloride	18.9	19.3	19.2	19.4	170
Magnesium	0.4540	0.4190	0.4500	0.4230	1.04
Potassium	0.3220	0.3330	0.3220	0.3170	3.79
Sodium	13.1	13.8	13.3	14.2	112
Sulfate	6.65	7.25	6.94	7.41	16.3
Borehole pH	7.65	7.69	8.10	8.09	6.17

Craft and Siegel (1997) found that under atmospheric conditions the recipes used to mix the brines could produce solutions supersaturated with calcite. However, after mixing all solutions were passed through a 0.45 μm filter to remove particulates. Thus, it may be assumed the solutions were saturated with respect to calcite.

Yeh (1993a and 1993b) measured the density and viscosity of a synthetic VPX 26 brine (Yeh's brine 2) and three Salado brines, QPBO2D, SB-139-B and L4P51. Table 5 lists measured density and dynamic viscosity values at 22° C, for VPX 26 and the Salado brine (QPBO2D) nearest in density to ERDA 6.

Table 5. Brine fluid properties.

Brine	Temperature (°C)	Density (Mg/m^3)	Temperature (°C)	Viscosity ($N \cdot s/m^2$)
VPX 26	22.1	1.0292	22.02	1.055×10^{-3}
QPBO2D	22.5	1.1993	22.05	2.355×10^{-3}
ERDA 6	22	1.191		

Column Apparatus

A schematic of the test apparatus is shown in Figure 7, and the more important components are listed in Table 6. Its major components were a column core holder, a syringe pump, a brine injection reservoir and an effluent collector. The column tracer test equipment was selected and assembled from generally off-the-shelf components to meet four requirements. First, materials which come in contact with the samples or brine must be nonreactive. Thus, all exposed surfaces were Teflon or Teflon coated. Second, the equipment testing conditions had to replicate as closely as possible the natural conditions in the Culebra, which required the maintenance of reservoir overburden pressure on the sample. Third, since tests continued for months at a time, most equipment had to be automatic and require minimum maintenance during operation. Therefore, automated syringe pumps and effluent collectors were used. Finally, due to the actinides used, the column apparatus had to fit into and be operated inside a glove box. This last requirement restricted some options and required keeping the operation as simple as possible.

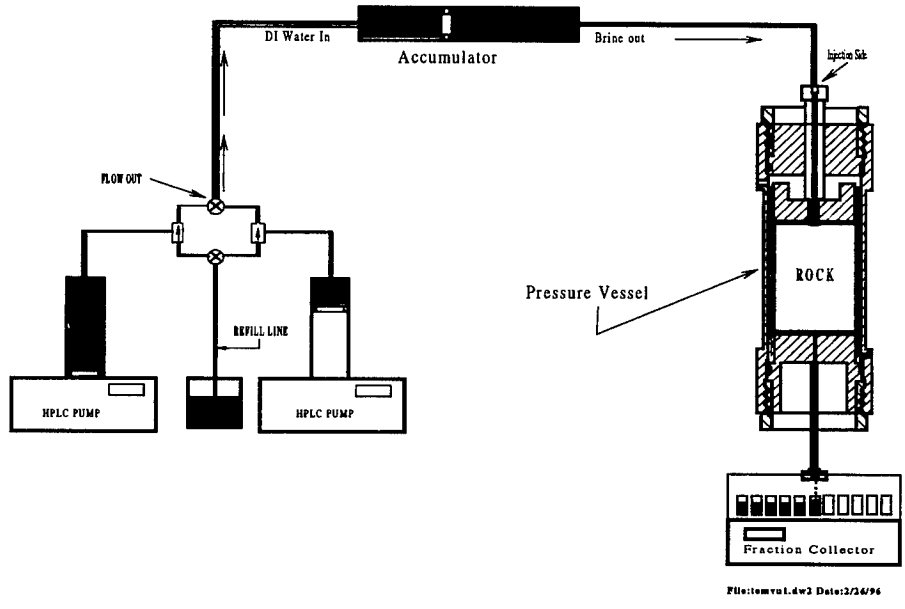

Figure 7. Schematic of test apparatus.

Table 6. Core column test equipment.

Equipment	Make	Model
High Pressure Core Holder	TEMCO	HCB-5.7
Brine Accumulator	TEMCO	CC200 150
Syringe Pumps	ISCO	500 D
Syringe Pump Controller	ISCO	621240026-91266
Fraction Collector	Spectra/Chrom	CF-1
Leachate pressure transducer	Taber	2412, (8-50 psi)
Overburden pressure transducer	Taber	2404, (0-1000 psi)
Thermocouple	TTEC	Type K

Aluminum was used to construct the column barrel and the end fittings were made of brass. Each core is held in a flexible sleeve between two distributor plates. Overburden loads are simulated by applying pressure in the annulus between the column and the sleeve. That pressure is also applied to the top distributor plate which is free to slide up and down, while the bottom plate is fixed. Thus, the core is subjected to the reservoir pressure in all three directions while allowing the effluent to exit at atmospheric pressure. The distributor plates are Teflon coated on all surfaces that come in contact with the core or leachate. A triaxial confining pressure of 725 psi was applied during all tests. This overburden pressure was computed using the rock density profile above the borehole. Since the density profile immediately above the cores is not known, one available from well H17 was used to compute the overburden pressure (Mercer and Snyder, 1990).

Brine was pumped from an accumulator into the core. The accumulator is a simple cylinder and piston sealed at both ends. Double, high pressure, liquid chromatography syringe pumps drive water into one end of the accumulator, which forces brine out the other. The accumulator prevents contamination and fouling of the pumps, while the double pump configuration allows automatic filling of the syringe pumps and insures continuous operation. Effluent was collected with a fraction collector operating in time mode set to provide approximately 5 ml per sample. Once a day the tubes were capped, swiped for contamination and removed from the glove box.

Differential leachate pressure, overburden pressure and column temperature were continuously monitored and recorded using pressure transducers, thermocouples and a personal computer based data acquisition system as indications of overall test conditions. The differential pressure can be used to compute core conductivity, but the precision of that measurement is limited and was not used. This is due to the design of the core holder and the operational limitations of running a continuous test inside a glove box. The differential pressure was measured across the entire column and includes losses at the inlet and exit. In addition, air bubbles had a tendency to form in the transducer lines, producing an unbalanced hydrostatic pressure equal to several inches of water.

Isotopes

SELECTION CRITERIA

Column tests require an isotope with a half-life greater than one day and less than 1,000 years. The one day minimum is necessary to achieve adequate transport time during the experiment. Obviously, measurable amounts of a tracer must remain at the end of a test to have any hope of measuring it in the column effluent. The 1,000 year maximum is dictated by the need to have measurable activity at molar concentrations below solubility limits. Radioassay methods, gamma spectrometry (γ Spec) and liquid scintillation counting (LSC), were used to measure effluent molar concentration. Those techniques measure isotope decays, not molar mass as chemical methods do. At a constant molar concentration, a short lived isotope undergoes more decays and is thus easier to detect than a longer life isotope of the same element. Since the actinide solubilities are generally low, measurable activities cannot be achieved with solutions of isotopes with half-lives greater than approximately 1,000 years. Using short half-life isotopes adds considerable experimental difficulty. Extra effort and planning are needed to ensure that sample spikes are delivered at the desired time since long storage is not possible. Such short lived isotopes were only considered if they have strong gamma emissions that make radioassays easier or tomography possible.

Since radioassays were used to quantify the effluent concentrations, the isotope's decay emission is important. Of the two radio assay methods used, γ Spec is preferable, since it does not require sample preparation and can easily distinguish different isotopes. Sample tubes can be directly loaded into the instrument and all gamma emitting isotopes measured simultaneously. LSC requires the sample to be mixed with a scintillation cocktail. It has poor energy resolution, but can differentiate alpha and beta emissions. Therefore, LSC may require knowledge of what isotopes are present in the sample. LSC does have the advantage over γ Spec in that its detection limit is generally an order of magnitude lower.

The total mix of isotope and emissions had to be considered to minimize interference in radioassays of the various tracers. These considerations also had to take into account any short-lived daughter products. Since daughters in-grow with their own half-lives, a short-lived daughter will soon equal the activity of the parent in any solution.

In addition to the feasibility criteria listed above, the isotope had to be available at economical prices. This implies that the isotope could either be obtained from commercial suppliers, or in the case of short-lived isotopes, separated from a stock of a long-life parent. Isotopes obtainable from dedicated reactor operations were investigated but found to be too costly and operationally impractical.

AMERICIUM

Americium has two isotopes that meet the feasibility criteria, 240 and 241. The first is not economically available, but ^{241}Am is an acceptable tracer candidate. It has a 59.5 keV gamma emission with a 35.7% yield and two alphas with energies at 5.44 and 5.49 MeV with 12.8% and 85.2% yields. Its long half-life of 432.2 years requires relatively high molar concentrations for γ

Spec analysis, but LSC can go two orders of magnitude lower. Certified stocks were obtained from Isotope Products Laboratories, Burbank California in HCl solutions.

NEPTUNIUM

Four Neptunium isotopes meet the selection criteria, 234, 235, 238 and 239. With a 1.1 year half-life 235, is the longest lived of the four, but only has an alpha emission. The other three isotopes have similar half-lives of two to four days and multiple gamma emissions. ^{239}Np has two high yield, high energy γ ray emissions and was chosen. It was obtained from a stock of its parent ^{243}Am purchased from Oak Ridge National Lab and its separation followed Newton et al. (1995a).

PLUTONIUM

Plutonium has five feasible isotopes, 236, 237, 238, 241 and 246. The only good gamma emitter, 246, is not available except by dedicated reactor operations. Three isotopes, 236, 237 and 238 are alpha emitters, and 241 is a beta emitter. ^{241}Pu with a 14.4 year half-life was chosen since its beta emission would have minimum interference from the other isotopes present in the effluent. Certified stocks were obtained from Isotope Products Laboratories, Burbank California in HCl solutions.

SODIUM

^{22}Na with a 2.6 year half-life was used as a conservative tracer in most tests. As will be shown in a latter section, sodium is a conservative solute in the calcium rich Culebra Dolomite. ^{22}Na is readily available and its positron emission produces 511 keV gamma's with a 180% yield. Certified samples were obtained from Isotope Products as a dilute chloride salt solution in water.

TRITIUM

Tritium (^{3}H), when bound as water provides the ultimate conservative tracer for transport studies. By definition, it moves with the ground water flow unhindered by adsorption. With a 12.28 year half-life and strong beta emission, it is easily detected by LSC. Its only drawback is that its emission interferes with the analysis of ^{241}Pu. Certified stocks were obtained from Amersham Corporation, Arlington Heights, Illinois.

THORIUM

Thorium has only three isotopes that meet the selection criteria, 227, 228 and 234. Both 227 and 234 have short half-lives, 18.7 and 24.1 days respectively, compared to 228's 1.9 years. None of the three thorium isotopes have a strong gamma emission, thus ^{228}Th was chosen for its longer half-life. ^{228}Th also had an advantage since it is readily available in large quantities. It is the daughter of ^{232}U and spikes were obtained from a large supply of its parent maintained by Inhalation Toxicology Research (ITRI). Depending on the specific test requirements, the ^{232}U and ^{228}Th were either separated or left combined.

URANIUM

Four uranium isotopes, 230, 231, 232 and 237, are feasible tracers, but only ^{232}U is economically available. It has one gamma at 57.8 keV with a 0.2% yield and two alphas at 5.26 and 5.32 MeV with 31% and 68.6% yields respectively. It was obtained from a large stock maintained by ITRI. Spikes were prepared and assayed by ITRI before use.

SPIKE PREPARATION

Injection spikes were prepared and assayed by ITRI (Newton et al., 1995b). They dispensed the desired isotope activity into Teflon bottles and then added brine supplied by SNL to bring the total spike volume between 10 and 20 ml. These procedures produce a spike of known isotope activity with an ionic strength slightly less than the brine itself. Actinide stocks were maintained at low pH until they were diluted with the appropriate brine to the desired spike activity. Only at the last step was the spike pH brought to the natural brine pH listed in Table 4.

Spike Injection

During the planning phase for these experiments, several reviewers expressed concern that actinide spikes would plate out in the injection apparatus and never reach the core. Thus, a procedure was developed to insure the tracer materials reached the core at the desired activity and in soluble form. Before each core was mounted, a small reservoir, approximately 5 cm in diameter and 1 cm deep was milled into its inlet end (Heath, 1995). The reservoir provides an approximately 20 ml volume, enough to hold a typical tracer spike. When a spike was ready for injection, the pumps where turned off and the upper inlet tubing removed. A 12" long Teflon tube, attached to a plastic syringe, was inserted into the core holder and used to empty the inlet reservoir. The syringe was then removed, reservoir brine discarded, and the tracer spike drawn into the syringe. Next, a sample of the spike, typically 1 to 5 ml, was dispensed from the syringe into a fraction collection tube labeled "START". The syringe tube was then reinserted into the core and the spike injected directly into the reservoir. The spike solutions remaining in the syringe and tubing were then placed in a tube labeled "END". Finally, the inlet tubing was reconnected, and the pumps started. This operation typically took 15 minutes. The START and END tubes were weighed, topped off to the standard 5 ml volume with deionized water and assayed. Since the tubes were filled from the same syringe and at the same time as the spike, they provide proof that the actinides reached the core. While the temporary flow interruption and inlet reservoir are undesirable, their effects are small compared to the total test time and core size.

Some experiments with Cores A and B used 500 or 2000 ml slugs of tracer to provide a constant concentration boundary condition. For those tests a dedicated "hot" accumulator was placed inside the glove box. Tracer was loaded into it along with the appropriate brine volume. The hot accumulator then replaced the normal accumulator by connecting it directly to the pump output and core inlet. After the slug was injected, the hot accumulator was disconnected and normal operation resumed.

Test Conditions

Test objectives, spike activity, spike volume, flow rate and brine used for each experiment are listed in Table 7. Twenty-six individual tests have been run on the five cores, most of which had multiple isotopes in the injection spike. In total, there have been five ^{3}H spikes, three spikes with ^{241}Pu and ^{241}Am, four ^{228}Th spikes, ten spikes of ^{239}Np and ^{232}U, and twenty-two spikes of ^{22}Na. ^{22}Na was used repeatedly to quantify and monitor the core hydraulics. Two tests, C5 and C7, were carried out with ERDA 6 brine to quantify the impact of brine type on transport. Tests B5 to B8 and D6 were performed at different flow rates to measure flow rate dependencies. Most tests were carried out at a total flow rate of 0.1 ml/min. That flow corresponds to a volume flux (or Darcy flux) of 9.8×10^{-6} cm/s (3.2 m/yr). Division of the volume flux by the fitted porosity for each test will yield the effective seepage velocities in the advective porosity. This flow is at the upper end of the estimated natural conditions (Ramsey et al., 1996).

An important feature of these tests is the multiple spike injection in the same core. This strategy has three specific benefits. First, the multiple spikes allow direct comparison in the same core of different isotopes while minimizing interference in the radioassays. Second, multiple spikes provide a direct measure of core behavior with time, allowing changes in the core to be detected by the behavior of ^{22}Na. Finally, and most important, the multiple spikes with continuous analysis make very long tests practical. Once an isotope has been injected in a core, it is analyzed for in all later effluent, which is important in the quantification of noneluting actinides. As an example, while Test C3 was nominally carried out for two liters, all column effluent after that time, (over 62 liters) has been assayed for both ^{241}Am and ^{241}Pu. Thus minimum R analysis on those two isotopes can confidently be based on an eluted volume of approximately 250 pore volumes.

Spike Concentration

Actinide concentrations are reported here as isotope activities per volume or activities per mass. To assist readers, Appendix A contains conversions curies to molar or gram mass units.

Table 8 lists the actinide spike activity and concentration for each test sorted by isotope. Concentrations presented in the table are the largest values occurring during the experiments. On injection, the spike is diluted by brine in the column headspace, and then undergoes hydrodynamic dispersion. Even a conservative solute spike will normally be diluted by an order of magnitude by the time it reaches the outlet. Aqueous concentration of retarded solutes will be quickly reduced due to adsorption on to the mineral surface as defined in Eq. 1.

Spike concentration are compared to measured and computed solubility in Table 9. Solubility of Am, Th, and Np were computed by Craft and Siegel (1997). Values corresponding to solutions both supersaturated with calcite and in equilibrium with dolomite are listed. The range in Pu solubility was obtained from measurements made by Nitsche et al. (1992 and 1994) in AIS brine. Uranium solubility during the tests is clearly demonstrated by its elution from the cores with moderate retardation, as shown in the results. Pu, Np and Th spike activities were well below solubilty. Americium had spike concentrations between 3.4 to 8.0×10^{-7} M necessitated by its the relatively low activity. Unfortunately, this was greater than the solubility

Table 7. Test conditions.

Test	Start Date	Brine	Tracer	Spike (ml)	Flow (ml/m)	Vol. (L)	Time (days)	Test Objective
A-1	4/5/95	AIS	0.641 μCi ^{3}H	20	0.5	2	0.7	Porosity
A-2	4/28/95	AIS	500 μCi ^{22}Na	500	0.02	0.5	11	Tomography
A-3	6/9/95	AIS	0.22 μCi ^{3}H	20	0.1	2	13	Flow effects
A-4	7/25/95	AIS	23 μCi ^{22}Na 156 μCi ^{239}Np	20	0.1	2	13	Tomography and Np Retardation
B-1	9/6/95	AIS	0.246 μCi ^{3}H	13	0.1	0.5		Porosity
B-2	9/22/95	AIS	8.69 μCi ^{22}Na 375 μCi ^{239}Np	18	0.1	2	13	Tomography and Np Retardation
B-3	10/4/95	AIS	8.23 μCi ^{22}Na 70.7 μCi ^{232}U 70.7 μCi ^{228}Th	13.7	0.1	2	13	Tomography, U and Th Retardation
B-4	11/6/95	AIS	300 μCi ^{22}Na	2000	0.1	4	30	Tomography
B-5	12/7/95	AIS	274 μCi ^{22}Na	2000	0.05	2	60	Tomography
B-6	1/30/96	AIS	4.22 μCi ^{22}Na 5.94μCi ^{232}U	17	0.05	2	60	U Retardation
B-7	4/16/96	AIS	9.0 μCi ^{22}Na 4.28 μCi ^{232}U	18	0.5	4		U Retardation
B-8	4/23/96	AIS	220 μCi ^{22}Na	2000	0.5	4		Tomography
C-1	5/1/95	AIS	1μCi ^{22}Na 10μCi ^{3}H	20	0.1	2	13.3	Porosity
C-2	6/19/95	AIS	3.7μCi ^{22}Na 10μCi ^{232}U 10μCi ^{228}Th	20	0.1	2	21	U and Th Retardation
C-3	7/10/95	AIS	3.3μCi ^{22}Na 20μCi ^{241}Pu 5.6μCi ^{241}Am	20	0.1	2	16	Pu and Am Retardation
C-4	7/26/95	AIS	11.5μCi ^{22}Na 78.3μCi ^{239}Np	10	0.1	2	49	Np Retardation
C-5	9/13/95	ERDA	3.4μCi ^{22}Na 26.8μCi ^{239}Np 4.8μCi ^{232}U 4.8μCi ^{228}Th	10	0.1	2	13	Brine Effects on Np, U and Th Retardation
C-6	10/18/95	AIS	5.3μCi ^{22}Na 175μCi ^{239}Np	8.5	0.1	2	13	Duplicate Np Retardation
C-7	11/17/95	ERDA	6.83μCi ^{22}Na 327μCi ^{239}Np 50μCi ^{232}U	10	0.1	2	13	Duplicate Brine Effects

Table 7. Test conditions (continued).

Test	Start Date	Brine	Tracer	Spike (ml)	Flow (ml/m)	Vol. (L)	Time (days)	Test Objective
D-1	8/29/95	AIS	0.35μCi ^{3}H	18	0.1	0.5	4.0	Porosity
D-2	9/13/95	AIS	3.4μCi ^{22}Na 4.8μCi ^{232}U 4.8μCi ^{228}Th 26.8μCi ^{239}Np	10	0.1	2	12	U, Th and Np Retardation
D-3	9/28/95	AIS	3.1μCi ^{22}Na 16.1μCi ^{241}Pu 4μCi-^{241}Am	10	0.1	2	13	Am and Pu Retardation
D-4	10/18/95	AIS	5.3μCi ^{22}Na 175μCi ^{239}Np	8.5	0.1	2	13	Duplicate Np Retardation
D-5	11/13/95	AIS	3.97μCi ^{22}Na 43.2μCi ^{232}U	10	0.1	2	13	U Retardation
D-6	1/30/96	AIS	3.4μCi ^{22}Na 53μCi ^{232}U	20	0.05	2	60	Flow Effects on U Retardation
E-1	12/20/95	AIS	3.17μCi ^{22}Na 40 μCi ^{232}U 156μCi ^{239}Np	20	0.1	2	12	Porosity, U and Np Retardation
E-2	1/16/96	AIS	3.07μCi ^{22}Na 20μCi ^{241}Pu 20μCi ^{241}Am	18.5	0.1	2	13	Am and Pu Retardation

determined at a later date. Therefore, to be conservative, it will be assumed that the injected americium concentration was equal to the solubility without dolomite equilibrium (6.46×10^{-9} molar).

Effluent Analysis

Effluent was collected in Fisher, 13 × 100 mm screw cap tubes (Catalog No. 14-956-4A). With the large number of tubes used, it was impractical to tare weigh each one, thus an average tare weight of 4.70 gm was used. Spot checks of tubes indicate their weights varied on average less than 0.01 gm, with a 0.1 gm maximum variance. Filled tubes were weighed to one milligram precision on a Mettler PM12000 balance.

Effluent tube activity was measured with a Canberra automatic gamma spectrometer (γ Spec), equipped with a large area germanium detector (Canberra Model GL2020R) and multichannel analyzer. This detector was calibrated with a multiple energy source standard with the same geometry as the sample tubes. All calibration sources were traceable to the National Institute of Standards and Technology (NIST).

Table 8. Injection spike concentrations.

Test	Tracer	Brine	Activity (uCi)	Spike (ml)	Activity (mCi/L)	mole/L (10^{-9})	Mass (ug/L)
C3	^{241}Am	AIS	5.6	20.0	0.28	338	81.6
D3	^{241}Am	AIS	4.0	10.0	0.40	484	117
E2	^{241}Am	AIS	12.2	18.5	0.66	797	192
A4	^{239}Np	AIS	156.0	20.0	7.80	0.14	0.03
B2	^{239}Np	AIS	375.0	18.0	20.8	0.38	0.09
C4	^{239}Np	AIS	78.3	10.0	7.83	0.14	0.03
C5	^{239}Np	ERDA 6	26.8	10.0	2.68	0.05	0.01
C6	^{239}Np	AIS	175.0	8.5	20.6	0.37	0.09
C7	^{239}Np	ERDA 6	327.0	10.0	32.7	0.59	0.14
D2	^{239}Np	AIS	26.8	10.0	2.68	0.05	0.01
D4	^{239}Np	AIS	175.0	8.5	20.6	0.37	0.09
E1	^{239}Np	AIS	464.0	20.0	23.2	0.42	0.10
C3	^{241}Pu	AIS	20.0	20.0	1.00	40.3	9.71
D3	^{241}Pu	AIS	16.1	10.0	1.61	64.8	15.6
E2	^{241}Pu	AIS	11.3	18.5	0.61	24.6	5.93
B3	^{228}Th	AIS	70.7	13.7	5.16	27.6	6.19
C2	^{228}Th	AIS	10.0	20.0	0.50	2.68	0.60
C5	^{228}Th	ERDA 6	4.8	10.0	0.48	2.57	0.58
D2	^{228}Th	AIS	4.8	10.0	0.48	2.57	0.58
B3	^{232}U	AIS	70.7	13.7	5.16	1040	241
B6	^{232}U	AIS	101.0	17.0	5.94	1196	278
B7	^{232}U	AIS	77.0	18.0	4.28	862	200
C2	^{232}U	AIS	10.0	20.0	0.50	101	23.4
C5	^{232}U	ERDA 6	4.8	10.0	0.48	96.7	22.4
C7	^{232}U	ERDA 6	50.0	10.0	5.00	1007	234
D2	^{232}U	AIS	4.8	10.0	0.48	96.7	22.4
D5	^{232}U	AIS	43.2	10.0	4.32	870	202
D6	^{232}U	AIS	53.0	20.0	2.65	534	124
E1	^{232}U	AIS	31.0	20.0	1.55	312	72.4

Some isotopes do not emit adequate gamma radiation and were quantified by their alpha or beta emissions. Approximately every fifth sample was analyzed by liquid scintillation counting (LSC) on a Canberra model 2550 TR/AB. The LSC is calibrated with an unquenched ^{14}C calibration standard traceable to NIST. Activity concentrations were computed as the ratio of the measured activity to the sample weight.

Table 9. Solubility of actinides in column brines.

Actinide	Brine	Solubility (Molar)	
Computed Data		*Without dolomite equilibrium*	*With dolomite equilibrium*
Am	VPX 28	6.46×10^{-9}	9.63×10^{-9}
Np	VPX 28	7.84×10^{-6}	1.10×10^{-5}
Np	ERDA 6	4.17×10^{-7}	9.51×10^{-7}
Th	VPX 28	1.90×10^{-7}	1.57×10^{-7}
Th	ERDA 6	3.98×10^{-7}	1.21×10^{-2}
Measured Data		*Low*	*High*
Pu	AIS	3.0×10^{-8}	7.6×10^{-7}

Minimum detection activities, MDA, for each isotope used and two important daughters of ^{228}Th (^{224}Ra and ^{212}Pb) are listed in Table 10 for both γ Spec and LSC. The MDA will vary for each isotope as a function of the analytical technique and interference from other isotopes in the sample. MDA levels are limited by machine sensitivity with no interference. The only major interference for the isotopes in these experiments occurs with the LSC analysis of ^{3}H and ^{241}Pu. The LSC cannot distinguish between those isotopes, thus ^{3}H use is limited to the initial hydraulic test of each core. ^{228}Th daughters produce some interference in both the γ Spec and LSC analysis. When they are present, the analysis is repeated for 30 to 45 days until they decay below interference levels.

^{232}U, is analyzed by both γ Spec and LSC since it has a weak, but measurable gamma ray (57 keV with 0.02% yield) and a strong alpha (5.32 MeV with 68.6% yield). The sensitivity by LSC is much better for this isotope and LSC results were used for all parameter fitting. The γ Spec does provide a quantitative comparison and documentation that the LSC is measuring ^{232}U. ^{241}Am was detected by both γ Spec or LSC. LSC has a much lower MDA but interference from ^{232}U obscures its analysis when uranium is present in the effluent. The strong ^{241}Am γ ray emission stills provides a reasonable detection limit in those cases.

A decay correction was automatically applied by the γ Spec software to identified isotopes. Following first order decay,

$$A = \frac{A_m}{e^{-\lambda(t_m - t_s)}} \tag{7}$$

with

$$\lambda = \ln(2)/t_{1/2} \tag{8}$$

Table 10. MDA for isotopes of interest.

Isotope	γ Spec(nCi/ml)[1]	LSC (pCi/ml)[2]
^{3}H		1.5
^{241}Am	0.06	0.1
^{239}Np	0.62	
^{212}Pb	0.02	
^{241}Pu		1.5
^{224}Ra	0.27	
^{228}Th	3.8	
^{232}U	1.2	0.1

1. γ Spec MDA analysis, 15 min. counts, performed 10-31-95. "WIPP Lab Notebook, WBS 1.1.5.1.5, Calibration and Equipment Records." Albuquerque, NM: Sandia National Laboratories. (Copy on file in the Sandia WIPP Central Files, Sandia National Laboratories, Albuquerque, NM as WPO#40975.)
2. LSC MDA analysis, 15 min. counts, performed 3-9-95. WIPP Lab Notebook, WBS 1.1.5.1.5, Calibration and Equipment Records." Albuquerque, NM: Sandia National Laboratories. (Copy on file in the Sandia WIPP Central Files, Sandia National Laboratories, Albuquerque, NM as WPO#40975.)

where A is the reported activity, A_m is the measured activity, λ is the first order decay constant, t_m is the time sample activity was measured, t_s is an initial sample time, and $t_{1/2}$ is the isotope half-life. Since a large number of samples were being analyzed, the initial sample time was always set to the time of spike injection, and not the time of sample elution. Generally, the difference between spike injection and sample analysis time was one to seven days. For isotopes with half-lives greater than a year, the timing is trivial and the activity difference is smaller than measurement precision. The only isotope where the timing correction is significant is ^{239}Np with a 2.355 day half-life.

Parameter fitting of the solute breakthrough requires sample elution time and activity in μCi/ml at elution. Sample elution time was computed by,

$$t_j = \frac{\left[\left(\sum_{i=1}^{j-1} m_i + \frac{1}{2} m_j\right)\Big/\rho\right] - DV}{Q} \tag{9}$$

where t_j is the midpoint time of sample j, m is the measure mass of sample i, ρ is the solution density given in Table 5, Q is the volume flow rate, and DV in the column exit dead volume. The column dead volume was calculated based on the geometry of the collection plate, (6.1 ml) and the length of the effluent tube, (0.021 ml/cm). For the short cores, C, D, and E this totaled 6.7 ml, while the long cores A and B, had more tubing and totaled 8.2 ml.

Sample activity per effluent mass was measured in μCi/gm and converted to volume activities by multiplication of the solution density given in Table 5. Activities at elution, Af_j were computed for ^{239}Np by,

$$Af_j = A_j e^{-\lambda(t_s - t_j)} \tag{10}$$

Parameter Fitting for Eluted Species

Effluent curves were analyzed using COLUMN (Budge, 1996). That code provides parameter fits to the data for two different models. The first is the standard homogeneous porous media, advection dispersion model, based on the analytical solution of Parker and van Genuchten (1984). The second is a dual porosity, fractured-matrix numerical model similar to the Performance Assessment transport model, SECO-TP (WIPP Performance Assessment, 1992-1993).

COLUMN performs automatic least-squares fits of effluent data to theoretical effluent curves calculated using either the single-porosity or dual-porosity models. The fits are calculated using Marquardt minimization in which the curvature matrix is inverted using singular value decomposition (SVD). The advantage of SVD over other matrix decompositions is that a meaningful answer is returned even if there are dependencies in the model parameters being fit. COLUMN reports fitted parameter values, uncertainties, and the nature of any parameter dependencies to the analyst. The code requires the effluent activities, the collection times and the location along the column at which the effluent is collected (generally equal to the column length). In addition, the analyst must specify the spike volume and concentration and initial estimates of all model parameters. The analyst must convert the effluent volumes to collection times using the known flow rate.

Each column experiment includes at least one nonsorbing tracer, such as ^{3}H or ^{22}Na. This tracer is used to determine the hydrological parameters for each model, which are then used in subsequent fits of the sorbing tracers to determine the chemical retardation.

SINGLE POROSITY MODEL

The single porosity model assumes that, at least on the macroscopic scale, the rock is homogeneous. The mean pore velocity is determined by the porosity, ϕ, and the distribution of pore velocities is characterized by the dispersion, D. Chemical sorption is characterized by the retardation coefficient, R. Flux weighted concentrations were used, as recommended by Parker and van Genuchten (1984). The single porosity model is a simple model for which effluent curves can be computed analytically and whose parameters are easy to interpret. COLUMN is able to find optimal fits to the single porosity model in a few seconds of computer time.

DUAL POROSITY MODEL

The dual porosity model assumes that the rock column is heterogeneous, and divides it into two portions: a macropore space, in which transport is dominated by advection, and a surrounding rock matrix in which advection is negligible, but into which molecular diffusion can

take place. The hydrological parameters that describe the column include the advective porosity and matrix porosity, ϕ_f and ϕ_m; the advective and matrix dispersions, D_f and D_m; and the matrix block size, B. Chemical sorption is characterized by the advective and matrix retardation coefficients, R_f and R_m. The dual porosity model is similar to that used in SECO/TP. It is a complex model, and COLUMN can take up to a day to fit experimental data to dual porosity curves.

Another difficulty is the lumped parameter nature of the dual porosity model. The functional form of the transport equations makes the individual parameter definitions ambiguous. In other words, for the data available from the column experiments, it is difficult to distinguish fits using very different parameter values. For example, a decrease in D_m can be almost exactly offset by a decrease in B. We have chosen fixed values for matrix tortuosity, ϕ_m and matrix diffusion, D_m for the analyses described here. This leaves the matrix block size, B, as the single parameter describing the effects of dual porosity. Parameters fixed in the dual-porosity analysis are listed in Table 11. For U and Np matrix dispersion is set to the free-solution diffusion coefficients for the respective ions. The value used is the average of the probable oxidation states for both actinides reported by Brush (1996a). Diffusion into the matrix is computed assuming a one-dimensional plate geometry. This is analogous to a fracture or layered system.

Table 11. Fixed parameters used in all dual porosity analyses.

Parameter	Value
Matrix dispersion, D_m	
Na	1.5×10^{-5} cm^2/sec
U	3×10^{-6} cm^2/sec
Np	2.2×10^{-6} cm^2/sec
Matrix porosity, ϕ_m	0.11
Advective tortuosity	1
Matrix tortuosity	0.067
Advection computational cell length	1 cm
Matrix computational cell length	0.001 cm

Parameter Fitting for Noneluted Species

Determination of actinide retardation in the column experiments is problematic for isotopes that do not appear in the effluent. In such cases, actual retardation coefficients cannot be computed, since lack of detection means only that the test may not have been run long enough, or that the solute eluted from the column at a concentration lower than the analysis detection limits. Nevertheless, minimum values can be calculated based on the known hydraulics of flow and instrument MDA.

Two cases that limit estimates of retardation coefficients are shown in Figure 8. The figure presents possible breakthrough curves, only one of which will apply in a given test. The first curve, labeled **A**, is for a solute that eluted during the sampling, but whose maximum activity concentration at the outlet was below the MDA of the analysis instrument. In that case, the

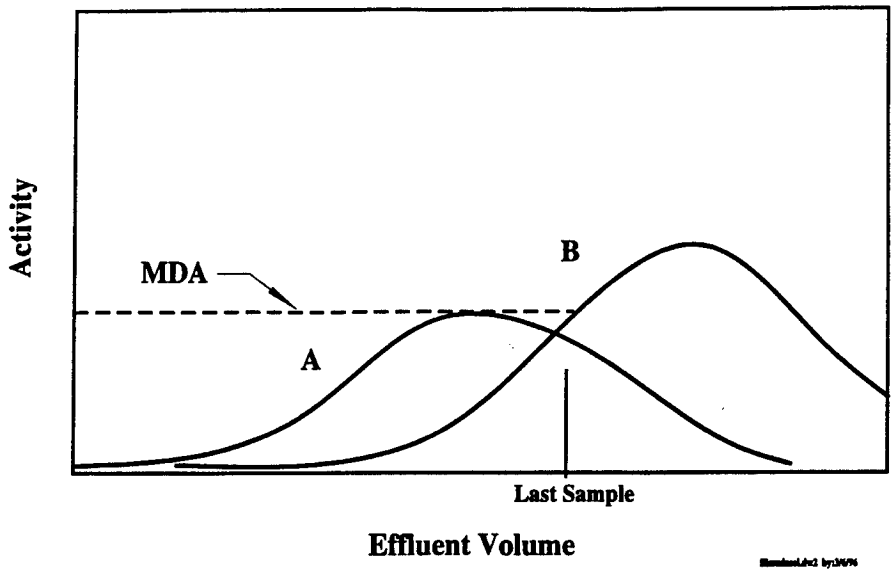

Figure 8. Possible breakthrough curves for non-eluting solutes.

minimum R will be that value that produces a peak equal to the MDA. The second curve, labeled **B**, is for a solute that would elute at activities higher than the MDA if the test was run longer. Solute may be in the effluent, but at activities below the MDA. In that case, minimum R is defined by the smallest retardation value that does not produce an activity greater than the MDA before the last sample. The limiting case, **A** or **B** is a function of the spike activity, dispersion, radioactive decay, total sampling volume and the MDA.

Minimum R was determined by trial and error runs of the single porosity model using the last sample volume, and assuming constant values of flow rate, dispersion, porosity and MDA. The MDA was set at the value listed in Table 10. Flow rate, porosity and dispersion were equated to the fitted values from the ^{22}Na breakthrough for the same test. Finally, R was varied over an appropriate range to determine the limiting case, **A** or **B**, and the minimum R.

Partition Coefficients and Dispersivity

The solute partition coefficient, k_d was computed from fitted R values by (Fetter, 1993, p. 119),

$$k_d = \frac{(R-1)\phi}{\rho_b} \tag{11}$$

With this definition, k_d will have the inverse units of the bulk density, ρ_b (cm^3/gm, or ml/gm). Since the bulk density is not known exactly in these samples a value of 2.4 gm/cm^3 from Table 2 was used. Considering the accuracy of the parameter fit for R and ϕ, that

assumption is adequate. In single porosity fits, the fitted value was used for ϕ, while for dual porosity fits the value of ϕ_m assumed as 0.11 (Table 11) was employed. The use of fitted porosity is a conservative practice, since the fitted values are less than or equal to the estimated total porosity, and k_d is linear with ϕ.

The effect of flow rate on dispersion can be reduced by calculation of the dispersivity, α,

$$\alpha = \frac{D - Dm}{v} \tag{12}$$

where D is the hydrodynamic dispersion, Dm is the molecular diffusion coefficient, and v is the seepage velocity (Fetter, 1993, p. 51). Molecular diffusion was assumed as 3×10^{-5} and 1.5×10^{-5} cm^2/s for ^{3}H and ^{22}Na respectively, which are representative values for those ions. The seepage velocity is given by,

$$v = \frac{Q}{A_{cs}\phi} \tag{13}$$

where A_{cs} is the column cross sectional area.

Daughter Product Analysis

At one time it was hoped that the minimum R of thorium could be lowered by observing the decay of its daughter products. ^{228}Th follows the decay chain:

$$^{228}\text{Th} \rightarrow {}^{224}\text{Ra} \rightarrow {}^{220}\text{Rn} \rightarrow {}^{216}\text{Po} \rightarrow {}^{212}\text{Pb} \rightarrow {}^{212}\text{Bi} \rightarrow {}^{208}\text{Tl(branch)}$$

$$\hookrightarrow {}^{212}\text{Po(branch)}$$

All daughters are shorted lived with ^{224}Ra having the longest half-life of 3.62 days. The daughters have multiple gamma, alpha and beta emissions which provide low MDA's for some. Since the ^{224}Ra is mobile, with a retardation of about two, all columns receiving ^{228}Th have ^{224}Ra and its daughters in the effluent. Repeated measurement for ^{224}Ra in the effluent shows its reduction with time, indicating that any ^{228}Th if present, must be at an activity less than the measured ^{224}Ra. The eventual reduction of ^{224}Ra below its MDA would indicate ^{228}Th was also below the ^{224}Ra MDA.

Unfortunately, the daughter product decay analysis is inconclusive due to the use of ^{232}U in the experiments. ^{232}U is the parent of ^{228}Th, and has been used in all cores. With repeated use of ^{232}U it has eluted at measurable activities over much of the effluent curve. All effluent samples with ^{232}U experience growth of ^{228}Th and its daughters. This situation makes any analysis based on the absence of the daughters problematic and generally inconclusive.

RESULTS

Effluent Curves

Measured breakthrough curves for eluting species are shown in Appendix B and listed in Appendix C. In general, the curves have the shape expected for advection-dispersion transport. ^{3}H, ^{22}Na, ^{232}U and ^{239}Np eluted in that general order. There was little difference between ^{3}H and ^{22}Na, indicating sodium is a conservative species in this salt rich system. Figure 9 shows their similarity in Test C1 once the activities are scaled to the maximum.

Due to equipment problems, Test A2 did not yield useful results. Two test spikes, C4-^{239}Np and C5-^{232}U, were unusable due to low initial spike activity. Both isotopes eluted, but at activities too low to provide useful data for parameter fitting. As a result of these tests, later spike activities were increased.

^{232}U eluted after a mild retardation in all experiments. Figure 10 shows Test E1 results, a typical ^{232}U breakthrough curve for both γ Spec and LSC results. ^{22}Na elutes at one pore volume followed by ^{232}U. Both analysis methods provide similar results, but the LSC has less noise and obtains useful measurements after ^{232}U has fallen below the γ Spec MDA.

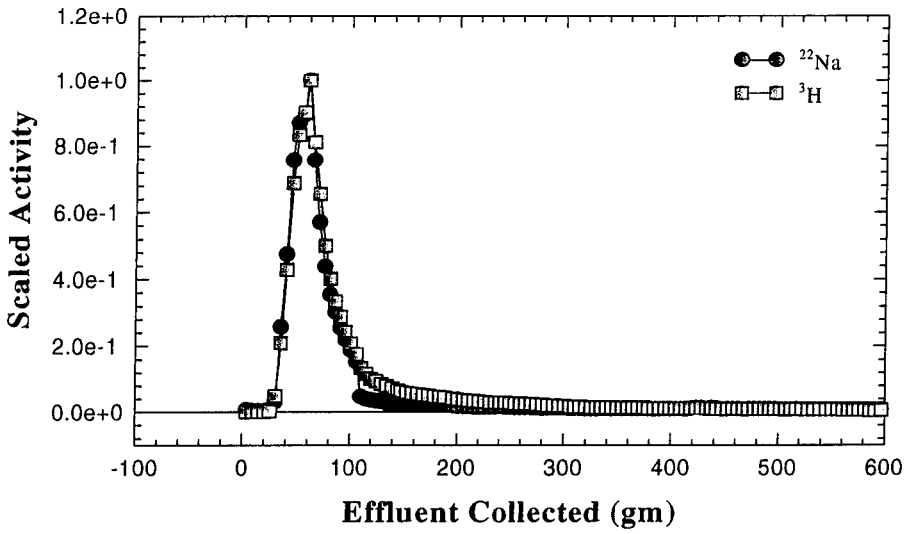

Figure 9. Comparison of ^{3}H and ^{22}Na effluent breakthrough in Test C1.

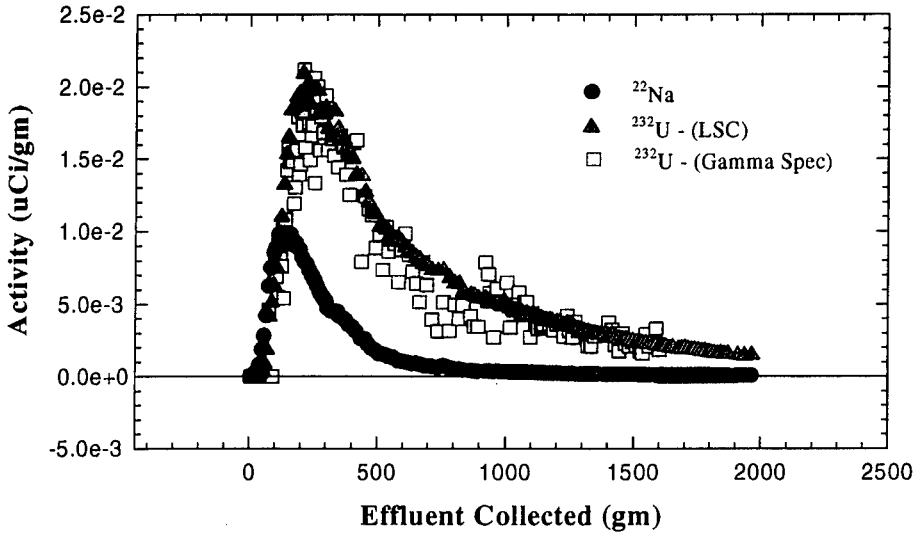

Figure 10. Comparison of γ Spec versus LSC in Test E1.

As mentioned previously, the short lived daughters of ^{228}Th require the holding of samples before LSC analysis. Figure 11 demonstrates the decay of the first and longest half-life daughter, ^{224}Ra, for test C2. The figure presents ^{224}Ra analysis of the samples at 5 different times, ^{22}Na activity, and the final analysis of ^{232}U by LSC. The first results, 6/21/95, show that the ^{224}Ra initially in equilibrium with the ^{228}Th breaks through with a retardation of about two. After breakthrough, the ^{224}Ra does not drop to zero, but instead declines until it reaches a level that represents the steady state balance between growth from the ^{228}Th in the column and transport out. Analysis of the same samples at later dates shows ^{224}Ra decreasing consistent with radioactive decay, until by 7/20/95 it is only slightly above the MDA. Finally, the ^{232}U LSC analysis carried out on 8/1/95 shows no interference. Since a daughter grows in a solution of its parent with its own half-life, the decay of ^{224}Ra is also proof that any ^{228}Th activity is below the MDA of the ^{224}Ra.

Eluted Species Parameter Fitting

The results of the analysis are summarized in Tables 12, 13 and 14 for the eluted species. The tables contain fitted porosity, dispersion and retardation values, and calculated values of partition coefficient, k_d and dispersivity, α. Also listed are values of the root mean squared error (RMS), between the measured and fitted effluent concentrations. RMS provides a method to compare the goodness-of-fit of the two models to a single breakthrough curve. The smaller the RMS, the better the fit. However, since RMS is a function of the absolute effluent activity, it should not be used to compare the fit between tests.

Most parameter fits were straightforward and require little explanation. The following paragraphs list a qualitative assessment of the data fits, and discusses the tests that experienced problems in their analysis. Plots of the curve fits are contained in Appendix B and listed in Appendix C.

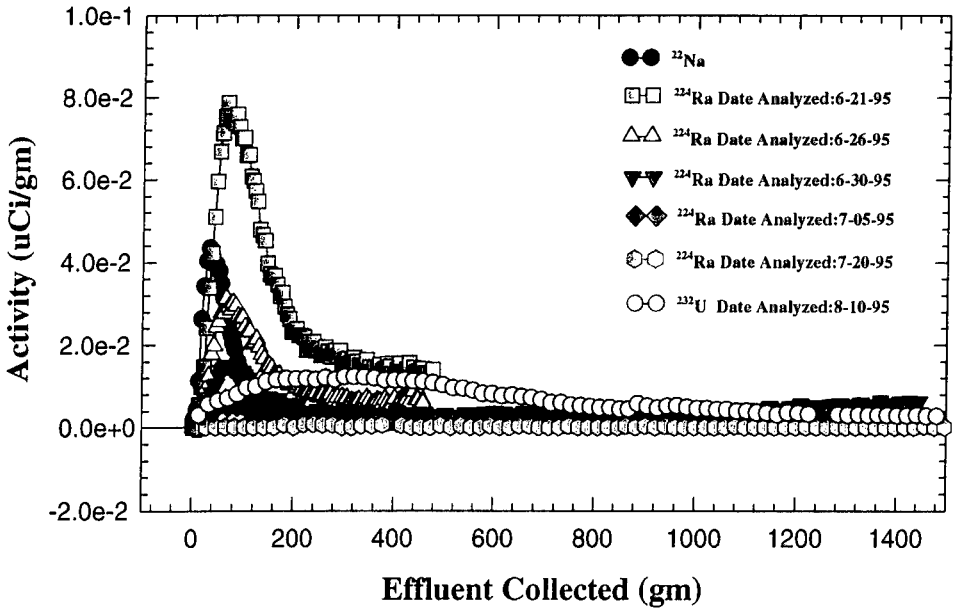

Figure 11. Thorium 228 daughters in Test C2.

TEST A1

Test A1 measured core porosity with ^{3}H. The measured ^{3}H effluent concentrations were well matched by both single and dual porosity models, with the dual model fitting the data slightly better.

TEST A2

Test A2 was intended to image ^{22}Na by tomography. The equipment was unable to maintain a steady 0.02 ml/min flow rate and after much difficulty the test was terminated. No useful results were obtained.

TEST A3

Test A3 was similar to Test A1 except it was carried out at one-fifth the flow rate, 0.1 ml/min. Both single and dual porosity models fit the data well, but provided lower porosity when compared to Test A1. The single porosity yielded 1.9% for Test A3 contrasted to 4.4% for Test A1 while the dual porosity yielded 1.5% for Test A3 versus 3.2% for Test A1. The lower porosity estimated by Test A3 compared to Test A1 may indicate that the pore structure changed, resulting in fewer pores transporting the solute. This may have resulted from fines relocating and blocking pores, or the degassing of the pore water and subsequent formation of air bubbles within the core.

Table 12. Parameter fitting for conservative solutes.

Test	Isotope	Single Porosity				Dual Porosity				
		ϕ %	D cm^2/s	α cm	RMS nCi/ml	ϕ_f %	^1D_f cm^2/s	α cm	B cm	RMS nCi/ml
A1	^3H	4.4	0.00372	0.3	0.20	3.2	0.00147	0.93	0.89	0.04
A2	^{22}Na			*Test*		*Failed*				
A3	^3H	1.9	0.00489	9.2	0.07	1.5	0.00465	7.06	6.00	0.06
A4	^{22}Na	2.1	0.00288	6.0	6.58	2.2	0.0025	5.45	13.5	11.4
B1	^3H	19.9	0.00134	26.4	0.03	7.9	0.00092	7.20	1.27	0.02
B2	^{22}Na	9.2	0.00118	10.7	1.01	6.0	0.00081	4.81	1.74	0.39
B3	^{22}Na	9.2	0.00142	12.9	0.69	4.9	0.00010	0.49	1.50	0.38
B4	^{22}Na	7.9	0.00207	16.2	6.90	8.0	0.002	15.8	12.0	8.34
B5	^{22}Na	7.9	0.00103	16.1	6.54	8.0	0.002	31.7	12.0	8.55
B6			*BTC*	*not*	*useable*	*due to*	*tailing*	*from*	*B5*	
B7	^{22}Na	13.0	0.00870	22.4	0.45	5.6	0.00656	7.25	0.58	0.12
B8	^{22}Na	8.3	0.00675	11.1	2.94	*Unable*	*to*	*fit*		

[1] Value of matrix retardation fixed at 1 for nonsorbing tracers.

Table 12. Parameter fitting for conservative solutes (continued).

Test	Isotope	Single Porosity				Dual Porosity				
		ϕ %	D cm^2/s	α cm	RMS nCi/ml	ϕ_f %	^2D_f cm^2/s	α cm	B cm	RMS nCi/ml
C1	^3H	3.2	0.00057	1.8	7.42	2.2	0.00030	0.65	1.21	6.08
C1	^{22}Na	2.5	0.00038	0.9	0.02	2.6	0.00038	0.98	8.33	0.03
C2	^{22}Na	8.5	0.00266	22.4	2.37	3.7	0.00439	16.1	2.70	1.45
C3	^{22}Na	3.3	0.00204	6.7	2.44	*Unable*	*to*	*Fit*		
C4	^{22}Na	4.8	0.00133	6.3	4.65	1.3	0.00033	0.42	0.57	1.89
C5	^{22}Na	4.3	0.00250	10.7	1.19	1.6	0.00206	3.32	1.14	0.92
C6	^{22}Na	5.9	0.00170	9.9	2.63	1.5	0.00096	1.40	0.79	1.33
C7	^{22}Na	2.0	0.00155	3.0	2.63	1.9	0.00151	2.86	8.50	2.62
D1	^3H[3]	14.3	0.00055	7.8	0.07	7.3	0.00047	3.40	0.78	0.04
D2	^{22}Na	8.0	0.00058	4.6	0.43	5.2	0.00046	2.37	1.05	0.21
D3	^{22}Na	8.9	0.00053	4.7	0.44	5.4	0.00042	2.25	0.88	0.42
D4	^{22}Na	9.7	0.00054	5.2	1.60	3.5	0.00035	1.21	0.67	0.81
D5	^{22}Na	9.7	0.00054	5.2	0.35	5.6	0.00034	1.89	0.76	0.31
D6	^{22}Na	9.6	0.00045	8.6	0.59	5.4	0.00020	2.14	0.73	0.60
E1	^{22}Na	18.3	0.00024	4.3	0.23	15.5	0.00022	3.38	1.46	0.15
E2	^{22}Na	23.8	0.00029	6.8	0.36	15.0	0.00025	3.71	0.88	0.37

[2] Value of matrix retardation fixed at 1 for nonsorbing tracers.
[3] Fit is for Co = 0.011 uCi/ml

Table 13. Parameter Fitting for U retardation.

Test	Single Porosity			Dual Porosity						
				Without Advective Retardation			With Advective Retardation			
	R	k_d cm^3/gm	RMS nCi/ml	R_m	k_d cm^3/gm	RMS nCi/ml	R_f	R_m	k_d cm^3/gm	RMS nCi/ml
B3	4.50	0.13	1.36	68.8	3.1	4.99	1.14	65.4	3.0	4.95
B6	6.40	0.18	1.24	*Unable*	*to*	*fit*	*Unable*	*to*	*fit*	
B7	3.70	0.15	0.30	63.6	2.9	2.19	4.35	1.00	0	0.48
C2	13.9	0.46	1.69	4577	210	3.52	16.2	4287	200	3.09
C5		*BTC*	*not*	*useable*	*due to*	*low*	*spike*	*activity*		
C7	3.23	0.02	2.28	2975	140	5.32	2.64	486	22	2.11
D5	18.1	0.69	0.78	1500	69	2.22	12.6	675	30	0.54
D6	10.1	0.36	1.42	332	15	7.22	9.77	71.5	3.2	2.08
E1	1.80	0.06	1.30	236	11	3.27	1.84	29.3	1.3	1.14

Table 14. Parameter fitting for Np retardation.

Test	Single Porosity			Dual Porosity						
				Without Advective Retardation			With Advective Retardation			
	R	k_d cm^3/gm	RMS nCi/ml	R_m	k_d cm^3/gm	RMS nCi/ml	R_f	R_m	k_d cm^3/gm	RMS nCi/ml
A4				*BTC*	*Not*	*Usable*				
B2				*BTC*	*Not*	*Usable*				
C4				*BTC*	*Not*	*Usable*				
C5*	22.2	0.38	1.75	2648	120	2.42	20.6	587	27	0.94
C6	77.5	1.88	0.37	5667	260	2.01	56.2	700	32	0.26
C7	75.1	0.62	2.28	*Unable*	*to*	*fit*	8.90	17421	800	1.71
D2	29.7	0.96	0.04	*Unable*	*to*	*fit*	18.3	10395	480	0.04
D4	37.0	1.46	0.25	5921	271	0.58	25.6	1095	50	0.07

*Test C5 results not considered reliable. See text for details.

TEST A4

A ^{22}Na and ^{239}Np spike was use in Test A4 to measure the latter's retardation. Sodium eluted and was well fit by both models. Porosity values were close to A3 fits. ^{239}Np was retarded enough that it did not elute at significant activities before its decay.

TEST B1

Fitting the ^{3}H spike for Test B1 yielded a good fit by the dual porosity model and a poor fit with the single porosity model. The single porosity fit yielded a porosity of 20%, which is considerably larger than the estimated total porosity of 15%.

TEST B2

Similar to A4, B2 spiked ^{22}Na and ^{239}Np to measure the latter's retardation. Sodium elution was fitted by both models with the dual porosity yielding a clearly better fit. Porosity values were lower than B1 fits, with the single porosity calculated as 9.2% and dual porosity as 6.0. ^{239}Np was retarded enough that it did not elute at useable activities before it decayed.

TEST B3

Test B3's objective was to measure uranium and thorium retardation. Thorium did not elute. As in the previous B tests, ^{22}Na tracer was fit better by the dual porosity model with values slightly lower than the B2 fits. The uranium eluted and was well fitted by the single porosity model with R = 4.5. In the dual models, measured activities were poorly fit if no advective retardation was assumed and adequately fitted if it was allowed.

TEST B4

A step injection of ^{22}Na was used in Test B4 for tomography imaging. Effluent fitting calculated good fits by both models with a single porosity value of 7.9% and a dual estimate of 8.0%.

TEST B5

Test B5 was similar to B4 with the exception that the flow rate was reduced to 0.05 ml/min. Both the single porosity fit of 7.9% and the dual porosity fit of 8.1% were consistent with B4.

TEST B6

Uranium retardation was measured at the low flow rate of 0.05 ml/min in Test B6. A high ^{22}Na tail activity from Test B5 was superimposed on the B6 effluent, which prevented a good fit by either pore model. Therefore, uranium retardation was fit using B5 parameters. The uranium R factor was 6.4 for the single porosity model. The dual porosity model was unable to fit the breakthrough curve.

TEST B7

Flow was increased in Test B7 to 0.5 ml/min, and a ^{22}Na and ^{232}U spike injected. The sodium effluent was fit well by both models, with the dual porosity estimate somewhat better. The estimated porosities were substantially different at 13.4% and 0.6% for the single and dual porosity models respectively. Uranium retardation at R = 3.7 was slightly less than previous tests.

TEST B8

Continuing at 0.5 ml/min, Test B8 was a step injection of ^{22}Na. A porosity of 8.3% was calculated by the single porosity fit, which is similar to B4 and B5 values. Surprisingly, the dual porosity model could not fit the measured effluent at the high flow rate.

TEST C1

Test C1 was a combined ^{3}H and ^{22}Na spike intended to test the suitability of using sodium as a conservative tracer in the Culebra cores. The two solutes eluted very similarly and provided similar fits by both pore models. With the single porosity model, ^{3}H provided a porosity of 3.2% while ^{22}Na yielded a value of 2.5%. That variation is within the fitting error. The dual porosity fitting computed fracture porosity of 2.2% and 2.6% for ^{3}H and ^{22}Na respectively.

TEST C2

Thorium and uranium retardation were measured in Test C2. Thorium did not elute above the MDA. ^{22}Na was fit well by both models. ^{232}U was well fitted by the single porosity model and the dual porosity model with fracture retardation. The no fracture retardation model provided a poor fit.

TEST C3

The objective of Test C3 was to measure ^{241}Pu and ^{241}Am retardation. Neither solute eluted. As for the ^{22}Na tracer, the dual porosity fit could not be completed because the fracture spacing, *B*, became so large that computer memory was exhausted. The magnitude of *B* determines the size of the matrix calculation grid.

TEST C4

^{239}Np and ^{22}Na were injected in Test C4. While measurable activities of ^{239}Np were detected in the effluent, the data were inadequate due to the rapid decay of the isotope. The ^{22}Na data provided porosity fits of 4.8% for the single and 1.3% for the fractures, with the fracture fit being noticeably better.

TEST C5

ERDA 6 brine was used in Test C5 to determine the impact on neptunium, uranium and thorium retardation resulting from the intrusion of a Salado brine into the Culebra. ^{228}Th did not elute above the MDA. ^{232}U eluted at activities too low to provide useful fitting data due to the low spike activity. The eluted ^{22}Na was fit somewhat better by the dual than the single porosity model. ^{239}Np eluted and was well fitted by the dual porosity model with advective retardation, but poorly fit by the other methods. Unfortunately, Test C5 results for ^{239}Np must be disregarded. As detailed by Brown (1995-1996, page 79), the ^{239}Np sample spike for the test experienced difficulties in preparation at ITRI. There is convincing evidence that the measured effluent ^{239}Np was not in solution, but instead was a nonrepresentative silicate colloid. It formed during the separation of the ^{239}Np from its parent, ^{243}Am, due to the use of concentrated HF acid in glass containers. The problem occurred only in Test C5 and did not affect the other ^{239}Np tests reported here.

TEST C6

Test C6 replicated C4 with the exception of using a higher ^{239}Np activity. Both ^{22}Na and ^{239}Np fittings were similar to Test C5 with the exception that neptunium had a larger single porosity retardation of 78.

TEST C7

Salado brine was again used in Test C7 to replicate C5. ^{22}Na elution yielded similar parameters as C5. Thorium did not elute. Neptunium exhibited retardation of 75 for the single porosity model, very close to the C6 retardation.

TEST D1

Test D1 measured the core porosity by ^{3}H. A single porosity fit gave could only be obtained if the concentration is left as a free parameter. This may be due to an incorrect input spike concentration. A very good fit is obtained for a porosity of 14.3% and an input spike concentration roughly half of that specified. That fitting is reported here and used in the dual porosity fit.

TEST D2

Uranium, thorium and neptunium retardation were measured in Test D2. ^{22}Na was well fit by both models with a single porosity fit of 8% and a fracture porosity of 5.2%. Neptunium was fit adequately by the dual porosity models, but not the single.

TEST D3

Test D3 injected ^{22}Na, ^{241}Am and ^{241}Pu. As in Test D2, ^{22}Na was well fit by both models with about the same porosity. The actinides did not elute above the MDA.

TEST D4

A replicate of Test D2 was carried out in D4. ^{22}Na fits were similar, while ^{239}Np retardation was somewhat lower.

TEST D5

Uranium retardation was measured in Test D5. Porosity values for ^{22}Na fits similar to previous tests with 9.7% and 5.6% for the single and dual porosity models respectively. ^{232}U retardation was fit at the relatively high values of 18 with single-porosity and 1500 with dual porosity without fracture retardation.

TEST D6

The flow rate was decreased to 0.05 ml/min in Test D6, and ^{232}U injected. Estimated porosity was similar to D5, but ^{232}U retardation was only about 60% the value fitted for Test D5.

TEST E1

Test E1's objective was porosity estimates, and ^{232}U and ^{239}Np retardation. Porosity fits were relatively high, 18.3% as fitted by the single porosity model. Uranium retardation was fit well by all three models, with the lowest R value estimates of any test.

TEST E2

Test E2 provided similar porosity estimates as E1. The injected ^{241}Am and ^{241}Pu did not elute above the MDA.

Single vs. Dual Porosity Models

It is possible to compare the applicability of the two porosity models by two steps. First, comparison of the fitted parameter values of ϕ and ϕ_f for the conservative solutes show that the dual porosity model provides ϕ_f values only slightly less than the single porosity model. This indicates that the "advective porosity" of the dual porosity model is largely the same void space as the porosity of the single model.

Second, a statistical test of the single and dual porosity models' ability to fit the effluent curves can be carried out using the Root Mean Squared error (RMS) between the measured and fitted effluent breakthrough curves for the conservative tracers. Two Student t, paired two sample for means tests were performed to determine if there is significant difference between the RMS of the single and dual porosity models. The two data sets tested where,

$$D_R = RMS_{single} - RMS_{dual} \tag{14}$$

and

$$D_N = (RMS_{single} - RMS_{dual}) / Injected\ Activity \tag{15}$$

Where D_R is the raw difference between the fits and D_N is the difference normalized by the injection activity. The hypotheses tested were:

$$\text{Ho: } D_R = 0 \tag{16}$$

$$\text{Ha: } D_R \neq 0 \tag{17}$$

and

$$\text{Ho: } D_N = 0 \tag{18}$$

$$\text{Ha: } D_N \neq 0 \tag{19}$$

The analysis was performed with Microsoft Excel. Both tests failed to reject Ho. Therefore, it can be concluded there is no significant difference between the two fittings. It is apparent the dual porosity model is providing essentially a single porosity fit to the data.

Test Comparisons

Figure 12 presents are fitted single porosity values from the column experiments. Each fit is labeled by tracer and any special condition of brine, injection mode or flow rate. Tests not labeled were carried out at the standard flow rate with AIS brine. Also shown is the estimated total porosity for each core. Figures 13 and 14 show fitted uranium and neptunium retardation respectively.

The variability of conditions between the tests was relatively large, which makes their direct comparison difficult. Likewise some of the duplicate tests do not provide comparison due to testing or fitting problems on one of the replicates. Thus, any difference between flow rates or brine type is subject to considerable ambiguity. Therefore, the following two paragraphs are only observations and not substantiated results.

FLOW RATE DEPENDENCIES

No clear trend can be seen in relation to flow rate. Porosity estimates in B core are similar in B4, B5 and B8 which span an order of magnitude in flow rate. Similarly, D6 and D5 have equivalent porosity fittings. In regards to uranium retardation, in B core, the high flow Test B7 had the lowest R value, while in D core the lower flow rate Test D6 had the lower R. If flow rate dependencies are present they are within the parameter fitting errors.

BRINE EFFECTS

As would be expected, brine type had no impact on core porosity estimates. Test C5 and C7 had similar porosity fittings as the other Core C tests. Comparing Tests C2 and C7 indicates that uranium retardation was reduced by a factor of four. However, comparing Tests C6 and C7 shows neptunium retardation is near constant. Considering that all the R values are near the range display by other tests, no conclusion is possible.

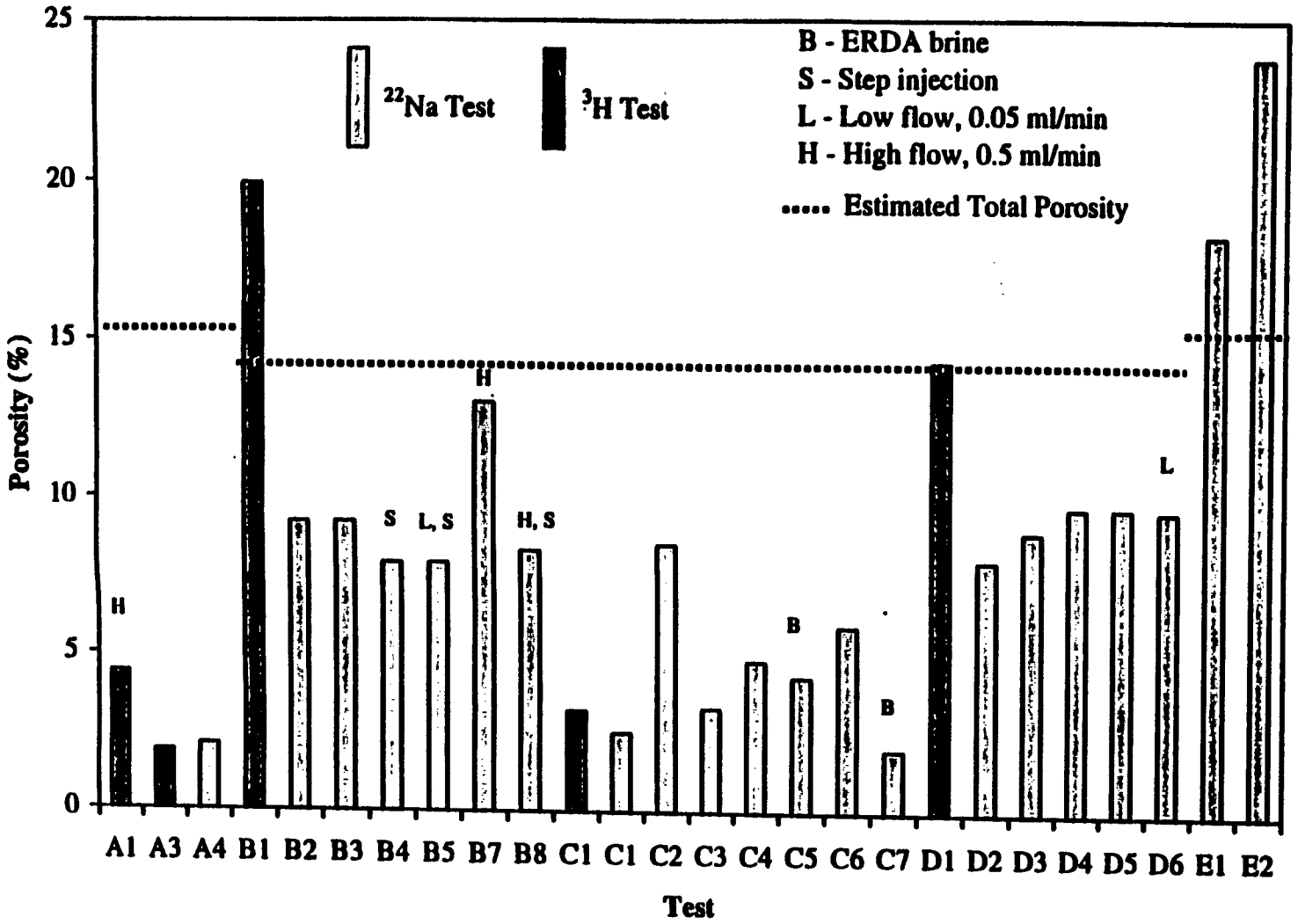

Figure 12. Porosity computed by conservative solute fittings.

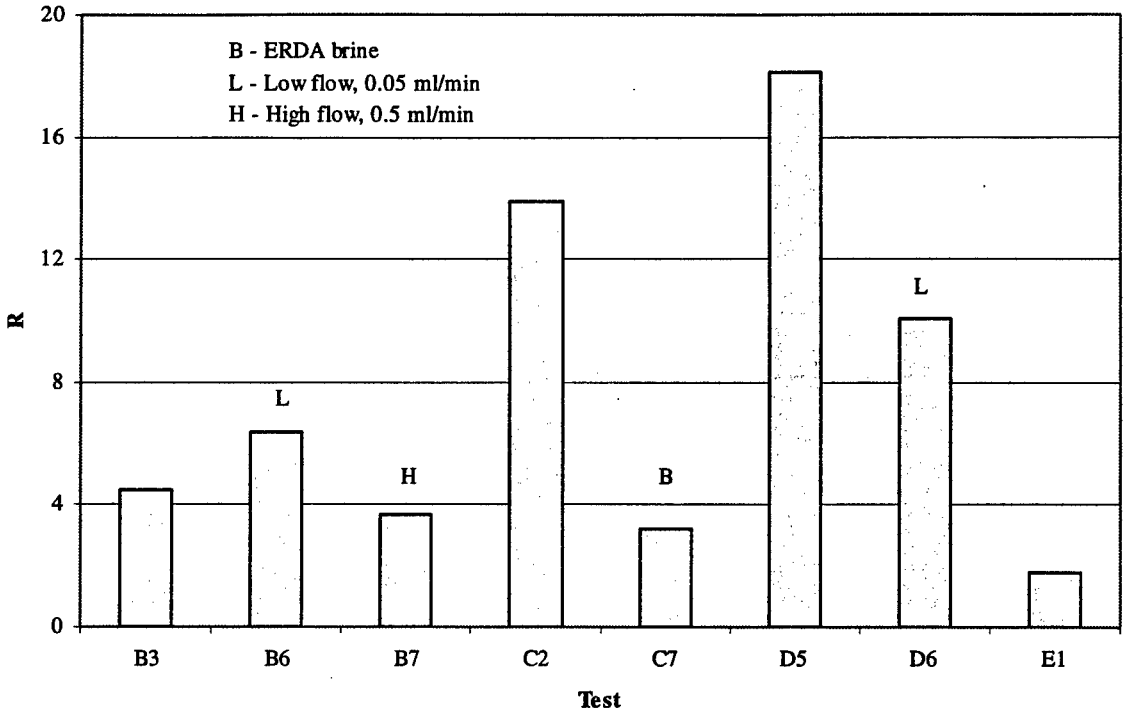

Figure 13. Fitted uranium retardation.

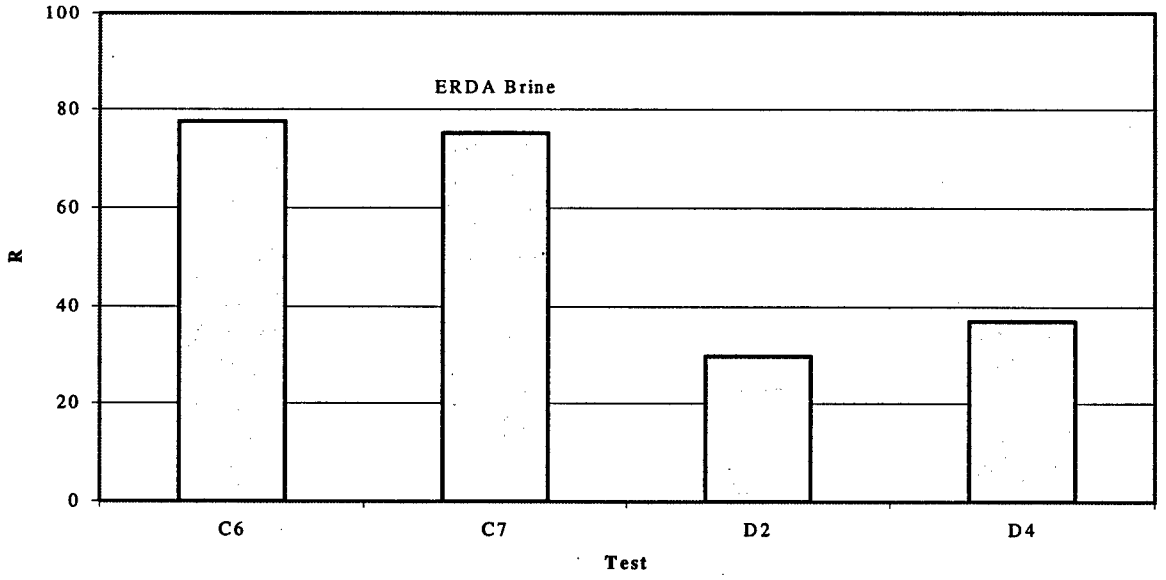

Figure 14. Fitted neptunium retardation.

Noneluted Species Minimum Retardation

Table 15 lists the limiting case, minimum R and minimum k_d for the noneluted species. All values were computed using the single porosity model and the procedures detailed earlier in the section Parameter Fitting for Noneluted Species. Effluent volumes where estimated based on Lucero (1997). For C Core, effluent volumes were projected to its September 4, 1997 termination date. Minimum R values were 520 to 18,000 for ^{241}Am based on the LSC MDA and an injection concentration equal to the solubility. Minimum R values were 9.1 to 47 for ^{228}Th, and 800 to 38,000 for ^{241}Pu. The range of these minimum R values is a function of the individual test conditions and does not indicate data uncertainty. The lower values are provided by the shorter duration tests, and nothing in the results of the eluting actinides would indicate that those tests will behave any differently for the noneluting species. Thus, it is recommended that the upper range value be used if a single R value is needed.

Table 15. Lower Bounds on Retardation for Noneluting Species.

Test	Element	Effluent Volume (L)	Limiting Case	Lower Limit of R	Lower Limit of k_d
C3	Am	71.4	B	18,000	254
D3	Am	48.2	B	2,800	35
E2	Am	15.0	B	520	53
C3	Pu	71.4	B	38,000	540
D3	Pu	48.2	B	3,700	140
E2	Pu	15.0	B	800	79
B3	Th	18	A	23	0.84
C2	Th	71.1	A	47	1.6
C5	Th	68.1	A	27	0.46
D2	Th	46	A	9.1	0.27

Relation of Transport Parameters to Other Estimates

The cores were estimated to have similar porosity, but fitted values differed greatly. Core E had fitted porosity values (0.18 and 0.24) greater than the estimated 0.15. On the other hand, all tests of A, B, C, and D Cores provided porosity values less than expected. The average of seven ^{22}Na fits on C core was 0.042 and the six D Core fits averaged 0.092. These results indicate that C and D Cores experienced significant preferential flow. The large fracture in Core C is possibly the cause of its preferential flow. The cause of the preferential flow in Core D is not believed to be a large fracture. Instead, visual examination suggests that any high permeability paths occur in the chalky material along bedding planes and possibly at connected vugs. Such paths are probably not continuous over the cores, but instead provide a loose network where flow converges and diverges in and out of the paths. The lack of continuous paths explains why the effluent curves are still well fitted by the single porosity model.

Fitted hydrodynamic dispersion coefficients were an order of magnitude greater than for uniform packed columns. This is shown using the classical Peclet diagram (Fetter, 1993, p. 54-56). The single porosity fit yielded dispersion coefficients, D for ^{22}Na of 0.0002 to 0.001 cm^2/s

with an average of 0.0006 cm^2/s. The aqueous molecular diffusion coefficient, D_m for NaCl is approximately 1.5 x 10^{-5} cm^2/s (Weast, 1985, Diffusion Coefficients of Strong Electrolytes). Taking the ratio of the average,

$$\frac{D}{D_m} = \frac{0.0006}{0.000015} = 40 \tag{20}$$

For packed columns that ratio would predict a Peclet number of 20, and falls in a region where advective dispersion dominates transport. The Peclet number is defined as the ratio of advective transport to diffusion,

$$P = \frac{vd}{D_m} \tag{21}$$

where d is a characteristic length normally defined as the mean grain diameter. The seepage velocity, v is given by Equation 13.

Solving Eqs. 21 and 13 for d yields,

$$d = \frac{PD_m A\phi}{Q} \tag{22}$$

Letting P = 20, D_m = 0.000015 cm^2/s, A = *165* cm^2, Q = 0.0017 cm^3/s and assuming ϕ = 0.15, Eq. 22 yields d = 4 cm. That value is clearly larger than any pore or particle in these cores.

Field scale dispersion is normally defined by the dispersivity, α, given in Equation 12. Table 12 lists the computed dispersivity values for each test that ranges from 0.3 to 26 cm. Gelhar (1986) has shown that field dispersivity can be estimated at 0.1 the transport distance. These experiments with 10 cm and 50 cm long cores had dispersivity of 0.09 to 0.8 the transport distance clearly indicating non-uniform advection. That is, flow in the cores is dominated by the spatially heterogeneous conductivity. Since only a portion of the pore space was accessed by the solute during the experiment, R and k_d values measured here are probably smaller than the core's full potential.

CONCLUSIONS

Two actinides eluted from the columns, U and Np. Retardation is lower for uranium, with R values of 2 to 18. Neptunium shows greater retardation and has R values of 30 to 78. The quoted retardation factors are for the single porosity model.

There is little evidence of dual porosity effects in the effluent curves, but porosity estimates and fitted dispersivity values indicate that significant preferential flow occurred in all cores. The time and space dimensions of these experiments place them at the lower end of the spectrum of Damkohler numbers (Holt, 1997). Thus, the evidence of preferential flow is to be expected. Since only a portion of the pore space was accessed by the solute during the experiment, R and k_d values measured here are probably smaller than the core's full potential.

Three actinides did not elute from the columns, Pu, Am and Th. Theoretical analysis shows that retardation is very high for plutonium and americium. Thorium is not yet well constrained, due to a high MDA. Minimum R values were 520 to 18,000 for Am, 9.1 to 47 for Th, and 800 to 38,000 for Pu. The range of these minimum R values is a function of the individual test conditions and does not indicate data uncertainty or measurement error.

No clear trend is apparent with regard to flow rate dependencies. Use of the Salado brine, ERDA 6, did not produced a significant change in actinide retardation compared to AIS.

REFERENCES

ASTM D412. 1997. *Standard Test Methods for Vulcanized Rubber and Thermoplastic Rubbers and Thermoplastic Elastomers - Tension.* ASTM D412. Philadelphia, PA: American Society for Testing and Materials.

ASTM D624. 1991 (Reapproved 1996). *Standard Test Method for Tear Strength of Convential Vulcanized Rubber and Thermoplastic Elastomers.* ASTM D624. Philadelphia, PA: American Society for Testing and Materials.

Bertram-Howery, S.G., M.G. Marietta, R.P. Rechard, P.N. Swift, D.R. Anderson, B.L. Baker, J.E. Bean, Jr., W. Beyeler, K.F. Brinster, R.V. Guzowski, J.C. Helton, R.D. McCurley, D.K. Rudeen, J.D. Schreiber, and P. Vaughn. 1990. *Preliminary Comparison with 40 CFR Part 191, Subpart B for the Waste Isolation Pilot Plant, December 1990.* SAND90-2347. Albuquerque, NM: Sandia National Laboratories.

Brown, G.O. 1995-1996. "WIPP Lab Notebook. WBS: 1.1.10.3.3. #100495." Albuquerque, NM: Sandia National Laboratories. (Copy on file in the Sandia WIPP Central Files, Sandia National Laboratories, Albuquerque, NM in records package WPO#40975.)

Brush, L.H. 1990. *Test Plan for Laboratory and Modeling Studies of Repository and Radionuclide Chemistry for the Waste Isolation Pilot Plant.* SAND90-0266. Albuquerque, NM: Sandia National Laboratories.

Brush, L.H. 1996a. "Revised Free-Solution Tracer Diffusion Coefficients ($D_{sol}s$) for Dissolved Pu, Am, U, Th, Np, Cm, and Ra in Boreholes and the Culebra for Use in PA Calculations to Support the WIPP CCA." Memorandum to M.S. Tierney, dated May 11, 1996. Albuquerque, NM: Sandia National Laboratories. (Copy on file in the Sandia WIPP Central Files, Sandia National Laboratories, Albuquerque, NM as WPO#38510; Reprinted in Appendix D.)

Brush, L.H. 1996b. "Ranges and Probability Distributions of Kds for Dissolved Pu, Am, U, Th, and Np in the Culebra for the PA Calculations to Support the WIPP CCA." Memorandum to M.S. Tierney, dated June 10, 1996. Albuquerque, NM: Sandia National Laboratories. (Copy on file in the Sandia WIPP Central Files, Sandia National Laboratories, Albuquerque, NM as WPO#38801; Reprinted in Appendix D.)

Budge, K. 1996. "Column: A Computer Program for Fitting Model Parameters to Column Flow Breakthrough Curves, Version 1.3." Albuquerque, NM: Sandia National Laboratories. (Copy on file in the Sandia WIPP Central Files, Sandia National Laboratories, Albuquerque, NM as WPO#37867.)

Craft, C.C., and M.D. Siegel. 1997. "Additional Calculations of Solubility-Limited Concentrations of Actinides for Injection Spikes Used in WIPP Core Column Experiments at Sandia National Laboratories." Memorandum to D. Lucero, dated June 9, 1997. Albuquerque, NM: Sandia National Laboratories. (Copy on file in the Sandia WIPP Central Files, Sandia National Laboratories, Albuquerque, NM in records package WPO#40975; Reprinted in Appendix D.)

Dosch, R.G. 1980. *Assessment of Potential Radionuclide Transport in Site-Specific Geologic Formations.* SAND79-2468. Albuquerque, NM: Sandia National Laboratories.

Dosch, R.G. 1981. *Solubility and Sorption Characteristics of Uranium(VI) Associated with Rock Samples and Brines/Groundwaters from WIPP and NTS.* SAND80-1595. Albuquerque, NM: Sandia National Laboratories.

Dosch, R.G., and A.W. Lynch. 1978. *Interaction of Radionuclides with Geomedia Associated with the Waste Isolation Pilot Plant (WIPP) Site in New Mexico.* SAND78-0297. Albuquerque, NM: Sandia National Laboratories.

Fetter, C.W. 1993. *Contaminant Hydrogeology.* New York, NY: Macmillan Publishing Company.

Gelhar, L.W. 1986. "Stochastic Subsurface Hydrology from Theory to Applications," *Water Resources Research.* Vol. 22, no. 9, 135S-145S.

Geotech. 1992. "Analytical Report to F. Gelbard, Project 6S0007000." Report dated April 15, 1992. Grand Junction, CO: Chem-Nuclear Geotech Analytical Laboratory (Vol. 1 on file in the Sandia WIPP Central Files, Sandia National Laboratories, Albuquerque, NM in WPO#48955.)

Heath, C.E. 1995. "WIPP Lab Notebooks. WBS: 1.1.5.1.5. #012795." Albuquerque, NM: Sandia National Laboratories. (Copy on file in the Sandia WIPP Central Files, Sandia National Laboratories, Albuquerque, NM in records package WPO#40975.)

Helton, J.C., J.W. Garner, R.D. McCurley, and D.K. Rudeen. 1991. *Sensitivity Analysis Techniques and Results for Performance Assessment at the Waste Isolation Pilot Plant.* SAND90-7103. Albuquerque, NM: Sandia National Laboratories.

Helton, J.C., J.W. Garner, R.P. Rechard, D.K. Rudeen, and P.N. Swift. 1992. *Preliminary Comparison with 40 CFR Part 191, Subpart B for the Waste Isolation Pilot Plant, December 1991. Volume 4: Uncertainty and Sensitivity Analysis Results.* SAND91-0893/4. Albuquerque, NM: Sandia National Laboratories.

Holt, R.M. 1997. *Conceptual Model for Transport Processes in the Culebra Dolomite Member, Rustler Formation.* SAND97-0194. Albuquerque, NM: Sandia National Laboratories.

Holt, R.M., and D.W. Powers. 1990. *Geologic Mapping of the Air Intake Shaft at the Waste Isolation Pilot Plant.* DOE-WIPP 90-051. Carlsbad, NM: Westinghouse Electric Corporation. (Available from the National Technical Information Service, Springfield, VA as DE91017780/XAB.)

Hsieh, H.T., G.O. Brown, M.L. Stone, and D.A. Lucero. 1997. "Measurement of Porous Media Component Content and Heterogeneity Using Gamma Ray Tomography," *Water Resources Research.* SAND96-2898J. Albuquerque, NM: Sandia National Laboratories. (Copy on file in the Sandia WIPP Central Files, Sandia National Laboratories, Albuquerque, NM as WPO#43583.)

Kelley, V.A., and G.J. Saulnier, Jr. 1990. *Core Analyses for Selected Samples from the Culebra Dolomite at the Waste Isolation Pilot Plant Site.* SAND90-7011. Albuquerque, NM: Sandia National Laboratories.

Lucero, D.A. 1995-1996. "WIPP Lab Notebooks." Multiple volumes. Albuquerque, NM: Sandia National Laboratories. (Copy on file in the Sandia WIPP Central Files, Sandia National Laboratories, Albuquerque, NM in records package WPO#40975.)

Lucero, D.A. 1997. "Memo of Record for Column Effluent Times." Memorandum to G. Perkins, dated February 3, 1997. Albuquerque, NM: Sandia National Laboratories. . (Copy on file in the Sandia WIPP Central Files, Sandia National Laboratories, Albuquerque, NM in records package WPO#40975; Reprinted in Appendix D.)

Lucero, D.A., F. Gelbard, Y.K. Behl, and J.A. Romero. 1995. "Test Plan for Laboratory Column Experiments for Radionuclide Adsorption Studies of the Culebra Dolomite Member of the Rustler Formation at the WIPP Site." Test Plan, TP 95-03. Albuquerque, NM: Sandia National Laboratories. (Copy on file in the Sandia WIPP Central Files, Sandia National Laboratories, Albuquerque, NM as WPO#22640.)

Lucero, D.A., Y.K. Behl, G.O. Brown, K.G. Budge, M. Dunn, A.J. Francis, J.B. Gillow, and H.W. Papenguth. 1996. "Laboratory Evaluation of Colloid Transport Under Simulated Subsurface Conditions at the Waste Isolation Pilot Plant (WIPP): 2. Large-Scale-Intact-Core Column Flow Experiments," *Experimental & Modeling Studies of Radionuclide Speciation in Real Systems.* SAND96-2741J. Albuquerque, NM: Sandia National Laboratories. (Copy on file in the Sandia WIPP Central Files, Sandia National Laboratories, Albuquerque, NM as WPO#42864.)

Lynch, A.W., and R.G. Dosch. 1980. *Sorption Coefficients for Radionuclides on Samples from the Water-Bearing Magenta and Culebra Members of the Rustler Formation.* SAND80-1064. Albuquerque, NM: Sandia National Laboratories.

Mackay, D.M., D.L. Freyberg, P.V. Roberts, and J.A. Cherry. 1986. "A Natural Gradient Experiment on Solute Transport in a Sand Aquifer 1. Approach and Overview of Plume Movement," *Water Resources Research.* Vol. 22, no. 13, 2017-2029.

Meigs, L.C., R.L. Beauheim, J.T. McCord, Y.W. Tsang, and R. Haggerty. 1997. "Design, Modelling, and Current Interpretations of the H-19 and H-11 Tracer Tests at the WIPP Site," *Field Tracer Experiments: Role in the Prediction of Radionuclide Migration: Synthesis and Proceeding of an NEA/EC Geotrap Workshop, Cologne, Germany, August 28-30, 1996.* SAND96-2796C. Paris: Nuclear Energy Agency, Organisation for Economic Co-Operation and Development. 157-169.

Mercer, J.W., and R.P. Snyder. 1990. *Basic Data Report for Drillholes H-17 and H-18 (Waste Isolation Pilot Plant—WIPP).* SAND89-0204. Albuquerque, NM: Sandia National Laboratories.

Newton, G.J., M.D. Hoover, and W.E. Bechton. 1995a. "Americium and Neptunium Separation by Ion- Exchange." ITRI SOP 1029. Albuquerque, NM: Inhalation Toxicology Research Institute. (Copy on file in the Sandia WIPP Central Files, Sandia National Laboratories, Albuquerque, NM in records package WPO#40975.)

Newton, G.J., W.E. Bechton, and K.R. Ahlert. 1995b. "Preparation and Transfer of Samples for Brine Penetration Studies." ITRI SOP 1037. Albuquerque, NM: Inhalation Toxicology Research Institute. (Copy on file in the Sandia WIPP Central Files, Sandia National Laboratories, Albuquerque, NM in records package WPO#40975.)

Nitsche, H., K. Roberts, R.C. Gatti, T. Prussin, K. Becraft, S.C. Leung, S.A. Carpenter, and C.F. Novak. 1992. *Plutonium Solubility and Speciation Studies in a Simulant of Air Intake Shaft Water from the Culebra Dolomite at the Waste Isolation Pilot Plant.* SAND92-0659. Albuquerque, NM: Sandia National Laboratories.

Nitsche, H., K. Roberts, R. Xi, T. Prussin, K. Becraft, I. Al Mahamid, H.B. Silber, S.A. Carpenter, R.C. Gatti, and C.F. Novak. 1994. "Long Term Plutonium Solubility and Speciation Studies in a Synthetic Brine," *Radiochimica Acta.* Vol. 66/67, 3-8.

Novak, C.F. 1992. *An Evaluation of Radionuclide Batch Sorption Data on Culebra Dolomite for Aqueous Compositions Relevant to the Human Intrusion Scenario for the Waste Isolation Pilot Plant.* SAND91-1299. Albuquerque, NM: Sandia National Laboratories.

Nowak, E.J. 1980. *Radionuclide Sorption and Migration Studies of Getters for Backfill Barriers.* SAND79-1110. Albuquerque, NM: Sandia National Laboratories.

Parker, J.C., and M.Th. van Genuchten. 1984. *Determining Transport Parameters from Laboratory and Field Tracer Experiments.* Virginia Agricultural Experimental Station Bulletin 84-3. Blacksburg, VA: Virginia Agricultural Experiment Station, Virginia Polytechnic Institute and State University. (Copy on file in the Sandia WIPP Central Files, Sandia National Laboratories, Albuquerque, NM as WPO#44584.)

Public Law 96-164. 1979. *Department of Energy National Security and Military Applications of Nuclear Energy Authorization Act of 1980.* (93 Stat. 1259).

Ramsey, J.L., M.G. Wallace, and H-N. Jow. 1996. "Analysis Package for the Culebra Flow and Transport Calculations (Task 3) of the Performance Assessment Calculations Supporting the Compliance Certification Application (CCA), AP-019." Albuquerque, NM: Sandia National Laboratories. (Copy on file in the Sandia WIPP Central Files, Sandia National Laboratories, Albuquerque, NM as WPO#40516.)

Sewards, T., M.L. Williams, and K. Keil. 1991. *Mineralogy of the Culebra Dolomite Member of the Rustler Formation.* SAND90-7008. Albuquerque, NM: Sandia National Laboratories.

Terra Tek. 1996. "Results of Porosity and Permeability Measurements of VPX 26-11 Core Sample." Letter report to Y. Behl. (Copy on file in the Sandia WIPP Central Files, Sandia National Laboratories, Albuquerque, NM in records package WPO#40975; Reprinted in Appendix D.)

Trauth, K.M., S.C. Hora, R.P. Rechard, and D.R. Anderson. 1992. *The Use of Expert Judgment to Quantify Uncertainty in Solubility and Sorption Parameters for Waste Isolation Pilot Plant Performance Assessment.* SAND92-0479. Albuquerque, NM: Sandia National Laboratories.

U.S. DOE (Department of Energy) and State of New Mexico. 1988. "Agreement for Consultation and Cooperation Between Department of Energy and the State of New Mexico on the Waste Isolation Pilot Plant." Updated April 18, 1988. Albuquerque, NM: U.S. Department of Energy, Albuquerque Operations Office and State of New Mexico. (Copy on file in the Sandia WIPP Central Files, Sandia National Laboratories, Albuquerque, NM as PA#00451.)

U.S. EPA (Environmental Protection Agency). 1993. "40 CFR Part 191 Environmental Radiation Protection Standards for the Management and Disposal of Spent Nuclear Fuel, High-Level and Transuranic Radioactive Wastes; Final Rule," *Federal Register.* Vol. 58, no. 242, 66,398-66,416.

Weast, R.C., ed. 1985. *CRC Handbook of Chemistry and Physics: A Ready-Reference Book of Chemical and Physical Data.* 66th ed. Boca Raton, FL: CRC Press. (Copy of 66th ed. on file in the Sandia WIPP Central Files, Sandia National Laboratories, Albuquerque, NM as WPO#46901.)

Weber, W.J., Jr., P.M. McGinley, and L.E. Katz. 1991. "Sorption Phenomena in Subsurface Systems: Concepts, Models and Effects on Contaminant Fate and Transport," *Water Research.* Vol. 25, no. 5, 499-528.

WIPP Performance Assessment Department. 1992-1993. *Preliminary Performance Assessment for the Waste Isolation Pilot Plant, December 1992. Volumes 1-5.* SAND92-0700/1-5. Albuquerque, NM: Sandia National Laboratories.

Yeh, S. 1993a. "Determination of the Viscosity of Synthetic Culebra Brines in the Temperature Range of 20°C to 30°C, Revised." Memorandum to Fred Gelbard, dated August 13, 1993. Albuquerque, NM: Sandia National Laboratories. (Copy on file in the Sandia WIPP Central Files, Sandia National Laboratories, Albuquerque, NM as WPO#8760.)

Yeh, S. 1993b. "Determination of the Viscosity of Salado Brines in the Temperature Range of 20°C to 35°C, Revised." Memorandum to Fred Gelbard, dated August 13, 1993. Albuquerque, NM: Sandia National Laboratories. (Copy on file in the Sandia WIPP Central Files, Sandia National Laboratories, Albuquerque, NM as WPO#8761.)

APPENDIX A

Activity to Concentration Conversions

Activity to Concentration Conversions

The rate of radioactive disintegration of an isotope is proportional to the time rate of change of its concentration and is described by first order decay (Knoll, 1989, p. 2-3). Expressed in traditional units, the activity of a sample is,

$$A = \frac{\lambda A_v M}{C} \tag{1}$$

where A is the radioactive activity (Ci), λ is the first order decay constant (s^{-1}), A_v is Avogadro's number (6.023×10^{23} atoms/mole), M is the number of moles of the isotope and C is a conversion from disintegration rate to activity (3.7×10^{10} Ci^{-1} s^{-1}). The rate constant is related to the radioactive half-life, $t_{1/2}$ by,

$$\lambda = \frac{\ln(2)}{t_{1/2}} \tag{2}$$

Solving Equations 1 and 2 for the number of moles of the isotope yields the desired result,

$$M = \frac{A C t_{1/2}}{\ln(2) A_v} \tag{3}$$

The mass of isotope can be found by multiplying Equation 3 by the isotope gram-atomic weight w,

$$m = wM \tag{4}$$

where m is the mass in grams. Values of w can be found in Weast (1985, Table of the Isotopes) and $t_{1/2}$ in Kocher (1981). Other sources may give slightly different values. Table A1 presents the results of applying Equations 3 and 4 to the isotopes used in the WIPP column retardation experiments. The half-lives given must be converted to units of seconds before application of Equation 3.

Table A1. Equivalent moles and gram mass to 1 curie of activity.

Isotope	Atomic Weight (gm)	Half Life	Moles per Curie	Grams per Curie
^{3}H	3.02	12.28 y	3.43×10^{-5}	1.03×10^{-4}
^{22}Na	21.99	2.602 y	7.28×10^{-6}	1.60×10^{-4}
^{232}U	232.04	72 y	2.0×10^{-4}	4.7×10^{-2}
^{228}Th	228.04	1.913 y	5.35×10^{-6}	1.20×10^{-3}
^{224}Ra	224.02	3.62 d	2.77×10^{-8}	6.15×10^{-6}
^{241}Am	241.06	432.2 y	1.21×10^{-3}	2.92×10^{-1}
^{241}Pu	241.06	14.4 y	4.03×10^{-5}	9.71×10^{-3}
^{239}Np	239.05	2.355 d	1.80×10^{-8}	4.31×10^{-6}

Appendix A References

Knoll, G.F. 1989. *Radiation Detection and Measurement.* 2nd ed. New York, NY: John Wiley & Sons.

Kocher, D.C. 1981. *Radioactive Decay Data Tables: A Handbook of Decay Data for Application to Radiation Dosimetry and Radiological Assessments.* DOE/TIC-11026. [Oak Ridge, TN]: Technical Information Center, U.S. Department of Energy; Springfield, VA: Available from National Technical Information Service. (Copy on file in the Sandia WIPP Central Files, Sandia National Laboratories, Albuquerque, NM as WPO#49497.)

Weast, R.C., ed. 1985. *CRC Handbook of Chemistry and Physics: A Ready-Reference Book of Chemical and Physical Data.* 66th ed. Boca Raton, FL: CRC Press.

APPENDIX B

Measured and Fitted Break Through Curves

List of Figures

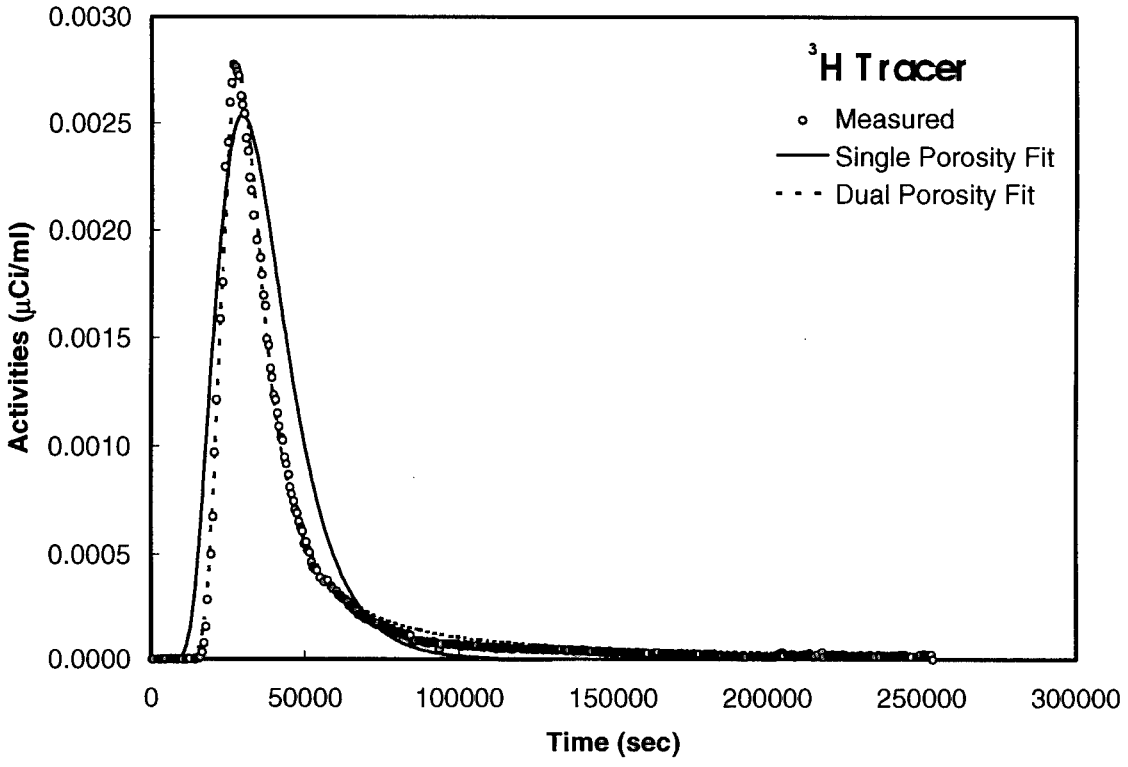

Figure B1. Test A1 measured and fitted ^{3}H effluent concentrations.

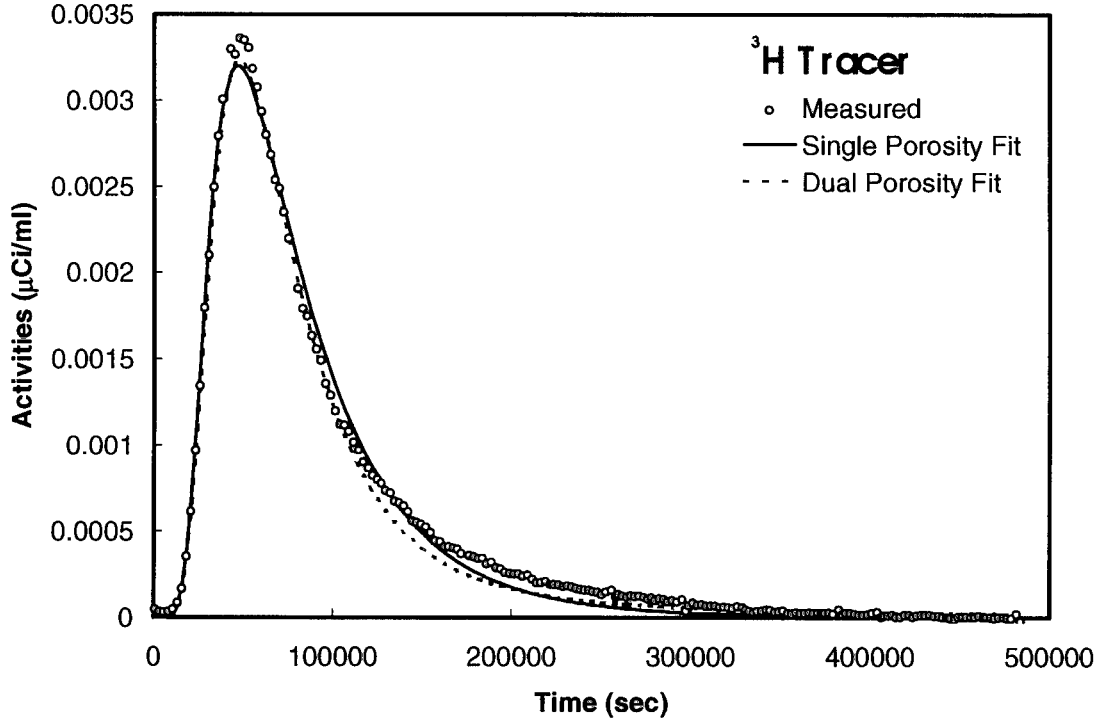

Figure B2. Test A3 measured and fitted ^{3}H effluent concentrations.

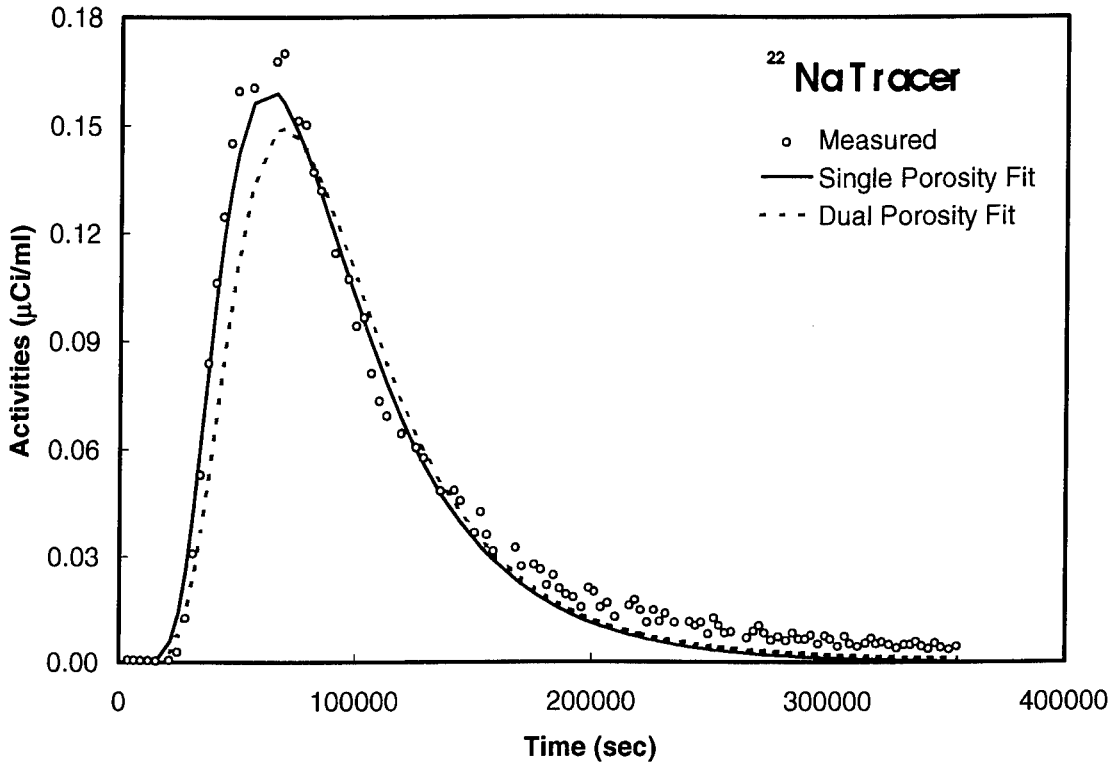

Figure B3. Test A4 measured and fitted ^{22}Na effluent concentrations.

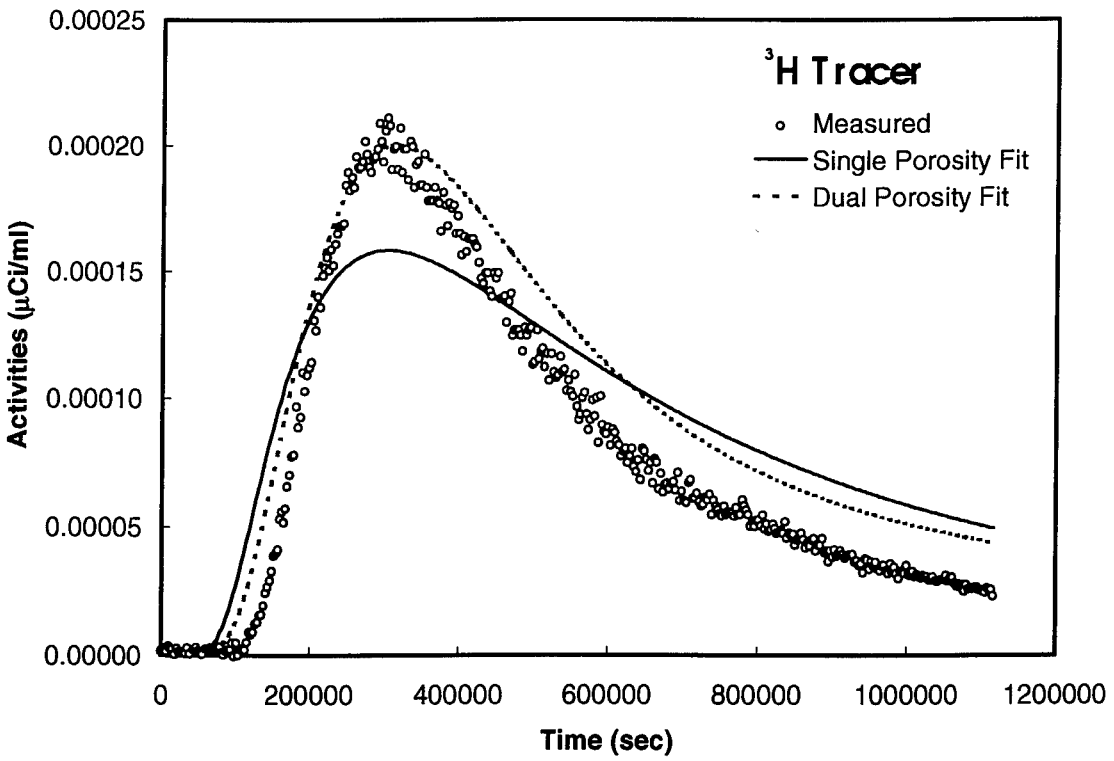

Figure B4. Test B1 measured and fitted ^{3}H effluent concentrations.

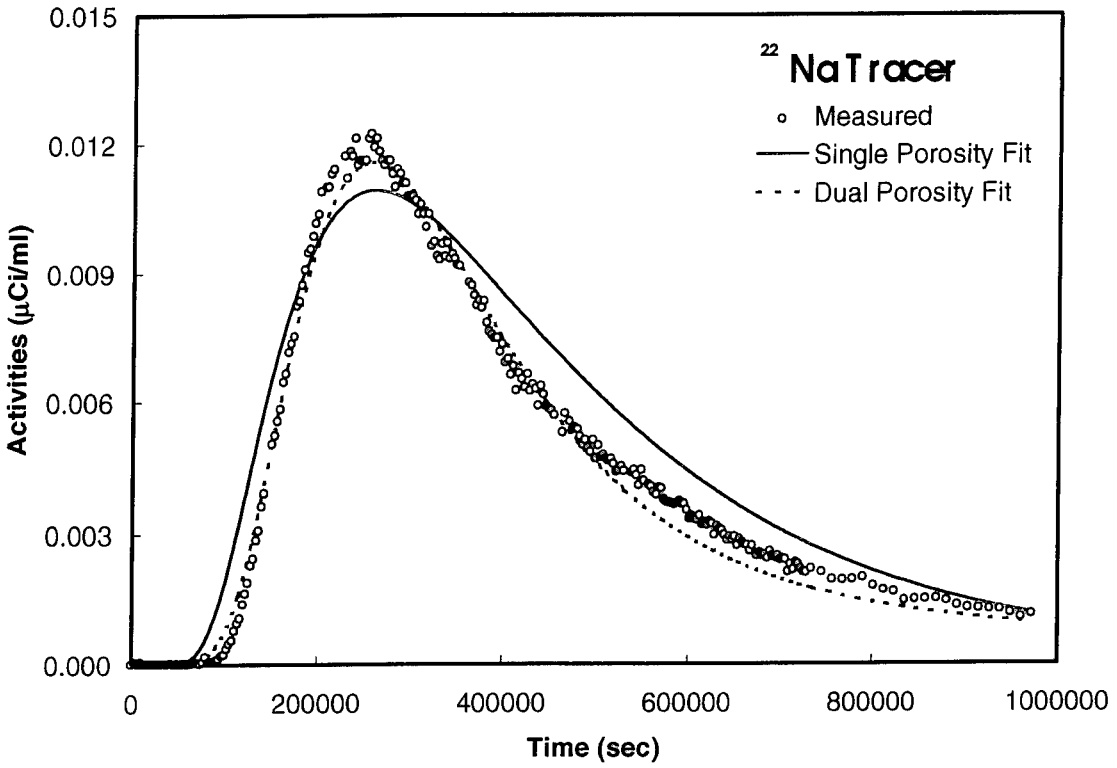

Figure B5. Test B2 measured and fitted ^{22}Na effluent concentrations.

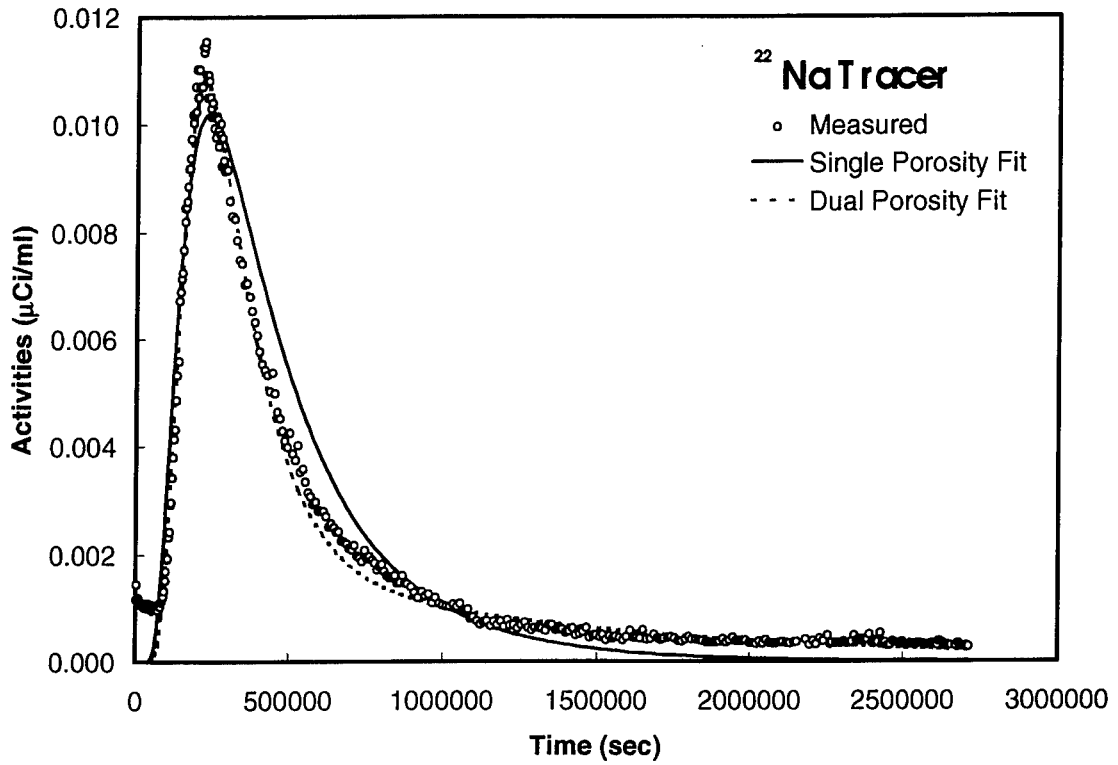

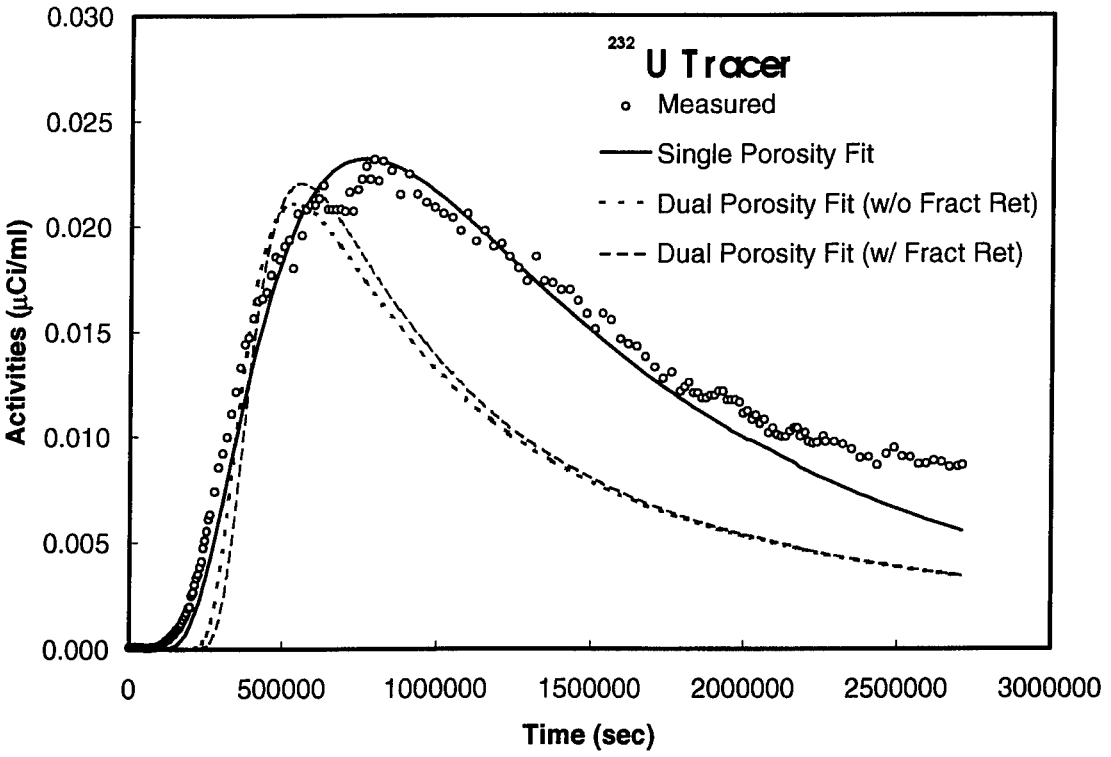

Figure B6. Test B3 measured and fitted ^{22}Na and ^{232}U effluent concentrations.

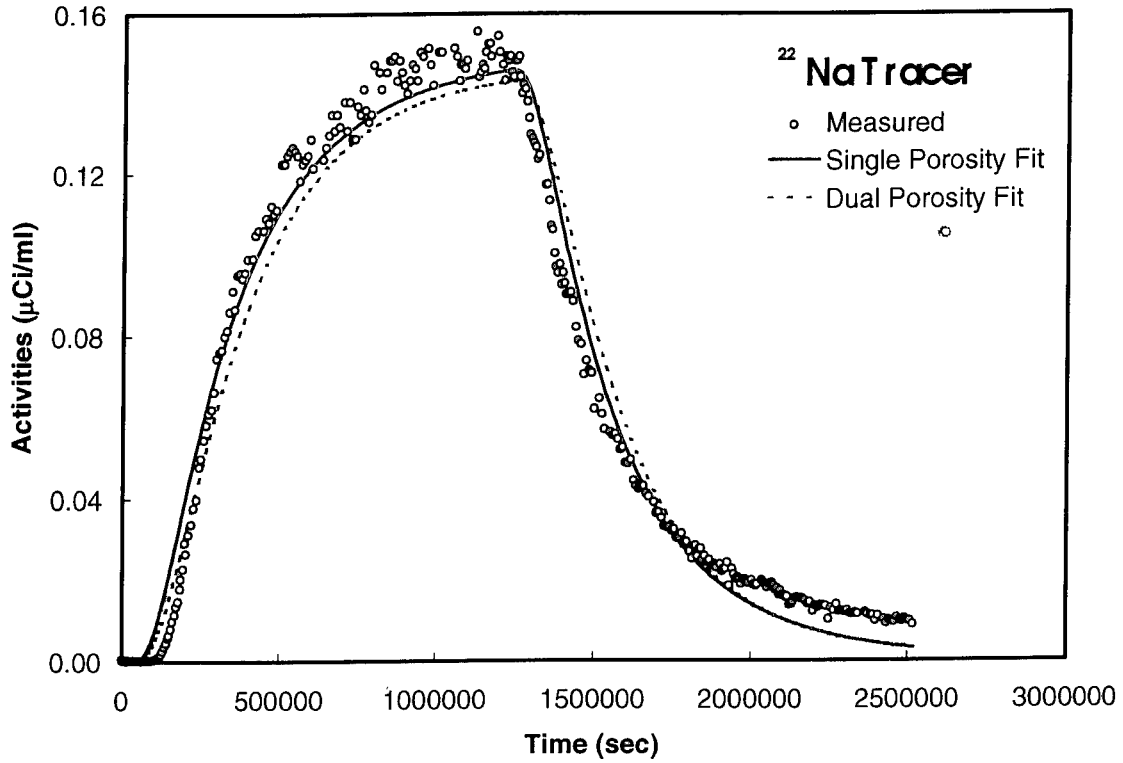

Figure B7. Test B4 measured and fitted ^{22}Na effluent concentrations.

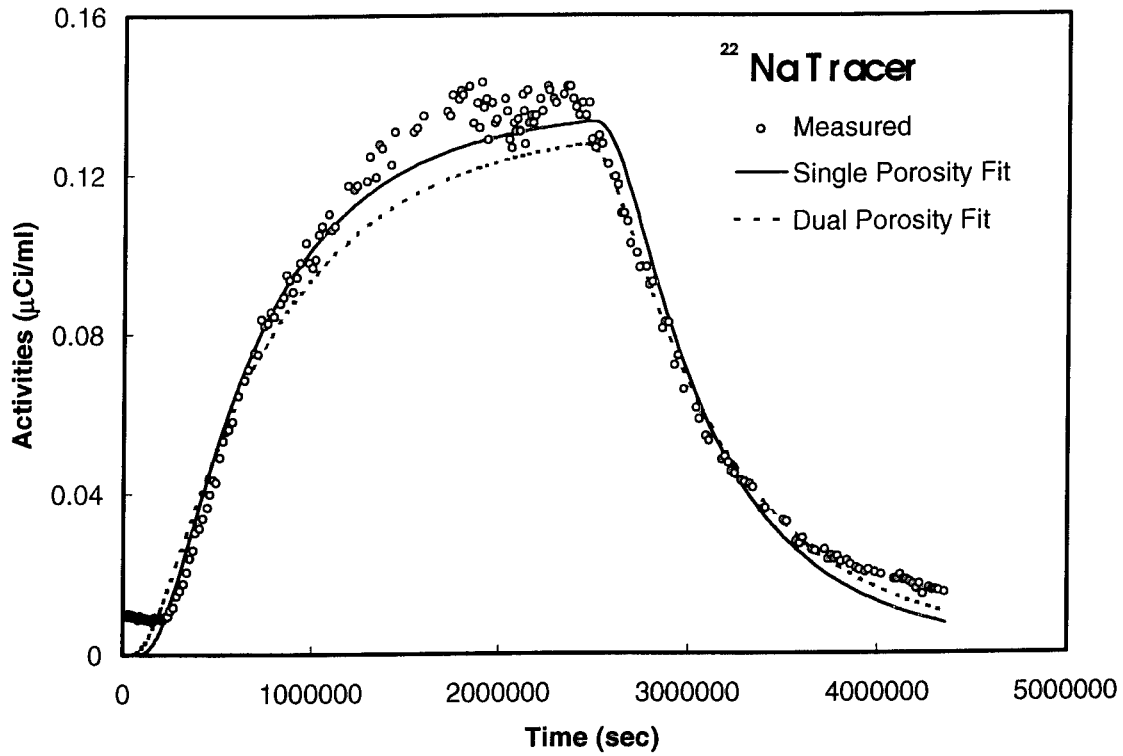

Figure B8. Test B5 measured and fitted ^{22}Na effluent concentrations.

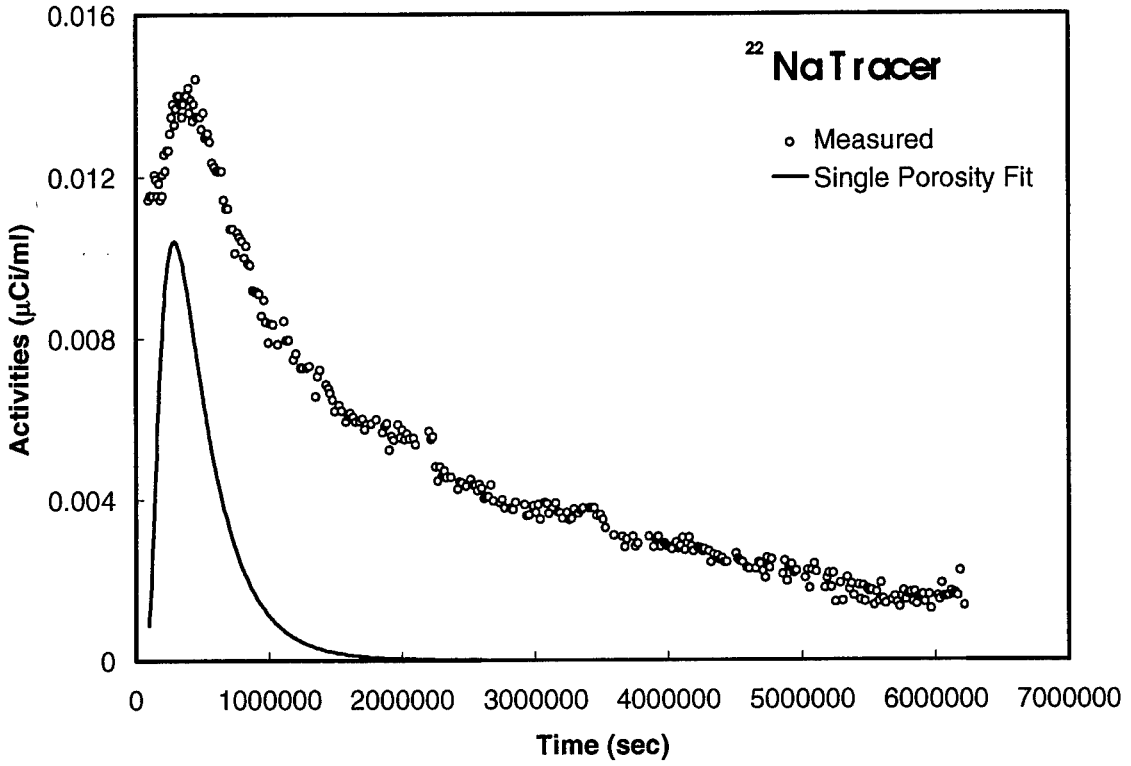

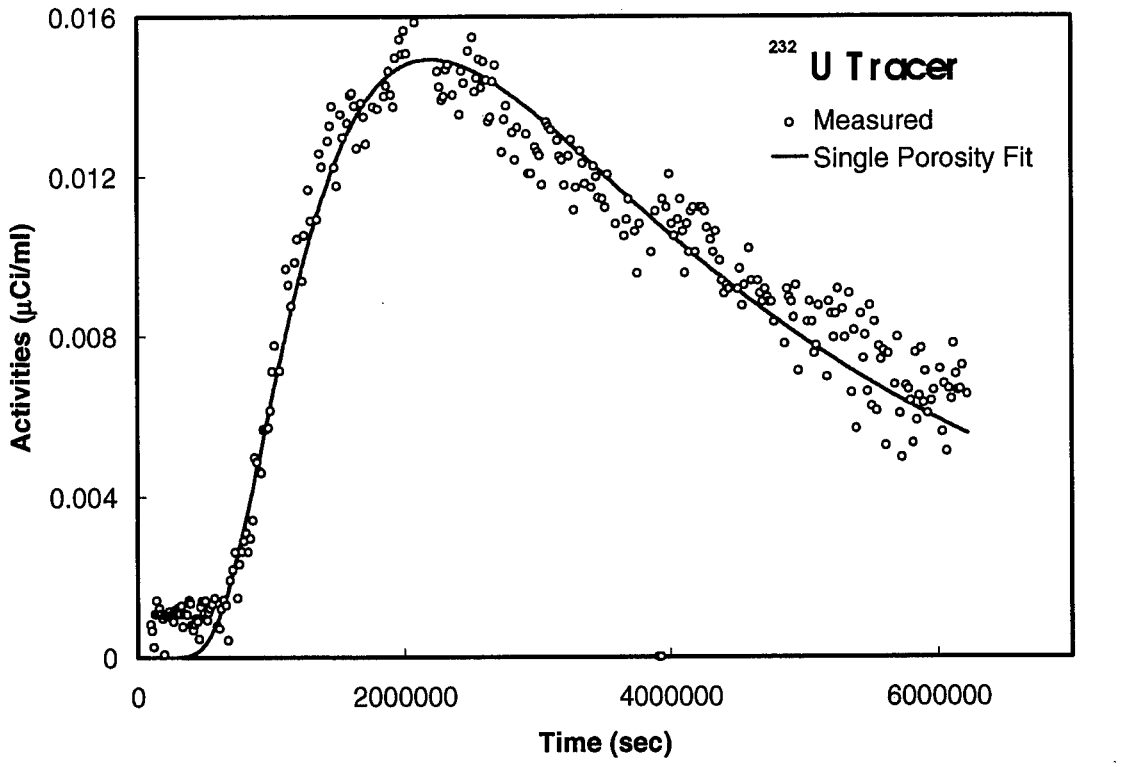

Figure B9. Test B6 measured and fitted ^{22}Na and ^{232}U effluent concentrations. See text for explanation for ^{22}Na curve.

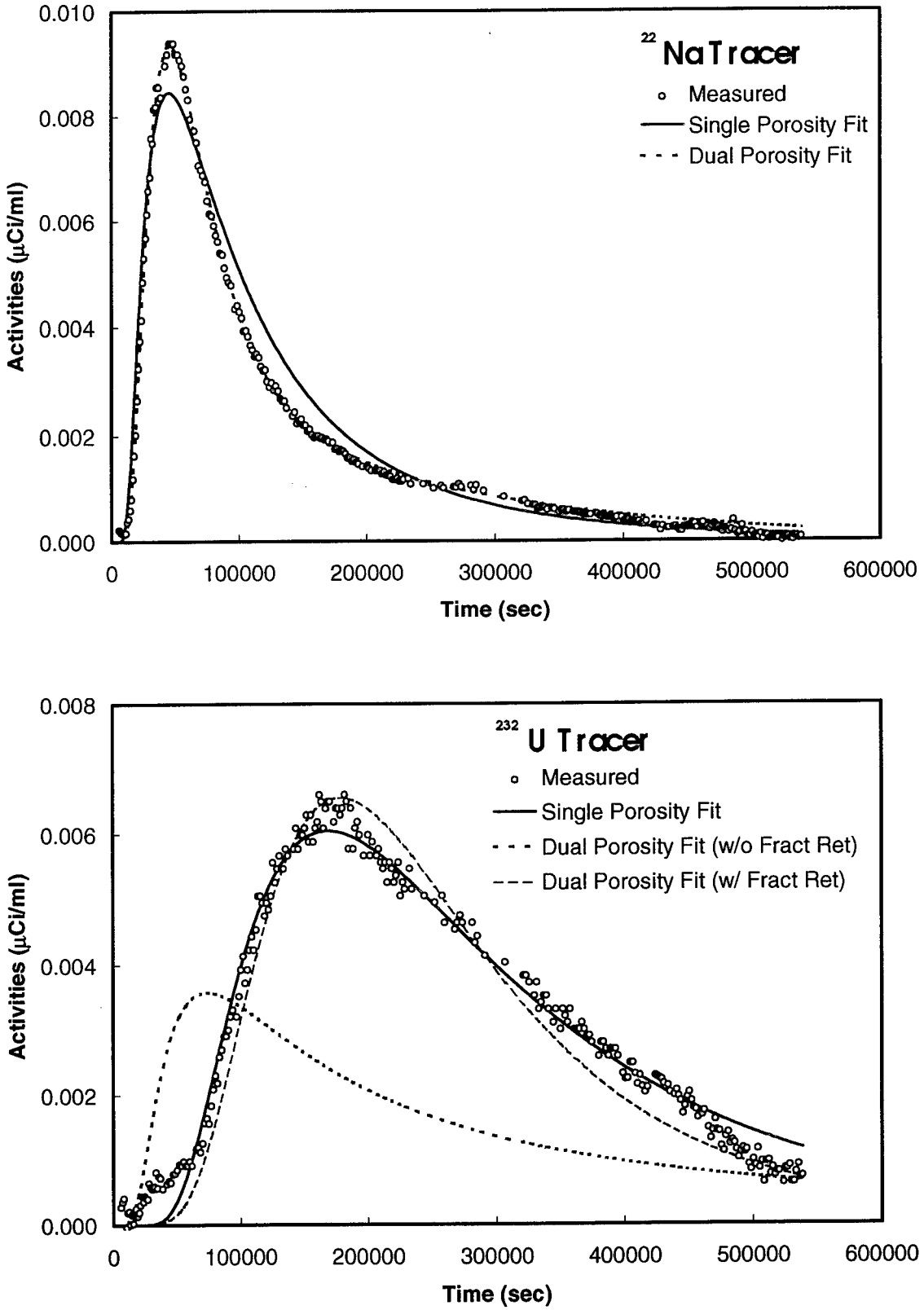

Figure B10. Test B7 measured and fitted ^{22}Na and ^{232}U effluent concentrations.

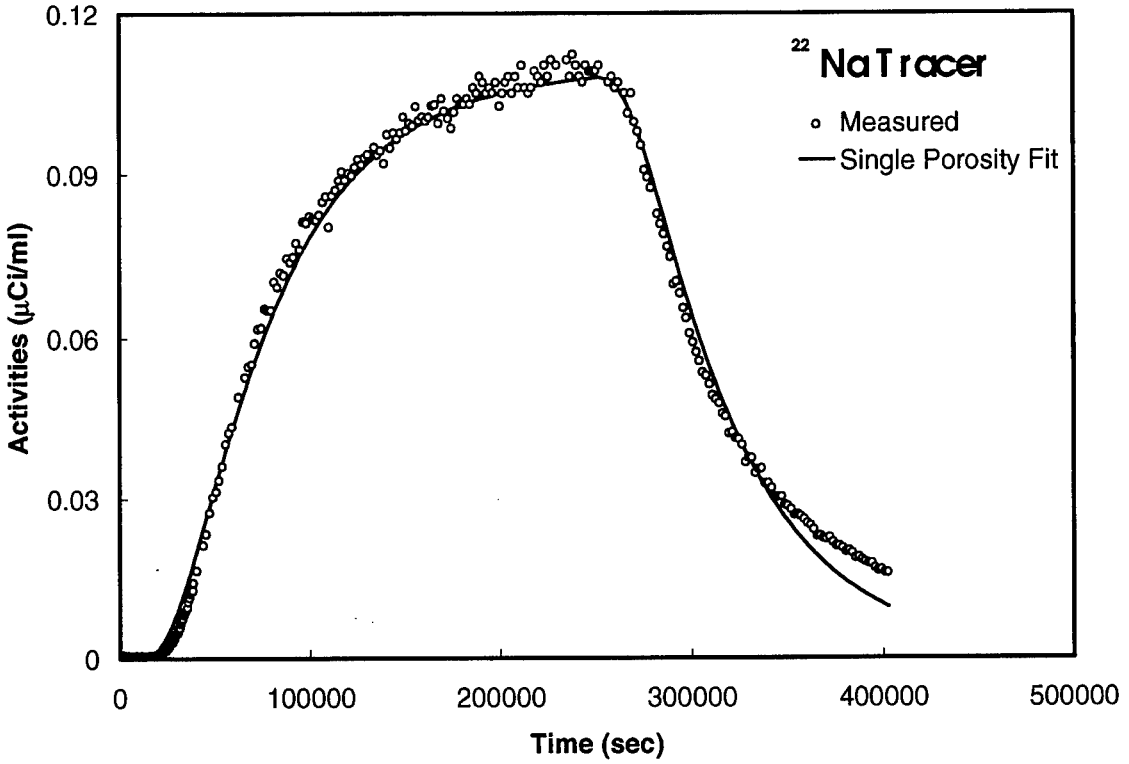

Figure B11. Test B8 measured and fitted ^{22}Na effluent concentrations.

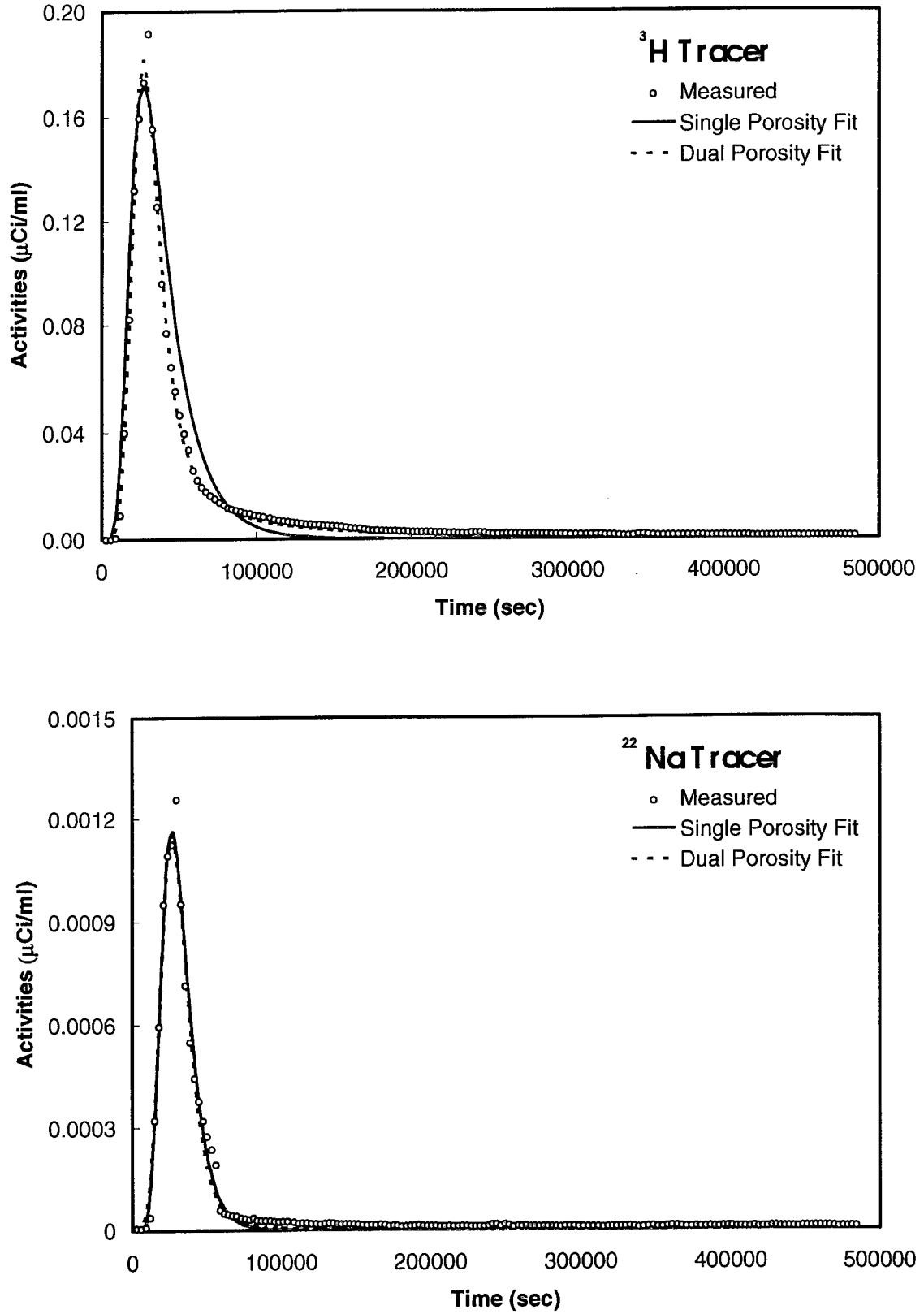

Figure B12. Test C1 measured and fitted ^{3}H and ^{22}Na effluent concentrations.

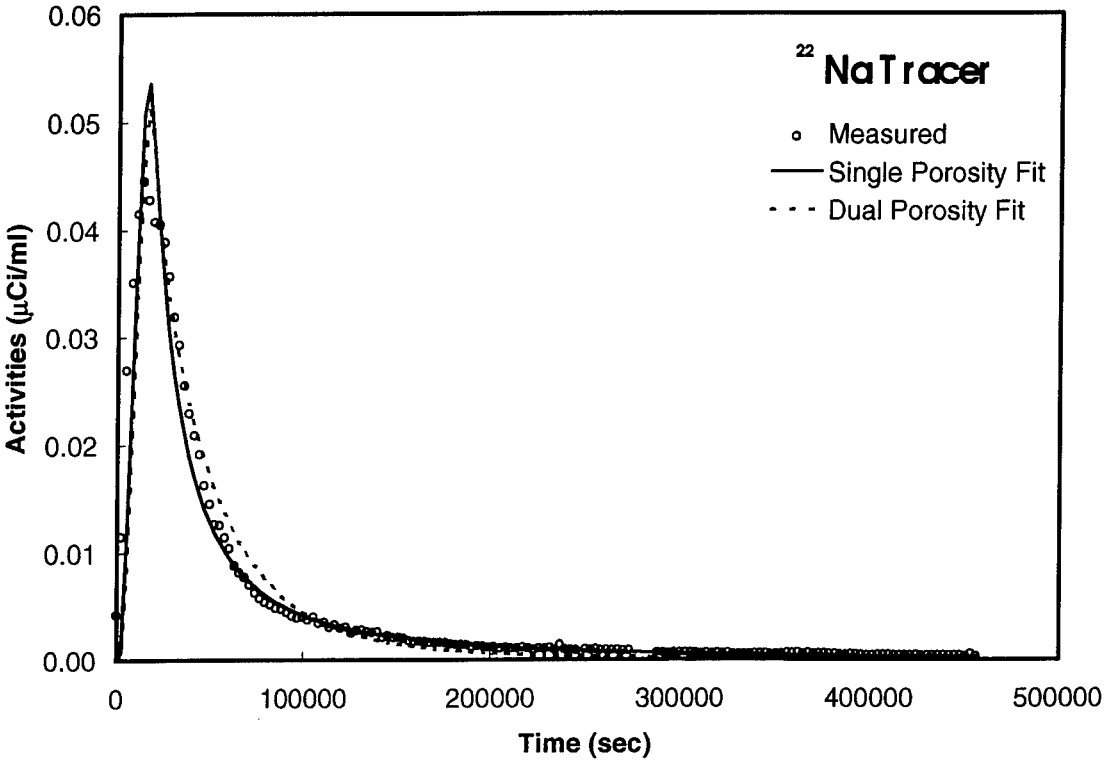

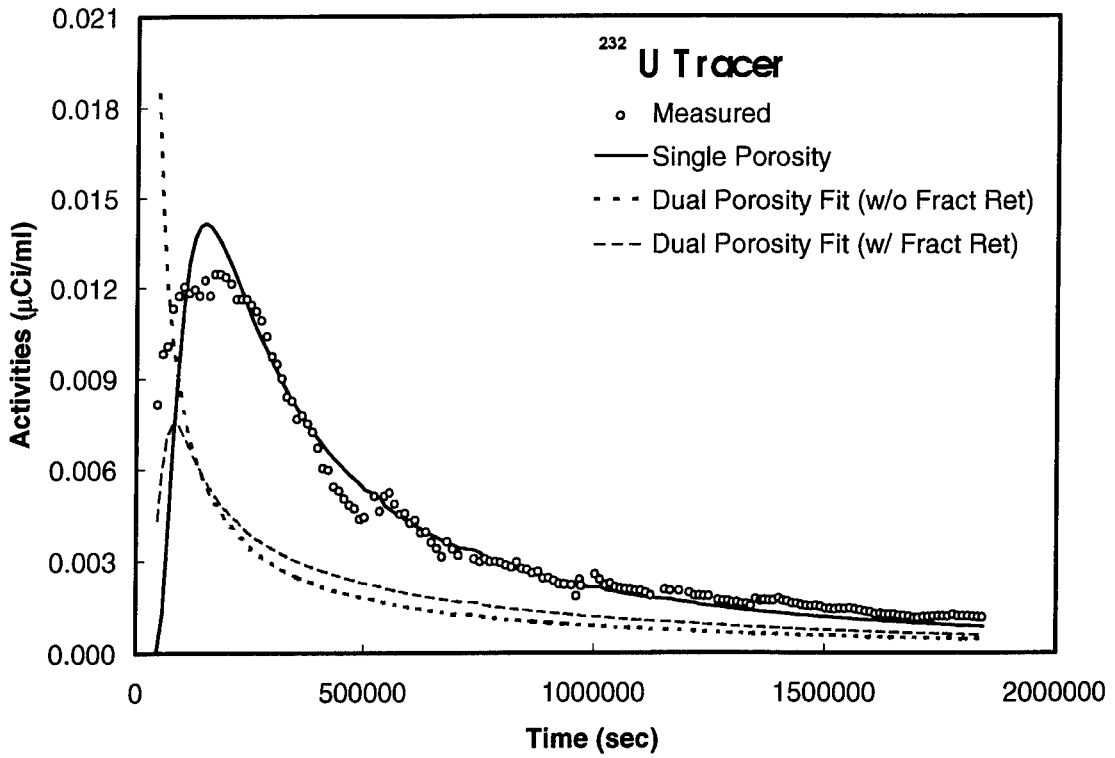

Figure B13. Test C2 measured and fitted ^{22}Na and ^{232}U effluent concentrations.

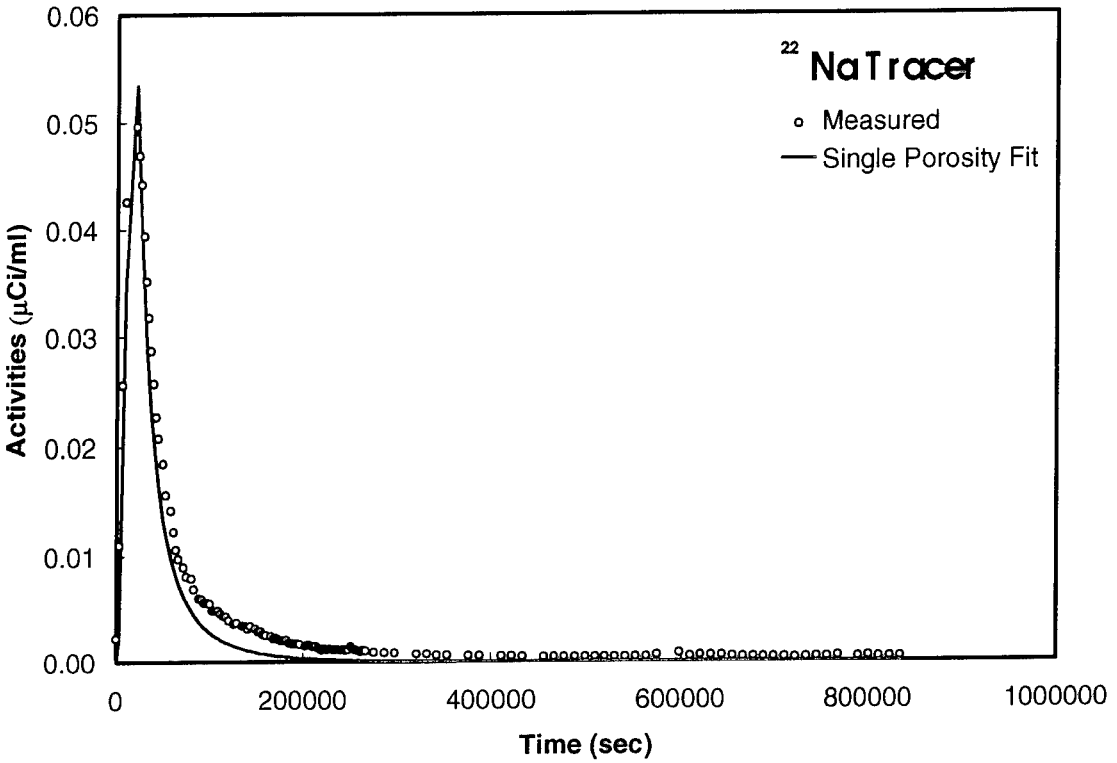

Figure B14. Test C3 measured and fitted ^{22}Na effluent concentrations.

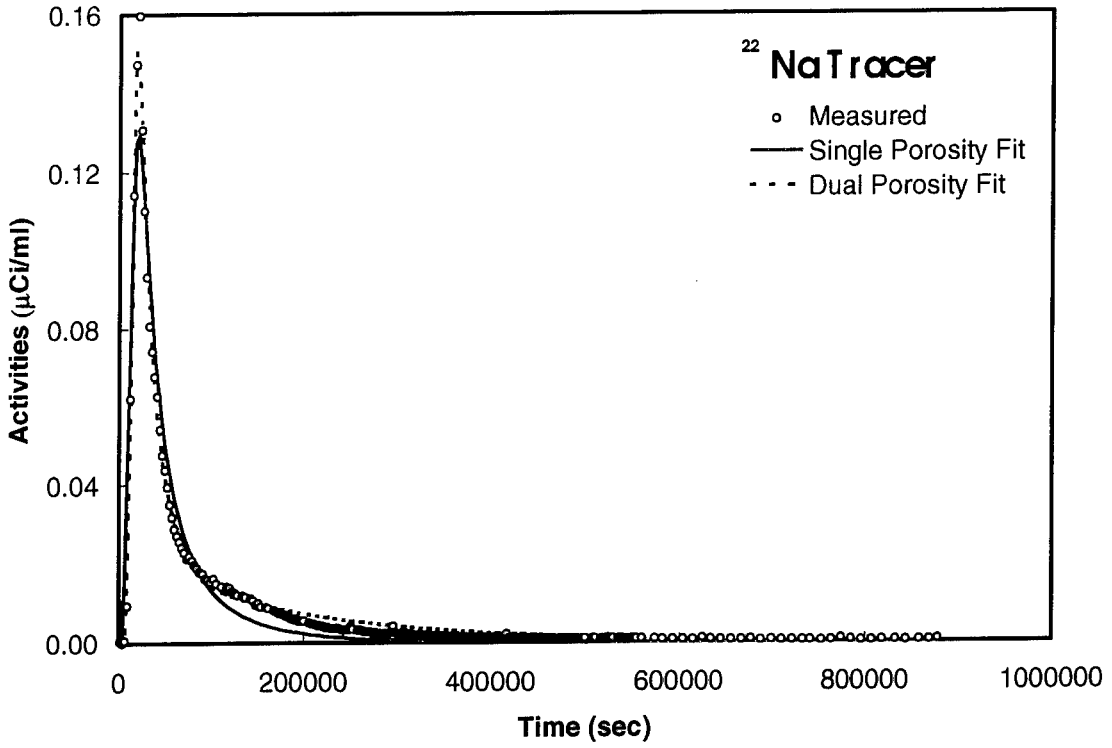

Figure B15. Test C4 measured and fitted ^{22}Na effluent concentrations.

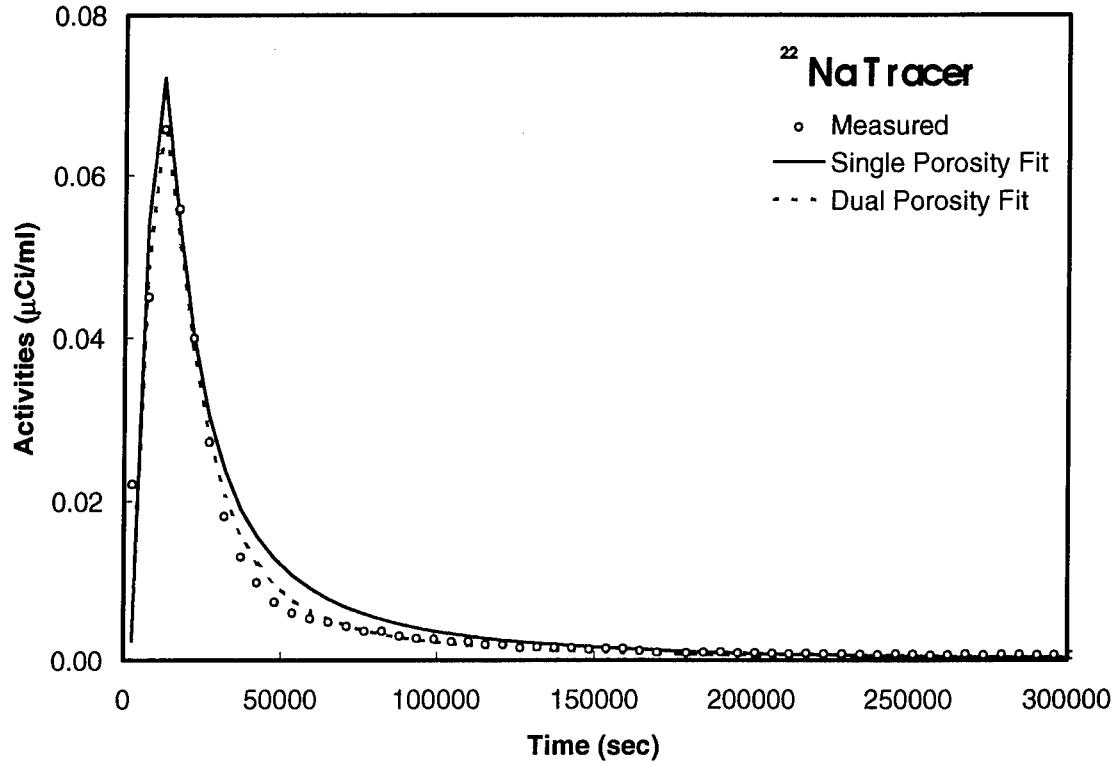

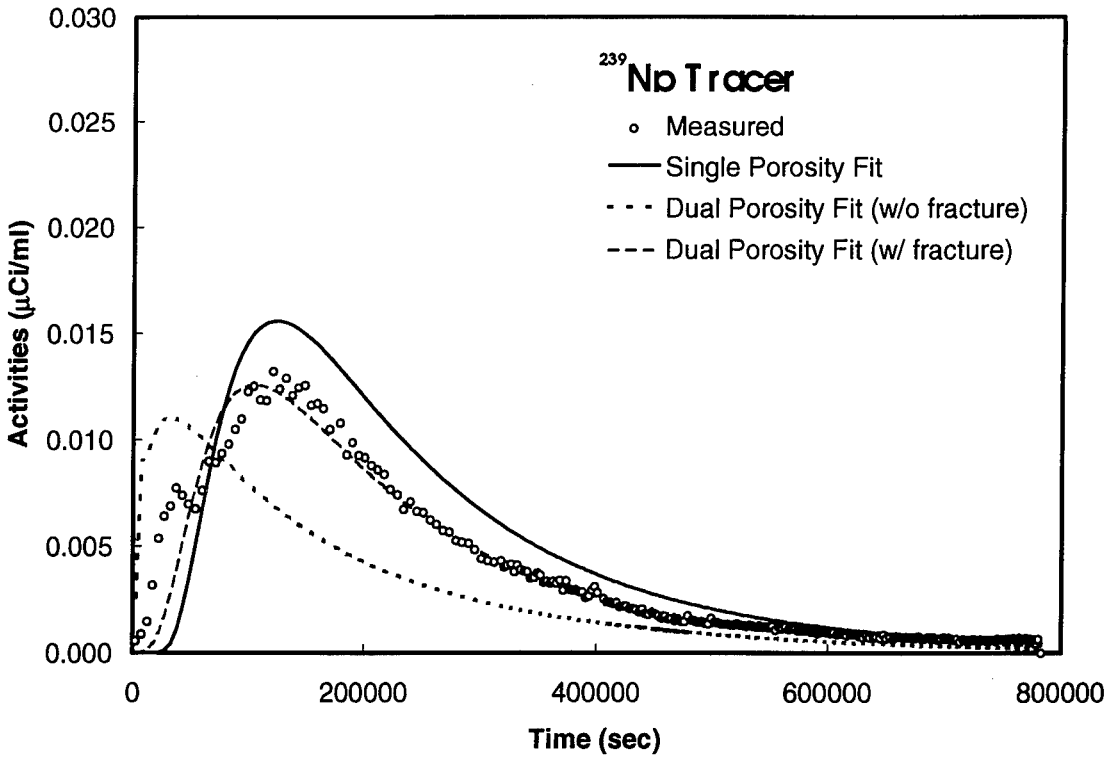

Figure B16. Test C5 measured and fitted ^{22}Na and ^{239}Np effluent concentrations. See text for explanation for ^{239}Np.

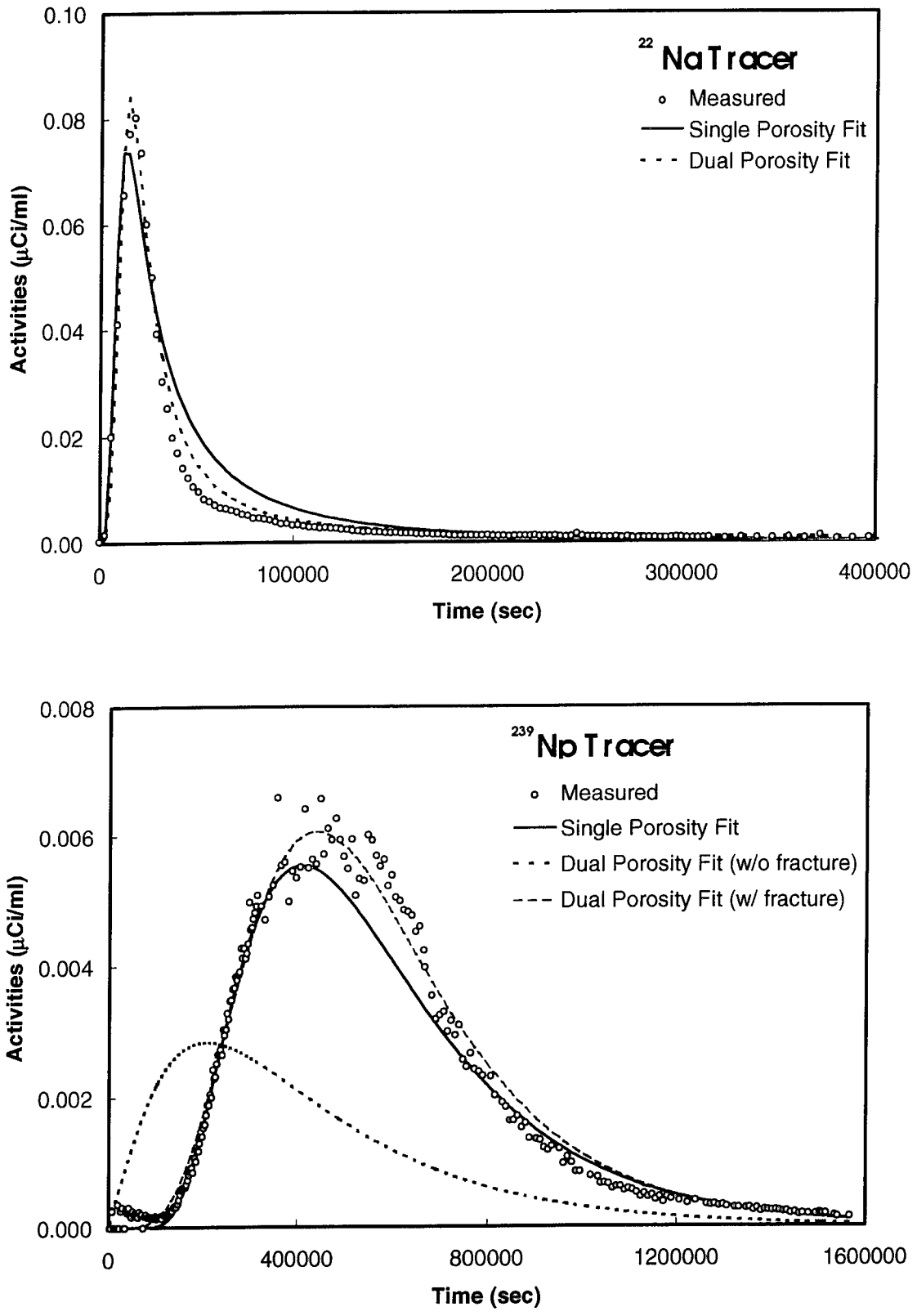

Figure B17. Test C6 measured and fitted ^{22}Na and ^{239}Np effluent concentrations.

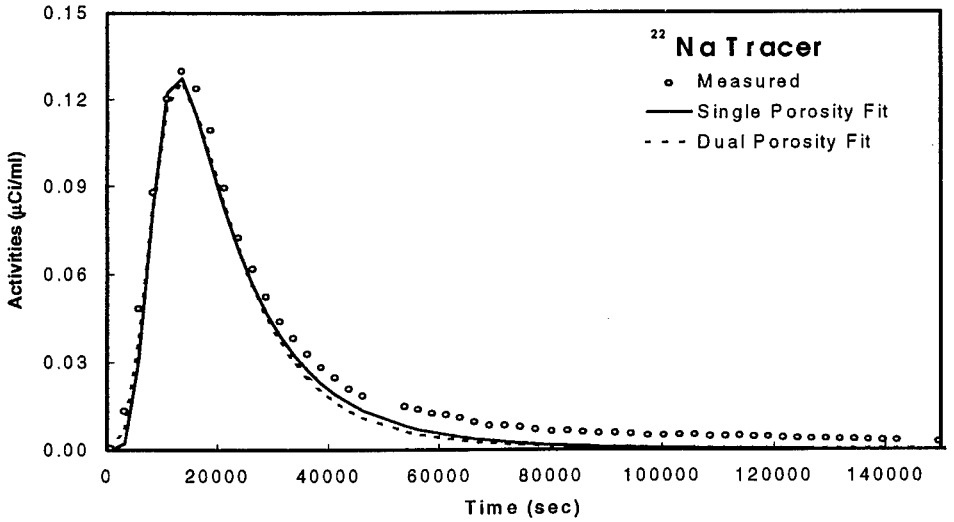

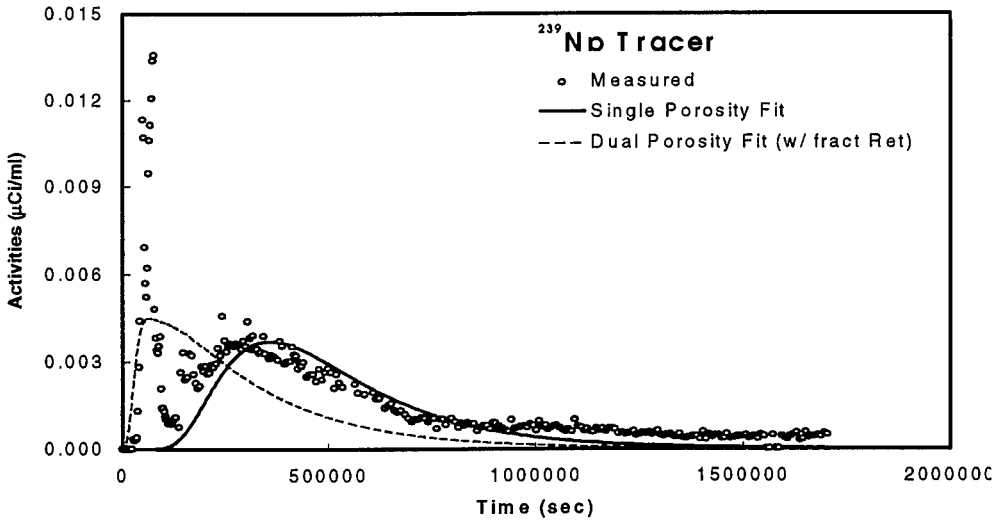

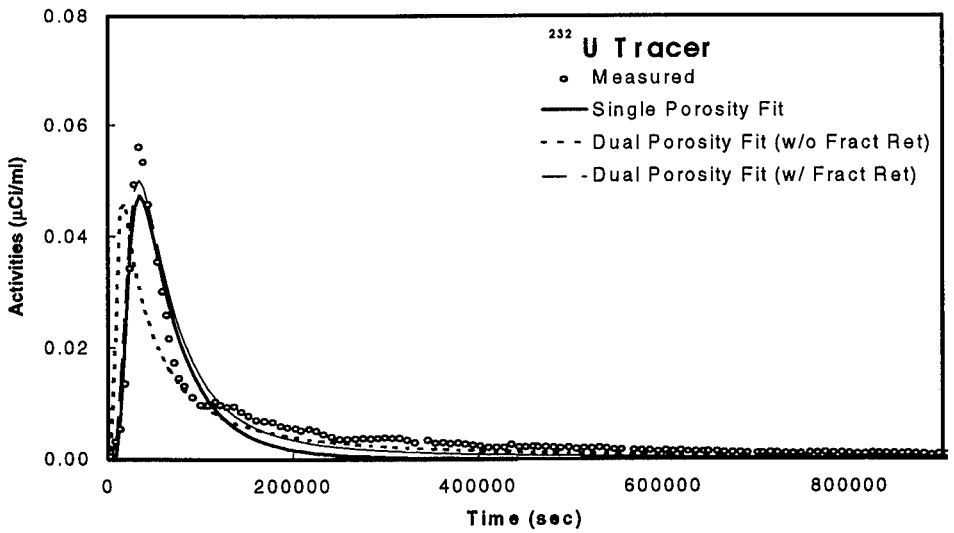

Figure B18. Test C7 measured and fitted ^{22}Na, ^{239}Np and ^{232}U effluent concentrations.

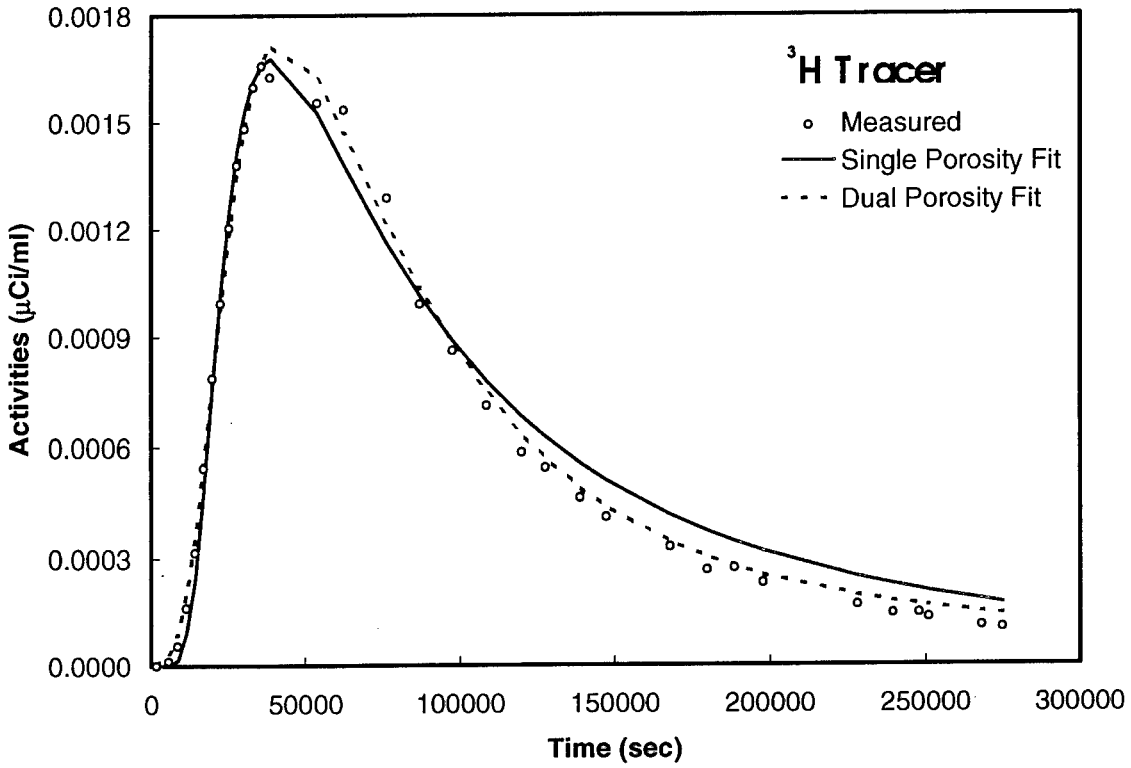

Figure B19. Test D1 measured and fitted ^{3}H effluent concentrations.

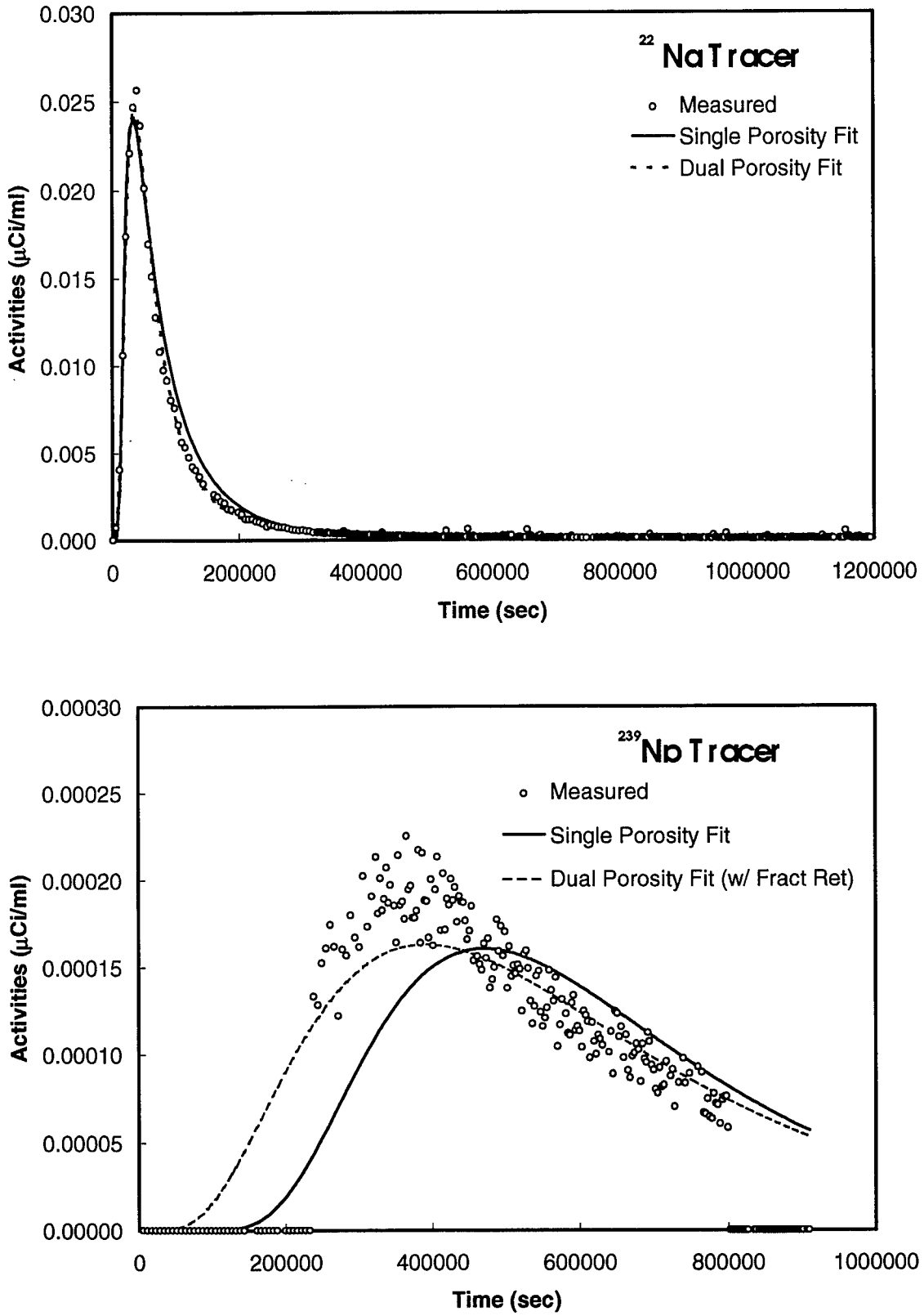

Figure B20. Test D2 measured and fitted ^{22}Na and ^{239}Np effluent concentrations.

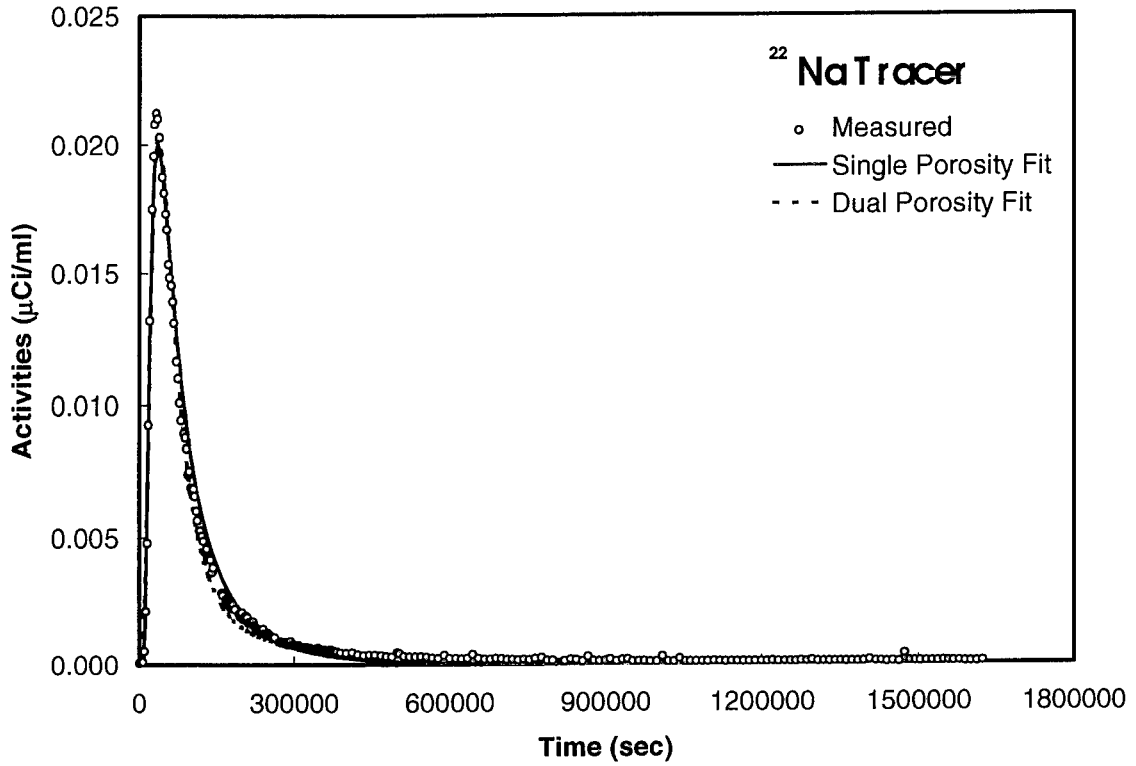

Figure B21. Test D3 measured and fitted ^{22}Na effluent concentrations.

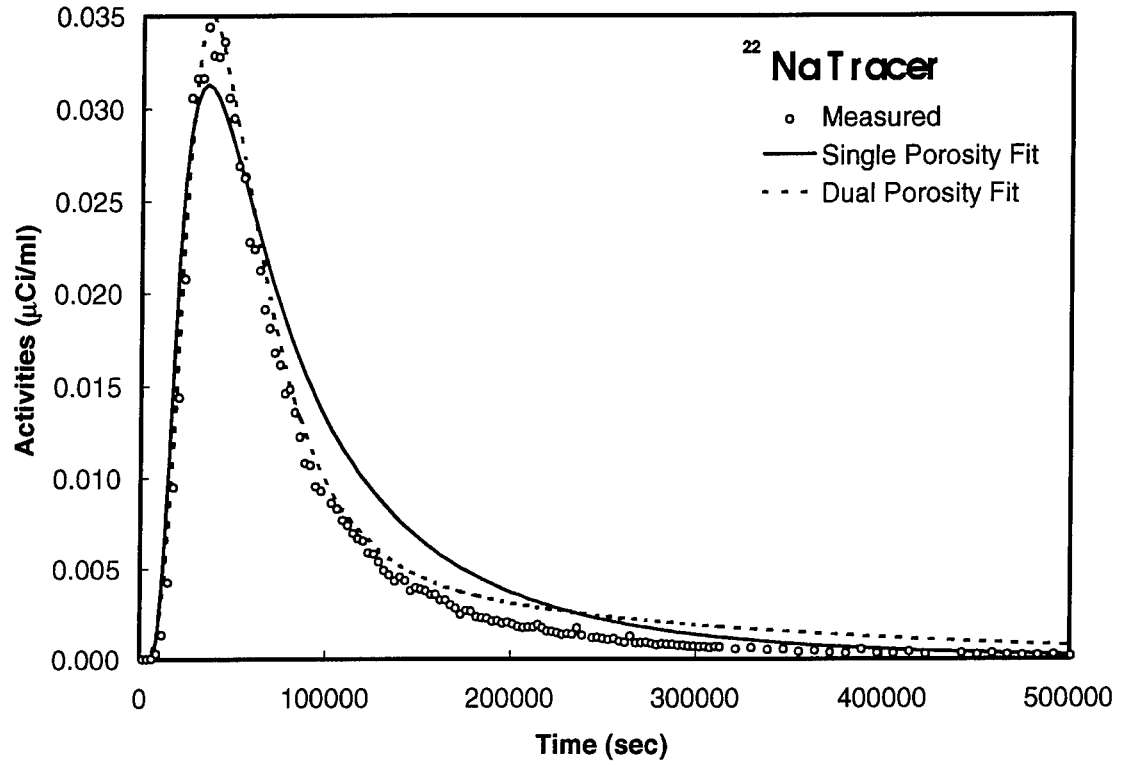

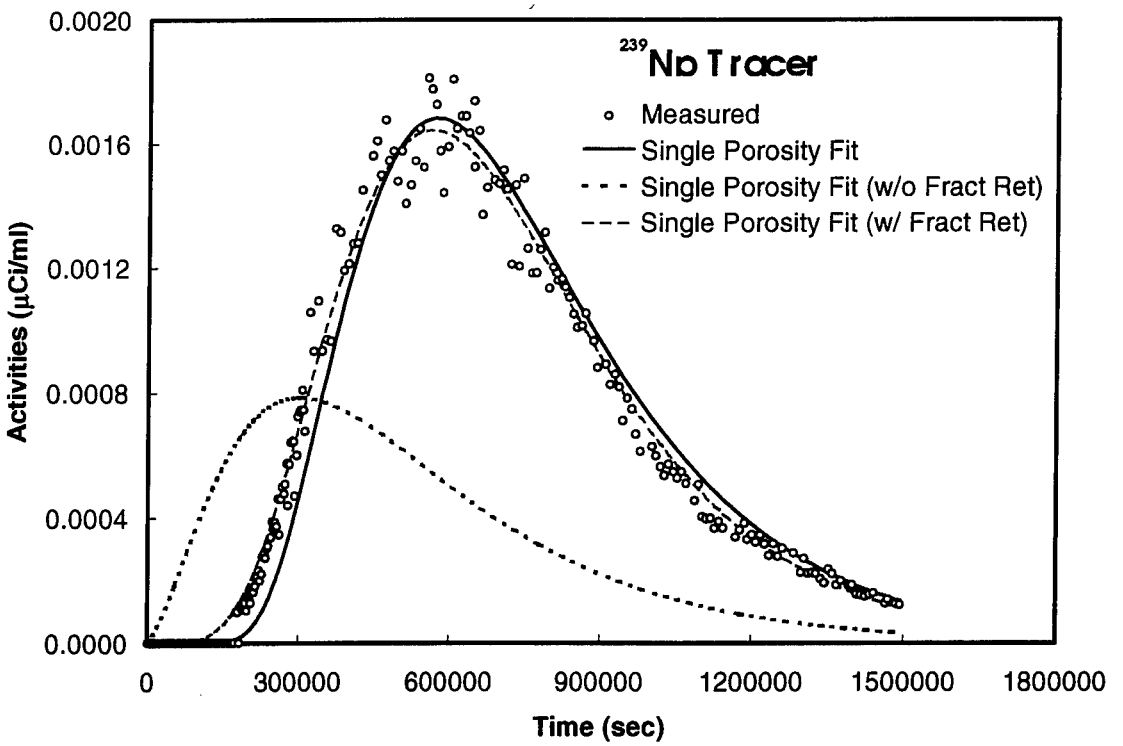

Figure B22. Test D4 measured and fitted ^{22}Na and ^{239}Np effluent concentrations.

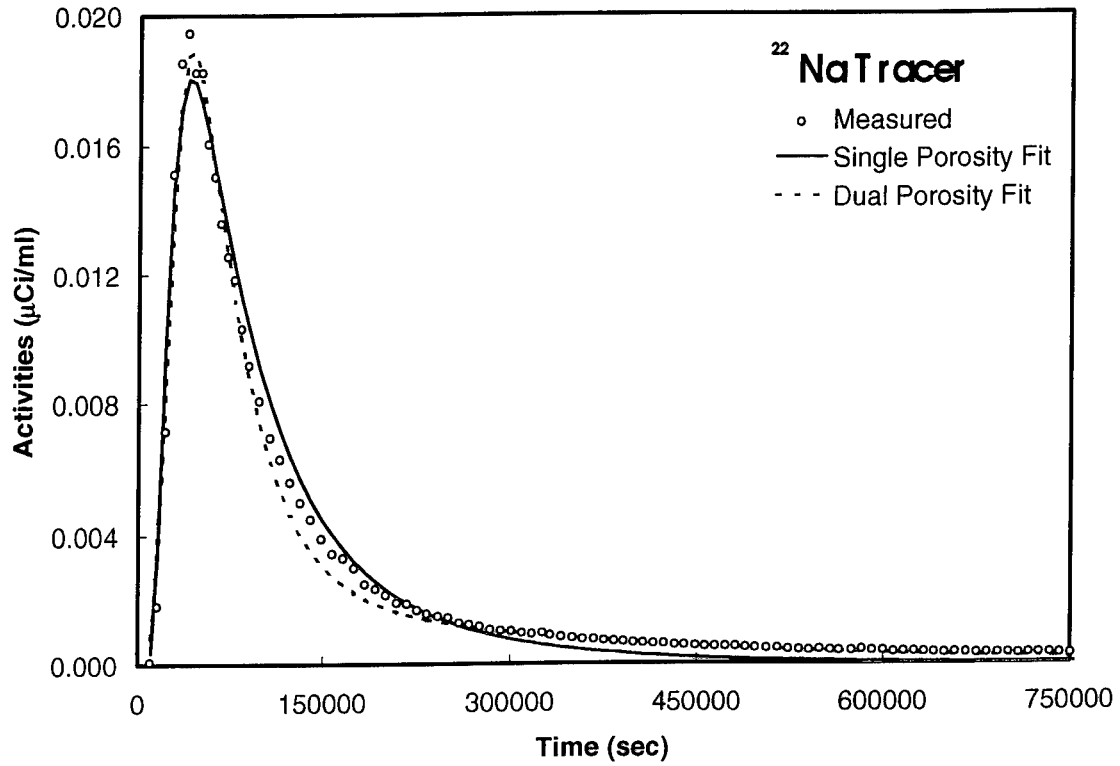

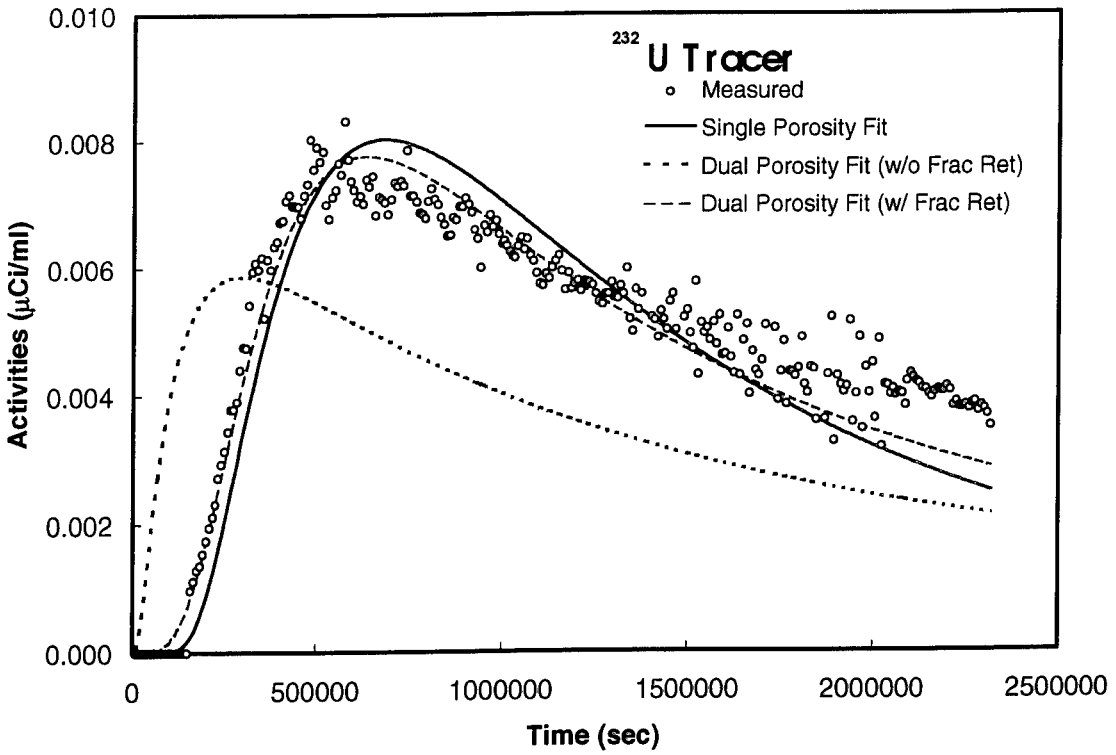

Figure B23. Test D5 measured and fitted ^{22}Na and ^{232}U effluent concentrations.

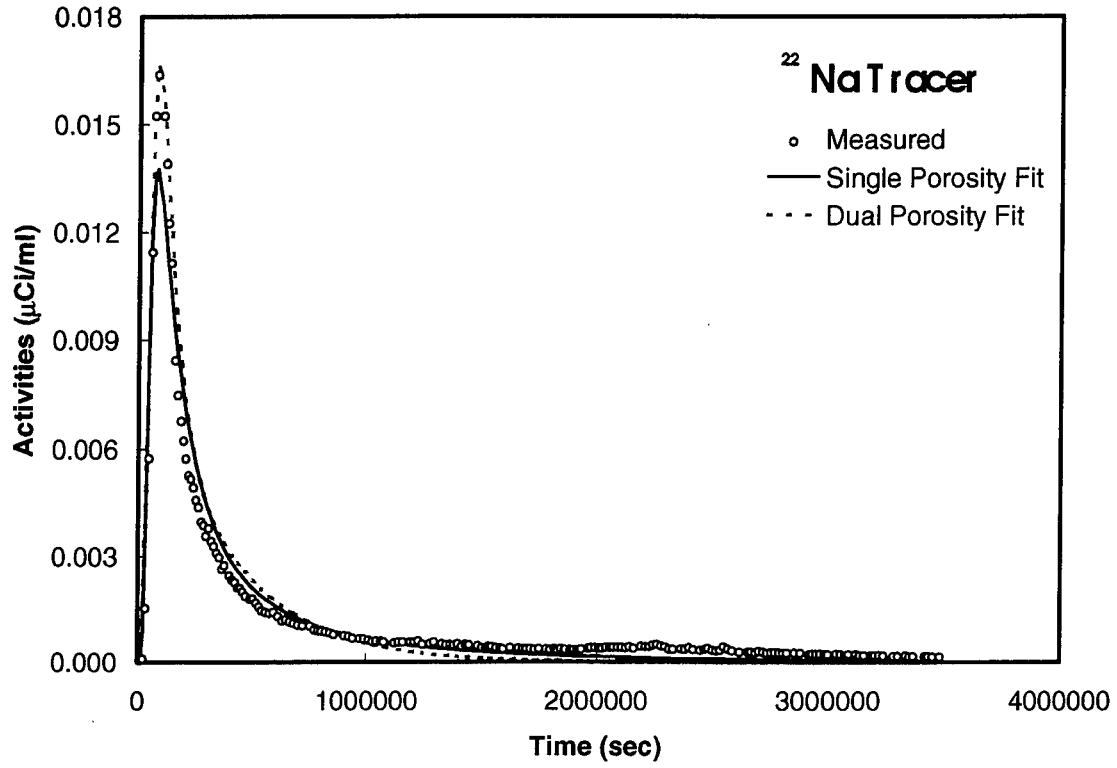

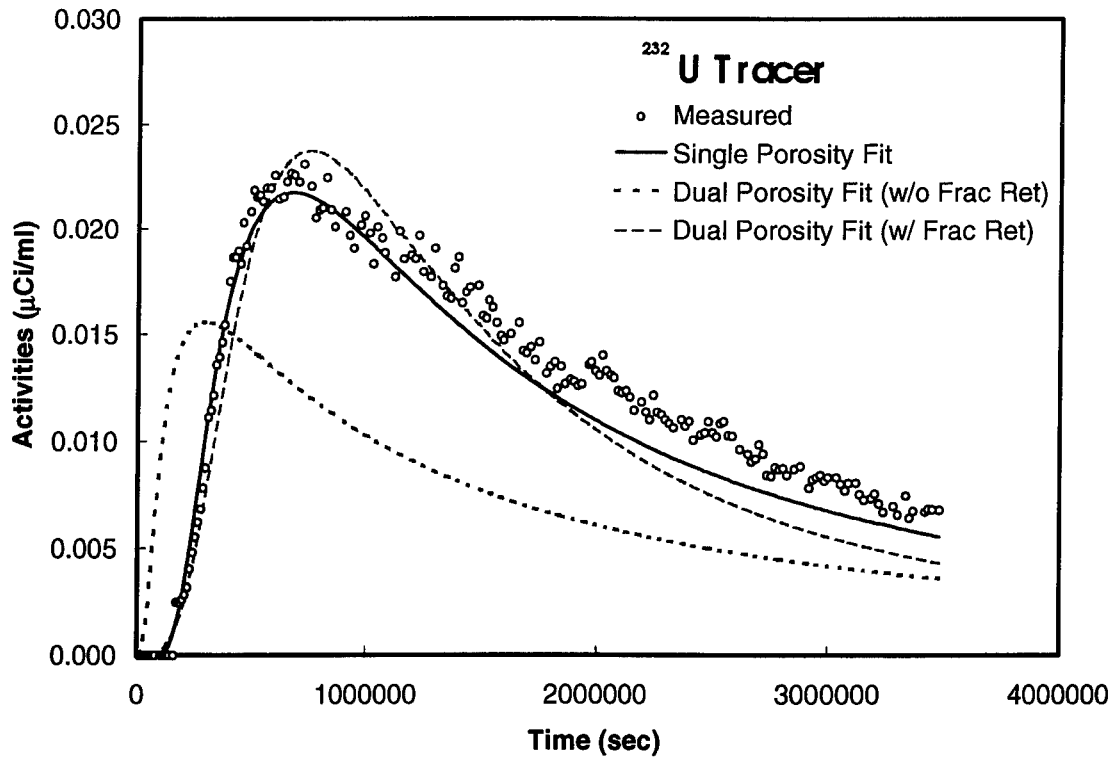

Figure B24. Test D6 measured and fitted ^{22}Na and ^{232}U effluent concentrations.

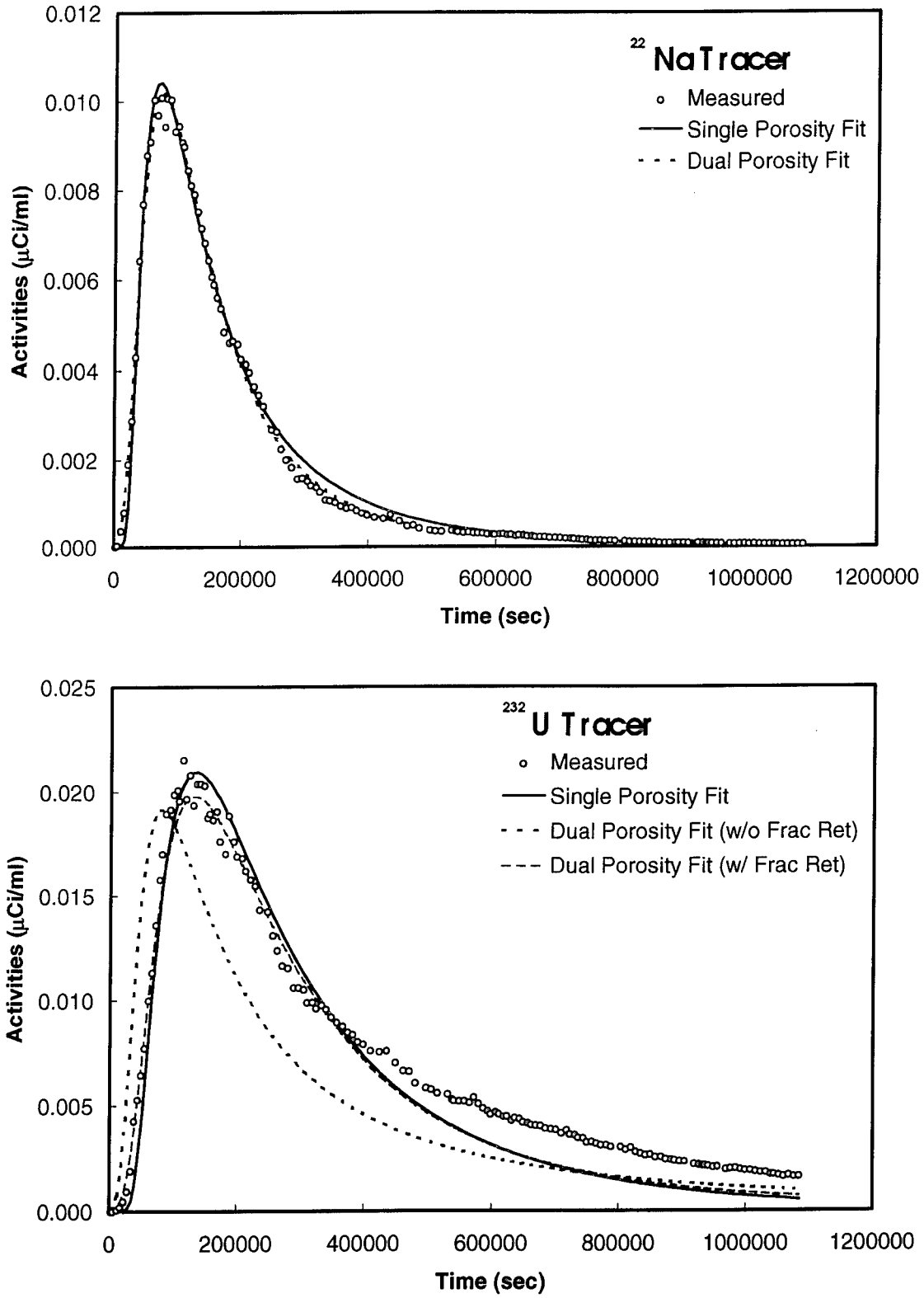

Figure B25. Test E1 measured and fitted ^{22}Na and ^{232}U effluent concentrations.

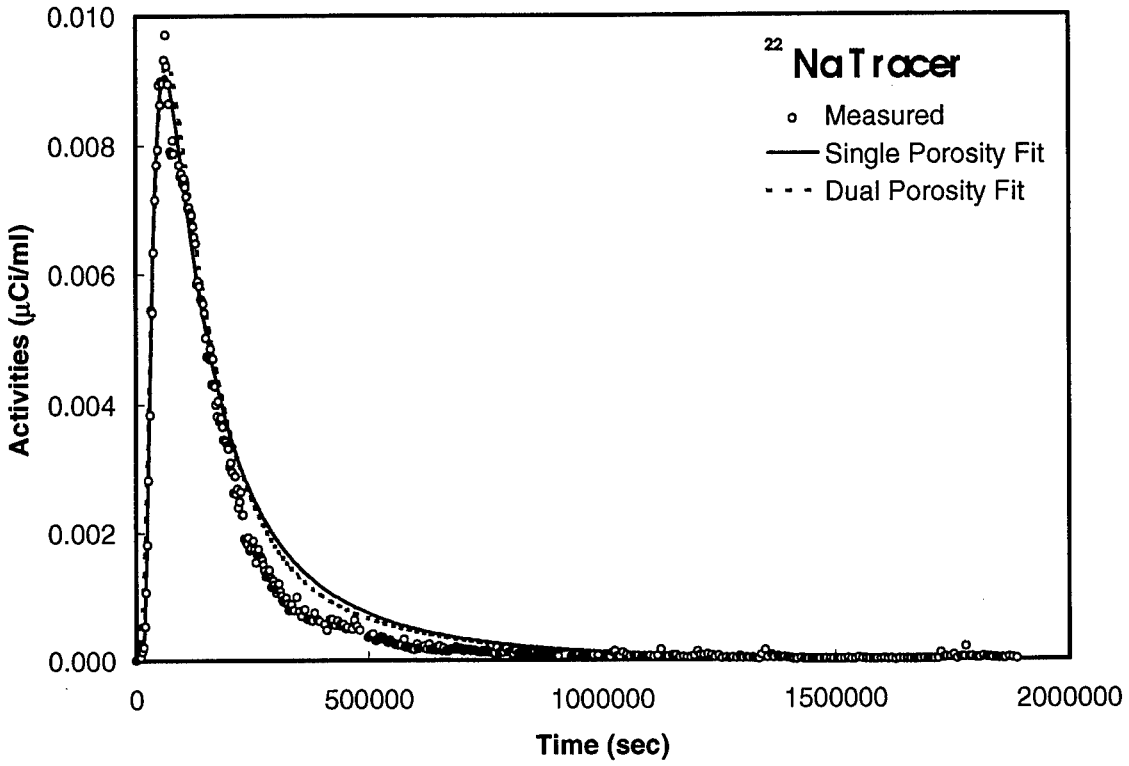

Figure B26. Test E2 measured and fitted ^{22}Na effluent concentrations.

APPENDIX C

MEASURED EFFLUENT CONCENTRATIONS FOR ^{3}H, ^{22}Na, ^{232}U and ^{239}Np.

List of Tables

Table C1. Test A1, ^{3}H.

Effluent *gm*	Activity *µCi / gm*	Effluent *gm*	Activity *µCi / gm*	Effluent *gm*	Activity *µCi / gm*
5	0.000001	290	0.002120	570	0.000247
10	0.000001	295	0.002010	575	0.000233
15	0.000000	305	0.001900	580	0.000228
20	-0.000001	315	0.001820	585	0.000224
30	-0.000001	320	0.001740	590	0.000207
35	-0.000001	325	0.001650	595	0.000200
40	-0.000001	330	0.001600	600	0.000200
45	0.000001	335	0.001450	605	0.000192
50	-0.000001	340	0.001420	610	0.000189
55	-0.000002	345	0.001320	615	0.000184
65	0.000001	350	0.001280	620	0.000184
70	0.000002	355	0.001200	625	0.000177
75	0.000000	360	0.001180	630	0.000172
80	0.000001	365	0.001120	635	0.000168
85	0.000000	370	0.001060	640	0.000160
90	0.000002	375	0.001010	645	0.000165
95	0.000002	380	0.000998	655	0.000159
100	0.000000	385	0.000920	660	0.000151
110	0.000001	390	0.000889	665	0.000151
115	0.000002	395	0.000840	670	0.000142
120	0.000002	400	0.000786	675	0.000142
135	0.000001	405	0.000754	680	0.000142
140	0.000003	410	0.000724	685	0.000134
145	0.000003	415	0.000685	690	0.000131
150	0.000012	420	0.000669	695	0.000123
155	0.000032	425	0.000633	700	0.000123
160	0.000074	430	0.000606	705	0.000127
165	0.000150	435	0.000590	710	0.000113
170	0.000276	440	0.000536	715	0.000115
180	0.000487	445	0.000542	720	0.000113
185	0.000655	450	0.000506	725	0.000106
190	0.000943	455	0.000494	730	0.000112
195	0.001180	460	0.000452	735	0.000110
205	0.001540	465	0.000429	740	0.000085
210	0.001710	470	0.000420	750	0.000085
215	0.002230	475	0.000414	760	0.000086
225	0.002340	485	0.000380	765	0.000085
230	0.002520	495	0.000361	770	0.000083
235	0.002610	505	0.000365	775	0.000078
240	0.002690	515	0.000340	780	0.000079
245	0.002680	520	0.000326	785	0.000074
250	0.002660	530	0.000315	790	0.000076
255	0.002640	535	0.000299	795	0.000077
260	0.002550	540	0.000297	800	0.000083
265	0.002510	545	0.000285	805	0.000077
270	0.002470	550	0.000279	810	0.000073
275	0.002360	555	0.000277	815	0.000044
280	0.002300	560	0.000265	820	0.000071
285	0.002180	565	0.000247	835	0.000069

Effluent *gm*	Activity *µCi / gm*	Effluent *gm*	Activity *µCi / gm*	Effluent *gm*	Activity *µCi / gm*
840	0.000070	1110	0.000047	1375	0.000028
845	0.000069	1115	0.000047	1380	0.000029
850	0.000068	1120	0.000048	1385	0.000031
855	0.000069	1125	0.000046	1390	0.000030
860	0.000067	1130	0.000044	1395	0.000028
865	0.000069	1135	0.000044	1410	0.000028
870	0.000066	1140	0.000042	1415	0.000030
875	0.000060	1145	0.000043	1420	0.000027
880	0.000061	1150	0.000045	1425	0.000032
885	0.000064	1155	0.000046	1435	0.000027
890	0.000067	1165	0.000043	1440	0.000026
895	0.000062	1170	0.000039	1445	0.000030
900	0.000064	1175	0.000043	1450	0.000028
905	0.000064	1185	0.000043	1455	0.000026
910	0.000061	1190	0.000039	1460	0.000029
915	0.000060	1195	0.000040	1465	0.000029
920	0.000062	1200	0.000038	1470	0.000024
930	0.000056	1205	0.000040	1475	0.000027
940	0.000054	1210	0.000039	1480	0.000027
945	0.000057	1215	0.000044	1485	0.000024
950	0.000055	1220	0.000039	1490	0.000029
955	0.000059	1225	0.000041	1495	0.000026
960	0.000054	1230	0.000039	1500	0.000024
965	0.000054	1235	0.000040	1505	0.000028
970	0.000057	1240	0.000038	1510	0.000024
975	0.000049	1250	0.000038	1515	0.000026
980	0.000052	1255	0.000039	1520	0.000026
985	0.000051	1260	0.000039	1525	0.000027
990	0.000051	1265	0.000036	1530	0.000022
995	0.000050	1270	0.000037	1535	0.000027
1000	0.000055	1275	0.000034	1540	0.000026
1005	0.000055	1280	0.000035	1550	0.000024
1010	0.000051	1285	0.000034	1555	0.000026
1015	0.000048	1290	0.000039	1560	0.000023
1020	0.000047	1295	0.000034	1565	0.000026
1025	0.000050	1300	0.000033	1570	0.000025
1030	0.000052	1305	0.000032	1575	0.000026
1035	0.000052	1310	0.000035	1580	0.000027
1040	0.000054	1315	0.000034	1585	0.000022
1045	0.000049	1320	0.000034	1590	0.000014
1050	0.000047	1325	0.000032	1595	0.000015
1060	0.000046	1330	0.000033	1600	0.000017
1065	0.000049	1335	0.000030	1610	0.000016
1070	0.000050	1340	0.000030	1615	0.000016
1075	0.000047	1345	0.000033	1620	0.000016
1080	0.000054	1350	0.000032	1625	0.000015
1085	0.000043	1355	0.000030	1630	0.000014
1095	0.000045	1360	0.000030	1635	0.000016
1100	0.000051	1365	0.000034	1640	0.000017
1105	0.000043	1370	0.000033	1645	0.000014

Effluent *gm*	Activity *µCi / gm*
1650	0.000015
1660	0.000014
1665	0.000015
1670	0.000013
1680	0.000015
1685	0.000015
1690	0.000013
1695	0.000014
1700	0.000014
1705	0.000016
1710	0.000015
1715	0.000014
1720	0.000016
1725	0.000014
1730	0.000013
1735	0.000012
1740	0.000012
1745	0.000014
1750	0.000013
1755	0.000021
1760	0.000027
1765	0.000021
1770	0.000031
1775	0.000018
1785	0.000021
1790	0.000021
1795	0.000024
1800	0.000024
1805	0.000014
1810	0.000015
1815	0.000018
1820	0.000022
1825	0.000019
1830	0.000024
1835	0.000019
1840	0.000022
1845	0.000028
1850	0.000017
1855	0.000013
1860	0.000018
1870	0.000025
1880	0.000032
1885	0.000012
1895	0.000020
1900	0.000020
1905	0.000017
1910	0.000024
1915	0.000022
1920	0.000014
1925	0.000020

Effluent *gm*	Activity *µCi / gm*
1930	0.000021
1935	0.000022
1940	0.000025
1945	0.000020
1950	0.000015
1955	0.000016
1960	0.000015
1965	0.000016
1970	0.000016
1975	0.000015
1980	0.000016
1985	0.000019
1990	0.000018
1995	0.000017
2000	0.000015
2005	0.000016
2010	0.000015
2015	0.000021
2020	0.000016
2025	0.000016
2030	0.000015
2040	0.000021
2045	0.000015
2055	0.000017
2060	0.000017
2065	0.000016
2070	0.000016
2075	0.000019
2080	0.000019
2085	0.000015
2090	0.000015
2095	0.000018
2100	0.000020
2105	0.000021
2110	0.000020
2115	0.000013
2120	0.000013
2125	0.000013
2130	0.000014
2145	0.000013
2150	0.000016
2155	0.000021
2165	0.000024
2170	0.000019
2175	0.000017
2180	0.000023
2185	0.000022
2190	0.000000

Table C2. Test A3, ^{3}H.

Effluent *gm*	Activity *µCi / gm*
1.10	0.000000
3.92	0.000028
7.55	0.000040
12.11	0.000047
16.53	0.000033
20.92	0.000032
25.27	0.000034
29.63	0.000049
33.94	0.000084
38.24	0.000164
42.51	0.000344
46.72	0.000594
51.05	0.000943
55.35	0.001305
59.63	0.001744
64.02	0.002038
68.37	0.002426
72.65	0.002714
77.00	0.002920
84.78	0.003202
89.01	0.003173
93.20	0.003265
97.42	0.003252
101.68	0.003209
105.88	0.003090
110.04	0.002989
114.22	0.002854
118.45	0.002724
122.60	0.002611
126.94	0.002467
131.19	0.002416
135.51	0.002282
139.78	0.002135
149.09	0.001851
153.70	0.001738
157.90	0.001697
162.20	0.001584
166.60	0.001510
171.02	0.001446
175.72	0.001319
180.32	0.001253
184.73	0.001167
189.17	0.001090
193.47	0.001084
197.77	0.001049
202.65	0.000988
207.15	0.000940
211.98	0.000875
216.48	0.000843
220.89	0.000799
225.27	0.000775
228.91	0.000753
233.36	0.000713
237.78	0.000699
242.18	0.000655
246.38	0.000642
250.54	0.000626
254.66	0.000594
258.98	0.000541
263.00	0.000533
267.29	0.000523
272.14	0.000505
276.48	0.000478
281.11	0.000431
285.47	0.000425
289.81	0.000398
294.04	0.000398
298.21	0.000389
302.39	0.000384
305.70	0.000360
313.89	0.000351
318.21	0.000342
322.30	0.000334
326.38	0.000333
330.68	0.000305
335.07	0.000312
339.49	0.000283
343.81	0.000273
348.06	0.000254
352.29	0.000251
356.47	0.000249
360.80	0.000249
365.23	0.000235
369.84	0.000239
374.05	0.000218
378.32	0.000198
382.58	0.000199
386.97	0.000202
391.06	0.000187
395.22	0.000189
399.42	0.000185
403.58	0.000174
407.73	0.000180
412.15	0.000175
416.08	0.000166
420.03	0.000162
424.15	0.000156
428.23	0.000154
432.18	0.000149
436.25	0.000145
440.33	0.000132
445.21	0.000143
451.24	0.000155
453.33	0.000118
455.98	0.000133
460.58	0.000123
464.32	0.000115
468.22	0.000122
472.39	0.000121
476.61	0.000122
480.78	0.000113
484.17	0.000106
487.78	0.000111
491.59	0.000099
495.65	0.000108
499.70	0.000104
503.95	0.000092
508.27	0.000095
512.42	0.000086
518.69	0.000103
519.96	0.000038
523.80	0.000069
527.92	0.000081
532.16	0.000072
536.46	0.000075
540.79	0.000066
545.12	0.000067
549.28	0.000066
553.44	0.000058
557.67	0.000061
561.63	0.000059
565.87	0.000053
571.35	0.000063
574.75	0.000057
577.85	0.000044
582.11	0.000036
585.56	0.000028
589.76	0.000037
593.88	0.000038
598.08	0.000044
602.13	0.000040
606.40	0.000031
610.20	0.000035
614.70	0.000038
618.45	0.000025
622.64	0.000020
626.80	0.000028
630.96	0.000023
635.09	0.000024

Effluent *gm*	Activity *µCi / gm*
639.24	0.000028
643.35	0.000026
647.47	0.000026
650.35	0.000021
654.13	0.000024
658.15	0.000025
662.36	0.000020
668.64	0.000044
670.49	0.000019
674.65	0.000025
678.71	0.000024
682.84	0.000021
687.14	0.000017
691.22	0.000017
695.35	0.000018
699.59	0.000024
705.35	0.000033
707.15	0.000000
710.68	0.000009
714.64	0.000011
718.71	0.000014
722.69	0.000004
726.79	0.000004
731.07	0.000017
734.94	0.000014
738.52	0.000004
742.57	0.000012
746.69	0.000016
750.82	0.000016
755.04	0.000013
759.05	0.000008
763.10	0.000008
766.83	0.000003
770.63	0.000000
774.49	-0.000005
778.29	-0.000008
782.24	0.000005
785.87	0.000004
789.68	0.000004
793.75	0.000000
797.64	0.000001
802.34	0.000009
805.31	0.000002
809.01	0.000001
812.96	0.000003
816.80	-0.000004
820.77	0.000003
824.85	0.000000
828.60	-0.000005
832.55	-0.000004
838.90	0.000021
840.39	-0.000022

Table C3. Test A4, ^{22}Na.

Effluent *gm*	Activity *μCi / gm*
1.82	0.000803
8.49	0.000681
17.21	0.000505
22.16	0.000530
27.42	0.000454
33.01	0.000405
38.58	0.000389
48.36	0.000562
53.96	0.002860
59.37	0.012100
64.70	0.029900
70.16	0.051500
75.43	0.081400
80.78	0.103000
86.11	0.121000
91.32	0.141000
96.41	0.155000
107.59	0.156000
124.43	0.163000
129.46	0.165000
140.57	0.147000
145.99	0.146000
151.62	0.133000
157.22	0.128000
167.54	0.111000
177.27	0.104000
183.17	0.091500
188.40	0.093800
194.20	0.078800
200.01	0.071400
205.72	0.067400
216.53	0.062600
227.16	0.058800
232.29	0.056100
244.92	0.047100
254.40	0.047200
258.94	0.044400
269.34	0.035700
273.33	0.041400
277.87	0.035100
283.07	0.030600
298.45	0.031600
303.18	0.026300
312.57	0.026900
317.02	0.025500
322.18	0.021100
326.59	0.023900
331.19	0.020300
336.26	0.018700
341.38	0.017900
348.05	0.015100
352.00	0.020400
355.94	0.019300
361.24	0.015100
365.92	0.016200
372.17	0.012400
381.40	0.015600
384.93	0.017000
389.20	0.014200
395.08	0.011000
398.96	0.014200
404.07	0.011200
407.85	0.013300
414.77	0.011000
425.54	0.011100
430.06	0.009930
433.74	0.011000
439.96	0.007670
442.99	0.012200
446.88	0.009990
451.60	0.008050
456.30	0.008310
468.07	0.006730
472.04	0.008650
475.18	0.010100
479.65	0.008030
485.45	0.006070
490.14	0.006940
496.05	0.005970
499.76	0.008020
504.58	0.006260
509.36	0.006290
513.07	0.007410
519.52	0.004870
523.17	0.007270
527.47	0.006240
534.40	0.004280
537.53	0.007170
542.16	0.005190
548.81	0.004280
553.57	0.005280
556.78	0.006620
560.94	0.005180
565.60	0.005470
570.40	0.004850
576.95	0.003940
581.58	0.004780
585.94	0.004790
589.41	0.005610
593.86	0.004440
599.55	0.003650
603.25	0.005250
608.25	0.003990
614.59	0.003480
619.27	0.004210

Table C4. Test B1, ^{3}H.

Effluent *gm*	Activity *µCi / gm*
4.42	0.000002
6.99	0.000002
10.35	0.000002
14.24	0.000003
18.48	0.000002
22.99	0.000002
27.62	0.000004
32.36	0.000003
37.25	0.000002
42.13	0.000000
47.09	0.000003
52.09	0.000001
57.15	0.000001
62.17	0.000001
67.11	0.000001
71.98	0.000003
76.74	0.000001
86.10	0.000002
90.83	0.000003
95.59	0.000002
100.28	0.000001
105.05	0.000000
114.57	0.000003
119.42	0.000002
124.25	0.000003
129.02	0.000002
133.89	0.000002
138.57	0.000001
140.60	0.000001
145.91	0.000003
150.65	0.000001
155.38	0.000000
160.11	0.000002
164.99	0.000001
169.84	0.000002
174.70	0.000005
179.56	0.000000
184.42	0.000005
189.29	0.000000
194.23	0.000002
199.19	0.000003
204.16	0.000002
209.09	0.000005
213.94	0.000009
218.83	0.000008
223.57	0.000009
228.52	0.000012
233.26	0.000013
237.92	0.000015
242.80	0.000015
247.54	0.000019
252.34	0.000024
257.13	0.000026
261.90	0.000028
266.57	0.000032
271.29	0.000038
275.87	0.000039
280.44	0.000040
285.05	0.000052
289.61	0.000054
292.54	0.000050
297.17	0.000055
302.49	0.000064
307.54	0.000068
312.49	0.000075
317.44	0.000076
322.34	0.000094
327.28	0.000086
332.24	0.000090
337.21	0.000107
342.27	0.000100
347.20	0.000106
352.21	0.000109
357.09	0.000111
361.96	0.000127
366.81	0.000123
371.66	0.000136
376.46	0.000132
381.20	0.000144
385.93	0.000147
390.55	0.000151
395.19	0.000146
399.82	0.000154
404.45	0.000148
409.18	0.000156
413.82	0.000160
418.50	0.000163
423.17	0.000163
427.83	0.000164
432.48	0.000179
437.12	0.000184
441.76	0.000177
446.48	0.000182
451.22	0.000178
455.95	0.000190
460.71	0.000186
465.47	0.000186
470.29	0.000188
475.10	0.000196
479.99	0.000191
484.86	0.000186
489.76	0.000184
494.60	0.000189
499.46	0.000190
504.33	0.000193
509.17	0.000203
513.98	0.000196
518.83	0.000188
523.57	0.000200
528.38	0.000205
533.13	0.000202
537.83	0.000185
542.65	0.000193
547.36	0.000194
552.14	0.000185
556.91	0.000201
561.78	0.000184
566.52	0.000193
571.23	0.000193
576.10	0.000181
580.87	0.000196
585.66	0.000194
590.58	0.000178
595.48	0.000187
599.72	0.000188
604.51	0.000179
609.45	0.000179
614.29	0.000191
619.19	0.000178
624.19	0.000173
629.11	0.000173
634.02	0.000173
638.96	0.000178
643.87	0.000173
648.85	0.000172
653.75	0.000161
658.66	0.000176
663.56	0.000171
668.44	0.000163
673.33	0.000172
678.15	0.000170
682.48	0.000171
687.40	0.000160
692.22	0.000167
697.08	0.000160
701.94	0.000152
706.79	0.000159
711.63	0.000153
716.47	0.000158

Effluent *gm*	Activity *µCi / gm*	Effluent *gm*	Activity *µCi / gm*	Effluent *gm*	Activity *µCi / gm*
721.27	0.000158	963.79	0.000106	1201.47	0.000069
726.04	0.000158	968.31	0.000094	1206.46	0.000058
730.76	0.000156	972.84	0.000089	1211.55	0.000062
735.74	0.000155	977.33	0.000091	1216.70	0.000058
740.62	0.000149	981.84	0.000097	1221.77	0.000058
745.58	0.000143	986.44	0.000099	1226.76	0.000065
750.76	0.000141	990.96	0.000091	1231.80	0.000066
755.90	0.000145	995.55	0.000085	1236.72	0.000059
760.95	0.000145	1000.12	0.000089	1241.82	0.000059
765.88	0.000138	1004.75	0.000096	1246.47	0.000061
770.72	0.000136	1009.39	0.000090	1251.31	0.000058
775.49	0.000145	1014.12	0.000097	1256.10	0.000056
780.27	0.000143	1018.75	0.000080	1260.92	0.000057
785.05	0.000145	1022.24	0.000098	1265.83	0.000060
789.84	0.000135	1027.06	0.000087	1270.66	0.000059
794.77	0.000135	1031.78	0.000085	1275.50	0.000061
799.64	0.000136	1036.47	0.000084	1280.38	0.000053
804.53	0.000126	1041.24	0.000086	1285.26	0.000059
809.33	0.000134	1046.02	0.000079	1290.10	0.000056
814.07	0.000137	1050.91	0.000085	1294.94	0.000055
818.77	0.000121	1055.76	0.000084	1299.74	0.000053
823.51	0.000123	1060.61	0.000081	1304.54	0.000053
828.17	0.000123	1065.52	0.000079	1309.06	0.000056
832.83	0.000123	1070.50	0.000075	1313.67	0.000053
837.47	0.000121	1075.48	0.000077	1318.30	0.000054
842.18	0.000115	1080.48	0.000078	1322.84	0.000054
846.90	0.000124	1085.39	0.000073	1327.31	0.000054
851.55	0.000121	1090.29	0.000075	1331.81	0.000052
856.27	0.000123	1095.19	0.000078	1336.33	0.000056
861.01	0.000124	1100.03	0.000071	1340.94	0.000053
865.82	0.000110	1104.79	0.000069	1345.56	0.000053
870.64	0.000111	1109.55	0.000074	1350.23	0.000059
875.27	0.000123	1114.41	0.000066	1354.91	0.000057
879.96	0.000112	1119.18	0.000078	1359.51	0.000055
884.71	0.000115	1123.89	0.000077	1364.14	0.000053
889.41	0.000116	1128.67	0.000074	1368.79	0.000049
894.31	0.000109	1133.41	0.000070	1373.37	0.000050
899.21	0.000114	1138.20	0.000073	1378.00	0.000049
904.29	0.000104	1143.08	0.000065	1382.58	0.000051
909.51	0.000114	1147.88	0.000074	1387.15	0.000051
915.07	0.000107	1152.68	0.000073	1391.74	0.000049
921.02	0.000105	1157.57	0.000063	1396.34	0.000053
925.58	0.000106	1162.30	0.000069	1400.92	0.000048
930.38	0.000113	1167.03	0.000062	1405.60	0.000050
935.19	0.000107	1171.93	0.000065	1410.31	0.000047
940.03	0.000108	1176.67	0.000065	1414.97	0.000048
944.86	0.000100	1181.52	0.000063	1419.67	0.000049
949.69	0.000104	1186.49	0.000065	1424.28	0.000048
954.43	0.000099	1191.37	0.000066	1428.89	0.000046
959.15	0.000098	1196.47	0.000063	1433.50	0.000046

Effluent *gm*	Activity *µCi / gm*
1438.07	0.000047
1442.78	0.000046
1447.34	0.000050
1451.90	0.000044
1456.54	0.000046
1461.22	0.000046
1465.84	0.000046
1470.51	0.000042
1475.33	0.000044
1480.03	0.000045
1484.79	0.000046
1489.58	0.000044
1494.42	0.000041
1499.16	0.000042
1503.99	0.000041
1508.80	0.000044
1513.54	0.000044
1518.35	0.000040
1523.25	0.000042
1528.13	0.000042
1533.04	0.000044
1537.87	0.000039
1542.74	0.000039
1547.53	0.000036
1552.29	0.000040
1556.94	0.000037
1561.60	0.000040
1566.34	0.000038
1570.97	0.000038
1575.67	0.000039
1580.40	0.000038
1585.13	0.000037
1589.88	0.000038
1594.60	0.000038
1599.32	0.000038
1604.11	0.000038
1608.88	0.000035
1613.54	0.000036
1618.36	0.000034
1623.11	0.000035
1627.94	0.000031
1632.68	0.000036
1637.49	0.000036
1642.38	0.000033
1647.24	0.000035
1652.08	0.000034
1656.93	0.000035
1661.86	0.000033
1666.70	0.000032
1671.58	0.000034

Effluent *gm*	Activity *µCi / gm*
1676.37	0.000034
1681.18	0.000032
1685.92	0.000031
1690.58	0.000035
1695.27	0.000031
1699.87	0.000033
1704.47	0.000031
1709.17	0.000029
1713.78	0.000032
1718.43	0.000032
1723.20	0.000031
1727.87	0.000034
1732.60	0.000030
1737.28	0.000030
1742.03	0.000032
1746.68	0.000030
1751.33	0.000031
1756.02	0.000030
1760.67	0.000029
1765.45	0.000030
1770.18	0.000029
1774.92	0.000030
1779.62	0.000029
1784.43	0.000029
1789.35	0.000030
1794.23	0.000028
1799.13	0.000028
1804.07	0.000028
1808.90	0.000029
1813.67	0.000029
1818.45	0.000030
1823.23	0.000028
1828.03	0.000029
1832.72	0.000029
1837.40	0.000027
1842.15	0.000026
1846.83	0.000027
1851.55	0.000026
1856.32	0.000027
1861.07	0.000024
1865.85	0.000027
1870.72	0.000025
1875.53	0.000026
1880.38	0.000025
1885.43	0.000026
1890.20	0.000026
1895.08	0.000025
1899.90	0.000025
1904.67	0.000024
1909.42	0.000024

Effluent *gm*	Activity *µCi / gm*
1914.17	0.000025
1918.97	0.000025
1923.82	0.000025
1928.70	0.000022

Table C5. Test B2, ^{22}Na.

Effluent *gm*	Activity *µCi / gm*	Effluent *gm*	Activity *µCi / gm*	Effluent *gm*	Activity *µCi / gm*
2.99	0.000050	230.66	0.002240	502.19	0.011000
6.67	0.000115	235.51	0.002390	507.01	0.010800
10.58	0.000023	240.36	0.002800	511.83	0.010800
14.94	0.000057	245.28	0.003000	516.69	0.010500
19.13	0.000026	250.07	0.003530	521.57	0.010500
23.53	0.000022	254.75	0.003820	526.37	0.010500
27.90	0.000065	268.91	0.004900	531.27	0.010400
32.47	0.000030	273.86	0.005100	536.26	0.010100
36.88	0.000027	278.86	0.005420	541.18	0.010300
41.31	0.000024	283.91	0.005680	546.15	0.010100
45.80	0.000027	288.93	0.006290	551.16	0.009800
50.21	0.000029	293.96	0.006480	556.18	0.010100
54.71	0.000027	299.05	0.006960	561.31	0.009380
59.28	0.000029	303.99	0.007150	566.45	0.009460
63.76	0.000027	308.99	0.007320	571.51	0.009150
68.32	0.000027	313.95	0.008020	576.54	0.009060
72.82	0.000025	318.82	0.008130	581.43	0.009420
77.31	0.000028	323.69	0.008490	586.24	0.009140
81.71	0.000024	328.59	0.008850	591.01	0.009440
86.32	0.000029	333.51	0.009230	595.73	0.009070
90.84	0.000020	338.49	0.009310	600.39	0.009180
95.42	0.000029	343.34	0.009590	605.07	0.009070
99.99	0.000022	348.16	0.009890	609.82	0.008940
104.70	0.000026	352.95	0.010100	614.55	0.008920
109.68	0.000027	357.69	0.010600	632.95	0.008550
114.68	0.000019	367.21	0.010700	637.65	0.008480
119.70	0.000028	372.02	0.010700	642.34	0.008240
124.63	0.000031	376.79	0.011000	647.17	0.008030
129.52	0.000053	381.60	0.011100	651.86	0.008140
134.40	0.000034	400.68	0.011400	656.62	0.007970
139.33	0.000028	405.71	0.010900	661.35	0.008130
144.26	0.000060	410.51	0.011500	666.15	0.007630
149.10	0.000183	415.35	0.011400	670.98	0.007430
153.92	0.000056	420.21	0.011800	675.77	0.007360
158.77	0.000078	425.13	0.011200	680.70	0.007270
163.59	0.000078	430.04	0.011300	685.70	0.007280
168.41	0.000100	435.08	0.011300	690.82	0.006960
173.18	0.000143	439.90	0.011300	695.86	0.007140
177.98	0.000207	444.65	0.011800	701.01	0.006720
182.85	0.000243	449.45	0.011900	706.19	0.006800
187.59	0.000356	454.21	0.011600	711.40	0.006440
192.38	0.000481	459.00	0.011800	716.62	0.006630
197.21	0.000560	463.81	0.011500	721.80	0.006090
202.01	0.000785	468.61	0.011300	727.00	0.006480
206.75	0.000953	473.45	0.011200	732.14	0.006350
211.58	0.001050	478.25	0.011300	737.27	0.006150
216.35	0.001360	483.02	0.011300	742.29	0.006450
221.14	0.001610	487.79	0.011000	747.29	0.006080
225.93	0.001860	492.66	0.010700	752.24	0.006230
		497.38	0.011100	757.15	0.006130

Effluent *gm*	Activity *µCi / gm*
762.12	0.005740
766.97	0.006190
771.85	0.005990
776.77	0.005730
781.76	0.005680
786.66	0.005640
791.62	0.005540
807.11	0.005150
811.94	0.005570
821.05	0.005400
825.84	0.005220
830.60	0.005260
835.37	0.005210
840.21	0.005060
845.15	0.004860
850.04	0.004990
854.87	0.004810
859.97	0.004720
864.71	0.004990
869.60	0.004580
874.27	0.004870
879.07	0.004610
883.88	0.004650
888.62	0.004580
893.31	0.004530
897.98	0.004560
902.77	0.004460
907.64	0.004290
912.47	0.004320
917.32	0.004400
922.10	0.004300
936.03	0.004260
940.63	0.004320
945.27	0.004200
949.98	0.003970
954.51	0.004320
959.33	0.004070
968.29	0.004000
972.86	0.003950
977.55	0.003830
982.25	0.003780
986.95	0.003930
991.64	0.003910
996.40	0.003660
1001.15	0.003630
1005.92	0.003600
1010.70	0.003590
1015.46	0.003550
1020.08	0.003590
1024.70	0.003640

Effluent *gm*	Activity *µCi / gm*
1029.37	0.003580
1033.97	0.003570
1038.60	0.003440
1043.30	0.003260
1047.96	0.003300
1052.61	0.003240
1057.28	0.003230
1061.92	0.003310
1066.62	0.003120
1071.31	0.003170
1075.96	0.003110
1080.58	0.003180
1085.19	0.003130
1089.87	0.002890
1094.52	0.003080
1099.28	0.003030
1104.01	0.002990
1108.87	0.002890
1113.80	0.002790
1118.56	0.002840
1123.33	0.002780
1128.15	0.002850
1133.04	0.002660
1137.80	0.002800
1142.54	0.002730
1147.29	0.002670
1152.02	0.002660
1156.82	0.002540
1161.65	0.002650
1169.90	0.002440
1174.71	0.002490
1179.57	0.002440
1184.41	0.002450
1189.30	0.002370
1194.10	0.002530
1198.98	0.002430
1203.72	0.002400
1208.55	0.002430
1213.24	0.002350
1218.06	0.002360
1222.78	0.002350
1227.73	0.002080
1232.91	0.002240
1237.86	0.002120
1242.24	0.002280
1247.02	0.002240
1251.85	0.002140
1256.77	0.002080
1261.71	0.002060
1271.21	0.002150

Effluent *gm*	Activity *µCi / gm*
1290.39	0.002080
1309.86	0.001910
1329.14	0.001900
1348.04	0.001910
1367.39	0.001950
1386.49	0.001760
1405.95	0.001660
1425.54	0.001630
1445.58	0.001440
1465.53	0.001450
1484.73	0.001460
1504.20	0.001470
1523.08	0.001420
1542.28	0.001320
1562.24	0.001270
1582.06	0.001260
1602.29	0.001230
1621.40	0.001230
1641.13	0.001160
1660.41	0.001050
1679.58	0.001120

Table C6. Test B3, ^{22}Na.

Effluent *gm*	Activity *µCi / gm*
6.30	0.000841
9.91	0.000951
14.23	0.000801
18.06	0.001071
22.49	0.000791
27.01	0.000821
31.35	0.000811
35.97	0.000741
40.61	0.000741
45.24	0.000691
49.95	0.000691
54.59	0.000731
59.29	0.000661
63.92	0.000671
68.61	0.000641
73.33	0.000637
78.12	0.000731
82.82	0.000631
87.57	0.000721
92.24	0.000649
97.06	0.000711
101.81	0.000592
106.49	0.000627
111.16	0.000671
115.48	0.000681
120.00	0.000651
124.56	0.000614
129.11	0.000681
133.75	0.000658
138.36	0.000597
142.99	0.000691
147.64	0.000731
152.39	0.000660
157.07	0.000741
161.79	0.000801
166.62	0.000851
171.48	0.000951
176.34	0.001131
181.14	0.001301
185.98	0.001511
190.88	0.001541
195.73	0.001921
200.91	0.002021
205.46	0.002511
210.27	0.002541
215.05	0.002981
219.83	0.003351
224.66	0.003681
229.60	0.003851
234.19	0.004381
238.96	0.004841
243.76	0.005091
248.65	0.005091
253.17	0.006191
257.76	0.006341
262.34	0.006581
267.04	0.006701
271.64	0.007121
276.20	0.007881
280.85	0.007631
285.48	0.007891
290.12	0.007991
294.87	0.008261
299.61	0.008571
304.28	0.008591
309.06	0.008761
313.81	0.009121
318.62	0.009551
323.39	0.009411
328.13	0.009581
332.79	0.010061
337.66	0.009601
342.18	0.010361
346.82	0.009861
351.48	0.009861
356.08	0.010361
360.67	0.010061
365.39	0.010061
369.97	0.010061
374.34	0.010761
378.75	0.010661
383.29	0.010761
387.70	0.010861
392.28	0.010261
396.99	0.010161
401.82	0.009861
406.06	0.010261
410.64	0.010161
415.43	0.009861
420.17	0.009661
424.99	0.009511
429.71	0.009761
434.49	0.009531
439.34	0.009311
444.14	0.009511
449.01	0.009151
453.94	0.009521
458.62	0.009481
463.53	0.009271
468.26	0.008981
472.99	0.009191
477.72	0.009391
482.52	0.008631
487.30	0.009131
492.10	0.008651
496.91	0.008731
501.77	0.008541
515.78	0.008561
530.07	0.008001
544.12	0.007731
558.19	0.007671
572.62	0.007291
587.59	0.006931
601.86	0.006871
616.39	0.006491
630.86	0.006511
645.24	0.006251
659.75	0.006001
674.15	0.005801
688.58	0.005561
703.25	0.005271
717.74	0.005041
732.50	0.004931
747.25	0.004831
761.57	0.004541
775.70	0.004871
790.00	0.004511
804.46	0.004171
818.70	0.004051
833.20	0.003821
847.66	0.003651
862.54	0.003531
877.54	0.003791
892.30	0.003421
906.94	0.003301
921.39	0.003571
935.83	0.003091
949.96	0.003141
964.24	0.002911
978.52	0.002721
993.01	0.002641
1007.51	0.002501
1022.18	0.002551
1037.39	0.002391
1051.70	0.002391
1066.00	0.002381
1080.44	0.002291
1094.94	0.002111
1109.54	0.002161

Effluent *gm*	Activity *µCi / gm*	Effluent *gm*	Activity *µCi / gm*	Effluent *gm*	Activity *µCi / gm*
1124.05	0.002091	1939.67	0.000340	2893.68	0.000072
1138.16	0.002011	1958.67	0.000381	2914.32	0.000152
1152.25	0.002021	1977.53	0.000397	2933.73	0.000094
1166.94	0.001851	1997.02	0.000310	2952.52	0.000057
1181.91	0.001831	2016.60	0.000393	2971.52	0.000079
1196.59	0.001801	2036.37	0.000334	2990.35	0.000102
1210.93	0.001721	2055.63	0.000390	3009.53	0.000109
1225.29	0.001691	2074.55	0.000295	3029.63	0.000081
1239.64	0.001771	2093.58	0.000424	3049.73	0.000039
1253.84	0.001581	2107.78	0.000320	3069.23	0.000030
1268.09	0.001541	2130.07	0.000329	3088.25	0.000065
1282.33	0.001481	2149.58	0.000266	3106.93	0.000112
1296.26	0.001681	2169.47	0.000329	3125.50	0.000061
1310.41	0.001531	2189.17	0.000367	3144.42	0.000066
1324.63	0.001571	2208.37	0.000277	3164.43	0.000046
1338.61	0.001501	2227.60	0.000238	3184.28	0.000044
1352.46	0.001451	2246.48	0.000269	3202.87	0.000012
1366.26	0.001331	2264.90	0.000281	3221.17	0.000014
1380.05	0.001391	2283.78	0.000261	3240.43	0.000013
1393.73	0.001431	2302.93	0.000223	3259.02	0.000008
1407.51	0.001301	2321.83	0.000329	3277.87	0.000027
1421.54	0.001231	2340.48	0.000322	3296.17	0.000072
1435.67	0.001191	2359.37	0.000230	3315.28	0.000013
1450.13	0.001191	2378.17	0.000248	3334.08	0.000047
1464.61	0.001231	2396.65	0.000251	3352.53	0.000104
1478.90	0.001091	2415.23	0.000193	3370.42	0.000035
1493.38	0.001101	2434.33	0.000213	3388.52	0.000036
1507.35	0.001231	2453.42	0.000267	3406.62	0.000034
1521.54	0.001081	2472.57	0.000145	3425.07	0.000051
1535.42	0.001071	2492.17	0.000170	3444.38	0.000006
1554.39	0.001021	2510.20	0.000206	3463.53	-0.000014
1573.54	0.000911	2529.08	0.000282	3483.85	-0.000016
1593.35	0.000821	2548.23	0.000102	3500.80	0.000026
1612.30	0.000931	2567.42	0.000141	3519.93	-0.000018
1631.81	0.000851	2586.53	0.000143	3538.47	0.000054
1650.87	0.000881	2605.82	0.000107	3557.38	0.000005
1670.17	0.000731	2623.10	0.000147	3577.78	-0.000019
1689.32	0.000821	2642.12	0.000060	3596.68	-0.000002
1708.78	0.000721	2660.98	0.000123	3615.98	0.000009
1728.42	0.000681	2679.83	0.000075	3635.07	0.000016
1748.30	0.000671	2698.77	0.000118	3654.22	0.000007
1768.10	0.000655	2718.17	0.000085	3673.33	-0.000001
1787.23	0.000701	2738.43	0.000049	3696.92	0.000009
1806.47	0.000656	2758.63	0.000111	3711.12	0.000022
1825.58	0.000721	2778.25	0.000218	3759.82	0.000062
1851.17	0.000602	2797.45	0.000086	3783.13	-0.000031
1869.72	0.000615	2817.33	0.000104	3801.97	0.000034
1883.17	0.000446	2835.08	0.000080	3821.03	-0.000024
1902.03	0.000475	2853.47	0.000238	3840.03	0.000081
1920.78	0.000400	2872.85	0.000063	3859.02	0.000032

Effluent *gm*	Activity *µCi / gm*
3882.42	0.000136
3896.50	-0.000029
3910.80	0.000006
3929.65	0.000006
3943.98	0.000007
3958.18	-0.000004
3972.57	0.000023
3987.47	-0.000014
4002.82	0.000002
4017.97	0.000020
4032.88	0.000135
4047.65	0.000033
4062.12	0.000069
4076.53	0.000040
4090.67	0.000068
4104.95	0.000066
4119.37	0.000153
4133.80	0.000007
4148.53	0.000051
4163.32	0.000009
4177.77	0.000174
4192.17	-0.000017
4206.57	0.000009
4220.92	-0.000047
4235.22	-0.000035
4248.43	0.000030
4261.77	0.000011
4275.42	0.000004
4289.58	-0.000027
4303.62	0.000018
4317.63	-0.000025
4331.37	-0.000033
4345.22	-0.000020
4358.83	-0.000023
4372.62	-0.000057
4386.22	-0.000014
4399.98	0.000000
4414.17	-0.000017
4429.07	-0.000059
4438.78	-0.000034
4453.28	-0.000027
4467.68	-0.000014
4481.82	-0.000024
4495.87	-0.000041
4505.07	0.000026
4514.32	0.000021
4527.97	-0.000006
4541.93	-0.000061
4556.83	-0.000041
4571.85	-0.000053
4596.55	-0.000046
4611.15	-0.000014
4625.67	-0.000044
4640.08	-0.000067
4654.53	-0.000052
4669.13	-0.000067

Table C7. Test B3, ^{232}U.

Effluent *gm*	Activity *µCi / gm*
6.30	0.000118
14.23	0.000108
22.49	0.000117
31.35	0.000107
40.61	0.000108
49.95	0.000110
59.29	0.000108
68.61	0.000105
78.12	0.000103
87.57	0.000103
97.06	0.000100
106.49	0.000102
115.48	0.000102
124.56	0.000100
133.75	0.000102
142.99	0.000111
152.39	0.000116
161.79	0.000110
171.48	0.000148
181.14	0.000174
190.88	0.000220
200.91	0.000259
210.27	0.000322
219.83	0.000400
229.60	0.000466
238.96	0.000526
248.65	0.000607
257.76	0.000699
267.04	0.000753
276.20	0.000886
285.48	0.000946
294.87	0.001050
304.28	0.001160
313.81	0.001350
323.39	0.001510
332.79	0.001670
342.18	0.001880
351.48	0.001930
360.67	0.002420
369.97	0.002600
378.75	0.002950
387.70	0.003240
396.99	0.003400
406.06	0.003730
415.43	0.004010
424.99	0.004630
434.49	0.004940
444.14	0.005380
453.94	0.005940
463.53	0.006130
487.30	0.007180
511.13	0.008310
534.73	0.008950
558.19	0.009700
582.55	0.010800
606.65	0.011800
630.86	0.012900
654.91	0.014000
678.96	0.014300
703.25	0.015200
727.56	0.016000
752.06	0.016100
775.70	0.016400
799.62	0.017200
823.48	0.018000
847.66	0.017900
872.71	0.018500
897.12	0.018800
921.39	0.017500
945.47	0.020000
968.94	0.019000
993.01	0.020200
1017.28	0.020400
1042.25	0.020400
1066.00	0.020700
1090.08	0.021300
1114.33	0.020200
1138.16	0.020200
1162.07	0.020200
1186.83	0.020200
1210.93	0.020100
1234.84	0.021000
1258.64	0.020100
1282.33	0.021100
1305.70	0.021600
1329.45	0.022200
1352.46	0.021600
1375.44	0.022500
1398.42	0.021500
1421.54	0.022400
1469.39	0.022000
1516.93	0.020900
1563.92	0.021800
1612.30	0.020900
1660.47	0.020500
1708.78	0.020300
1758.18	0.020000
1806.47	0.019800
1851.17	0.019200
1892.62	0.020000
1939.67	0.018700
1987.17	0.019200
2036.37	0.018500
2084.10	0.018600
2130.07	0.018000
2179.38	0.017500
2227.60	0.016900
2274.22	0.018000
2321.83	0.016900
2369.17	0.016800
2415.23	0.016500
2463.02	0.016500
2510.20	0.016000
2557.85	0.015400
2605.82	0.014700
2651.48	0.015400
2698.77	0.015100
2748.62	0.014200
2797.45	0.014000
2843.18	0.013900
2893.68	0.013400
2943.02	0.012900
2990.35	0.012400
3039.68	0.012700
3088.25	0.011800
3111.52	0.012000
3134.93	0.012200
3159.42	0.011700
3184.28	0.011700
3207.12	0.011500
3230.63	0.011500
3254.32	0.011600
3278.02	0.011600
3300.87	0.011800
3324.78	0.011800
3348.18	0.011400
3370.53	0.011400
3393.23	0.011400
3415.87	0.011300
3439.42	0.010800
3463.43	0.010900
3488.57	0.010500
3510.38	0.010700
3533.80	0.010300
3557.23	0.010500
3582.48	0.009880
3606.33	0.010100
3630.28	0.009790
3654.08	0.009690

Effluent gm	Activity $\mu Ci / gm$
3678.05	0.009690
3701.63	0.009960
3727.83	0.010100
3759.98	0.009730
3787.83	0.009870
3806.68	0.009490
3830.48	0.009390
3854.22	0.009420
3887.13	0.009720
3901.22	0.009490
3948.73	0.009450
3997.72	0.009330
4047.65	0.009130
4095.43	0.008720
4143.62	0.008730
4192.17	0.008400
4240.72	0.008910
4284.80	0.009190
4331.37	0.008790
4377.13	0.008740
4424.13	0.008440
4467.68	0.008450
4509.60	0.008590
4551.77	0.008530
4596.55	0.008310
4644.97	0.008320
4669.13	0.008400

Table C8. Test B4, ^{22}Na.

Effluent *gm*	Activity *µCi / gm*
2.09	0.000599
3.72	0.000554
5.84	0.000463
8.93	0.000416
10.54	0.000549
13.26	0.000389
14.75	0.000571
18.09	0.000452
21.75	0.000340
25.52	0.000329
29.55	0.000361
33.68	0.000526
38.42	0.000241
43.14	0.000314
46.50	0.000405
50.99	0.000314
55.50	0.000311
60.08	0.000287
64.70	0.000316
69.28	0.000300
73.91	0.000267
78.54	0.000283
83.18	0.000266
87.83	0.000295
92.51	0.000301
97.24	0.000293
101.93	0.000289
106.60	0.000286
111.33	0.000297
116.14	0.000229
120.92	0.000311
125.79	0.000280
130.59	0.000262
135.52	0.000283
140.35	0.000274
145.32	0.000344
150.16	0.000309
155.07	0.000405
160.01	0.000290
164.86	0.000327
169.73	0.000309
174.56	0.000298
179.33	0.000355
184.13	0.000472
188.84	0.000509
193.61	0.000608
198.27	0.000730
202.98	0.000936
207.60	0.001070
212.23	0.001170
216.83	0.001420
221.41	0.001830
230.36	0.002530
241.44	0.003570
250.41	0.004540
259.76	0.005660
265.01	0.006460
274.72	0.007930
284.62	0.009770
294.58	0.011400
304.33	0.013400
314.17	0.014600
323.95	0.017600
328.85	0.020000
338.66	0.022400
347.87	0.028400
352.49	0.025900
366.40	0.030300
380.65	0.032800
394.89	0.036800
409.66	0.038800
424.37	0.046400
434.01	0.048400
448.24	0.052900
462.30	0.056500
476.44	0.059200
490.42	0.060100
504.50	0.064300
518.22	0.072400
532.00	0.073800
546.17	0.074400
560.53	0.077700
574.79	0.079200
588.96	0.083600
602.97	0.088500
616.84	0.084200
630.43	0.092300
644.30	0.092800
658.39	0.091600
672.66	0.092900
687.08	0.096300
715.53	0.096400
729.61	0.102000
743.86	0.103000
772.12	0.103000
786.30	0.106000
800.55	0.105000
815.15	0.109000
829.77	0.107000
844.44	0.108000
872.74	0.119000
886.61	0.119000
900.39	0.121000
914.41	0.122000
928.14	0.123000
942.06	0.122000
956.19	0.121000
970.57	0.115000
984.51	0.119000
999.03	0.120000
1013.45	0.121000
1027.93	0.125000
1041.99	0.118000
1098.00	0.120000
1112.82	0.123000
1127.51	0.126000
1141.67	0.131000
1155.71	0.127000
1169.79	0.131000
1183.92	0.128000
1211.65	0.134000
1226.17	0.127000
1240.54	0.134000
1255.55	0.125000
1270.57	0.125000
1284.97	0.133000
1299.68	0.131000
1314.21	0.137000
1328.69	0.132000
1343.21	0.129000
1357.89	0.131000
1372.41	0.143000
1400.12	0.141000
1414.69	0.137000
1443.38	0.141000
1457.37	0.144000
1471.26	0.144000
1485.04	0.145000
1498.86	0.139000
1512.74	0.144000
1527.11	0.141000
1541.81	0.138000
1556.80	0.136000
1571.73	0.139000
1586.42	0.143000
1600.96	0.142000
1615.40	0.139000
1629.47	0.146000
1643.74	0.145000

Effluent *gm*	Activity *μCi / gm*
1671.57	0.147000
1686.00	0.143000
1700.67	0.138000
1729.32	0.146000
1743.68	0.146000
1813.80	0.147000
1828.38	0.145000
1843.33	0.139000
1848.22	0.143000
1858.22	0.143000
1873.33	0.142000
1883.25	0.144000
1936.62	0.151000
1946.38	0.140000
1956.33	0.141000
1966.18	0.143000
1975.83	0.142000
1985.38	0.146000
1994.83	0.148000
2004.33	0.148000
2013.73	0.145000
2050.58	0.150000
2060.17	0.146000
2079.78	0.143000
2089.73	0.139000
2099.57	0.145000
2109.23	0.144000

Table C9. Test B5, ^{22}Na.

Effluent *gm*	Activity *µCi / gm*
31.44	0.009730
36.03	0.009220
40.50	0.009830
44.96	0.009510
49.51	0.009640
54.21	0.009600
58.90	0.009030
63.73	0.009370
68.63	0.009300
73.34	0.009240
78.11	0.009010
82.86	0.008480
87.65	0.009320
92.22	0.009100
96.75	0.008900
101.36	0.008560
105.93	0.008840
110.61	0.008820
115.32	0.008490
120.19	0.008420
124.93	0.008690
129.79	0.008280
134.76	0.008630
139.76	0.008350
144.93	0.007980
149.89	0.008550
154.50	0.009080
159.57	0.008500
164.37	0.008650
169.17	0.008580
174.20	0.008550
179.05	0.008740
183.75	0.008550
188.44	0.008800
193.65	0.008360
198.71	0.008870
203.93	0.008960
208.99	0.009320
214.16	0.009220
224.22	0.010500
239.10	0.011400
253.17	0.014100
267.47	0.015400
282.67	0.017000
297.28	0.019900
311.65	0.023200
325.61	0.025200
335.08	0.029400
354.85	0.030500
369.75	0.032900
389.12	0.035400
399.01	0.038600
414.02	0.042200
429.71	0.041600
445.12	0.047600
459.61	0.051600
473.79	0.054000
488.77	0.054500
503.87	0.056400
532.72	0.062700
560.02	0.066500
575.27	0.069100
605.24	0.073100
619.55	0.072700
634.88	0.081300
649.47	0.079700
665.35	0.080500
678.23	0.083100
692.60	0.082000
721.99	0.085200
736.61	0.086800
751.02	0.092200
765.61	0.090900
780.78	0.088100
795.33	0.091600
809.99	0.095200
838.17	0.100000
852.67	0.095200
867.42	0.094000
882.22	0.095900
896.45	0.102000
910.85	0.104000
940.40	0.107000
954.57	0.103000
968.82	0.104000
1027.15	0.114000
1055.00	0.113000
1069.73	0.114000
1112.89	0.115000
1127.43	0.121000
1155.79	0.116000
1169.54	0.124000
1183.50	0.123000
1227.32	0.119000
1241.84	0.127000
1330.52	0.127000
1344.75	0.128000
1374.29	0.131000
1481.51	0.132000
1495.88	0.131000
1523.79	0.137000
1537.85	0.135000
1551.97	0.132000
1580.75	0.131000
1595.03	0.138000
1623.31	0.126000
1638.69	0.134000
1652.53	0.135000
1681.14	0.130000
1710.89	0.124000
1739.81	0.124000
1754.25	0.124000
1784.49	0.126000
1799.22	0.125000
1814.72	0.127000
1830.57	0.130000
1845.23	0.133000
1860.21	0.129000
1904.11	0.130000
1919.08	0.133000
1938.85	0.133000
1945.73	0.135000
1997.85	0.139000
2012.08	0.136000
2026.74	0.138000
2040.27	0.138000
2054.02	0.135000
2068.19	0.133000
2082.99	0.131000
2097.18	0.134000
2111.49	0.131000
2125.70	0.134000
2140.00	0.125000
2155.10	0.123000
2169.93	0.126000
2184.59	0.124000
2213.30	0.119000
2243.74	0.116000
2257.84	0.114000
2272.66	0.107000
2286.36	0.107000
2301.64	0.105000
2315.71	0.099500
2343.92	0.097300
2358.33	0.093800
2388.92	0.093900
2402.36	0.089500
2416.54	0.090200
2461.31	0.078900

Effluent *gm*	Activity *µCi / gm*
2475.49	0.080500
2489.25	0.080400
2518.54	0.069900
2533.50	0.072100
2560.81	0.063800
2619.43	0.059500
2632.75	0.056700
2662.95	0.052600
2677.87	0.051400
2735.46	0.046800
2749.88	0.047500
2764.27	0.046000
2778.41	0.044000
2793.71	0.043400
2823.23	0.041800
2837.49	0.041400
2861.52	0.040900
2875.96	0.040100
2918.95	0.034700
2933.87	0.035000
3016.41	0.032100
3030.48	0.031800
3073.55	0.027000
3088.87	0.026500
3102.30	0.027700
3146.58	0.025100
3161.53	0.024800
3205.81	0.025100
3220.28	0.022700
3234.47	0.023600
3249.53	0.022900
3263.38	0.023500
3278.19	0.022200
3307.23	0.022400
3321.94	0.021400
3348.75	0.020600
3363.56	0.020100
3390.72	0.019700
3404.70	0.020100
3434.51	0.019400
3462.88	0.018900
3520.32	0.017900
3535.78	0.017700
3548.97	0.018800
3563.51	0.017600
3578.53	0.017600
3592.97	0.017200
3606.69	0.016600
3621.29	0.015500
3635.86	0.016700

Effluent *gm*	Activity *µCi / gm*
3651.40	0.014200
3679.63	0.015700
3693.86	0.015100
3707.13	0.015300
3722.14	0.015000
3749.36	0.014500

Table C10. Test B6, ^{22}Na.

Effluent *gm*	Activity *µCi / gm*
95.61	0.011100
104.65	0.011200
113.68	0.011200
123.27	0.011200
133.22	0.011700
143.05	0.011600
153.12	0.011200
162.86	0.011500
172.70	0.011100
181.74	0.011200
186.49	0.011700
195.72	0.012200
205.04	0.011800
214.54	0.012300
224.03	0.012300
233.50	0.012700
242.58	0.013100
251.61	0.013400
261.28	0.012900
271.10	0.013300
280.97	0.013600
290.96	0.013600
300.55	0.013400
310.08	0.013100
319.59	0.013400
329.19	0.013600
339.55	0.013600
349.45	0.013800
359.05	0.013200
368.42	0.013500
378.09	0.013000
387.65	0.013400
396.51	0.014000
405.72	0.013100
415.59	0.013100
426.37	0.013100
436.54	0.012800
446.98	0.013200
460.61	0.012600
465.73	0.012600
475.46	0.012700
489.92	0.012500
506.15	0.012000
520.52	0.011900
534.43	0.011800
548.62	0.011800
564.66	0.011800
578.77	0.011100
592.01	0.010900
606.75	0.010900
622.27	0.010400
639.01	0.010400
652.38	0.009810
666.13	0.010300
680.67	0.010200
695.72	0.010100
710.66	0.009680
723.58	0.009980
736.69	0.009560
750.52	0.009520
765.58	0.008910
781.44	0.008860
795.32	0.008870
808.53	0.008830
822.60	0.008290
837.88	0.008670
852.91	0.008150
866.85	0.007670
881.34	0.008100
896.13	0.008090
928.38	0.007630
970.76	0.008180
986.78	0.007720
1002.20	0.007730
1029.20	0.007260
1044.34	0.007400
1075.75	0.007060
1089.94	0.007060
1115.55	0.007060
1131.28	0.007090
1172.83	0.006380
1186.33	0.006860
1201.81	0.007010
1241.94	0.006660
1257.04	0.006570
1267.54	0.006470
1282.81	0.006300
1296.94	0.006030
1324.98	0.006170
1340.42	0.006040
1369.19	0.005760
1382.51	0.005910
1396.66	0.005980
1413.07	0.005880
1429.22	0.005760
1457.09	0.005780
1472.71	0.005830
1488.55	0.005590
1531.26	0.005720
1562.39	0.005820
1604.34	0.005520
1619.05	0.005670
1634.48	0.005730
1648.38	0.005100
1661.60	0.005420
1675.42	0.005320
1704.36	0.005710
1718.61	0.005390
1732.04	0.005580
1746.73	0.005340
1761.78	0.005480
1776.96	0.005360
1804.68	0.005370
1819.15	0.005220
1904.38	0.005540
1917.81	0.005350
1932.12	0.005410
1946.80	0.004680
1961.72	0.004340
1976.05	0.004680
1990.07	0.004470
2003.89	0.004590
2018.33	0.004420
2048.18	0.004430
2089.76	0.004140
2104.53	0.004310
2120.16	0.004290
2145.80	0.004210
2174.78	0.004380
2189.24	0.004240
2204.47	0.004230
2217.66	0.004100
2231.91	0.004260
2247.60	0.004160
2262.27	0.003910
2276.35	0.003960
2289.60	0.003950
2305.44	0.004240
2319.85	0.003850
2362.38	0.003810
2377.58	0.003870
2392.51	0.003670
2433.47	0.003680
2448.22	0.003650
2464.09	0.003820
2521.02	0.003760
2534.86	0.003490
2549.02	0.003520
2576.30	0.003720

Effluent *gm*	Activity *µCi / gm*
2591.17	0.003580
2606.46	0.003760
2621.19	0.003410
2648.93	0.003800
2663.97	0.003780
2678.48	0.003550
2719.11	0.003790
2734.50	0.003590
2750.01	0.003570
2764.15	0.003440
2792.00	0.003570
2807.83	0.003400
2823.98	0.003420
2838.07	0.003660
2865.64	0.003550
2881.28	0.003620
2897.08	0.003680
2937.66	0.003670
2952.39	0.003670
2967.44	0.003670
2982.31	0.003490
3009.76	0.003520
3025.24	0.003400
3040.58	0.003200
3096.64	0.003020
3151.32	0.002980
3166.07	0.002740
3180.26	0.002930
3219.31	0.002990
3234.52	0.002750
3249.41	0.002820
3323.37	0.002980
3351.80	0.002740
3366.81	0.002930
3383.46	0.002990
3399.32	0.002750
3424.73	0.002820
3440.57	0.002760
3456.29	0.002720
3471.18	0.002680
3498.64	0.002840
3513.68	0.002700
3527.87	0.002760
3540.87	0.002950
3554.35	0.002650
3567.79	0.002830
3582.45	0.002960
3596.74	0.002750
3611.11	0.002630
3639.14	0.002710

Effluent *gm*	Activity *µCi / gm*
3654.33	0.002700
3668.74	0.002630
3682.33	0.002680
3709.28	0.002630
3723.95	0.002350
3738.91	0.002540
3765.51	0.002520
3779.11	0.002410
3794.44	0.002460
3809.96	0.002350
3823.50	0.002370
3881.01	0.002570
3895.10	0.002440
3908.98	0.002390
3923.58	0.002350
3952.59	0.002230
3966.77	0.002200
4010.71	0.002200
4025.87	0.002350
4039.74	0.002320
4054.46	0.002150
4068.34	0.001980
4081.89	0.002460
4096.08	0.002230
4110.02	0.002430
4178.98	0.002080
4193.52	0.002390
4208.74	0.001920
4222.87	0.002250
4236.88	0.002310
4250.92	0.002120
4265.86	0.002160
4324.14	0.001980
4338.68	0.002170
4352.83	0.001740
4366.19	0.002170
4380.36	0.002320
4395.15	0.002140
4448.55	0.001750
4461.80	0.001990
4476.26	0.002100
4491.21	0.001760
4504.89	0.002110
4519.61	0.001400
4548.44	0.001870
4563.61	0.001430
4592.70	0.002000
4607.76	0.001710
4622.41	0.001840
4636.42	0.001560

Effluent *gm*	Activity *µCi / gm*
4664.61	0.001820
4679.04	0.001450
4694.40	0.001790
4708.89	0.001420
4723.35	0.001730
4737.15	0.001670
4752.20	0.001690
4767.18	0.001320
4781.24	0.001640
4796.28	0.001420
4810.56	0.001870
4825.95	0.001480
4841.85	0.001370
4884.46	0.001450
4899.35	0.001530
4914.19	0.001390
4929.25	0.001290
4957.05	0.001680
4971.93	0.001460
4986.07	0.001590
5000.91	0.001630
5015.46	0.001400
5025.37	0.001650
5040.71	0.001340
5054.44	0.001540
5068.78	0.001560
5078.11	0.001580
5092.03	0.001400
5119.85	0.001580
5133.56	0.001240
5174.58	0.001550
5189.05	0.001460
5202.55	0.001850
5217.09	0.001540
5231.32	0.001530
5245.81	0.001560
5260.42	0.001670
5275.12	0.001580
5288.96	0.001620
5303.23	0.001560
5318.37	0.002160
5348.19	0.001310

Table C11. Test B6, ^{232}U.

Effluent *gm*	Activity *µCi / gm*
95.61	0.000804
104.65	0.000655
113.68	0.000246
123.27	0.001052
133.22	0.001381
143.05	0.001106
153.12	0.001201
162.86	0.001057
172.70	0.000959
181.74	0.000077
186.49	0.001032
195.72	0.001034
205.04	0.001002
214.54	0.001111
224.03	0.001025
233.50	0.000942
242.58	0.000879
251.61	0.001151
261.28	0.001107
271.10	0.001212
280.97	0.001064
290.96	0.001255
300.55	0.000747
310.08	0.001049
319.59	0.001055
329.19	0.001045
339.55	0.001388
349.45	0.001316
359.05	0.000786
368.42	0.000662
378.09	0.000802
387.65	0.000943
396.51	0.000872
405.72	0.000456
415.59	0.001235
426.37	0.001372
436.54	0.001074
446.98	0.001371
460.61	0.000903
465.73	0.001094
475.46	0.001202
489.92	0.001298
506.15	0.001431
520.52	0.000752
534.43	0.000699
548.62	0.001185
564.66	0.001407
578.77	0.001273
592.01	0.000422
606.75	0.001873
622.27	0.002129
639.01	0.002557
652.38	0.001441
666.13	0.002253
680.67	0.002564
695.72	0.002822
710.66	0.003017
723.58	0.002558
736.69	0.002887
750.52	0.003317
765.58	0.004831
781.44	0.004728
795.32	0.004505
808.53	0.004462
822.60	0.005505
837.88	0.005500
852.91	0.005549
866.85	0.005969
881.34	0.006923
896.13	0.007549
928.38	0.006928
970.76	0.009399
986.78	0.009009
1002.20	0.008499
1029.20	0.009571
1044.34	0.010133
1075.75	0.009100
1089.94	0.010221
1115.55	0.011337
1131.28	0.010581
1172.83	0.010614
1186.33	0.012200
1201.81	0.011895
1241.94	0.012511
1257.04	0.012874
1267.54	0.013353
1282.81	0.011870
1296.94	0.011423
1324.98	0.013142
1340.42	0.012596
1369.19	0.012940
1382.51	0.013625
1396.66	0.013674
1413.07	0.013371
1429.22	0.012344
1457.09	0.013422
1472.71	0.013089
1488.55	0.012441
1531.26	0.013348
1562.39	0.013281
1604.34	0.013604
1619.05	0.013854
1634.48	0.014199
1648.38	0.013631
1661.60	0.013333
1675.42	0.014530
1704.36	0.014978
1718.61	0.014609
1732.04	0.015195
1746.73	0.014635
1761.78	0.015819
1776.96	0.015927
1804.68	0.015397
1819.15	0.015945
1904.38	0.016164
1917.81	0.016034
1932.12	0.015895
1946.80	0.014200
1961.72	0.013823
1976.05	0.013501
1990.07	0.013588
2003.89	0.014252
2018.33	0.014355
2048.18	0.013628
2089.76	0.013159
2104.53	0.014206
2120.16	0.013920
2145.80	0.014701
2174.78	0.015030
2189.24	0.013700
2204.47	0.014044
2217.66	0.014496
2231.91	0.013807
2247.60	0.014442
2262.27	0.013988
2276.35	0.012988
2289.60	0.013080
2305.44	0.013953
2319.85	0.014364
2362.38	0.012246
2377.58	0.013034
2392.51	0.013363
2433.47	0.012723
2448.22	0.012051
2464.09	0.012828
2521.02	0.012676
2534.86	0.011722
2549.02	0.011729
2576.30	0.012359

Effluent *gm*	Activity *µCi / gm*
2591.17	0.012245
2606.46	0.012163
2621.19	0.011457
2648.93	0.012961
2663.97	0.012860
2678.48	0.012773
2719.11	0.012526
2734.50	0.012136
2750.01	0.012054
2764.15	0.011438
2792.00	0.012155
2807.83	0.012540
2823.98	0.010842
2838.07	0.011382
2865.64	0.012262
2881.28	0.011970
2897.08	0.011475
2937.66	0.011373
2952.39	0.011900
2967.44	0.011633
2982.31	0.011135
3009.76	0.011100
3025.24	0.010900
3040.58	0.011700
3096.64	0.010200
3151.32	0.011100
3166.07	0.010300
3180.26	0.009300
3219.31	0.010500
3234.52	0.009800
3249.41	0.010800
3323.37	0.011100
3351.80	0.010900
3366.81	0.011700
3383.46	0.010500
3399.32	0.010200
3424.73	0.010600
3440.57	0.011100
3456.29	0.010300
3471.18	0.009300
3498.64	0.010500
3513.68	0.009800
3527.87	0.010800
3540.87	0.010900
3554.35	0.009800
3567.79	0.010900
3582.45	0.010900
3596.74	0.010800
3611.11	0.010400
3639.14	0.010100

Effluent *gm*	Activity *µCi / gm*
3654.33	0.009800
3668.74	0.010300
3682.33	0.009600
3709.28	0.009100
3723.95	0.008800
3738.91	0.009000
3765.51	0.008900
3779.11	0.008900
3794.44	0.009400
3809.96	0.008500
3823.50	0.009000
3881.01	0.009900
3895.10	0.009100
3908.98	0.009100
3923.58	0.008800
3952.59	0.008600
3966.77	0.008900
4010.71	0.008700
4025.87	0.008600
4039.74	0.008600
4054.46	0.008100
4068.34	0.007580
4081.89	0.008900
4096.08	0.008700
4110.02	0.008600
4178.98	0.008200
4193.52	0.009000
4208.74	0.006920
4222.87	0.008100
4236.88	0.008600
4250.92	0.008100
4265.86	0.007350
4324.14	0.007540
4338.68	0.008500
4352.83	0.006760
4366.19	0.008600
4380.36	0.008300
4395.15	0.007730
4448.55	0.008300
4461.80	0.008900
4476.26	0.008400
4491.21	0.007730
4504.89	0.008800
4519.61	0.006390
4548.44	0.007900
4563.61	0.005520
4592.70	0.008300
4607.76	0.007210
4622.41	0.007790
4636.42	0.006410

Effluent *gm*	Activity *µCi / gm*
4664.61	0.008500
4679.04	0.006060
4694.40	0.008100
4708.89	0.005960
4723.35	0.007510
4737.15	0.007190
4752.20	0.007400
4767.18	0.005100
4781.24	0.007340
4796.28	0.006570
4810.56	0.007740
4825.95	0.005890
4841.85	0.004820
4884.46	0.006550
4899.35	0.006470
4914.19	0.006190
4929.25	0.005160
4957.05	0.007360
4971.93	0.005720
4986.07	0.006310
5000.91	0.007470
5015.46	0.006150
5025.37	0.006890
5040.71	0.005880
5054.44	0.006190
5068.78	0.006450
5078.11	0.006950
5092.03	0.005430
5119.85	0.006600
5133.56	0.004960
5174.58	0.006480
5189.05	0.006240
5202.55	0.007580
5217.09	0.006840
5231.32	0.006450
5245.81	0.006470
5260.42	0.007050
5275.12	0.006340
5288.96	0.006910
5303.23	0.006470
5318.37	0.007900
5348.19	0.004690

Table C12. Test B7, ^{22}Na.

Effluent *gm*	Activity *μCi / gm*
65.54	0.000220
74.51	0.000180
83.62	0.000150
101.60	0.000170
110.92	0.000160
120.21	0.000360
129.60	0.000420
139.06	0.000590
148.51	0.000790
157.79	0.001160
167.21	0.001590
176.57	0.001960
186.15	0.002580
195.61	0.003150
205.15	0.003640
214.73	0.004010
224.66	0.004700
233.67	0.005130
243.29	0.005510
252.89	0.005950
262.37	0.006390
272.03	0.006650
281.46	0.007370
291.19	0.007270
300.48	0.007910
310.22	0.007940
319.70	0.008310
329.13	0.008310
343.50	0.008120
372.16	0.008710
386.72	0.008910
401.02	0.009110
415.36	0.009110
429.34	0.009110
443.68	0.008910
457.60	0.008910
472.07	0.008810
486.42	0.008710
500.64	0.008510
514.99	0.008270
529.34	0.008080
543.97	0.007720
572.64	0.007500
587.27	0.007290
601.74	0.006860
616.15	0.006780
630.75	0.006680
645.26	0.006560
659.35	0.006210
673.98	0.005960
688.36	0.005930
703.09	0.005740
717.11	0.005560
731.48	0.005440
746.21	0.005230
760.39	0.005200
774.99	0.004960
789.39	0.004780
803.95	0.004690
818.41	0.004640
846.50	0.004210
860.88	0.004270
874.86	0.004160
889.58	0.004050
904.10	0.003810
918.33	0.003820
932.86	0.003720
947.45	0.003550
961.69	0.003470
976.12	0.003350
990.84	0.003400
1004.83	0.003340
1019.39	0.003180
1033.60	0.003110
1047.49	0.003120
1062.17	0.002910
1076.24	0.002820
1090.92	0.002890
1105.36	0.002770
1119.86	0.002830
1134.32	0.002740
1149.13	0.002600
1163.39	0.002570
1176.99	0.002570
1191.57	0.002440
1232.27	0.002300
1246.67	0.002370
1261.33	0.002170
1276.02	0.002200
1290.37	0.002240
1304.23	0.002130
1318.98	0.002130
1333.04	0.002030
1348.20	0.002060
1362.81	0.001960
1377.46	0.001910
1391.91	0.001940
1406.37	0.001940
1416.14	0.001890
1430.58	0.001910
1444.73	0.001870
1458.91	0.001880
1473.20	0.001840
1500.94	0.001820
1515.56	0.001690
1529.95	0.001710
1544.48	0.001660
1558.93	0.001680
1573.45	0.001660
1588.07	0.001620
1601.99	0.001540
1616.77	0.001540
1630.95	0.001480
1645.46	0.001510
1660.02	0.001460
1674.50	0.001430
1703.26	0.001390
1732.09	0.001390
1746.25	0.001350
1760.68	0.001310
1789.00	0.001310
1803.54	0.001310
1818.13	0.001310
1832.52	0.001250
1847.04	0.001280
1861.28	0.001220
1875.89	0.001220
1890.51	0.001200
1904.98	0.001140
1919.39	0.001150
1934.17	0.001160
1948.22	0.001120
1962.80	0.001120
1975.51	0.001150
2007.67	0.001160
2023.31	0.001060
2107.63	0.001060
2175.48	0.000990
2226.53	0.001030
2243.08	0.000980
2310.89	0.001010
2327.74	0.001000
2344.59	0.001060
2361.40	0.001010
2428.00	0.001030
2444.64	0.000960
2461.31	0.001040
2511.59	0.000930
2648.04	0.000820

Effluent *gm*	Activity *µCi / gm*
2768.01	0.000740
2785.02	0.000760
2807.05	0.000690
2839.28	0.000680
2855.38	0.000670
2871.68	0.000610
2888.01	0.000630
2904.00	0.000630
2920.01	0.000620
2936.20	0.000590
2966.83	0.000610
2982.80	0.000600
3015.02	0.000540
3031.31	0.000580
3046.71	0.000580
3062.43	0.000540
3078.42	0.000570
3110.04	0.000540
3126.16	0.000540
3142.24	0.000530
3158.12	0.000530
3174.04	0.000500
3190.19	0.000490
3206.13	0.000490
3222.16	0.000490
3270.42	0.000500
3286.64	0.000460
3302.81	0.000450
3319.12	0.000460
3335.39	0.000440
3351.80	0.000450
3368.08	0.000430
3384.62	0.000410
3400.77	0.000440
3433.34	0.000440
3449.87	0.000370
3466.35	0.000350
3482.91	0.000390
3499.30	0.000360
3515.89	0.000360
3532.04	0.000350
3548.65	0.000360
3564.83	0.000310
3581.56	0.000320
3598.24	0.000360
3650.44	0.000280
3664.46	0.000280
3678.62	0.000270
3692.63	0.000200
3706.77	0.000270

Effluent *gm*	Activity *µCi / gm*
3734.61	0.000230
3748.72	0.000230
3777.43	0.000250
3791.80	0.000260
3806.15	0.000220
3820.36	0.000180
3834.91	0.000180
3849.36	0.000250
3863.67	0.000250
3877.76	0.000270
3891.96	0.000270
3906.41	0.000290
3920.98	0.000320
3935.07	0.000230
3963.02	0.000300
3977.35	0.000330
4006.15	0.000250
4020.69	0.000210
4035.17	0.000260
4049.73	0.000310
4064.14	0.000270
4078.53	0.000240
4092.95	0.000190
4107.38	0.000160
4121.82	0.000220
4136.13	0.000190
4150.42	0.000160
4164.90	0.000200
4179.81	0.000380
4193.61	0.000170
4208.03	0.000120
4222.29	0.000140
4236.99	0.000270
4251.08	0.000140
4262.30	0.000160
4276.72	0.000080
4291.20	0.000080
4305.69	0.000140
4320.36	0.000080
4334.63	0.000080
4348.84	0.000050
4363.56	0.000110
4378.00	0.000020
4392.49	0.000100
4392.49	0.000090
4406.97	0.000020
4406.97	0.000050
4420.86	0.000030
4420.86	0.000040
4435.48	0.000040

Effluent *gm*	Activity *µCi / gm*
4435.48	0.000000
4450.20	0.000050
4450.20	0.000030
4464.74	0.000060
4464.74	0.000020
4479.09	0.000010
4479.09	0.000070
4507.87	0.000080
4507.87	0.000030
4518.92	0.000060
4518.92	0.000100
4533.31	0.000090
4533.31	0.000020
4547.48	0.000050
4547.48	0.000030
4561.93	0.000040
4576.56	0.000040
4591.07	0.000000
4605.29	0.000050
4619.63	0.000030
4634.06	0.000060

Table C13. Test B7, ^{232}U.

Effluent *gm*	Activity *µCi / gm*
65.54	0.000270
74.51	0.000350
83.62	0.000400
101.60	-0.000040
110.92	0.000190
120.21	0.000200
129.60	0.000010
139.06	0.000160
148.51	0.000020
157.79	0.000140
167.21	0.000250
176.57	0.000130
186.15	0.000190
195.61	0.000300
205.15	0.000430
214.73	0.000350
224.66	0.000430
233.67	0.000400
243.29	0.000390
252.89	0.000620
262.37	0.000560
272.03	0.000530
281.46	0.000530
291.19	0.000570
300.48	0.000790
310.22	0.000550
319.70	0.000720
329.13	0.000700
343.50	0.000540
372.16	0.000610
386.72	0.000650
401.02	0.000630
415.36	0.000760
429.34	0.000770
443.68	0.000820
457.60	0.000900
472.07	0.000880
486.42	0.000950
500.64	0.000880
514.99	0.000880
529.34	0.000950
543.97	0.000880
572.64	0.001130
587.27	0.001160
601.74	0.001090
616.15	0.001220
630.75	0.001530
645.26	0.001590
659.35	0.001520
673.98	0.001780
688.36	0.002020
703.09	0.002230
717.11	0.002120
731.48	0.002510
746.21	0.002610
760.39	0.002810
774.99	0.002810
789.39	0.002910
803.95	0.003110
818.41	0.003210
846.50	0.003110
860.88	0.003410
874.86	0.003810
889.58	0.004010
904.10	0.003610
918.33	0.003810
932.86	0.004110
947.45	0.004310
961.69	0.004110
976.12	0.004410
990.84	0.004910
1004.83	0.004910
1019.39	0.004810
1033.60	0.004610
1047.49	0.004810
1062.17	0.004710
1076.24	0.004910
1090.92	0.005410
1105.36	0.005110
1119.86	0.005310
1134.32	0.005510
1149.13	0.005310
1163.39	0.005310
1176.99	0.005610
1191.57	0.005510
1232.27	0.005610
1246.67	0.005910
1261.33	0.005610
1276.02	0.005810
1290.37	0.005810
1304.23	0.005910
1318.98	0.006110
1333.04	0.005710
1348.20	0.006110
1362.81	0.005710
1377.46	0.005910
1391.91	0.006010
1406.37	0.006410
1416.14	0.006310
1430.58	0.005910
1444.73	0.006210
1458.91	0.006310
1473.20	0.006310
1500.94	0.006010
1515.56	0.006210
1529.95	0.006210
1544.48	0.006110
1558.93	0.006210
1573.45	0.006410
1588.07	0.006310
1601.99	0.005610
1616.77	0.006210
1630.95	0.005610
1645.46	0.005910
1660.02	0.006010
1674.50	0.005810
1703.26	0.005510
1732.09	0.005810
1746.25	0.005510
1760.68	0.005710
1789.00	0.005510
1803.54	0.005610
1818.13	0.005410
1832.52	0.005310
1847.04	0.005410
1861.28	0.005110
1875.89	0.005410
1890.51	0.005310
1904.98	0.005110
1919.39	0.005210
1934.17	0.005410
1948.22	0.004910
1962.80	0.005110
1975.51	0.005010
2007.67	0.005310
2023.31	0.005010
2107.63	0.004910
2175.48	0.004810
2226.53	0.004910
2243.08	0.004510
2310.89	0.004410
2327.74	0.004510
2344.59	0.004610
2361.40	0.004510
2428.00	0.004510
2444.64	0.004210
2461.31	0.004310
2511.59	0.004010
2648.04	0.003910

Effluent *gm*	Activity *µCi / gm*
2768.01	0.003710
2785.02	0.003710
2807.05	0.003610
2839.28	0.003410
2855.38	0.003610
2871.68	0.003210
2888.01	0.003310
2904.00	0.003410
2920.01	0.003410
2936.20	0.003210
2966.83	0.003010
2982.80	0.003210
3015.02	0.002910
3031.31	0.003210
3046.71	0.003110
3062.43	0.003010
3078.42	0.003210
3110.04	0.002910
3126.16	0.002910
3142.24	0.002910
3158.12	0.003010
3174.04	0.002910
3190.19	0.002810
3206.13	0.002810
3222.16	0.002710
3270.42	0.002510
3286.64	0.002710
3302.81	0.002710
3319.12	0.002610
3335.39	0.002510
3351.80	0.002610
3368.08	0.002610
3384.62	0.002610
3400.77	0.002510
3433.34	0.002250
3449.87	0.002170
3466.35	0.002180
3482.91	0.002410
3499.30	0.002410
3515.89	0.002240
3532.04	0.002090
3548.65	0.002220
3564.83	0.002050
3581.56	0.001970
3598.24	0.002040
3650.44	0.002220
3664.46	0.002200
3678.62	0.002180
3692.63	0.002160
3706.77	0.002100

Effluent *gm*	Activity *µCi / gm*
3734.61	0.002070
3748.72	0.001970
3777.43	0.001930
3791.80	0.002000
3806.15	0.001910
3820.36	0.001840
3834.91	0.001650
3849.36	0.001760
3863.67	0.001890
3877.76	0.001970
3891.96	0.001840
3906.41	0.001730
3920.98	0.001710
3935.07	0.001590
3963.02	0.001630
3977.35	0.001690
4006.15	0.001440
4020.69	0.001280
4035.17	0.001400
4049.73	0.001560
4064.14	0.001400
4078.53	0.001390
4092.95	0.001160
4107.38	0.001090
4121.82	0.001310
4136.13	0.001370
4150.42	0.001200
4164.90	0.001250
4179.81	0.001210
4193.61	0.001110
4208.03	0.000990
4222.29	0.001070
4236.99	0.001130
4251.08	0.001080
4262.30	0.001110
4276.72	0.000880
4291.20	0.000810
4305.69	0.000960
4320.36	0.000870
4334.63	0.001120
4348.84	0.000830
4363.56	0.000930
4378.00	0.000620
4392.49	0.000930
4392.49	0.000940
4406.97	0.000740
4406.97	0.000840
4420.86	0.000730
4420.86	0.000780
4435.48	0.000780

Effluent *gm*	Activity *µCi / gm*
4435.48	0.000610
4450.20	0.000830
4450.20	0.000830
4464.74	0.000870
4464.74	0.000620
4479.09	0.000620
4479.09	0.000770
4507.87	0.000880
4507.87	0.000690
4518.92	0.000710
4518.92	0.000930
4533.31	0.000940
4533.31	0.000740
4547.48	0.000840
4547.48	0.000730
4561.93	0.000780
4576.56	0.000780
4591.07	0.000610
4605.29	0.000830
4619.63	0.000830
4634.06	0.000870

Table C14. Test B8, ^{22}Na.

Effluent *gm*	Activity *µCi / gm*
4.58	0.000530
9.65	0.000547
25.36	0.000528
29.77	0.000585
34.46	0.000542
39.25	0.000489
44.05	0.000533
48.84	0.000510
53.64	0.000531
58.44	0.000483
63.32	0.000477
68.23	0.000506
72.99	0.000507
77.62	0.000529
82.46	0.000514
87.31	0.000503
97.41	0.000483
106.36	0.000559
111.24	0.000496
116.04	0.000485
120.91	0.000509
125.80	0.000403
130.80	0.000516
135.58	0.000537
140.54	0.000529
145.30	0.000531
150.15	0.000530
155.01	0.000589
159.79	0.000579
164.62	0.000589
169.58	0.000597
174.36	0.000664
179.28	0.000688
184.32	0.000727
188.84	0.000842
193.80	0.000846
198.55	0.000966
203.37	0.001000
208.32	0.001170
213.06	0.001370
217.97	0.001520
222.81	0.001670
227.68	0.001870
232.52	0.002190
237.30	0.002430
242.08	0.002760
246.88	0.002990
251.70	0.003410
256.58	0.003620
261.24	0.004110
266.05	0.004580
270.91	0.004810
275.80	0.005380
280.70	0.005650
285.52	0.006390
290.25	0.007060
295.08	0.007230
299.92	0.008050
304.70	0.008690
309.56	0.008780
314.44	0.009350
319.17	0.010300
323.94	0.011100
328.79	0.011900
333.63	0.012400
338.45	0.012500
343.24	0.013800
357.70	0.016100
386.52	0.020700
401.05	0.022800
415.47	0.026500
430.07	0.029300
444.56	0.030300
458.97	0.032500
473.58	0.035100
487.91	0.039100
502.42	0.041100
517.15	0.042200
545.94	0.047700
577.09	0.051300
591.77	0.053200
606.54	0.053500
620.56	0.057400
635.02	0.059900
649.76	0.060100
664.18	0.063600
678.75	0.063300
693.41	0.063300
707.80	0.068400
722.43	0.067300
736.78	0.069900
751.45	0.069500
766.07	0.072500
780.57	0.071800
795.16	0.072800
809.52	0.075200
824.25	0.074000
839.88	0.079000
854.32	0.078800
868.73	0.079900
883.38	0.079500
897.99	0.079200
912.72	0.080200
927.29	0.082500
941.99	0.083500
956.84	0.078100
971.12	0.083700
985.65	0.084600
1000.17	0.086300
1014.69	0.087900
1029.16	0.086400
1043.67	0.087600
1058.35	0.087200
1072.80	0.088700
1087.28	0.090100
1101.74	0.089100
1116.31	0.090400
1130.85	0.091000
1159.99	0.092300
1174.58	0.090900
1189.22	0.091700
1204.06	0.089400
1218.07	0.094600
1232.65	0.092200
1247.18	0.094900
1261.83	0.093800
1276.50	0.094900
1290.92	0.097700
1303.55	0.095200
1318.11	0.096600
1332.57	0.096100
1347.20	0.099600
1361.70	0.097100
1376.22	0.097700
1390.84	0.097000
1405.31	0.097600
1419.97	0.099800
1434.42	0.099900
1449.33	0.096600
1463.57	0.101000
1478.17	0.098800
1492.92	0.097500
1507.86	0.095700
1521.72	0.098700
1536.28	0.101000
1550.92	0.100000
1565.41	0.100000
1579.96	0.101000
1594.63	0.100000

Effluent *gm*	Activity *µCi / gm*
1609.13	0.103000
1623.78	0.102000
1638.35	0.105000
1652.86	0.104000
1667.44	0.102000
1682.01	0.103000
1696.64	0.102000
1711.08	0.104000
1726.08	0.099700
1739.97	0.102000
1754.63	0.104000
1768.69	0.105000
1783.33	0.102000
1797.94	0.105000
1812.63	0.103000
1827.06	0.107000
1841.75	0.103000
1856.42	0.102000
1871.06	0.103000
1885.80	0.106000
1900.24	0.105000
1914.82	0.104000
1929.31	0.107000
1943.84	0.105000
1958.44	0.108000
1982.64	0.107000
2028.65	0.108000
2042.87	0.105000
2057.15	0.109000
2071.47	0.107000
2085.97	0.105000
2100.54	0.104000
2115.12	0.107000
2129.68	0.106000
2144.30	0.106000
2159.04	0.106000
2173.67	0.107000
2217.03	0.104000
2231.76	0.105000
2246.24	0.103000
2260.86	0.104000
2289.98	0.102000
2304.77	0.098400
2318.87	0.102000
2333.39	0.096700
2347.92	0.095100
2362.25	0.092600
2377.01	0.088200
2391.67	0.086900
2405.99	0.085000

Effluent *gm*	Activity *µCi / gm*
2434.94	0.080300
2449.48	0.078500
2463.74	0.076700
2478.28	0.074400
2492.80	0.072700
2507.34	0.067800
2521.76	0.068400
2536.28	0.066200
2550.86	0.063500
2565.35	0.061800
2580.01	0.059000
2594.52	0.057500
2608.90	0.055700
2623.39	0.054100
2638.09	0.052000
2652.64	0.051400
2667.11	0.049900
2681.62	0.047900
2696.25	0.047200
2710.81	0.046500
2725.40	0.044500
2739.92	0.044100
2754.75	0.041000
2769.53	0.041100
2784.01	0.040100
2798.31	0.039900
2812.75	0.038900
2827.54	0.035700
2841.78	0.036500
2856.29	0.036500
2870.70	0.033600
2885.16	0.034400
2899.62	0.034500
2914.42	0.031900
2928.84	0.031900
2943.55	0.031000
2958.18	0.029300
2972.91	0.029300
2987.46	0.029300
3002.43	0.028000
3016.24	0.027700
3030.75	0.027100
3045.44	0.026000
3059.93	0.026200
3074.44	0.025800
3088.95	0.025300
3103.55	0.024600
3118.12	0.024100
3132.74	0.023400
3147.49	0.022300

Effluent *gm*	Activity *µCi / gm*
3161.58	0.022300
3176.01	0.021900
3190.12	0.021800
3204.45	0.022000
3218.92	0.021100
3233.50	0.020500
3248.00	0.020500
3262.44	0.020100
3276.81	0.019500
3291.28	0.019600
3305.96	0.019200
3320.42	0.018300
3334.79	0.018500
3349.25	0.018000
3363.83	0.017600
3378.41	0.017300
3393.03	0.017300
3407.71	0.016400
3422.24	0.016000
3436.71	0.016200
3451.46	0.015700
3466.14	0.015500

Table C15. Test C1, ^{3}H.

Effluent *gm*	Activity *µCi / gm*
3.65	0.000007
9.43	0.000005
14.83	0.000010
20.23	0.000014
25.35	0.000508
30.11	0.009010
34.94	0.038900
40.11	0.079700
45.33	0.128000
50.60	0.155000
55.73	0.168000
60.12	0.186000
65.26	0.151000
70.46	0.122000
75.81	0.092900
81.07	0.074800
85.93	0.062300
90.61	0.053600
95.47	0.045300
100.66	0.038700
105.86	0.032700
110.52	0.025100
115.22	0.021700
119.94	0.019100
124.74	0.017500
129.62	0.016000
134.75	0.014900
139.94	0.013600
145.15	0.012400
148.21	0.011500
153.30	0.011000
158.45	0.010600
163.37	0.010100
168.57	0.009540
173.77	0.009290
178.89	0.008790
183.66	0.008440
188.41	0.008160
190.78	0.007560
195.87	0.007660
201.11	0.007250
206.25	0.006900
210.88	0.006610
215.95	0.006410
221.15	0.006070
226.40	0.005810
231.42	0.005700
236.12	0.005530
240.84	0.005510
245.63	0.005260
250.27	0.005190
255.10	0.004930
259.90	0.004920
265.10	0.004810
270.32	0.004630
275.48	0.004440
280.57	0.004260
285.67	0.003920
290.82	0.003800
295.78	0.003690
300.61	0.003540
305.73	0.003260
310.33	0.003110
315.13	0.003100
320.29	0.002950
325.29	0.002920
330.36	0.002820
334.96	0.002830
339.86	0.002760
344.91	0.002710
349.71	0.002650
354.71	0.002440
359.38	0.002510
364.38	0.002500
369.50	0.002520
374.55	0.002500
379.32	0.002410
384.52	0.002250
389.55	0.002250
394.67	0.002170
399.30	0.002130
404.08	0.002010
409.06	0.002010
414.18	0.001930
418.78	0.002350
423.46	0.002290
428.29	0.002220
433.21	0.002070
437.84	0.001920
442.50	0.001780
447.72	0.001690
452.49	0.001810
457.52	0.001900
462.53	0.001880
467.57	0.001860
472.47	0.001820
477.57	0.001790
482.64	0.001760
487.36	0.001780
492.01	0.001770
497.09	0.001760
502.14	0.001710
507.16	0.001640
512.22	0.001650
517.08	0.001600
522.58	0.001540
528.18	0.001490
533.82	0.001450
539.58	0.001420
545.25	0.001410
550.94	0.001360
555.89	0.001340
560.84	0.001320
565.86	0.001280
570.88	0.001300
576.03	0.001190
581.21	0.001140
586.27	0.001020
591.27	0.001030
596.91	0.001140
602.37	0.001350
607.80	0.001330
613.28	0.001240
618.72	0.001090
624.16	0.001050
629.72	0.001050
635.22	0.001040
640.82	0.001050
646.34	0.001020
651.96	0.000995
657.50	0.000964
663.04	0.000978
668.69	0.000952
673.76	0.000949
678.76	0.000920
683.73	0.000922
688.81	0.000850
693.91	0.000824
698.91	0.000838
703.91	0.000846
709.01	0.000833
714.01	0.000856
719.04	0.000823
724.04	0.000820
729.07	0.000783
734.12	0.000798
739.16	0.000804
744.22	0.000800
749.28	0.000775

Effluent *gm*	Activity *µCi / gm*
754.34	0.000781
759.42	0.000752
764.50	0.000738
769.56	0.000733
774.66	0.000712
779.86	0.000717
784.97	0.000706
790.05	0.000728
795.14	0.000682
800.34	0.000679
805.56	0.000665
810.69	0.000680
815.78	0.000682
820.88	0.000665
825.99	0.000656
831.03	0.000679
836.16	0.000647
841.26	0.000625

Table C16. Test C1, ^{22}Na.

Effluent *gm*	Activity *µCi / gm*
3.65	0.000007
9.43	0.000004
14.83	0.000005
20.23	0.000005
25.35	0.000008
30.11	0.000036
34.94	0.000312
40.11	0.000578
45.33	0.000922
50.60	0.001060
55.73	0.001090
60.12	0.001220
65.26	0.000923
70.46	0.000695
75.81	0.000532
81.07	0.000431
85.93	0.000366
90.61	0.000309
95.47	0.000266
100.66	0.000229
105.86	0.000185
110.52	0.000056
115.22	0.000048
119.94	0.000044
124.74	0.000041
129.62	0.000039
134.75	0.000034
139.94	0.000031
145.15	0.000029
148.21	0.000034
153.30	0.000027
158.45	0.000026
163.37	0.000025
168.57	0.000025
173.77	0.000024
178.89	0.000023
183.66	0.000024
188.41	0.000023
190.78	0.000029
195.87	0.000021
201.11	0.000018
206.25	0.000019
210.88	0.000019
215.95	0.000017
221.15	0.000017
226.40	0.000017
231.42	0.000017
236.12	0.000018
240.84	0.000018
245.63	0.000016
250.27	0.000016
255.10	0.000015
259.90	0.000015
265.10	0.000015
270.32	0.000014
275.48	0.000014
280.57	0.000012
285.67	0.000013
290.82	0.000013
295.78	0.000014
300.61	0.000014
305.73	0.000011
310.33	0.000011
315.13	0.000011
320.29	0.000010
325.29	0.000010
330.36	0.000010
334.96	0.000012
339.86	0.000012
344.91	0.000010
349.71	0.000011
354.71	0.000010
359.38	0.000010
364.38	0.000010
369.50	0.000009
374.55	0.000011
379.32	0.000009
384.52	0.000008
389.55	0.000010
394.67	0.000010
399.30	0.000009
404.08	0.000010
409.06	0.000009
414.18	0.000008
418.78	0.000011
423.46	0.000014
428.29	0.000014
433.21	0.000010
437.84	0.000014
442.50	0.000012
447.72	0.000007
452.49	0.000010
457.52	0.000009
462.53	0.000010
467.57	0.000008
472.47	0.000009
477.57	0.000009
482.64	0.000009
487.36	0.000010
492.01	0.000009
497.09	0.000010
502.14	0.000008
507.16	0.000009
512.22	0.000008
517.08	0.000009
522.58	0.000007
528.18	0.000008
533.82	0.000007
539.58	0.000007
545.25	0.000008
550.94	0.000007
555.89	0.000008
560.84	0.000008
565.86	0.000008
570.88	0.000007
576.03	0.000008
581.21	0.000008
586.27	0.000007
591.27	0.000006
596.91	0.000007
602.37	0.000008
607.80	0.000008
613.28	0.000006
618.72	0.000007
624.16	0.000008
629.72	0.000011
635.22	0.000011
640.82	0.000008
646.34	0.000007
651.96	0.000007
657.50	0.000007
663.04	0.000006
668.69	0.000007
673.76	0.000007
678.76	0.000006
683.73	0.000007
688.81	0.000008
693.91	0.000008
698.91	0.000008
703.91	0.000007
709.01	0.000007
714.01	0.000006
719.04	0.000007
724.04	0.000007
729.07	0.000006
734.12	0.000007
739.16	0.000007
744.22	0.000007
749.28	0.000007

Effluent gm^{-}	Activity $\mu Ci / gm$
754.34	0.000007
759.42	0.000006
764.50	0.000006
769.56	0.000007
774.66	0.000006
779.86	0.000007
784.97	0.000008
790.05	0.000007
795.14	0.000007
800.34	0.000008
805.56	0.000007
810.69	0.000007
815.78	0.000008
820.88	0.000006
825.99	0.000006
831.03	0.000006
836.16	0.000008
841.26	0.000007

Table C17. Test C2, ^{22}Na.

Effluent *gm*	Activity *µCi / gm*	Effluent *gm*	Activity *µCi / gm*	Effluent *gm*	Activity *µCi / gm*
2.41	0.001700	234.56	0.002750	477.86	0.000939
5.33	0.001760	239.33	0.002570	503.61	0.000662
8.65	0.004190	244.25	0.002510	508.80	0.000688
12.95	0.011200	249.06	0.002610	513.98	0.000648
17.81	0.026200	253.90	0.002050	519.13	0.000692
22.81	0.034100	258.65	0.002250	524.29	0.000668
27.64	0.040300	263.48	0.002070	529.31	0.000658
32.37	0.043300	268.33	0.002130	534.32	0.000661
37.25	0.041600	273.11	0.002000	539.19	0.000646
41.96	0.039600	277.89	0.001780	544.12	0.000568
46.65	0.039400	282.79	0.001700	549.09	0.000618
51.31	0.037800	287.58	0.001760	553.87	0.000579
55.99	0.034700	292.30	0.001700	558.82	0.000617
60.61	0.031000	297.10	0.001640	563.82	0.000553
65.22	0.028500	301.92	0.001650	568.62	0.000617
69.90	0.024800	306.72	0.001620	573.44	0.000557
74.56	0.022300	311.58	0.001560	578.22	0.000546
79.13	0.020300	316.44	0.001500	583.00	0.000546
83.72	0.018600	321.21	0.001460	587.86	0.000565
88.54	0.015800	326.01	0.001450	592.74	0.000590
93.24	0.014100	330.94	0.001410	597.53	0.000601
97.87	0.012300	335.92	0.001230	602.37	0.000581
102.49	0.012200	340.90	0.001290	607.19	0.000541
107.02	0.011100	345.84	0.001280	612.09	0.000576
111.62	0.010100	350.94	0.001180	616.97	0.000562
116.15	0.008590	356.15	0.001240	621.86	0.000620
120.77	0.007940	361.28	0.001080	626.61	0.000598
125.35	0.007560	366.37	0.001210	631.44	0.000702
130.29	0.006880	371.60	0.001090	636.32	0.000578
135.31	0.006170	376.76	0.001080	640.92	0.000626
140.31	0.005660	381.85	0.001210	645.73	0.000562
145.39	0.005300	386.85	0.001070	650.59	0.000583
150.48	0.005070	391.71	0.000974	655.35	0.000596
155.63	0.004770	396.60	0.001100	660.14	0.000576
160.68	0.004660	401.43	0.001050	664.99	0.000546
165.70	0.004350	406.14	0.001110	669.84	0.000496
170.63	0.004080	410.79	0.000952	674.66	0.000496
175.58	0.003880	415.64	0.001430	679.58	0.000525
180.53	0.003940	420.42	0.000984	684.58	0.000504
185.47	0.003690	425.38	0.000953	689.46	0.000502
190.32	0.003940	430.19	0.000934	694.36	0.000458
195.27	0.003400	438.43	0.000992	699.34	0.000454
200.23	0.003460	443.24	0.000907	704.39	0.000484
205.20	0.003000	448.01	0.001010	709.23	0.000491
210.11	0.003230	452.89	0.000890	714.28	0.000493
215.10	0.002940	457.81	0.000956	719.18	0.000425
220.00	0.003020	457.81	0.000956	724.01	0.000433
224.91	0.002510	462.71	0.000890	728.76	0.000447
229.76	0.002730	467.74	0.000960	733.71	0.000437
		472.85	0.000850	738.63	0.000499

Effluent gm	Activity $\mu Ci / gm$
743.49	0.000389
748.42	0.000416
753.40	0.000417
758.43	0.000402
763.33	0.000415
768.22	0.000397
773.17	0.000414
778.09	0.000424
782.98	0.000349
787.89	0.000556
792.75	0.000348

Table C18. Test C2, ^{232}U.

Effluent *gm*	Activity *µCi / gm*
0.00	0.002860
12.95	0.005450
32.37	0.006270
51.31	0.006900
69.90	0.007930
88.54	0.009540
107.02	0.009800
125.35	0.011000
145.39	0.011400
165.70	0.011700
185.47	0.011500
205.20	0.011600
224.91	0.011400
244.25	0.011900
263.48	0.011400
282.79	0.012100
301.92	0.012100
321.21	0.012000
340.90	0.011800
361.28	0.011300
381.85	0.011300
401.43	0.011300
420.42	0.011100
438.43	0.010900
457.81	0.010600
477.86	0.010100
498.49	0.009440
519.13	0.009220
539.19	0.008750
558.82	0.008160
578.22	0.008020
597.53	0.007440
616.97	0.007560
636.32	0.007290
655.35	0.007030
674.66	0.006520
694.36	0.005860
714.28	0.005800
733.71	0.005280
753.40	0.005130
773.17	0.004900
792.75	0.004690
812.62	0.004580
832.66	0.004250
852.62	0.004310
869.38	0.004970
907.10	0.004490
926.61	0.004970
945.41	0.005080
964.48	0.004720
984.34	0.004390
1004.33	0.004430
1024.13	0.004110
1043.79	0.004210
1063.37	0.003800
1083.46	0.003840
1103.45	0.003510
1123.36	0.003310
1143.36	0.003040
1164.12	0.003520
1184.21	0.003290
1204.73	0.003100
1224.95	0.002990
1283.16	0.002890
1303.18	0.002990
1323.71	0.002900
1343.69	0.002880
1363.30	0.002860
1382.33	0.002780
1402.20	0.002730
1421.74	0.002870
1441.56	0.002680
1461.31	0.002650
1481.30	0.002530
1500.78	0.002580
1520.65	0.002360
1539.96	0.002380
1559.54	0.002280
1579.23	0.002200
1598.99	0.002180
1619.00	0.002140
1644.47	0.001800
1663.70	0.002320
1676.27	0.002130
1679.77	0.002490
1732.32	0.002330
1751.23	0.002160
1770.03	0.002190
1788.85	0.002090
1807.72	0.002040
1826.42	0.002030
1845.13	0.002010
1863.77	0.001970
1882.30	0.001980
1901.17	0.001920
1920.35	0.001830
1939.48	0.002010
1992.15	0.001970
2011.22	0.001980
2046.57	0.001920
2085.02	0.001830
2104.43	0.001830
2122.63	0.001800
2139.25	0.001800
2156.67	0.001690
2192.17	0.001650
2209.93	0.001640
2227.35	0.001590
2244.93	0.001610
2262.25	0.001560
2279.53	0.001550
2296.70	0.001500
2313.77	0.001710
2331.07	0.001660
2348.53	0.001680
2361.77	0.001670
2379.62	0.001670
2396.93	0.001730
2415.55	0.001640
2430.62	0.001630
2447.63	0.001580
2464.63	0.001550
2481.85	0.001520
2499.63	0.001500
2517.52	0.001470
2535.52	0.001500
2553.50	0.001460
2571.12	0.001400
2589.02	0.001410
2606.75	0.001390
2624.53	0.001410
2642.68	0.001410
2662.17	0.001420
2681.47	0.001380
2700.22	0.001360
2719.10	0.001310
2738.07	0.001290
2757.08	0.001240
2775.98	0.001260
2794.60	0.001220
2808.48	0.001220
2825.68	0.001220
2844.12	0.001190
2862.20	0.001170
2879.98	0.001150
2897.63	0.001110
2915.72	0.001110
2932.48	0.001130
2951.17	0.001130

Effluent *gm*	Activity *µCi / gm*
2969.98	0.001150
2988.22	0.001180
3006.38	0.001180
3024.95	0.001150
3043.12	0.001210
3061.98	0.001180
3080.88	0.001180
3099.88	0.001170
3118.98	0.001160
3137.50	0.001140
3156.47	0.001120
3172.58	0.000000

Table C19. Test C3, ^{22}Na.

Effluent *gm*	Activity *µCi / gm*
0.00	0.000473
10.27	0.002190
16.21	0.010700
21.41	0.024900
25.87	0.041400
45.40	0.048200
50.17	0.045600
54.89	0.043000
59.59	0.038300
64.35	0.034200
68.97	0.030900
73.42	0.027900
77.88	0.025000
82.26	0.022000
86.71	0.020200
96.52	0.017900
101.02	0.015200
110.72	0.013800
115.32	0.011900
119.89	0.010300
124.49	0.009490
134.22	0.008710
138.88	0.007890
148.75	0.007690
153.38	0.006710
162.98	0.005870
167.75	0.005780
172.63	0.005480
177.51	0.005470
182.33	0.005360
187.30	0.004760
192.24	0.004700
197.10	0.004700
201.87	0.004440
206.78	0.004210
211.74	0.004180
216.90	0.003840
227.02	0.003550
232.02	0.003620
242.23	0.003370
247.06	0.003320
251.83	0.003110
256.33	0.003280
265.54	0.003080
270.27	0.002820
274.95	0.002810
279.76	0.002540
284.43	0.002480
294.33	0.002400
299.13	0.002170
303.90	0.002210
308.63	0.002040
313.32	0.001980
318.02	0.001990
322.68	0.002010
327.51	0.001750
332.47	0.001730
337.28	0.001670
342.11	0.001680
346.97	0.001660
357.22	0.001460
362.15	0.001540
367.24	0.001490
372.40	0.001410
377.35	0.001470
382.43	0.001270
387.53	0.001100
392.57	0.001250
397.58	0.001160
402.50	0.001190
407.44	0.001140
412.18	0.001140
416.79	0.001130
421.51	0.001070
426.22	0.001170
430.99	0.001040
435.77	0.001170
440.54	0.001430
444.33	0.001180
448.48	0.001080
453.14	0.001020
457.79	0.000905
462.54	0.001030
467.23	0.001020
481.78	0.000868
501.08	0.000818
520.54	0.000794
560.28	0.000688
578.70	0.000656
597.47	0.000605
616.50	0.000579
656.43	0.000562
676.03	0.000548
714.74	0.000520
733.59	0.000513
752.20	0.000485
790.74	0.000447
809.56	0.000437
828.26	0.000424
847.65	0.000419
866.77	0.000398
884.95	0.000394
901.53	0.000419
920.43	0.000392
939.51	0.000436
958.59	0.000465
977.44	0.000461
996.80	0.000605
1036.33	0.000768
1056.44	0.000468
1075.70	0.000568
1095.57	0.000553
1115.18	0.000545
1134.86	0.000497
1153.76	0.000449
1172.78	0.000401
1191.97	0.000379
1210.81	0.000375
1230.34	0.000357
1249.64	0.000348
1269.15	0.000368
1288.54	0.000439
1307.59	0.000463
1327.67	0.000525
1365.78	0.000452
1384.58	0.000510
1403.70	0.000430
1423.21	0.000412
1442.23	0.000409
1461.62	0.000407
1481.52	0.000402
1491.95	0.000420
1511.19	0.000438
1531.39	0.000431
1549.74	0.000452
1569.02	0.000464
1588.16	0.000426
1607.12	0.000419
1627.66	0.000457
1647.02	0.000497
1666.27	0.000513
1684.37	0.000527
1702.57	0.000517
1720.57	0.000519
1739.12	0.000498
1757.53	0.000506
1776.33	0.000501
1795.37	0.000544

Table C20. Test C4, ^{22}Na.

Effluent *gm*	Activity *µCi / gm*	Effluent *gm*	Activity *µCi / gm*	Effluent *gm*	Activity *µCi / gm*
3.34	0.000360	268.63	0.009660	520.44	0.002560
11.49	0.000329	273.26	0.008880	524.93	0.002360
21.15	0.000628	283.00	0.008660	529.58	0.002230
25.88	0.009140	287.63	0.008490	534.25	0.002260
30.84	0.060200	297.34	0.008040	539.06	0.002150
35.76	0.111000	301.96	0.007620	543.77	0.002220
40.72	0.143000	306.56	0.007270	548.40	0.002120
45.72	0.155000	311.32	0.007130	553.05	0.001940
50.87	0.127000	315.89	0.006990	557.64	0.001950
55.96	0.107000	320.49	0.006560	562.32	0.001890
61.05	0.090600	325.10	0.006340	566.89	0.002060
66.25	0.078400	329.88	0.005940	571.54	0.001900
71.27	0.072000	334.49	0.005750	576.17	0.001840
76.34	0.065700	339.19	0.005860	580.83	0.001770
81.22	0.060800	343.89	0.005380	585.53	0.001860
86.06	0.052600	348.60	0.005310	590.18	0.001650
90.88	0.046200	353.47	0.005330	594.81	0.001750
95.53	0.042500	363.35	0.004920	599.53	0.001660
100.02	0.038300	368.21	0.004680	604.06	0.001640
104.56	0.034000	373.08	0.004570	608.56	0.001680
109.15	0.030900	378.04	0.004320	613.27	0.001630
113.79	0.028000	382.96	0.004270	617.93	0.001560
118.39	0.026300	387.85	0.004040	622.51	0.001470
123.03	0.024900	392.77	0.003810	627.21	0.001600
127.65	0.023500	397.72	0.003790	631.99	0.001550
132.36	0.022300	402.64	0.003620	636.74	0.001530
137.09	0.020700	407.44	0.003680	641.61	0.001300
141.77	0.021300	412.25	0.003530	646.37	0.001400
146.46	0.020200	416.97	0.003620	650.94	0.001450
151.09	0.019200	421.70	0.003200	655.77	0.001310
155.90	0.018500	426.46	0.003130	660.48	0.001460
160.91	0.017500	431.19	0.003240	665.48	0.001290
166.04	0.016900	435.50	0.003200	670.26	0.001350
171.10	0.015800	438.98	0.003990	674.73	0.001280
176.26	0.015500	443.24	0.003340	679.72	0.001290
181.44	0.014900	453.09	0.003160	684.37	0.001290
186.29	0.015800	457.68	0.003080	688.94	0.001270
191.23	0.014600	462.39	0.002860	693.86	0.001250
201.25	0.013900	467.11	0.002700	698.52	0.001310
211.23	0.013700	471.78	0.002730	703.02	0.001340
216.07	0.013500	476.41	0.002580	707.57	0.001260
220.93	0.012600	481.14	0.002540	712.12	0.001230
225.72	0.012200	485.90	0.002480	716.61	0.001440
230.54	0.011700	490.68	0.002340	721.22	0.001200
240.22	0.011600	495.56	0.002240	724.86	0.002050
244.93	0.011300	500.51	0.002170	729.65	0.001150
254.82	0.010900	505.39	0.002290	734.14	0.001250
259.45	0.010400	509.99	0.002260	738.83	0.001110
264.04	0.009380	514.02	0.002580	743.35	0.001080
		516.12	0.004060	748.04	0.001080

Effluent *gm*	Activity *μCi / gm*	Effluent *gm*	Activity *μCi / gm*	Effluent *gm*	Activity *μCi / gm*
752.71	0.001120	1133.50	0.000602	2145.72	0.000332
757.39	0.001160	1152.41	0.000572	2164.27	0.000287
762.10	0.001080	1170.60	0.000747	2197.32	0.000312
766.87	0.001100	1189.02	0.000530	2216.47	0.000282
771.53	0.001060	1208.11	0.000576	2235.62	0.000271
775.78	0.001130	1226.65	0.000554	2251.58	0.000331
780.56	0.001080	1245.80	0.000520	2271.27	0.000310
785.63	0.001010	1265.09	0.000496	2290.55	0.000288
790.68	0.001020	1279.38	0.000501	2309.32	0.000296
795.69	0.000992	1299.40	0.000444	2328.13	0.000291
800.72	0.000966	1318.00	0.000464	2345.02	0.000485
805.81	0.000976	1336.52	0.000843	2364.03	0.000353
810.77	0.000896	1355.21	0.000454	2391.33	0.000339
815.68	0.000856	1374.65	0.000449	2410.90	0.000277
820.54	0.000949	1393.57	0.000416	2429.67	0.000308
824.94	0.001050	1412.81	0.000465	2448.28	0.000270
830.00	0.000961	1437.00	0.000460	2466.68	0.000262
834.83	0.000918	1456.84	0.000431	2485.13	0.000272
839.43	0.000912	1481.21	0.000480	2503.85	0.000251
844.00	0.001010	1499.25	0.000488	2522.98	0.000247
848.76	0.001020	1514.82	0.000630	2541.92	0.000277
853.44	0.000893	1542.00	0.000446	2560.48	0.000263
858.21	0.000826	1560.33	0.000429	2578.38	0.000257
863.03	0.000897	1583.99	0.000429	2596.38	0.000249
867.79	0.000937	1608.42	0.000413	2614.48	0.000235
882.81	0.000930	1627.65	0.000392	2633.02	0.000272
887.52	0.000875	1651.78	0.000383	2651.43	0.000269
897.48	0.000819	1669.97	0.000423	2670.20	0.000272
902.34	0.000983	1688.40	0.000379	2688.87	0.000229
907.01	0.000829	1706.97	0.000383	2707.48	0.000237
910.20	0.001090	1725.58	0.000362	2723.70	0.000227
914.93	0.000899	1744.83	0.000347	2742.05	0.000361
919.59	0.000909	1764.18	0.000325	2760.75	0.000240
929.28	0.000883	1783.63	0.000301	2779.47	0.000208
933.88	0.000985	1803.10	0.000326	2798.03	0.000245
938.68	0.000830	1821.82	0.000346	2817.17	0.000225
943.36	0.000857	1859.40	0.000351	2836.73	0.000233
948.10	0.000783	1878.27	0.000386	2855.12	0.000322
952.85	0.000834	1902.93	0.000293	2874.00	0.000216
957.66	0.000875	1922.23	0.000315	2892.75	0.000203
962.39	0.000793	1939.97	0.000487	2911.65	0.000231
972.23	0.000766	1958.87	0.000320	2930.18	0.000374
992.83	0.000773	1983.22	0.000333	2947.72	0.000192
1007.22	0.000748	2002.43	0.000310	2965.62	0.000245
1025.38	0.000725	2021.23	0.000302	2984.60	0.000267
1043.93	0.000665	2050.95	0.000315	3003.33	0.000235
1062.27	0.000643	2069.97	0.000315	3022.22	0.000220
1080.25	0.000861	2088.92	0.000322	3041.02	0.000227
1095.26	0.000675	2108.02	0.000325	3059.98	0.000182
1114.04	0.000649	2126.50	0.000281	3079.15	0.000157

Effluent *gm*	Activity *µCi / gm*
3098.33	0.000276
3117.82	0.000159
3136.87	0.000171
3155.07	0.000160
3173.88	0.000199
3192.97	0.000174
3211.70	0.000170
3230.38	0.000157
3249.78	0.000155
3269.28	0.000167
3285.82	0.000269
3304.53	0.000250
3323.52	0.000189
3342.25	0.000161
3361.15	0.000166
3380.43	0.000167
3399.47	0.000170
3418.90	0.000155
3437.73	0.000151
3456.83	0.000171
3475.83	0.000165
3494.67	0.000145
3513.75	0.000178
3532.25	0.000185
3550.78	0.000185
3569.22	0.000184
3587.62	0.000166
3606.02	0.000168
3624.38	0.000217
3642.82	0.000184
3661.57	0.000183
3676.38	0.000198
3695.28	0.000162
3713.88	0.000205
3732.63	0.000168
3751.30	0.000138
3770.08	0.000172
3788.98	0.000178
3807.77	0.000172
3826.78	0.000173
3845.72	0.000162
3864.53	0.000159
3883.62	0.000155
3902.55	0.000136
3921.43	0.000143
3940.60	0.000147
3959.47	0.000155
3978.88	0.000153
3997.53	0.000347
4016.48	0.000151

Effluent *gm*	Activity *µCi / gm*
4035.57	0.000162
4051.87	0.000157
4070.87	0.000135
4090.03	0.000258
4109.02	0.000140
4127.87	0.000175
4146.38	0.000167
4165.30	0.000133
4184.12	0.000153
4202.93	0.000154
4222.38	0.000161
4241.92	0.000150
4260.73	0.000438
4279.62	0.000160
4298.08	0.000158
4316.78	0.000146
4335.73	0.000178
4354.38	0.000096
4369.68	0.000170
4387.92	0.000141
4406.18	0.000106
4424.18	0.000101
4441.82	0.000101
4459.73	0.000113
4477.88	0.000109
4495.92	0.000112
4510.18	0.000130
4528.30	0.000108
4546.17	0.000118
4564.53	0.000096
4582.47	0.000108
4600.72	0.000113
4619.12	0.000117
4637.60	0.000102
4656.18	0.000098
4674.82	0.000099
4693.45	0.000115
4711.87	0.000134
4730.13	0.000118
4748.68	0.000103
4767.38	0.000120
4786.03	0.000096
4805.02	0.000092
4824.07	0.000102
4842.73	0.000132
4861.50	0.000098
4875.67	0.000091

Table C21. Test C5, ^{22}Na.

Effluent *gm*	Activity *µCi / gm*	Effluent *gm*	Activity *µCi / gm*	Effluent *gm*	Activity *µCi / gm*
6.24	0.008200	543.27	0.000675	873.86	0.000346
15.69	0.018600	554.27	0.000592	879.46	0.000383
25.42	0.037800	565.48	0.000653	884.85	0.000366
34.87	0.055200	576.51	0.000637	890.27	0.000429
44.39	0.046900	587.40	0.000611	895.83	0.000377
54.04	0.033500	598.45	0.000593	901.31	0.000354
63.96	0.022900	609.56	0.000557	906.79	0.000385
74.23	0.015200	620.60	0.000599	912.30	0.000371
84.54	0.010900	631.86	0.000436	917.86	0.000411
95.15	0.008230	643.36	0.000516	923.40	0.000370
106.30	0.006150	649.11	0.000485	928.87	0.000347
117.66	0.005000	654.79	0.000465	934.40	0.000354
129.22	0.004420	660.45	0.000502	939.95	0.000426
140.84	0.004100	666.10	0.000449	945.55	0.000340
152.36	0.003610	671.67	0.000457	951.18	0.000356
163.74	0.003080	677.43	0.000504	956.74	0.000359
174.81	0.003110	682.98	0.000482	961.06	0.000436
185.86	0.002570	688.66	0.000469	969.68	0.000470
196.82	0.002340	694.42	0.000493	974.71	0.000393
207.61	0.002250	699.94	0.000553	980.16	0.000451
218.42	0.001980	705.37	0.000454	985.61	0.000431
229.44	0.001970	710.68	0.000443	991.10	0.000394
240.35	0.001690	716.15	0.000529	996.63	0.000497
251.22	0.001580	721.64	0.000463	1002.13	0.000494
262.28	0.001320	727.25	0.000423	1007.56	0.000401
272.82	0.001420	732.78	0.000471	1013.06	0.000410
283.61	0.001370	738.24	0.000424	1018.59	0.000421
294.35	0.001270	743.70	0.000475	1024.10	0.000440
305.20	0.001180	749.25	0.000398	1029.51	0.000476
315.96	0.001230	754.60	0.000460	1035.03	0.000443
326.86	0.001230	760.05	0.000412	1040.53	0.000382
337.54	0.000990	765.46	0.000449	1046.02	0.000405
348.43	0.000870	770.95	0.000406	1051.56	0.000393
366.70	0.000833	776.49	0.000442	1057.24	0.000366
377.42	0.000868	781.97	0.000403	1062.71	0.000436
388.17	0.000883	787.60	0.000473	1068.20	0.000368
399.08	0.000816	793.24	0.000391	1073.80	0.000421
410.08	0.000777	798.26	0.000459	1079.30	0.000362
420.91	0.000747	802.61	0.000452	1084.77	0.000317
431.73	0.000675	807.62	0.000398	1090.29	0.000357
442.63	0.000732	818.52	0.000422	1095.83	0.000424
453.88	0.000703	824.15	0.000767	1101.36	0.000338
465.18	0.000704	829.79	0.000411	1106.97	0.000360
476.54	0.000631	835.26	0.000414	1112.74	0.000396
487.87	0.000584	840.83	0.000358	1118.34	0.000395
499.04	0.000707	846.33	0.000492	1123.84	0.000361
510.24	0.000648	851.93	0.000889	1129.36	0.000389
521.29	0.000569	857.37	0.000395	1135.29	0.000332
532.26	0.000602	862.93	0.000376	1140.72	0.000344
		868.37	0.000415	1146.22	0.000374

Effluent *gm*	Activity *µCi / gm*	Effluent *gm*	Activity *µCi / gm*	Effluent *gm*	Activity *µCi / gm*
1151.77	0.000369	1423.51	0.000329	1708.57	0.000261
1157.18	0.000365	1429.03	0.000332	1714.33	0.000194
1162.90	0.000378	1434.61	0.000340	1719.77	0.000257
1168.43	0.000359	1440.24	0.000370	1725.38	0.000235
1173.91	0.000373	1446.01	0.000354	1730.82	0.000230
1179.45	0.000365	1451.42	0.000401	1736.22	0.000250
1185.21	0.000355	1457.21	0.000335	1741.72	0.000254
1190.53	0.000363	1463.00	0.000346	1747.17	0.000249
1195.96	0.000333	1468.68	0.000301	1752.68	0.000249
1201.43	0.000311	1474.25	0.000365	1758.15	0.000247
1206.97	0.000334	1479.82	0.000383	1763.53	0.000250
1212.37	0.000353	1485.49	0.000350	1768.63	0.000254
1217.89	0.000364	1490.82	0.000364	1774.30	0.000258
1223.33	0.000314	1496.19	0.000364	1779.83	0.000308
1228.76	0.000376	1501.60	0.000337	1785.28	0.000297
1234.20	0.000381	1506.99	0.000349	1790.82	0.000259
1239.52	0.000369	1512.26	0.000359	1796.62	0.000268
1245.19	0.000307	1517.51	0.000367	1802.52	0.000253
1250.74	0.000319	1522.85	0.000297	1808.32	0.000279
1256.43	0.000342	1528.21	0.000343	1814.12	0.000256
1262.16	0.000321	1533.45	0.000390	1819.68	0.000257
1267.91	0.000341	1538.86	0.000342	1825.37	0.000302
1273.74	0.000445	1544.00	0.000351	1831.07	0.000238
1279.52	0.000325	1549.34	0.000326	1836.57	0.000265
1285.29	0.000370	1554.66	0.000372	1842.17	0.000200
1291.17	0.000348	1560.02	0.000316	1847.73	0.000252
1296.91	0.000483	1565.44	0.000385	1849.15	0.000595
1302.70	0.000391	1570.68	0.000363	1854.08	0.000290
1308.45	0.000361	1575.98	0.000321	1859.55	0.000251
1314.57	0.000330	1581.43	0.000295	1864.97	0.000000
1319.90	0.000369	1586.79	0.000333	1870.52	0.000257
1325.59	0.000333	1592.29	0.000319	1876.00	0.000278
1331.17	0.000338	1597.78	0.000306	1882.03	0.000239
1336.58	0.000360	1603.27	0.000390	1887.40	0.000254
1341.77	0.000432	1614.69	0.000271	1893.05	0.000234
1347.17	0.000313	1626.08	0.000258	1898.62	0.000240
1352.49	0.000334	1631.67	0.000357	1904.07	0.000303
1357.76	0.000450	1637.25	0.000349	1909.57	0.000279
1363.21	0.000340	1642.70	0.000325	1915.08	0.000240
1368.58	0.000379	1648.19	0.000358	1920.57	0.000321
1373.94	0.000344	1653.69	0.000326	1926.12	0.000264
1379.23	0.000285	1658.69	0.000337	1931.50	0.000322
1384.61	0.000337	1664.26	0.000315	1937.02	0.000240
1389.96	0.000325	1669.75	0.000460	1943.43	0.000156
1395.34	0.000331	1675.33	0.000290	1948.15	0.000292
1400.74	0.000328	1680.85	0.000335	1954.07	0.000211
1404.84	0.000364	1686.47	0.000307	1959.53	0.000231
1408.05	0.000480	1691.92	0.000248	1968.07	0.000209
1412.75	0.000383	1697.52	0.000294	1973.72	0.000239
1417.91	0.000375	1702.98	0.000255	1979.30	0.000242

Effluent *gm*	Activity *µCi / gm*
1985.27	0.000194
1990.33	0.000225
1995.80	0.000233
2001.18	0.000271
2006.85	0.000244
2012.47	0.000284
2018.13	0.000231
2023.63	0.000229
2029.17	0.000226
2034.77	0.000231
2040.32	0.000229
2045.78	0.000198
2051.27	0.000256
2056.82	0.000277
2062.43	0.000243
2067.97	0.000241
2073.47	0.000232
2078.92	0.000000
2084.57	0.000181
2090.08	0.000222
2095.63	0.000216
2101.22	0.000237
2106.58	0.000203
2112.43	0.000236
2118.32	0.000215
2123.37	0.000254
2129.63	0.000192
2135.27	0.000226
2140.72	0.000251
2146.53	0.000251
2151.30	0.000306
2157.12	0.000208
2162.43	0.000218
2167.85	0.000241
2173.20	0.000210
2178.55	0.000220
2183.78	0.000262
2189.23	0.000246
2194.67	0.000223
2200.08	0.000231
2205.42	0.000239
2210.98	0.000202
2216.50	0.000220
2221.65	0.000234
2227.25	0.000215
2232.68	0.000202
2238.13	0.000224
2243.72	0.000218
2249.15	0.000284
2254.73	0.000243

Effluent *gm*	Activity *µCi / gm*
2260.33	0.000305
2266.08	0.000209
2271.82	0.000210
2277.17	0.000242
2282.58	0.000229
2288.43	0.000265
2294.02	0.000277
2298.77	0.000356
2303.42	0.000232
2307.68	0.000293
2312.57	0.000238
2317.25	0.000251
2321.92	0.000304
2327.88	0.000231
2333.95	0.000250
2339.98	0.000220
2345.87	0.000253
2351.65	0.000274
2357.13	0.000235
2362.52	0.000216
2367.78	0.000221
2372.92	0.000251
2378.10	0.000222
2383.17	0.000263
2388.33	0.000244
2393.42	0.000247
2398.43	0.000231
2403.57	0.000279
2408.53	0.000239
2413.73	0.000241
2418.68	0.000226
2423.78	0.000253
2428.77	0.000219
2433.65	0.000232
2438.67	0.000235
2443.72	0.000286
2448.72	0.000241
2453.77	0.000262
2458.70	0.000359
2463.68	0.000239
2468.53	0.000264
2473.43	0.000221
2478.28	0.000209
2483.15	0.000395
2488.02	0.000207
2492.88	0.000274
2497.67	0.000273
2502.63	0.000223
2507.53	0.000246
2512.50	0.000235

Effluent *gm*	Activity *µCi / gm*
2512.50	0.000000
2517.42	0.000245
2522.25	0.000474
2527.10	0.000238
2531.93	0.000260
2536.93	0.000202
2541.78	0.000216
2546.58	0.000243
2551.40	0.000240
2556.32	0.000232
2561.12	0.000211
2565.85	0.000230
2570.77	0.000226
2575.40	0.000364
2580.20	0.000267
2584.80	0.000234
2589.65	0.000254
2594.27	0.000298
2599.07	0.000209
2603.88	0.000261
2608.48	0.000264
2613.43	0.000219
2618.05	0.000262
2622.47	0.000234
2627.27	0.000227
2631.92	0.000235
2636.62	0.000262
2641.27	0.000256
2645.92	0.000232
2650.78	0.000275
2655.28	0.000232
2660.05	0.000213
2664.77	0.000270
2669.40	0.000231
2674.08	0.000222
2678.57	0.000245
2683.08	0.000261
2687.88	0.000337
2690.13	0.000411
2692.35	0.000401
2696.72	0.000299
2701.23	0.000242
2705.82	0.000267
2710.38	0.000260
2715.05	0.000275
2724.63	0.000289
2729.42	0.000303
2734.33	0.000369
2739.12	0.000286
2744.00	0.000284

Effluent *gm*	Activity *µCi / gm*
2748.72	0.000258
2753.48	0.000267
2758.18	0.000256
2762.92	0.000243
2767.57	0.000278
2772.30	0.000248
2777.03	0.000274
2781.63	0.000274
2786.57	0.000231
2800.33	0.000176
2819.43	0.000179
2838.42	0.000141
2857.28	0.000163
2876.47	0.000152
2895.98	0.000179
2915.27	0.000166
2934.32	0.000165
2953.37	0.000183
2972.48	0.000178
2991.43	0.000162
3010.78	0.000137
3030.07	0.000165
3049.32	0.000174
3068.48	0.000172
3084.88	0.000192
3103.98	0.000183

Table C22. Test C5, ^{239}Np.

Effluent *gm*	Activity *µCi / gm*
6.24	0.000000
15.69	0.000487
25.42	0.000774
34.87	0.001310
44.39	0.002880
54.04	0.004910
63.96	0.006000
74.23	0.006550
84.54	0.007490
95.15	0.007300
106.30	0.007040
117.66	0.006940
129.22	0.007990
140.84	0.009610
152.36	0.009740
163.74	0.010400
174.81	0.011100
185.86	0.012100
196.82	0.012900
207.61	0.014700
218.42	0.015300
229.44	0.014800
240.35	0.015000
251.22	0.017100
262.28	0.016300
272.82	0.017300
283.61	0.016500
294.35	0.017300
305.20	0.017800
315.96	0.016800
326.86	0.017200
337.54	0.017200
348.43	0.016200
366.70	0.017000
377.42	0.014900
388.17	0.016100
399.08	0.015400
410.08	0.015500
420.91	0.015200
431.73	0.015100
442.63	0.015000
453.88	0.014000
465.18	0.013800
476.54	0.012800
487.87	0.013700
499.04	0.013100
510.24	0.013200
521.29	0.012800
532.26	0.012600
543.27	0.012200
554.27	0.012300
565.48	0.011600
576.51	0.011700
587.40	0.011800
598.45	0.011300
609.56	0.010500
620.60	0.010500
631.86	0.010500
643.36	0.010800
649.11	0.010200
654.79	0.010500
660.45	0.010700
666.10	0.009940
671.67	0.010800
677.43	0.010400
682.98	0.010300
688.66	0.010300
694.42	0.009600
699.94	0.009780
705.37	0.010400
710.68	0.010300
716.15	0.009290
721.64	0.009600
727.25	0.009420
732.78	0.009790
738.24	0.009610
743.70	0.010100
749.25	0.008730
754.60	0.010200
760.05	0.009150
765.46	0.009120
770.95	0.009160
776.49	0.009040
781.97	0.009060
787.60	0.008330
793.24	0.008680
798.26	0.009610
802.61	0.010200
807.62	0.009520
818.52	0.008520
824.15	0.008130
829.79	0.008200
835.26	0.008080
840.83	0.008280
846.33	0.007660
851.93	0.007770
857.37	0.007920
862.93	0.007620
868.37	0.007570
873.86	0.007550
879.46	0.007140
884.85	0.007740
890.27	0.007090
895.83	0.006890
901.31	0.007390
906.79	0.007120
912.30	0.006900
917.86	0.006540
923.40	0.006980
928.87	0.006360
934.49	0.006590
939.95	0.006270
945.55	0.006580
951.18	0.006270
956.74	0.006280
961.06	0.007510
969.68	0.006640
974.71	0.006600
980.16	0.006390
985.61	0.006500
991.10	0.006270
996.63	0.006280

Table C23. Test C6 ^{22}Na.

Effluent *gm*	Activity *µCi / gm*
0.01	0.000206
4.60	0.000374
9.25	0.001640
14.12	0.019500
19.06	0.040000
24.23	0.063800
29.23	0.075000
34.29	0.078000
39.25	0.071600
44.26	0.058400
49.28	0.048600
54.13	0.038200
58.99	0.029500
63.87	0.024600
68.65	0.019300
73.45	0.016600
78.16	0.013800
82.94	0.012000
87.65	0.010400
92.37	0.009480
97.18	0.008060
102.07	0.007680
106.80	0.006990
111.61	0.006460
116.52	0.006330
121.41	0.006010
126.26	0.005730
131.01	0.005260
135.97	0.005040
140.77	0.004510
145.81	0.004540
150.60	0.004430
155.47	0.004180
160.44	0.003890
165.40	0.003530
170.43	0.003500
175.39	0.003260
180.47	0.003320
185.33	0.003060
190.32	0.002830
195.33	0.002830
200.05	0.002620
204.87	0.002810
209.66	0.002590
214.43	0.002590
219.14	0.002410
223.97	0.002320
228.78	0.002170
233.52	0.002140
238.19	0.001990
243.00	0.002040
247.79	0.001910
252.54	0.001900
257.37	0.001740
262.26	0.001750
266.90	0.001810
271.47	0.001710
276.06	0.001660
280.73	0.001670
285.32	0.001550
290.08	0.001530
294.84	0.001480
299.65	0.001460
304.47	0.001460
309.37	0.001370
314.20	0.001330
319.12	0.001270
324.03	0.001140
329.06	0.001270
333.66	0.001270
338.29	0.001220
343.06	0.001240
347.78	0.001330
352.50	0.001210
357.29	0.001170
361.97	0.001130
366.76	0.001050
371.56	0.001210
376.34	0.001100
381.15	0.001140
385.92	0.001180
390.16	0.001220
394.21	0.001070
398.61	0.001140
403.22	0.001080
407.91	0.001110
412.68	0.001010
417.37	0.000924
422.26	0.001020
426.98	0.001470
431.72	0.001040
436.58	0.000916
441.40	0.000936
446.34	0.000902
451.25	0.000882
456.20	0.000840
461.24	0.000923
466.35	0.000805
471.22	0.000924
476.26	0.000749
481.35	0.000717
486.38	0.000825
490.86	0.000779
495.91	0.000786
500.84	0.000671
505.70	0.000758
510.56	0.000811
515.26	0.000851
519.55	0.000801
524.38	0.000732
529.22	0.000681
534.11	0.000745
539.00	0.000692
543.86	0.000800
548.29	0.000648
562.54	0.000805
577.06	0.000659
591.06	0.000748
604.95	0.000828
618.98	0.000629
633.65	0.001120
647.41	0.000496
662.51	0.000541
676.06	0.000595
690.63	0.000472
704.90	0.000592
718.85	0.000539
733.28	0.000465
747.46	0.000484
762.24	0.000573
776.46	0.000501
788.97	0.000485
803.61	0.000508
818.18	0.000453
832.53	0.000605
846.71	0.000400
860.79	0.000404
874.54	0.000497
888.73	0.000441
903.64	0.000597
917.45	0.000414
933.47	0.000457
947.74	0.000369
962.52	0.000457
976.93	0.000391
991.26	0.000454
1005.45	0.000385
1019.65	0.000402
1033.87	0.000387

Effluent *gm*	Activity *µCi / gm*
1048.76	0.000348
1063.40	0.000410
1078.65	0.000327
1093.67	0.000344
1108.29	0.000315
1122.63	0.000284
1136.97	0.000246
1151.26	0.000407
1155.85	0.000412
1181.83	0.000391
1196.15	0.000414
1210.33	0.000371
1224.82	0.000343
1238.95	0.000336
1252.90	0.000467
1266.16	0.000434
1279.81	0.000303
1294.13	0.000288
1307.88	0.000346
1321.95	0.000313
1336.34	0.000303
1351.32	0.000386
1366.23	0.000408
1394.67	0.000298
1409.03	0.000312
1436.26	0.000299
1449.87	0.000315
1464.28	0.000312
1477.44	0.000310
1491.87	0.000299
1506.60	0.000296
1520.95	0.000262
1535.32	0.000284
1561.03	0.000318
1575.10	0.000387
1588.78	0.000295
1603.09	0.000352
1617.66	0.000315
1646.48	0.000523
1661.19	0.000262
1675.67	0.000313
1690.15	0.000244
1704.63	0.000218
1718.95	0.000317
1758.27	0.000284
1784.58	0.000277
1794.18	0.000284
1808.68	0.000402
1823.18	0.000272
1837.83	0.000306

Effluent *gm*	Activity *µCi / gm*
1852.28	0.000473
1866.70	0.000291
1881.08	0.000328
1895.57	0.000363
1910.32	0.000383
1924.48	0.000500
1938.82	0.000480
1953.15	0.000253
1967.47	0.000255
1981.87	0.000442

Table C24. Test C6, ^{239}Np.

Effluent *gm*	Activity *µCi / gm*
0.01	0.000000
4.60	0.000000
9.25	0.000000
14.12	0.000000
19.06	0.000261
24.23	0.000000
29.23	0.000000
34.29	0.000000
39.25	0.000373
44.26	0.000000
49.28	0.000275
54.13	0.000331
58.99	0.000000
63.87	0.000000
68.65	0.000313
73.45	0.000248
78.16	0.000345
82.94	0.000231
87.65	0.000196
92.37	0.000299
97.18	0.000220
102.07	0.000266
106.80	0.000215
111.61	0.000200
116.52	0.000292
121.41	0.000247
126.26	0.000251
131.01	0.000000
135.97	0.000220
140.77	0.000255
145.81	0.000203
150.60	0.000205
155.47	0.000221
160.44	0.000212
165.40	0.000192
170.43	0.000189
175.39	0.000240
180.47	0.000181
185.33	0.000225
190.32	0.000230
195.33	0.000237
200.05	0.000197
204.87	0.000273
209.66	0.000272
214.43	0.000279
219.14	0.000304
223.97	0.000288
228.78	0.000372
233.52	0.000348
238.19	0.000387
243.00	0.000483
247.79	0.000513
252.54	0.000497
257.37	0.000567
262.26	0.000688
266.90	0.000822
271.47	0.000948
276.06	0.001000
280.73	0.001030
285.32	0.001030
290.08	0.001120
294.84	0.001260
299.65	0.001400
304.47	0.001520
309.37	0.001630
314.20	0.001520
319.12	0.001940
324.03	0.001860
329.06	0.002180
333.66	0.002190
338.29	0.002430
343.06	0.002800
347.78	0.002680
352.50	0.002970
357.29	0.003090
361.97	0.003410
366.76	0.003760
371.56	0.003770
376.34	0.004140
381.15	0.004090
385.92	0.005000
390.16	0.004770
394.21	0.004860
398.61	0.005310
403.22	0.005660
407.91	0.005720
412.68	0.005940
417.37	0.005830
422.26	0.006730
426.98	0.006610
431.72	0.006850
436.58	0.007490
441.40	0.007360
446.34	0.008090
451.25	0.008190
456.20	0.008680
461.24	0.008810
466.35	0.009310
471.22	0.009270
476.26	0.009570
481.35	0.009780
486.38	0.010800
490.86	0.010500
495.91	0.011000
500.84	0.010700
505.70	0.011000
510.56	0.011500
515.26	0.013300
519.55	0.012300
524.38	0.012500
529.22	0.013000
534.11	0.013400
539.00	0.013800
543.86	0.014400
548.29	0.014300
562.54	0.014100
577.06	0.015600
591.06	0.016600
604.95	0.021500
618.98	0.018600
633.65	0.019300
647.41	0.017700
662.51	0.019900
676.06	0.020100
690.63	0.021300
704.90	0.025500
718.85	0.022500
733.28	0.023700
747.46	0.024100
762.24	0.029300
776.46	0.026100
788.97	0.028700
803.61	0.028700
818.18	0.031200
832.53	0.030400
846.71	0.029900
860.79	0.029700
874.54	0.033100
888.73	0.029100
903.64	0.031400
917.45	0.032200
933.47	0.037600
947.74	0.038200
962.52	0.037700
976.93	0.037700
991.26	0.039500
1005.45	0.037700
1019.65	0.040000
1033.87	0.038600

Effluent *gm*	Activity *µCi / gm*
1048.76	0.039300
1063.40	0.039300
1078.65	0.040300
1093.67	0.041000
1108.29	0.040000
1122.63	0.041900
1136.97	0.039600
1151.26	0.037600
1155.85	0.035200
1181.83	0.032500
1196.15	0.034100
1210.33	0.035600
1224.82	0.033300
1238.95	0.036100
1252.90	0.034400
1266.16	0.037300
1279.81	0.031800
1294.13	0.031300
1307.88	0.034900
1321.95	0.032600
1336.34	0.033000
1351.32	0.033200
1366.23	0.034900
1394.67	0.031500
1409.03	0.031400
1436.26	0.031200
1449.87	0.028300
1464.28	0.029200
1477.44	0.031300
1491.87	0.028900
1506.60	0.031100
1520.95	0.027200
1535.32	0.028500
1561.03	0.028900
1575.10	0.027100
1588.78	0.026800
1603.09	0.029100
1617.66	0.029900
1646.48	0.025100
1661.19	0.028300
1675.67	0.026900
1690.15	0.023700
1704.63	0.024400
1718.95	0.024300
1758.27	0.025000
1784.58	0.022100
1794.18	0.023000
1808.68	0.023300
1823.18	0.021600
1837.83	0.022900
1852.28	0.023600
1866.70	0.021900
1881.08	0.023900
1895.57	0.023600
1910.32	0.022600
1924.48	0.020100
1938.82	0.023100
1953.15	0.021600
1967.47	0.023100
1981.87	0.020500

Table C25. Test C7, ^{22}Na.

Effluent *gm*	Activity *µCi / gm*
6.99	0.000330
11.70	0.000552
16.74	0.011200
21.84	0.040700
26.87	0.073800
32.14	0.101000
37.41	0.109000
42.59	0.104000
47.56	0.091800
52.63	0.075100
57.64	0.060900
62.61	0.051900
67.59	0.044000
72.40	0.037000
77.29	0.032100
82.31	0.027600
87.27	0.023900
92.18	0.020800
97.17	0.017600
102.39	0.015600
117.22	0.012500
122.02	0.011700
126.98	0.010600
131.97	0.010100
136.90	0.009240
142.21	0.007950
147.66	0.006960
153.17	0.006930
158.59	0.006520
164.25	0.005790
170.09	0.005220
175.56	0.005420
181.14	0.005080
187.01	0.004700
192.68	0.004690
198.50	0.004410
204.39	0.004030
210.00	0.004030
215.45	0.004170
220.73	0.004180
226.32	0.003680
231.60	0.003750
236.63	0.003870
241.60	0.003560
246.75	0.003660
252.00	0.003280
257.10	0.003250
262.11	0.003050
267.14	0.003100
272.28	0.002890
277.31	0.002880
282.28	0.002850
287.42	0.002610
292.07	0.002650
307.57	0.002290
318.69	0.002000
329.76	0.001990
341.21	0.001810
352.75	0.001670
363.95	0.001800
375.64	0.001450
387.10	0.001600
397.13	0.001590
408.20	0.001440
419.00	0.001330
428.42	0.001540
437.72	0.001260
447.71	0.001160
457.77	0.001250
468.23	0.001010
479.19	0.001030
490.87	0.001020
502.59	0.000964
513.59	0.001070
524.89	0.001010
536.47	0.000980
547.46	0.001030
558.61	0.000962
569.42	0.000937
580.01	0.000868
590.51	0.001010
600.83	0.000903
610.98	0.000858
621.27	0.000821
626.41	0.000916
636.56	0.000916
647.22	0.000866
658.48	0.000841
670.19	0.000741
681.29	0.000814
687.02	0.000765
697.46	0.000821
708.23	0.000789
719.22	0.000762
729.92	0.000733
740.44	0.000759
751.30	0.000726
761.76	0.000723
783.06	0.000695
793.64	0.000694
804.36	0.000714
815.70	0.000650
827.08	0.000594
838.43	0.000608
850.51	0.000622
861.91	0.000621
871.97	0.000554
881.58	0.000633
892.23	0.000599
902.37	0.000653
913.08	0.000559
923.68	0.000640
934.41	0.000652
939.78	0.000600
950.41	0.000581
961.26	0.000581
977.46	0.000466
993.91	0.000458
1010.86	0.000483

Table C26. Test C7, ^{239}Np.

Effluent *gm*	Activity *µCi / gm*
6.99	0.000000
11.70	0.000000
16.74	0.000000
21.84	0.000000
26.87	0.000000
32.14	0.000000
37.41	0.000000
42.59	0.000000
47.56	0.000000
52.63	0.000000
57.64	0.000000
62.61	0.000000
67.59	0.000290
72.40	0.000247
77.29	0.000297
82.31	0.000277
87.27	0.000331
92.18	0.001130
97.17	0.002470
102.39	0.003910
117.22	0.010300
122.02	0.009810
126.98	0.006390
131.97	0.005310
136.90	0.004910
142.21	0.005880
147.66	0.009010
153.17	0.010200
158.59	0.010800
164.25	0.011800
170.09	0.013200
175.56	0.013500
181.14	0.004840
187.01	0.003870
192.68	0.003470
198.50	0.003400
204.39	0.003680
210.00	0.004070
215.45	0.002190
220.73	0.001490
226.32	0.001500
231.60	0.001390
236.63	0.001220
241.60	0.001110
246.75	0.001090
252.00	0.000969
257.10	0.001010
262.11	0.001060
267.14	0.000986
272.28	0.001060
277.31	0.001120
282.28	0.001190
287.42	0.001250
292.07	0.001300
307.57	0.000919
318.69	0.003270
329.76	0.004210
341.21	0.003060
352.75	0.003230
363.95	0.004400
375.64	0.004370
387.10	0.003550
397.13	0.003170
408.20	0.002990
419.00	0.003160
428.42	0.004190
437.72	0.004000
447.71	0.004340
457.77	0.004000
468.23	0.004130
479.19	0.004610
490.87	0.004590
502.59	0.004880
513.59	0.005870
524.89	0.005530
536.47	0.008030
547.46	0.006670
558.61	0.006080
569.42	0.006580
580.01	0.006820
590.51	0.006780
600.83	0.006880
610.98	0.007130
621.27	0.007080
626.41	0.007140
636.56	0.007070
647.22	0.007780
658.48	0.007530
670.19	0.009480
681.29	0.008410
687.02	0.007640
697.46	0.008830
708.23	0.007860
719.22	0.008030
729.92	0.007880
740.44	0.008040
751.30	0.009580
761.76	0.008210
783.06	0.008060
793.64	0.008500
804.36	0.008510
815.70	0.008530
827.08	0.008470
838.43	0.010500
850.51	0.010200
861.91	0.008570
871.97	0.008930
881.58	0.009060
892.23	0.009280
902.37	0.011000
913.08	0.010300
923.68	0.010300
934.41	0.009040
939.78	0.009860
950.41	0.009580
961.26	0.010200
977.46	0.008710
993.91	0.009260
1010.86	0.009450
1027.87	0.008790
1043.67	0.010700
1060.25	0.009480
1075.76	0.010800
1091.79	0.011600
1107.61	0.011300
1123.99	0.009220
1134.60	0.011500
1151.16	0.010500
1168.07	0.010000
1233.72	0.011700
1249.53	0.010300
1282.11	0.010600
1327.12	0.011800
1343.59	0.010700
1360.15	0.011100
1392.95	0.009430
1408.08	0.010200
1423.75	0.011000
1439.91	0.009600
1456.39	0.009400
1472.28	0.010100
1494.83	0.009260
1514.24	0.008560
1530.45	0.007840
1547.39	0.008740
1564.67	0.009000
1581.67	0.009610
1598.65	0.009770
1615.34	0.008850

Effluent *gm*	Activity *µCi / gm*
1632.04	0.010000
1646.98	0.010500
1661.58	0.007250
1677.78	0.010900
1694.57	0.010900
1710.58	0.009210
1723.90	0.011400
1740.73	0.012200
1757.30	0.011100
1774.37	0.009010
1789.97	0.011000
1806.53	0.010500
1822.90	0.012000
1839.35	0.011400
1855.93	0.012100
1872.55	0.008890
1889.38	0.010700
1906.07	0.011900
1922.82	0.012400
1939.05	0.010800
1954.07	0.014700
1970.40	0.014700
1986.73	0.013300
2003.30	0.012500
2019.58	0.011700
2035.87	0.011100
2052.43	0.018800
2069.67	0.013800
2086.30	0.014600
2102.58	0.015600
2118.93	0.016500
2134.77	0.015900
2151.10	0.018800
2167.12	0.017900
2182.85	0.014500
2198.13	0.022800
2214.87	0.018500
2232.63	0.020000
2243.93	0.017000
2259.18	0.019100
2273.72	0.021000
2288.18	0.022100
2304.37	0.020200
2319.33	0.018600
2334.78	0.017600
2350.48	0.019800
2367.17	0.018700
2383.87	0.031900
2401.38	0.025400
2417.72	0.024800
2433.23	0.021400
2448.78	0.023900
2464.82	0.021300
2480.35	0.021600
2496.05	0.026500
2511.83	0.024800
2528.83	0.028400
2545.85	0.024600
2562.88	0.029900
2579.68	0.030200
2595.23	0.029200
2611.22	0.023800
2633.87	0.025400
2649.17	0.024100
2665.22	0.025700
2681.82	0.028300
2693.12	0.030700
2704.38	0.023800
2721.72	0.027000
2739.27	0.030600
2755.37	0.029900
2771.77	0.033500
2787.27	0.029600
2802.57	0.033500
2817.52	0.038800
2833.33	0.030200
2849.65	0.028900
2866.17	0.032000
2882.48	0.034900
2899.13	0.030300
2915.67	0.029600
2931.63	0.037300
2947.43	0.029500
2962.97	0.028100
2978.92	0.031800
2995.17	0.034000
3008.62	0.036100
3022.22	0.037900
3039.02	0.029000
3054.18	0.053100
3069.67	0.030300
3086.03	0.045200
3101.97	0.039900
3117.52	0.046700
3132.82	0.048100
3148.28	0.038400
3163.33	0.040200
3176.87	0.054600
3193.98	0.041100
3211.22	0.044000
3227.28	0.049300
3243.80	0.052300
3260.40	0.055100
3276.73	0.060600
3293.13	0.048900
3309.88	0.056600
3326.57	0.059200
3337.88	0.049800
3354.13	0.070300
3370.82	0.064500
3415.83	0.074300
3462.53	0.075800
3478.47	0.065800
3491.10	0.058900
3506.48	0.081000
3522.87	0.091900
3539.18	0.108000
3555.55	0.059200
3570.90	0.067400
3586.73	0.120000
3603.40	0.084500
3619.42	0.097100
3635.03	0.098800
3651.17	0.108000
3667.73	0.102000
3683.68	0.130000
3699.33	0.121000

Table C27. Test C7, ^{232}U.

Effluent gm	Activity $\mu Ci / gm$
6.99	0.000097
11.70	0.000375
16.74	0.002565
21.84	0.004497
26.87	0.011348
32.14	0.028743
37.41	0.041366
42.59	0.047035
47.56	0.044758
52.63	0.038277
57.64	0.029630
62.61	0.025202
67.59	0.021704
72.40	0.018117
77.29	0.014483
82.31	0.012173
87.27	0.011006
92.18	0.009259
97.17	0.008075
102.39	0.008014
117.22	0.008652
122.02	0.008095
126.98	0.007833
131.97	0.007907
136.90	0.007089
142.21	0.006465
147.66	0.005798
153.17	0.005629
158.59	0.005539
164.25	0.004964
170.09	0.004716
175.56	0.004544
181.14	0.004278
187.01	0.004502
192.68	0.004170
198.50	0.003701
204.39	0.003270
210.00	0.002907
215.45	0.002963
220.73	0.003002
226.32	0.003055
231.60	0.002993
236.63	0.003095
241.60	0.003199
246.75	0.003113
252.00	0.003053
257.10	0.002752
262.11	0.002409
267.14	0.002755
272.28	0.002364
277.31	0.002392
282.28	0.002252
287.42	0.002305
292.07	0.002201
307.57	0.002078
318.69	0.001922
329.76	0.001696
341.21	0.001691
352.75	0.001697
363.95	0.002117
375.64	0.001762
387.10	0.001773
397.13	0.001789
408.20	0.001745
419.00	0.001761
428.42	0.001659
437.72	0.001608
447.71	0.001665
457.77	0.001471

Table C28. Test D1, ^{3}H.

Effluent *gm*	Activity *µCi / gm*
1.41	0.000012
5.92	0.000014
14.14	0.000017
19.19	0.000024
24.19	0.000055
29.03	0.000120
33.82	0.000209
38.56	0.000336
43.27	0.000468
48.03	0.000590
52.76	0.000702
56.82	0.000691
61.44	0.000834
66.08	0.000918
70.82	0.000956
75.56	0.000931
101.78	0.000889
116.87	0.000854
138.80	0.000763
158.81	0.000621
176.75	0.000538
196.06	0.000455
215.42	0.000382
228.49	0.000349
247.91	0.000306
262.36	0.000283
297.96	0.000231
317.98	0.000188
333.04	0.000185
348.68	0.000163
401.05	0.000127
420.72	0.000110
435.25	0.000111
440.21	0.000097
469.83	0.000089
481.50	0.000085

Table C29. Test D2, ^{22}Na.

Effluent *gm*	Activity *µCi / gm*
3.17	0.000000
10.30	0.000043
19.15	0.000697
28.80	0.003950
38.44	0.010300
48.06	0.016900
57.93	0.021500
67.64	0.024000
77.42	0.024900
87.24	0.023000
97.37	0.019600
107.73	0.016500
117.77	0.014700
128.05	0.012400
138.21	0.010500
148.12	0.009490
158.36	0.008920
168.52	0.007830
178.39	0.007390
188.13	0.006460
198.08	0.005490
207.27	0.005210
217.01	0.004640
227.13	0.004110
235.87	0.003910
245.39	0.003560
255.24	0.003160
285.15	0.002550
294.63	0.002420
304.13	0.002160
313.55	0.002070
323.03	0.001730
332.53	0.001690
351.30	0.001560
360.95	0.001450
369.89	0.001200
379.66	0.001170
389.32	0.001150
398.97	0.001070
408.59	0.001000
418.53	0.000906
428.37	0.000773
438.29	0.000850
447.97	0.000801
457.60	0.000753
467.25	0.000723
476.68	0.000724
486.29	0.000649
496.02	0.000591
506.04	0.000570
515.78	0.000537
525.41	0.000581
535.03	0.000514
544.95	0.000503
554.92	0.000432
565.07	0.000433
570.04	0.000454
575.01	0.000446
579.84	0.000419
584.70	0.000395
589.44	0.000417
594.26	0.000425
599.14	0.000383
607.94	0.000386
612.91	0.000372
617.68	0.000343
622.49	0.000369
627.31	0.000392
632.34	0.000339
636.74	0.000497
641.22	0.000364
645.81	0.000342
650.41	0.000348
654.98	0.000306
659.79	0.000315
664.56	0.000324
669.26	0.000280
673.97	0.000345
678.88	0.000276
683.68	0.000298
688.68	0.000284
693.64	0.000278
698.72	0.000294
703.76	0.000301
708.65	0.000290
717.15	0.000279
721.98	0.000279
726.97	0.000276
731.76	0.000247
736.54	0.000305
740.38	0.000410
745.27	0.000285
750.14	0.000235
754.96	0.000242
759.88	0.000215
764.93	0.000249
769.37	0.000238
774.08	0.000217
778.89	0.000221
783.85	0.000234
788.65	0.000253
793.52	0.000216
801.94	0.000234
806.97	0.000204
811.85	0.000223
816.88	0.000204
821.87	0.000199
826.24	0.000246
831.31	0.000202
836.39	0.000158
841.41	0.000216
846.35	0.000176
851.24	0.000189
856.25	0.000180
861.15	0.000183
865.97	0.000176
870.97	0.000172
875.98	0.000158
880.88	0.000185
885.83	0.000235
890.77	0.000186
895.65	0.000146
900.54	0.000154
905.40	0.000195
910.30	0.000142
915.03	0.000504
919.93	0.000159
924.72	0.000171
929.54	0.000175
934.43	0.000141
939.30	0.000159
944.05	0.000204
948.88	0.000184
953.94	0.000152
959.04	0.000161
964.09	0.000133
969.08	0.000144
973.93	0.000592
978.76	0.000152
983.64	0.000157
988.61	0.000197
993.56	0.000124
998.50	0.000147
1007.34	0.000160

Table C30. Test D2, ^{239}Np.

Effluent *gm*	Activity *µCi / gm*
3.17	0.000000
10.30	0.000000
19.15	0.000000
28.80	0.000000
38.44	0.000000
48.06	0.000000
57.93	0.000000
67.64	0.000000
77.42	0.000000
87.24	0.000000
97.37	0.000000
107.73	0.000000
117.77	0.000000
128.05	0.000000
138.21	0.000000
148.12	0.000000
158.36	0.000000
168.52	0.000000
178.39	0.000000
188.13	0.000000
198.08	0.000000
207.27	0.000000
217.01	0.000000
227.13	0.000000
235.87	0.000000
245.39	0.000000
255.24	0.000000
285.15	0.000000
294.63	0.000000
304.13	0.000000
313.55	0.000000
323.03	0.000000
332.53	0.000000
351.30	0.000000
360.95	0.000000
369.89	0.000000
379.66	0.000000
389.32	0.000000
398.97	0.000000
408.59	0.000000
418.53	0.000292
428.37	0.000287
438.29	0.000347
447.97	0.000373
457.60	0.000412
467.25	0.000390
476.68	0.000300
486.29	0.000401
496.02	0.000400
506.04	0.000468
515.78	0.000443
525.41	0.000437
535.03	0.000558
544.95	0.000487
554.92	0.000546
565.07	0.000624
570.04	0.000534
575.01	0.000600
579.84	0.000550
584.70	0.000576
589.44	0.000636
594.26	0.000580
599.14	0.000617
607.94	0.000590
612.91	0.000528
617.68	0.000696
622.49	0.000609
627.31	0.000621
632.34	0.000594
636.74	0.000760
641.22	0.000662
645.81	0.000676
650.41	0.000618
654.98	0.000624
659.79	0.000644
664.56	0.000774
669.26	0.000590
673.97	0.000783
678.88	0.000691
683.68	0.000695
688.68	0.000624
693.64	0.000757
698.72	0.000619
703.76	0.000749
708.65	0.000830
717.15	0.000676
721.98	0.000814
726.97	0.000692
731.76	0.000771
736.54	0.000763
740.38	0.000832
745.27	0.000788
750.14	0.000827
754.96	0.000749
759.88	0.000821
764.93	0.000816
769.37	0.000820
774.08	0.000782
778.89	0.000741
783.85	0.000771
788.65	0.000843
793.52	0.000707
801.94	0.000731
806.97	0.000717
811.85	0.000709
816.88	0.000788
821.87	0.000755
826.24	0.000818
831.31	0.000686
836.39	0.000717
841.41	0.000759
846.35	0.000905
851.24	0.000822
856.25	0.000905
861.15	0.000823
865.97	0.000905
870.97	0.000740
875.98	0.000878
880.88	0.000793
885.83	0.000834
890.77	0.000817
895.65	0.000854
900.54	0.000848
905.40	0.000719
910.30	0.000915
915.03	0.000934
919.93	0.000884
924.72	0.000781
929.54	0.000710
934.43	0.000778
939.30	0.000891
944.05	0.000917
948.88	0.000779
953.94	0.000734
959.04	0.000772
964.09	0.000818
969.08	0.000967
973.93	0.000901
978.76	0.000870
983.64	0.000967
988.61	0.000709
993.56	0.000801
998.50	0.000910
1007.34	0.000869
1012.23	0.000797
1016.72	0.000797
1020.96	0.000938
1025.45	0.000976
1030.06	0.000838

Effluent *gm*	Activity *µCi / gm*	Effluent *gm*	Activity *µCi / gm*	Effluent *gm*	Activity *µCi / gm*
1034.74	0.000863	1321.39	0.001180	0.00	0.000000
1039.52	0.000852	1325.77	0.000885	0.00	0.000000
1044.18	0.000790	1330.54	0.000885	0.00	0.000000
1048.90	0.000956	1335.33	0.001010	0.00	0.000000
1053.71	0.000945	1340.18	0.000879	0.00	0.000000
1058.52	0.000926	1345.08	0.000871	0.00	0.000000
1063.31	0.000771	1349.73	0.001080	0.00	0.000000
1068.19	0.000940	1354.52	0.001010	0.00	0.000000
1073.08	0.000861	1359.26	0.001010	0.00	0.000000
1077.93	0.000811	1364.13	0.000867	0.00	0.000000
1082.08	0.000907	1369.88	0.001070	0.00	0.000000
1087.04	0.000897	1374.30	0.001110	0.00	0.000000
1091.60	0.000877	1378.65	0.001120	0.00	0.000000
1106.69	0.000867	1383.14	0.000865	0.00	0.000000
1111.37	0.000978	0.00	0.000000	0.00	0.000000
1116.05	0.000776	0.00	0.000000	0.00	0.000000
1120.61	0.001100	0.00	0.000000	0.00	0.000000
1125.25	0.001100	0.00	0.000000	0.00	0.000000
1130.02	0.000989	0.00	0.000000	0.00	0.000000
1135.04	0.001050	0.00	0.000000	0.00	0.000000
1140.27	0.000900	0.00	0.000000	0.00	0.000000
1145.38	0.001030	0.00	0.000000	0.00	0.000000
1150.51	0.000851	0.00	0.000000	0.00	0.000000
1155.44	0.000819	0.00	0.000000	0.00	0.000000
1160.35	0.000943	0.00	0.000000	0.00	0.000000
1165.29	0.000971	0.00	0.000000	0.00	0.000000
1170.27	0.001030	0.00	0.000000	0.00	0.000000
1175.01	0.001010	0.00	0.000000	0.00	0.000000
1179.71	0.000839	0.00	0.000000	0.00	0.000000
1184.07	0.001060	0.00	0.000000	0.00	0.000000
1188.14	0.000982	0.00	0.000000	0.00	0.000000
1192.39	0.000968	0.00	0.000000	0.00	0.000000
1195.84	0.001150	0.00	0.000000	0.00	0.000000
1200.59	0.001110	0.00	0.000000	0.00	0.000000
1205.31	0.000980	0.00	0.000000	0.00	0.000000
1210.08	0.000959	0.00	0.000000	0.00	0.000000
1214.84	0.000853	0.00	0.000000	0.00	0.000000
1219.56	0.000835	0.00	0.000000	0.00	0.000000
1224.34	0.000999	0.00	0.000000	0.00	0.000000
1229.33	0.000892	0.00	0.000000	0.00	0.000000
1234.45	0.000911	0.00	0.000000	0.00	0.000000
1239.54	0.001070	0.00	0.000000	0.00	0.000000
1249.27	0.001000	0.00	0.000000	0.00	0.000000
1253.86	0.001050	0.00	0.000000	0.00	0.000000
1258.50	0.000815	0.00	0.000000	0.00	0.000000
1268.50	0.000991	0.00	0.000000	0.00	0.000000
1278.76	0.001180	0.00	0.000000	0.00	0.000000
1283.79	0.001020	0.00	0.000000	0.00	0.000000
1293.58	0.001110	0.00	0.000000	0.00	0.000000
1312.63	0.001200	0.00	0.000000	0.00	0.000000

Effluent *gm*	**Activity** *μCi / gm*
0.00	0.000000
0.00	0.000000
0.00	0.000000
0.00	0.000000
0.00	0.000000
0.00	0.000000
0.00	0.000000
0.00	0.000000
0.00	0.000000
0.00	0.000000
0.00	0.000000
0.00	0.000000
0.00	0.000000
0.00	0.000000
0.00	0.000000
0.00	0.000000
0.00	0.000000
0.00	0.000000
0.00	0.000000
0.00	0.000000
0.00	0.000000
0.00	0.000000
0.00	0.000000
0.00	0.000000
0.00	0.000000
0.00	0.000000
0.00	0.000000
0.00	0.000000
0.00	0.000000
0.00	0.000000
0.00	0.000000
0.00	0.000000
0.00	0.000000
0.00	0.000000
0.00	0.000000
0.00	0.000000
0.00	0.000000
0.00	0.000000
0.00	0.000000
0.00	0.000000
0.00	0.000000
0.00	0.000000
0.00	0.000000
0.00	0.000000

Table C31. Test D3, ^{22}Na.

Effluent *gm*	Activity *µCi / gm*
1.71	0.000125
4.64	0.000081
8.02	0.000065
11.61	0.000066
15.54	0.000077
19.63	0.000159
23.81	0.000115
28.12	0.000533
32.52	0.002060
36.88	0.004660
41.29	0.009000
45.86	0.012800
53.35	0.017000
57.70	0.019000
62.12	0.020200
66.58	0.020600
71.02	0.020400
78.16	0.019700
87.84	0.018200
92.63	0.017600
97.33	0.016800
102.23	0.016200
107.13	0.014900
112.06	0.014400
116.90	0.014100
121.59	0.013500
126.37	0.012700
134.73	0.011300
139.56	0.010700
144.45	0.009810
149.44	0.009190
158.37	0.008700
163.21	0.008550
168.04	0.008150
172.96	0.007210
177.76	0.007330
182.53	0.006700
187.19	0.006600
191.78	0.006670
196.40	0.006420
201.10	0.005860
205.83	0.005510
210.61	0.005120
215.25	0.005110
220.02	0.004910
224.81	0.004730
229.72	0.004320
234.55	0.004430
239.31	0.004110
248.03	0.004040
252.69	0.003540
257.30	0.003740
285.67	0.002790
290.48	0.002690
299.82	0.002520
304.72	0.002470
309.63	0.002380
314.46	0.002230
319.19	0.002360
324.01	0.002320
328.73	0.002140
343.38	0.001960
348.16	0.001860
352.33	0.002020
357.41	0.001780
362.08	0.001880
366.19	0.001900
370.46	0.001830
375.03	0.001630
379.59	0.001660
384.27	0.001420
388.90	0.001660
393.66	0.001530
398.46	0.001450
402.94	0.001350
407.84	0.001320
412.70	0.001340
417.61	0.001290
422.55	0.001400
427.50	0.001210
432.67	0.001170
437.60	0.001250
442.27	0.001160
447.12	0.001100
451.96	0.001100
456.96	0.001040
461.91	0.001050
475.27	0.000878
480.33	0.000923
485.32	0.000856
490.16	0.000882
495.26	0.000842
500.16	0.000874
505.09	0.000799
509.82	0.000851
514.50	0.000925
519.30	0.000765
524.07	0.000774
531.64	0.000758
536.46	0.000733
541.33	0.000756
546.22	0.000689
556.25	0.000681
561.23	0.000670
566.13	0.000653
571.03	0.000667
575.85	0.000634
580.65	0.000651
585.65	0.000610
590.67	0.000588
595.64	0.000611
600.63	0.000644
605.66	0.000651
610.61	0.000600
615.56	0.000561
620.65	0.000591
625.63	0.000571
630.55	0.000538
635.30	0.000549
640.17	0.000525
644.89	0.000588
649.68	0.000531
654.67	0.000540
659.54	0.000485
664.25	0.000478
669.15	0.000514
678.93	0.000472
698.90	0.000457
718.28	0.000470
737.84	0.000402
756.51	0.000357
774.68	0.000369
793.89	0.000368
813.47	0.000352
830.98	0.000322
848.37	0.000318
865.64	0.000469
873.22	0.000431
889.16	0.000334
907.61	0.000316
926.44	0.000308
944.64	0.000307
964.18	0.000278
983.29	0.000253
1002.39	0.000231
1022.01	0.000365
1041.20	0.000235
1060.37	0.000228
1079.84	0.000215

Effluent *gm*	Activity *µCi / gm*
1098.66	0.000230
1117.22	0.000392
1136.02	0.000238
1155.47	0.000197
1174.44	0.000197
1193.14	0.000210
1212.25	0.000225
1231.16	0.000191
1248.77	0.000171
1267.45	0.000151
1285.96	0.000174
1305.10	0.000160
1324.24	0.000221
1343.66	0.000255
1362.65	0.000144
1381.52	0.000143
1420.78	0.000124
1439.94	0.000174
1459.58	0.000159
1479.20	0.000109
1497.38	0.000296
1516.00	0.000124
1535.37	0.000116
1555.14	0.000118
1571.08	0.000185
1591.06	0.000108
1609.48	0.000154
1626.73	0.000180
1645.51	0.000101
1664.91	0.000114
1683.42	0.000103
1703.37	0.000092
1723.57	0.000092
1742.98	0.000291
1761.88	0.000101
1780.23	0.000094
1799.78	0.000197
1819.08	0.000090
1835.82	0.000101
1854.43	0.000093
1874.55	0.000094
1893.53	0.000100
1912.92	0.000104
1932.32	0.000085
1951.42	0.000098
1970.67	0.000082
1990.62	0.000076
2010.65	0.000089
2029.88	0.000088
2049.25	0.000101

Effluent *gm*	Activity *µCi / gm*
2068.75	0.000079
2087.83	0.000093
2107.27	0.000104
2126.02	0.000095
2145.17	0.000083
2163.98	0.000087
2182.78	0.000086
2200.53	0.000104
2217.93	0.000082
2236.22	0.000130
2254.58	0.000088
2273.18	0.000078
2292.32	0.000094
2311.03	0.000080
2330.43	0.000079
2348.98	0.000092
2367.88	0.000086
2386.65	0.000087
2405.42	0.000092
2424.87	0.000147
2444.83	0.000081
2463.98	0.000083
2482.90	0.000062
2502.17	0.000093
2521.32	0.000070
2539.02	0.000375
2558.63	0.000081
2575.27	0.000090
2592.85	0.000089
2611.52	0.000084
2630.45	0.000080
2649.62	0.000095
2668.73	0.000102
2683.47	0.000082
2700.25	0.000089
2719.88	0.000077
2739.07	0.000068
2758.23	0.000069
2777.00	0.000069
2796.48	0.000072

Table C32. Test D4, ^{22}Na.

Effluent *gm*	Activity *µCi / gm*
4.81	0.000178
8.25	0.000022
12.21	0.000013
16.46	0.000013
20.96	0.000040
25.63	0.000295
30.58	0.001310
35.54	0.004120
40.14	0.009230
45.29	0.014000
50.12	0.020200
54.91	0.029700
59.87	0.030700
64.78	0.030700
69.71	0.033400
74.56	0.031900
79.21	0.031800
83.71	0.032600
88.57	0.029700
93.44	0.028600
98.36	0.026100
103.16	0.025500
108.20	0.022100
113.12	0.021700
117.98	0.020600
122.88	0.018600
127.77	0.017600
132.84	0.016300
137.76	0.015700
142.66	0.014200
147.41	0.014400
152.07	0.013200
157.00	0.011900
161.98	0.010500
166.85	0.010400
171.93	0.009250
176.91	0.009040
186.81	0.008380
191.84	0.008070
196.81	0.007440
201.69	0.007210
206.44	0.006740
211.11	0.006480
215.61	0.006350
220.52	0.005720
225.31	0.005640
230.34	0.005240
235.15	0.004770
240.13	0.004520
245.07	0.004210
250.05	0.004390
254.87	0.004220
259.93	0.003670
264.64	0.003830
269.43	0.003760
274.05	0.003660
278.69	0.003450
283.33	0.003490
288.05	0.003160
292.80	0.003150
297.60	0.002910
302.51	0.002720
307.43	0.002400
312.11	0.002590
317.03	0.002540
321.97	0.002260
326.88	0.002230
331.67	0.002200
336.54	0.002020
341.16	0.002060
345.87	0.001930
350.61	0.001980
355.21	0.001870
360.07	0.001750
364.92	0.001700
369.72	0.001730
374.39	0.001720
378.18	0.001840
382.46	0.001670
386.98	0.001490
391.63	0.001490
396.43	0.001420
401.12	0.001300
405.76	0.001360
410.27	0.001320
415.09	0.001680
419.82	0.001280
429.56	0.001160
434.40	0.001150
439.31	0.001110
444.35	0.001050
449.26	0.001120
454.32	0.000944
459.40	0.000894
464.43	0.001230
469.34	0.000862
474.19	0.000878
478.98	0.000887
483.72	0.000801
488.68	0.000769
493.50	0.000823
498.32	0.000780
503.27	0.000777
508.14	0.000734
512.98	0.000747
518.02	0.000701
522.82	0.000694
527.88	0.000674
532.60	0.000652
537.47	0.000619
542.22	0.000659
546.96	0.000627
561.46	0.000516
576.11	0.000620
590.65	0.000491
604.94	0.000537
619.31	0.000423
633.97	0.000457
648.36	0.000354
663.08	0.000337
677.33	0.000555
691.89	0.000323
706.66	0.000330
721.27	0.000423
735.59	0.000293
768.92	0.000333
783.32	0.000271
797.41	0.000321
811.13	0.000242
825.26	0.000216
839.59	0.000215
854.01	0.000245
869.11	0.000176
884.63	0.000156
900.31	0.000184
915.83	0.000538
930.89	0.000140
945.47	0.000159
959.89	0.000158
974.22	0.000137
988.38	0.000154
1002.78	0.000134
1014.63	0.000113
1030.07	0.000195
1045.44	0.000105
1060.60	0.000107
1075.50	0.000112
1090.02	0.000087
1103.06	0.000100

Effluent *gm*	Activity *µCi / gm*
1117.51	0.000091
1122.22	0.000153
1135.39	0.000102
1148.75	0.000084
1163.56	0.000080
1189.77	0.000088
1204.11	0.000075
1218.13	0.000104
1232.27	0.000072
1246.63	0.000081
1260.38	0.000083
1274.58	0.000062
1288.03	0.000074
1302.86	0.000055
1317.91	0.000059
1332.79	0.000039
1347.46	0.000067
1361.81	0.000050
1376.41	0.000056
1391.01	0.000064
1406.24	0.000031
1420.26	0.000055
1432.21	0.000054
1446.79	0.000032
1461.25	0.000046
1475.87	0.000039
1490.12	0.000040
1504.10	0.000057
1530.76	0.000037
1544.95	0.000186
1573.77	0.000074
1588.60	0.000077
1603.16	0.000026
1617.86	0.000459
1632.61	0.000029
1647.15	0.000024
1661.75	0.000023
1676.18	0.000165
1690.83	0.000063
1730.23	0.000052
1743.88	0.000065
1758.52	0.000051
1773.08	0.000056
1787.58	0.000072
1802.40	0.000054
1816.95	0.000067
1831.38	0.000062
1846.42	0.000058
1876.07	0.000054
1888.38	0.000093
1902.13	0.000053
1916.48	0.000069
1931.02	0.000046
1945.22	0.000045
1959.47	0.000036
1973.88	0.000048

Table C33. Test D4, ^{22}Na.

Effluent *gm*	Activity *µCi / gm*
4.81	0.000178
8.25	0.000022
12.21	0.000013
16.46	0.000013
20.96	0.000040
25.63	0.000295
30.58	0.001310
35.54	0.004120
40.14	0.009230
45.29	0.014000
50.12	0.020200
54.91	0.029700
59.87	0.030700
64.78	0.030700
69.71	0.033400
74.56	0.031900
79.21	0.031800
83.71	0.032600
88.57	0.029700
93.44	0.028600
98.36	0.026100
103.16	0.025500
108.20	0.022100
113.12	0.021700
117.98	0.020600
122.88	0.018600
127.77	0.017600
132.84	0.016300
137.76	0.015700
142.66	0.014200
147.41	0.014400
152.07	0.013200
157.00	0.011900
161.98	0.010500
166.85	0.010400
171.93	0.009250
176.91	0.009040
186.81	0.008380
191.84	0.008070
196.81	0.007440
201.69	0.007210
206.44	0.006740
211.11	0.006480
215.61	0.006350
220.52	0.005720
225.31	0.005640
230.34	0.005240
235.15	0.004770
240.13	0.004520
245.07	0.004210
250.05	0.004390
254.87	0.004220
259.93	0.003670
264.64	0.003830
269.43	0.003760
274.05	0.003660
278.69	0.003450
283.33	0.003490
288.05	0.003160
292.80	0.003150
297.60	0.002910
302.51	0.002720
307.43	0.002400
312.11	0.002590
317.03	0.002540
321.97	0.002260
326.88	0.002230
331.67	0.002200
336.54	0.002020
341.16	0.002060
345.87	0.001930
350.61	0.001980
355.21	0.001870
360.07	0.001750
364.92	0.001700
369.72	0.001730
374.39	0.001720
378.18	0.001840
382.46	0.001670
386.98	0.001490
391.63	0.001490
396.43	0.001420
401.12	0.001300
405.76	0.001360
410.27	0.001320
415.09	0.001680
419.82	0.001280
429.56	0.001160
434.40	0.001150
439.31	0.001110
444.35	0.001050
449.26	0.001120
454.32	0.000944
459.40	0.000894
464.43	0.001230
469.34	0.000862
474.19	0.000878
478.98	0.000887
483.72	0.000801
488.68	0.000769
493.50	0.000823
498.32	0.000780
503.27	0.000777
508.14	0.000734
512.98	0.000747
518.02	0.000701
522.82	0.000694
527.88	0.000674
532.60	0.000652
537.47	0.000619
542.22	0.000659
546.96	0.000627
561.46	0.000516
576.11	0.000620
590.65	0.000491
604.94	0.000537
619.31	0.000423
633.97	0.000457
648.36	0.000354
663.08	0.000337
677.33	0.000555
691.89	0.000323
706.66	0.000330
721.27	0.000423
735.59	0.000293
768.92	0.000333
783.32	0.000271
797.41	0.000321
811.13	0.000242
825.26	0.000216
839.59	0.000215
854.01	0.000245
869.11	0.000176
884.63	0.000156
900.31	0.000184
915.83	0.000538
930.89	0.000140
945.47	0.000159
959.89	0.000158
974.22	0.000137
988.38	0.000154
1002.78	0.000134
1014.63	0.000113
1030.07	0.000195
1045.44	0.000105
1060.60	0.000107
1075.50	0.000112
1090.02	0.000087
1103.06	0.000100

Effluent *gm*	Activity *µCi / gm*
1117.51	0.000091
1122.22	0.000153
1135.39	0.000102
1148.75	0.000084
1163.56	0.000080
1189.77	0.000088
1204.11	0.000075
1218.13	0.000104
1232.27	0.000072
1246.63	0.000081
1260.38	0.000083
1274.58	0.000062
1288.03	0.000074
1302.86	0.000055
1317.91	0.000059
1332.79	0.000039
1347.46	0.000067
1361.81	0.000050
1376.41	0.000056
1391.01	0.000064
1406.24	0.000031
1420.26	0.000055
1432.21	0.000054
1446.79	0.000032
1461.25	0.000046
1475.87	0.000039
1490.12	0.000040
1504.10	0.000057
1530.76	0.000037
1544.95	0.000186
1573.77	0.000074
1588.60	0.000077
1603.16	0.000026
1617.86	0.000459
1632.61	0.000029
1647.15	0.000024
1661.75	0.000023
1676.18	0.000165
1690.83	0.000063
1730.23	0.000052
1743.88	0.000065
1758.52	0.000051
1773.08	0.000056
1787.58	0.000072
1802.40	0.000054
1816.95	0.000067
1831.38	0.000062
1846.42	0.000058
1876.07	0.000054
1888.38	0.000093

Effluent *gm*	Activity *µCi / gm*
1902.13	0.000053
1916.48	0.000069
1931.02	0.000046
1945.22	0.000045
1959.47	0.000036
1973.88	0.000048

Table C34. Test D5, ^{22}Na.

Effluent *gm*	Activity *µCi / gm*
26.97	0.000091
36.58	0.001780
46.62	0.006940
56.78	0.014700
66.66	0.018000
76.22	0.018900
85.72	0.017700
95.40	0.017700
104.89	0.015600
114.34	0.014600
122.81	0.013200
133.04	0.012200
143.20	0.011500
153.37	0.010000
163.58	0.008890
178.35	0.007850
192.86	0.006760
206.72	0.006120
220.92	0.005440
235.09	0.004850
250.01	0.004360
264.85	0.003800
279.69	0.003350
295.27	0.003210
310.22	0.002920
325.38	0.002420
340.08	0.002280
354.82	0.002100
369.78	0.001860
383.32	0.001840
397.17	0.001660
410.76	0.001530
425.63	0.001450
439.68	0.001400
454.86	0.001250
468.68	0.001210
482.22	0.001140
497.25	0.001050
511.93	0.001010
526.57	0.001000
540.98	0.000928
554.77	0.000911
568.67	0.000930
579.89	0.000867
595.18	0.000820
610.01	0.000800
624.25	0.000748
638.77	0.000742
652.99	0.000696
666.76	0.000687
679.96	0.000669
693.74	0.000649
707.83	0.000633
722.03	0.000620
736.81	0.000614
751.73	0.000574
765.15	0.000566
779.68	0.000537
793.10	0.000519
807.28	0.000525
821.33	0.000518
835.26	0.000517
849.53	0.000497
862.91	0.000491
878.38	0.000469
893.22	0.000457
909.02	0.000436
923.46	0.000427
937.60	0.000406
952.19	0.000433
966.84	0.000412
978.57	0.000400
996.29	0.000403
1010.37	0.000420

APPENDIX D

Reprinted Memorandums

Appendix D Errata

The following modifications should be made to Appendix D.

Page	Comment
D-4 - D-6	Brush (1987) should read Brush (1988)
D-5	Brush, L.H.; Add closing parentheses after D_{sol}s. WPO# is 37400.
D-6	The following references should be added: Higgo, J.J.W, T.G. Cole, L.V.C. Rees, and D.S. Cronan. 1987. Diffusion of Radionuclides through Deep-Sea Sediments. DOE/RW/87.053. London, UK: Department of the Environment. (Copy on file in the Sandia WIPP Central Files, Sandia National Laboratories, Albuquerque, NM as WPO#49299.) Li, Y., and S. Gregory. 1974. "Diffusion of Ions in Sea Water and in Deep-Sea Sediments," Geochimica et Cosmochimica Acta. Vol. 38, no. 5, 703-714.
D-24	Sewards et al., 1992: "Brearly" should read "Brearley."
D-24	Sewards et al., 1991: S.J. Lambert and C.L. Stein were also authors.
D-24	Siegel et al., 1991: Correct page numbers are 2-1 through 2-164. This is chapter 2 of SAND88-0196.
D-93	Callout for "Novak (1996)" should read "Novak and Moore (1996)."
D-94	Drez, 1996. Title word "Estimate" is singular. WPO # is 35552.
D-95	"Weiner, R." should read "Weiner, R.F."
D-109	Callout for "Siegel, 1996a" should read "Siegel, 1996."
D-111	Callout for "Novak and Babb, 1995" should read "Babb and Novak, 1995."
D-113	Reference for "Lucero et al., 1995": "Geldbard" should read "Gelbard."
D-113	Reference for "Novak, C.F. and Babb, S.C." Should read "Babb, S.C., and Novak, C.F." WPO # is 28119.
D-113	Reference for "Siegel, M.D.": Date should read "July 17, 1996." WPO # is 38231.

List of Reprinted Memorandums

Brush, L.H. 1996a. "Revised Free-Solution Tracer Diffusion Coefficients (D_{sol}s) for Dissolved Pu, Am, U, Th, Np, Cm, and Ra in Boreholes and the Culebra for Use in PA Calculations to Support the WIPP CCA." Memorandum to M.S. Tierney, dated May 11, 1996. Albuquerque, NM: Sandia National Laboratories. (Copy on file in the Sandia WIPP Central Files, Sandia National Laboratories, Albuquerque, NM as WPO#38510.)

Brush, L.H. 1996b. "Ranges and Probability Distributions of Kds for Dissolved Pu, Am, U, Th, and Np in the Culebra for the PA Calculations to Support the WIPP CCA." Memorandum to M.S. Tierney, dated June 10, 1996. Albuquerque, NM: Sandia National Laboratories. (Copy on file in the Sandia WIPP Central Files, Sandia National Laboratories, Albuquerque, NM as WPO#38801.)

Craft, C.C., and M.D. Siegel. 1997. "Additional Calculations of Solubility-Limited Concentrations of Actinides for Injection Spikes Used in WIPP Core Column Experiments at Sandia National Laboratories." Memorandum to D. Lucero, dated June 9, 1997. Albuquerque, NM: Sandia National Laboratories. (Copy on file in the Sandia WIPP Central Files, Sandia National Laboratories, Albuquerque, NM in WPO#40975; Reprinted in Appendix D.)

Lucero, D.A. 1997. "Memo of Record for Column Effluent Times." Memorandum to G. Perkins, dated February 3, 1997. Albuquerque, NM: Sandia National Laboratories. . (Copy on file in the Sandia WIPP Central Files, Sandia National Laboratories, Albuquerque, NM in records package WPO#40975.)

Terra Tek. 1996. "Results of Porosity and Permeability Measurements of VPX 26-11 Core Sample." Letter report to Y. Behl. (Copy on file in the Sandia WIPP Central Files, Sandia National Laboratories, Albuquerque, NM in records package WPO#40975.)

Yeh, S. 1993a. "Revised Viscosity Measurements of Culebra Brines." Memorandum to F. Gelbard, dated August 13, 1993. Albuquerque, NM: Sandia National Laboratories. (Copy on file in the Sandia WIPP Central Files, Sandia National Laboratories, Albuquerque, NM in records package WPO#8760.)

Yeh, S. 1993b. "Viscosity Measurements of Salado Brines." Memorandum to F. Gelbard, dated August 13, 1993. Albuquerque, NM: Sandia National Laboratories. (Copy on file in the Sandia WIPP Central Files, Sandia National Laboratories, Albuquerque, NM in records package WPO#8761.)

WPO 38510

Sandia National Laboratories

Albuquerque, New Mexico 87185-1341

date: May 11, 1996

to: M. S. Tierney, MS-1328 (Org. 6741)

L. H. Brush

INFORMATION ONLY

from: L. H. Brush, MS-1341 (Org. 6748)

subject: Revised Free-Solution Tracer Diffusion Coefficients (D_{sol}s) for Dissolved Pu, Am, U, Th, Np, Cm, and Ra in Boreholes and the Culebra for Use in the PA Calculations to Support the WIPP CCA

This memorandum revises the free-solution tracer diffusion coefficients (D_{sol}s) recommended by Brush (1996) for use in the long-term performance-assessment (PA) calculations to support the Waste Isolation Pilot Plant (WIPP) Compliance Certification Application (CCA). After submission of this memorandum, C. T. Stockman suggested a better way of using the D_{sol}s for Pu, U, and Np in the PA calculations (see below).

Brush (1996) modified the D_{sol}s for Pu, U, and Np from Brush (1987) (see Table 1) slightly to be consistent with the oxidation states of Pu, U, and Np predicted for WIPP disposal rooms and assumed for boreholes and the Culebra. Actinide Source Term Program and the Dissolved Actinide Retardation Research Program personnel have predicted that Pu will speciate as Pu(III) or Pu(IV), but not as Pu(V) nor Pu(VI), U will speciate as U(IV) or U(VI), and Np will speciate as Np(IV) or Np(V), but not as Np(VI), in WIPP disposal rooms, boreholes, and the Culebra. Because Brush (1996) believed that PA personnel required fixed values of D_{sol} for Pu, U, and Np for the calculations to support the WIPP CCA, he recommend that PA use the mean of the D_{sol}s for Am(III) and Th(IV) compiled by Brush (1987) for Pu, the mean of the D_{sol}s for Th(IV) and U(VI) from Brush (1987) for U, and the mean of the D_{sol}s for Th(IV) and Np(V) from Brush (1987) for Np.

However, Stockman suggested that PA personnel sample D_{sol}s for Pu, U, and Np the same way they will sample the oxidation states for these elements in WIPP disposal rooms and the Culebra for predictions of solubilities and K_ds, respectively. PA will sample solubilities and K_ds for *either* Pu(III), U(IV), and Np(IV), *or* Pu(IV), U(VI), and Np(V) in any given vector. PA will specify the oxidation states of these elements by sampling "oxstat," a parameter with a uniform distribution of 0 to 1. If the sampled value of oxstat is 0.5 or less, PA will use the solubilities predicted for Pu(III), U(IV), and Np(IV). If oxstat is greater than 0.5, PA will use solubilities for Pu(IV), U(VI), and Np(V). Therefore, I recommend that, if oxstat is 0.5 or less, PA use the D_{sol}s for

SWCF-A:1.1.10.3.1: TD: QA: Nonsalado Adsorption Studies

Am(III), Th(IV), and Th(IV) compiled by Brush (1987) for Pu(III), U(IV), and Np(IV), respectively, for that vector (see Table 2). If oxstat is greater than 0.5, I recommend that PA use the D_{sol}s for Th(IV), U(VI), and Np(V) from Brush (1987) for Pu(IV), U(VI), and Np(V), respectively.

REFERENCES

Brush, L.H. 1987. *Feasibility of Disposal of High-Level Radioactive Wastes into the Seabed: Review of Laboratory Investigations of Radionuclide Migration through Deep-Sea Sediments.* SAND87-2438. Albuquerque, NM: Sandia National Laboratories.

Brush, L.H. "Free-Solution Tracer Diffusion Coefficients (D_{sol}s for Dissolved Pu, Am, U, Th, Np, Cm, and Ra in Boreholes and the Culebra for Use in the PA Calculations to Support the WIPP CCA." Unpublished memorandum to M.S. Tierney, May 2, 1996. Albuquerque, NM: Sandia National Laboratories.

Table 1. Values of D_{sol} from Brush (1987). Table includes only the elements needed for the PA calculations to support the WIPP CCA. Table retyped by L. H. Brush on May 2, 1996. Table checked by L. J. Storz on May 2, 1996.

Element	Species for Which D_{sol} Was Determined	Temperature at Which D_{sol} Was Determined (C)	D_{sol}, cm^2/sec
Pu	Pu^{4+}, PuO_2^+	4	3×10^{-6}
Am	Am^{3+}	4	3×10^{-6}
U	UO_2^{2+}	25	4.26×10^{-6}
Th	Th^{4+}	18	1.53×10^{-6}
Np	NpO_2^+	4	3×10^{-6}
Cm	Cm^{3+}	4	3×10^{-6}
Ra	Ra^{2+}	0	4.02×10^{-6}

Values for Pu^{4+} and PuO_2^+, Am^{3+}, and NpO_2^+ from Higgo et al. (1987); values for UO_2^{2+}, Th^{4+}, and Ra^{2+} from Li and Gregory (1974); value for Am^{3+} applied to Cm^{3+} by oxidation-state analogy.

Table 2. Revised Values of D_{sol} for Use in the PA Calculations to Support the WIPP CCA. Table compiled by L. H. Brush on May 11, 1996. Table checked by L. J. Storz on May 13, 1996.

Element	Oxidation State for Which D_{sol} Was Estimated	D_{sol}, cm^2/sec
Pu	Pu(III)	3×10^{-6}
	Pu(IV)	1.53×10^{-6}
Am	Am(III)	3×10^{-6}
U	U(IV)	1.53×10^{-6}
	U(VI)	4.26×10^{-6}
Th	Th(IV)	1.53×10^{-6}
Np	Np(IV)	1.53×10^{-6}
	Np(V)	3×10^{-6}
Cm	Cm(III)	3×10^{-6}
Ra	Ra(II)	4.02×10^{-6}

Distribution:

MS 1320 E. J. Nowak (Org. 6831)
MS 1320 R. V. Bynum (Org. 6831)
MS 1320 H. W. Papenguth (Org. 6748)
MS 1320 W. G. Perkins (Org. 6748)
MS 1320 M. D. Siegel (Org. 6748)
MS 1324 P. B. Davies (Org. 6115)
MS 1324 A. R. Lappin (Org. 6115)
MS 1324 L. C. Meigs (Org. 6115)
MS 1328 H. Jow (Org. 6741)
MS 1328 D. R. Anderson (Org. 6749)
MS 1328 M. A. Martell (Org. 6749)
MS 1328 J. L. Ramsey (Org. 6749)
MS 1328 C. T. Stockman (Org. 6749)
MS 1335 M. S. Y. Chu (Org. 6801)
MS 1337 W. D. Weart (Org. 6000)
MS 1341 J. T. Holmes (Org. 6748)
MS 1341 L. H. Brush (Org. 6748)
MS 1341 R. C. Moore (Org. 6748)
MS 1341 C. F. Novak (Org. 6748)
MS 1341 L. J. Storz (Org. 6748)
MS 1341 Y. Wang (Org. 6748)
MS1341 K. W. Larson (Org. 6751)
MS 1343 R. F. Weiner (Org. 6751)
MS 1395 L. E. Shephard (Org. 6800)
MS 1395 M. G. Marietta (Org. 6821)
MS 1330 SWCF (Org. 6352), WBS 1.1.10.3.1 (2)

WPO.. 38801

Sandia National Laboratories

Albuquerque, New Mexico 87185-1341

date: June 10, 1996

to: M. S. Tierney, MS-1328 (Org. 6741)

L. H. Brush

INFORMATION ONLY

from: L. H. Brush, MS-1341 (Org. 6748)

subject: Ranges and Probability Distributions of K_ds for Dissolved Pu, Am, U, Th, and Np in the Culebra for the PA Calculations to Support the WIPP CCA

INTRODUCTION

This memorandum contains ranges and probability distributions of matrix distribution coefficients (K_ds) for dissolved Pu, Am, U, Th, and Np under conditions expected during transport in the Culebra Dolomite member of the Rustler Formation. In this memo, a matrix K_d is the equilibrium ratio of the mass of Pu, Am, U, Th, or Np adsorbed on the solid phase(s) per unit mass of solid(s) divided by the concentration of that element in the aqueous phase (see, for example, Freeze and Cherry, 1979). Performance-assessment (PA) personnel require K_ds for Pu, Am, U, Th, and Np for their calculations to support the Waste Isolation Pilot Plant (WIPP) Compliance Certification Application (CCA) (Ramsey, 1996). (We will include this memorandum and all of the other memoranda cited herein in the parameter and analysis records packages for these K_ds.) Actually, PA requires K_ds for various isotopes of these elements; but Ramsey (1996) did not specify them. However, Garner (1996) stated that PA needs K_ds for ^{239}Pu, ^{241}Am, ^{234}U, and ^{230}Th. It is reasonable to assume that, in view of the small differences among the masses of different isotopes of these elements, one can apply a K_d determined for one isotope to any other isotope of the same element. We are submitting K_ds for Np in case PA requires them for sensitivity calculations to show that omitting this element does not affect the long-term performance of the repository significantly.

We, the Sandia-National-Laboratories (SNL), and SNL-subcontractor personnel working on or familiar with the dissolved-actinide Retardation Research Program (RRP) or related aspects of PA, have established these ranges and distributions from results obtained by the RRP through May 31, 1996 (see Table 1 below). These ranges and distributions pertain to dolomite-rich rock in the matrix (intact rock between the fractures) of the Culebra. (We use the terms

SWCF-A:1.1.10.3.1:PDD:QA: Culebra Dissolved Actinide Distribution Coefficients (K_ds), WPO#38231

"matrix" and "fractures" in a general sense, corresponding to transport pathways with relatively low and high transmissivities, respectively. Our use of these terms is consistent with the double-porosity conceptual model of the Culebra proposed by L. Meigs and her colleagues at SNL and its subcontractors.) The ranges and distributions in Table 1 *do not* include K_ds for the clay-rich rock associated with fracture surfaces and dispersed in the matrix of the Culebra. We believe that, based on Sewards (1991) and Sewards et al. (1991, 1992) and recent, yet-to-be published studies of Culebra mineralogy, clay minerals such as corrensite (an ordered mixture of chlorite and saponite) *are* present on fracture surfaces *and* in the matrix of the Culebra at concentrations high enough to increase the retardation of Pu, Am, U, Th, and Np relative to that observed in laboratory studies with dolomite-rich rock (see Description of Laboratory Studies Used to Determine Matrix K_ds below). However, we *have not* included K_ds for clay minerals in these ranges and distributions because we do not have sufficient laboratory data for clay-rich rock under expected Culebra conditions at this time. Furthermore, we *have not* taken any credit for sorption by clay minerals on fractures. We believe that omitting K_ds for clays is conservative.

FRACTURE-SURFACE K_ds

We recommend that PA personnel set the fracture-surface K_ds (actually, K_as) for Pu, Am, U, Th, and Np in the Culebra to zero. A distribution coefficient expressed on a per-unit-surface-area basis, or K_a, is the equilibrium ratio of the mass of Pu, Am, U, Th, or Np adsorbed on the solid phase(s) per unit area of solid(s) divided by the concentration of that element in the aqueous phase (Freeze and Cherry, 1979). We also recommend that PA not include sorption by a discrete layer of material associated with fracture surfaces. Setting these K_as to zero will not affect the predicted retardation of actinide elements by the Culebra because: (1) we *have not* taken credit for sorption by clay minerals on fracture surfaces; (2) the surface area of the dolomite-rich rock lining the fractures is very small relative to that of the dolomite-rich rock in the matrix. WIPP Performance Assessment Department (1992) discussed sorption on fractures in detail.

MATRIX K_ds

This section briefly describes the laboratory studies used to determine matrix K_ds for dissolved Pu, Am, U, Th, and Np, and the modeling study used to predict the oxidation-state distributions of these elements under conditions expected in the Culebra. It then discusses the methodologies used to establish ranges and probability distributions of these K_ds.

Description of Laboratory Studies Used to Determine Matrix K_ds

The RRP carried out several laboratory studies of the sorption of Pu, Am, U, Th, and Np by dolomite-rich rock from the Culebra. Papenguth and Behl (1996) described these studies in detail. These studies used different experimental methods and considered the effects of several factors on actinide sorption in the Culebra. The results used to establish ranges and probability distributions of matrix K_ds for Pu, Am, U, Th, and Np in the Culebra appear in Appendices B through F, respectively, of this memorandum. (These lengthy appendices are available on request to anyone who did not receive them with this memo.) Detailed descriptions of these laboratory studies and the complete results will appear as SNL and/or SNL subcontractor reports by the time of submission of the CCA.

I. Triay and her group at Los Alamos National Laboratory (LANL) carried out an empirical study of the sorption of Pu(V), Am(III), U(VI), Th(IV), and Np(V) by samples of dolomite-rich rock from the Culebra. Triay used four synthetic fluids, Brine A, ERDA-6, AISinR, and H-17, for her experiments with dolomite-rich rock. Brine A, developed by Molecke (1983) to simulate fluids equilibrated with K- and Mg-bearing minerals in overlying potash-rich zones in the Salado Formation prior to entering WIPP disposal rooms, is also similar to intergranular Salado brines at or near the stratigraphic horizon of the repository. These brines could accumulate in WIPP disposal rooms after filling and sealing, and flow from the repository into the Culebra in the event of human intrusion into the repository. ERDA-6 simulates brines that occur in isolated but occasionally large reservoirs in the underlying Castile Formation (Popielak et al., 1983). These brines could flow through the repository and into the Culebra in the event of human intrusion. AISinR simulates brine sampled from the Culebra in the WIPP Air Intake Shaft (AIS). H-17 simulates Culebra brine from the H-17 Hydropad. Triay also studied the effects of the partial pressure of CO_2 (and, hence, dissolved CO_2 concentration and, to some extent, pH) on sorption. She carried out experiments on the bench top (in contact with atmospheric CO_2, which contains about 0.035% CO_2) and in glove boxes with atmospheres containing 0.24, 1.4, and 4.1% CO_2. The CO_2 partial pressures in these runs were $10^{-3.5}$, $10^{-2.73}$, $10^{-1.98}$, and $10^{-1.50}$ atm, respectively, the range of P_{CO2} calculated for Culebra ground waters by Siegel et al. (1991). Furthermore, Triay studied the effects of dissolved actinide concentration on sorption. These experiments yielded sorption isotherms, plots of the quantity of radionuclide sorbed by the solid phase or phases versus the final dissolved radionuclide concentration, or plots of K_ds versus the final dissolved radionuclide concentration. (We will include these isotherms in the parameter and analysis records packages for these K_ds.) These plots in turn provided information on the nature of the reaction(s) responsible for removal of radionuclides from solution. Finally, Triay studied the effects of equilibration time (3-days and 1-, 3-, 6-, or 8-weeks) and direction of reaction (sorption or desorption) on sorption. Triay crushed the samples, selected the 75-to-500-μm

size fraction (significantly larger than the mean dolomite grain diameter of about 2 μm), washed these subsamples with dilute HCl to remove crystallographically strained surfaces, fine particles of dolomite, and Fe- and Mn-oxyhydroxides, and pretreated them with the same type of brine to be used for the actual experiment for periods of time for the most part identical to those of the sorption and desorption runs. Triay carried out each of the pretreatments and the actual experiments with 20 ml of brine and 1 g of rock. During the runs that yielded the K_ds to be used by PA, she used one actinide element at a time. At the end of her runs, Triay separated the aqueous and solid phases by sequential filtration to 0.2 μm, analyzed the solutions by liquid scintillation counting (LSC), and determined K_ds from the differences between the initial and the final radionuclide concentrations in the solutions. She carried out most of her experiments, and all of the runs that yielded the K_ds to be used by PA, with samples of dolomite-rich rock taken from AIS core segments adjacent to those used for the column-transport study (see below). X-ray-diffraction analysis of this rock failed to detect clay minerals in most cases. Because the detection limit of this technique is about 1%, the rock that yielded the K_ds for PA contains a lower concentration of clay minerals than the Culebra as a whole (estimated, based on previously published and ongoing studies of Culebra mineralogy, to be about 1 to 5%). Triay also carried out a few experiments with dolomite from the H-19 Hydropad and clay-rich rock from the lower, unnamed member of the Rustler. (The clay minerals in the lower member are identical to those lining fracture surfaces and dispersed in the matrix of the Culebra.) This study yielded a large number of K_ds for actual samples of nearly pure Culebra dolomite and actinide-bearing synthetic fluids closely resembling those that could actually flow through the Culebra after human intrusion.

P. V. Brady and his colleagues at SNL and LANL carried out a mechanistic study of the sorption of Pu(V), Am(III), Nd(III) (a nonradioactive analog of Am(III) and Pu(III)), U(VI), Th(IV), and Np(V) from synthetic 0.05, 0.5, and 5 M NaCl solutions by samples of well characterized, pure dolomite from Norway. Brady used a limited-residence-time (1 min.) reaction vessel to minimize the extent of dolomite dissolution, actinide precipitation, and other reactions unrelated to sorption during his experiments. This allowed him to study the effects of pH (from about 3 or 4 to 9 or 10 in most cases), the CO_2 concentration of the headspace (atmospheric, 0.5, and 5%), and the concentrations of potentially significant cations and anions on sorption in the absence of complexities caused by other reactions. Brady crushed the samples, selected the <106-μm size fraction, washed them with dilute HCl, and pretreated them overnight in an NaCl solution with the same concentration to be used for the actual experiments, and a solution-to-solid ratio of 100 ml per g of dolomite. He carried out the actual experiments with several actinide elements at a time, and a solution-to-solid ratio of 200 ml/g. After his runs, Brady separated the aqueous and solid phases with a 0.22-μm filter, analyzed the solutions by inductively coupled plasma emission/mass spectrometry, and determined K_ds from the differences between the initial and the final radionuclide concentrations in the solutions. Although

this study did not yield K_ds for actual samples of Culebra rock nor for synthetic Culebra fluids, it did yield results that have proven highly useful for interpreting the results of the empirical sorption study at LANL, and for extending the empirical data to the basic conditions (pH values of about-9 to 10) expected to result from use of an MgO backfill in WIPP disposal rooms (see below).

D. A. Lucero and his colleagues at SNL have studied actinide transport through intact, 5.7-inch-diameter cores obtained from the Culebra in the WIPP AIS. Lucero obtained the cores used for this study from 16-to-18-ft.-long horizontal boreholes aligned in the current direction of ground-water flow in the vicinity of the AIS (see Predictions of Actinide Oxidation States in the Culebra below) and stored them under conditions that minimized evaporation of pore water. Prior to his experiments, Lucero cut 4-to-20-inch sections from the original cores and potted them in Neoprene. He then placed the potted core sections in Al core holders, mounted them vertically in a glove box, and pressurized them to about 50 atm, the *in situ* pressure at the depths (716 and 721 ft.) from which these cores were obtained. Lucero carried out spike injections or, in a few experiments, continuous injections of Pu(V), Am(III), U(VI), Th(IV), and/or Np(V) by introducing synthetic AISinR or, in a few runs, synthetic ERDA-6 with low concentrations of the radionuclide(s) into a cavity cut in the top of each core. He then pumped additional brine through these cores at low flow rates (0.1 ml/min and, in a few runs, 0.05 ml/min) for periods of up to 237 days (equivalent to pumping up to 34.2 pore volumes of brine through these cores). These flow rates are at or close to the upper limit of the range of *in situ* fluid velocities. He collected the effluent continuously and analyzed it every 5 ml by γ spectrometry or LSC. He also used scanning γ emission tomography to image the cores. By injecting different radionuclides at different times and, in some cases, by using different brines, Lucero carried out multiple, sequential experiments with the same core. Because this study quantified actinide sorption from fluids flowing through intact samples of Culebra rock, it complements the static empirical and mechanistic sorption studies with crushed Culebra rock or pure dolomite. However, this study did not yield K_ds directly. For U and Np, which were moderately retarded by sorption, the observed delays between the elution peaks of nonsorbed radionuclides (such as ^{3}H or ^{22}Na) and those of U and Np yielded discrete values for the retardation factors R, which were then used, along with porosities determined with the nonsorbing tracers, to calculate K_ds. For Pu, Am, and Th, which were strongly retarded by sorption, Lucero did not observe breakthrough, even after pumping brine through these cores for 61, 118, and 211 days (Pu and Am) and 133, 146, and 237 days (Th) (equivalent to 8.83, 17.0, and 30.4 pore volumes for Pu and Am, and 19.1, 21.0, and 34.2 pore volumes for Th). Therefore, he was only able to calculate minimum values of R and K_d. These minimum values depend on factors such as the initial concentration of each radionuclide, the volume of brine pumped through the core, and the analytical detection limit for the radionuclide.

Because oxidation state significantly affects the chemical behavior, including sorption, of the actinide elements, predictions of the oxidation-state distributions of Pu, U, and Np in the Culebra are necessary to establish ranges and probability distributions of matrix K_ds for use in the PA calculations. For Pu, U, and Np, the following oxidation states are possible in low-temperature, geochemical systems: Pu(III), Pu(IV), Pu(V), and Pu(VI); U(IV) and U(VI); and Np(IV), Np(V), and Np(VI). For Am and Th, only one oxidation state, Am(III) or Th(IV), respectively, is possible.

We have used experimentally based predictions of the oxidation-state distributions of Pu, U, and Np in WIPP disposal rooms from the Actinide Source Term Program (ASTP) to specify the oxidation states of these elements in the Culebra. Based on a laboratory study carried out under expected WIPP conditions by D. Clark and his colleagues at LANL and previously published results obtained for applications other than the WIPP Project, ASTP personnel have predicted that Pu will speciate as Pu(III) or Pu(IV), but not as Pu(V) nor Pu(VI), that U will speciate as U(IV) and U(VI), and that Np will speciate as Np(IV) and Np(V), but not as Np(VI), in deep (Castile and Salado) brines in the repository. To evaluate the applicability of these predictions to the Culebra, H. W. Stockman of SNL carried out a modeling study of the oxidation states of Pu, U, and Np in the Culebra (see below). This study showed that Culebra fluids are poorly poised (have limited capacity to either oxidize or reduce actinide elements). Therefore, it is reasonable to use the oxidation-state distributions of Pu, U, and Np predicted for WIPP disposal rooms to specify the oxidation states of these elements in the Culebra. Using the ASTP predictions for the Culebra will ensure consistency between the oxidation-state distributions of these elements in WIPP disposal rooms and at the point of injection of deep (Castile or Salado) brines into the Culebra following human intrusion into the repository. This will in turn obviate the need to specify redox reactions in the Culebra, and the need to incorporate possible, concomitant dissolution and/or precipitation reactions in SECO, the PA model for Culebra flow and transport.

ASTP and PA personnel will calculate solubilities for *either* Pu(III), U(IV), and Np(IV), *or* Pu(IV), U(VI), and Np(V) in any given vector. PA will specify the oxidation states of these elements by sampling "oxstat," a parameter with a uniform probability distribution of 0 to 1. If the sampled value of oxstat is 0.5 or less, PA will use the solubilities predicted for Pu(III), U(IV), and Np(IV). (These solubilities are also sampled parameters.) If oxstat is greater than 0.5, PA will use solubilities for Pu(IV), U(VI), and Np(V). We recommend that PA use the ranges and distributions of K_ds for the oxidation states of Pu, U, and Np sampled for each vector.

This approach is equivalent to assuming that the oxidation-state distributions of Pu, U, and Np predicted for WIPP disposal rooms will be maintained along the

entire off-site transport pathway in the Culebra. (Previous PA calculations have predicted that, in the absence of climatic change, fluid will flow from the point of injection into the Culebra to the south or the southeast, and that the distance from the point of injection to the boundary of the Land Withdrawal Area will be about 2.5 or 3 km.) This assumption is certainly reasonable at the point of injection of deep brines into the Culebra and for some, perhaps significant, distance along the flow path. Because, in general, redox equilibrium is not observed in low-temperature aqueous solutions (see, for example, Lindberg and Runnells, 1984), the oxidation states of Pu, U, and Np predicted for the repository *could* persist along the entire flow path in the Culebra. At some point, however, the oxidation-state distributions of these elements *might* equilibrate with ambient conditions in the Culebra.

To evaluate the applicability of ASTP predictions to the Culebra, Stockman used the EQ3/6 geochemical software package (Daveler and Wolery, 1992; Wolery, 1992a, 1992b; Wolery and Daveler, 1992) to predict the oxidation-state distributions of Pu, U, and Np after mixing deep (Castile and Salado) brines containing these elements with Culebra brines. Stockman made various assumptions as to: (1) which naturally occurring or waste-derived dissolved species will control redox conditions in the deep brines after injection into the Culebra; (2) which naturally occurring dissolved or solid species control redox conditions in Culebra brines; (3) whether to use the data base in EQ3/6, or to modify it based on recently published studies of actinide chemistry. By calculating oxidation-state distributions of Pu, U, and Np before and after mixing deep brines with Culebra brines *under all possible combinations of these assumptions*, Stockman showed that Culebra fluids are poorly poised (have limited capacity to either oxidize or reduce actinide elements). Therefore, it is reasonable to assume that the oxidation-state distributions of Pu, U, and Np predicted for WIPP disposal rooms will be maintained along the entire off-site transport pathway.

Predictions of Brine Mixing in the Culebra

Brine composition could also affect the sorptive behavior of actinide elements in the Culebra. Therefore, predictions of the extent to which deep (Castile and Salado) and Culebra brines mix in the Culebra are necessary to specify weighting factors to combine the ranges and probability distributions of matrix K_ds for dissolved Pu, Am, U, Th, and Np established for deep and Culebra brines and obtain an overall range and distribution for a given element or elemental oxidation state.

Opinions differ significantly on the extent to which deep and Culebra brines will mix in the Culebra. One extreme of a range of possibilities is that, because of the density difference between deep and Culebra brines and/or limited spreading due to heterogeneity, a "slug" of deep brine will flow along the entire off-site transport pathway without significant mixing. The other extreme is that, because

of relatively high heterogeneity, hydrodynamic dispersion will result in rapid mixing, and the composition of the injected fluid will resemble that of Culebra ground water on the order of hundreds of meters from the point of injection.

We are submitting these ranges and distributions to PA concurrently with the submission of Culebra hydrologic parameters by personnel from Geohydrology Department 6115. Therefore, we could not carry out brine-mixing calculations with the current hydrologic parameters prior to establishing these ranges and distributions. In the absence of mixing calculations, E. J. Nowak, Manager of Chemical & Disposal Room Processes Department 6831, instructed us to take the following, conservative approach: (1) establish *separate* ranges and distributions for deep and the Culebra brines for each actinide element or elemental oxidation state; (2) recommend that PA personnel use the range and distribution that results in less retardation for each element or elemental oxidation state.

Methods Used to Establish Ranges of Matrix K_ds

This subsection briefly describes the methods used to establish ranges of matrix K_ds for dissolved Pu, Am, U, Th, and Np under conditions expected in the Culebra. We carried out most of the work described in this subsection at a meeting held April 1 and 2, 1996, here at the BDM Building. Sixteen SNL and SNL-subcontractor personnel working on or familiar with the RRP or related aspects of PA participated in all or part of this meeting. Two US DOE Carlsbad-Area-Office and Carlsbad-Technical-and-Administrative-Contractor personnel observed all or part of it. Appendix A (see below) contains the invitation to, agenda for, and list of the participants and observers at this meeting. (This and the other six appendices are available on request to anyone who did not receive them with this memorandum.) Detailed descriptions, including all of the empirical-sorption, mechanistic-sorption, and column-transport data considered and included or excluded, appear in Appendices B through F, respectively. Appendix G contains the results of experiments on the effects of four organic ligands on these K_ds.

At this meeting, we decided to establish *experimentally obtained* ranges for Am(III), U(VI), Th(IV), and Np(V), and to use the experimentally obtained ranges for Am(III) and Th(IV), and the oxidation-state analogy to establish ranges for Pu(III), and Pu(IV), U(IV), and Np(IV). Based on the ASTP predictions of oxidation-state distributions for Pu, U, and Np in WIPP disposal rooms *and* Stockman's predictions for the Culebra *under most of the possible combinations of assumptions* (see Predictions of Actinide Oxidation States in the Culebra above), we *did not* plan to establish an experimentally obtained range for Pu(V), nor to use the experimentally obtained range for U(VI) and the oxidation-state analogy to establish ranges for Pu(VI) and Np(VI).

We established *separate* ranges for the deep (Castile and Salado) and the Culebra brines for each actinide element or elemental oxidation state (see

Predictions of Brine Mixing in the Culebra above). However, we *did not* establish separate ranges for the two deep brines studied by Triay and her group in the LANL empirical sorption study (Brine A and ERDA-6) because the PA calculations carried out with the multiphase flow code Brine and Gas Flow to support the WIPP CCA have predicted that, in some vectors, the brine in WIPP disposal rooms will comprise mainly Castile brine; in other vectors, it will comprise mainly Salado brine; and in the rest, it will comprise various proportions of these and Culebra brines that will seep into the repository from above. (The latter brines will resemble Castile brines after reacting with Salado minerals.) Therefore, we established one range for Brine A and ERDA-6 to simulate these compositional variations. Similarly, the Culebra off-site transport pathway predicted by previous PA calculations (see Predictions of Actinide Oxidation States in the Culebra) contains ground waters that resemble *both* Culebra fluids used by Triay (AISinR and H-17). Therefore, we established one range and distribution for these fluids to simulate possible compositional variations along the flow path.

For U(VI), Th(IV), and Np(V) (see Appendices , we used the following methods to establish separate, *experimentally obtained* ranges for the deep and the Culebra brines. First, we considered *all* of the 6-week sorption data from the empirical study by Triay, the only experiments in which she has extensively studied the effects of dissolved actinide concentration on sorption. Because these are the only experiments carried out using a range of dissolved radionuclide concentrations, they are the only runs for which sorption isotherms have provided information on the nature of the reaction(s) responsible for removal of radionuclides from solution. (We will include these isotherms in the parameter and analysis records packages for these K_ds.) At the time of this meeting, Triay had not completed the 6-week desorption experiments. We would not, however, have included the results of the 6-week desorption runs, and did not include any data from the 3-day, nor the 1- nor 3-week desorption runs because these data could be artificially higher than those obtained from the sorption runs. Possible reasons for this include: (1) removal of a weakly sorbed actinide species concentrated in the aqueous phase by discarding the solution at the conclusion of a sorption experiment, thereby concentrating a strongly sorbed species prior to the start of a desorption run; (2) saturation of a sorption site with a high K_d followed by removal of the dissolved actinide after a sorption experiment, thereby resulting in sorption of a higher proportion of the actinide on the sorption site with a high K_d during the desorption run.

To establish the *initial* ranges for the deep brines, we first considered *all* the data obtained from the 6-week sorption experiments carried out with Brine A and ERDA-6 on the bench top (in contact with ambient atmospheric CO_2). Atmospheric CO_2 has a partial pressure of about $10^{-3.5}$ atm, the lowest CO_2 partial pressure used in the LANL study. This partial pressure is equivalent to a CO_2 content of 0.033% in the LANL study. We did not use data from runs equilibrated with higher partial pressures of CO_2 for the initial ranges for the deep

brines because we anticipate that an MgO backfill will be emplaced in WIPP disposal rooms to remove CO_2. Next, we discarded the data from runs in which the difference between the activity of the radionuclide in a standard (the radionuclide-bearing brine with which runs were started) and that in a control (a run conducted identically to that of an actual run, but without any rock) exceeded 3σ, where the standard deviation σ equals the square root of the total number of LSC counts. Discarding these data yielded the *initial* ranges for deep brines.

To establish the *initial* ranges for the Culebra brines (AISinR and H-17), we first considered *all* the data obtained from the 6-week sorption experiments carried out on the bench top (0.033% CO_2) and in glove boxes with atmospheres containing 0.24 and 1.4% CO_2. These three atmospheres had CO_2 partial pressures of $10^{-3.5}$, $10^{-2.73}$, and $10^{-1.98}$ atm, respectively. Siegel now considers this range more likely for groundwaters in the predicted off-site transport pathway than the previous range of $10^{-3.5}$ to $10^{-1.50}$ atm calculated for the Culebra as a whole by Siegel et al. (1991). We also discarded the data from runs in which the difference between the activity of the radionuclide in a standard and that in a control exceeded 3σ to obtain the *initial* ranges for Culebra brines.

We then compared these initial ranges with the data from the mechanistic sorption study by Brady and his colleagues at SNL and LANL. For the most part, we used Brady's data to extend Triay's empirical sorption data for the deep brines to the basic conditions expected to result from the use of an MgO backfill in WIPP disposal rooms. We assumed that, if mixing is sufficient to produce fluids with compositions similar to those of Culebra brines, the pH of these mixtures will also be similar to those of Culebra brines. Therefore, we *did not* use Brady's data to extend Triay's data for the Culebra brines to basic conditions. So far, Brady has reported data obtained with 0.05 and 0.5 M NaCl solutions, but not with 5 M NaCl. Therefore, we used only his data for 0.5 M NaCl and atmospheric CO_2 (the lowest CO_2 partial pressure used in this study) to extend Triay's data for the deep brines to basic conditions. This comparison yielded our *revised* ranges for the deep brines.

Next, we compared the revised ranges with the data from the transport study with intact Culebra cores by Lucero and his colleagues at SNL. Lucero carried out his experiments under ambient atmospheric conditions; therefore, the CO_2 content of these experiments was probably similar to that in the LANL bench-top runs. Because Lucero *did not* observe breakthrough of Th(IV) (nor of Pu(V) nor Am(III)), it was only possible to determine minimum values of K_d for Th(IV) (and for Pu(V) and Am(III)). This minimum K_d (and those for Pu(V)) are consistent with the revised ranges based on the empirical and mechanistic sorption studies. Lucero *did* observe breakthrough of U(VI) and Np(V) in his experiments. Therefore, it was possible to determine actual K_ds for these elements. In most cases, the K_ds determined for U(VI) and Np(V) from the transport study are less than the lower limits of the ranges obtained for these elements from the sorption studies. Therefore, we extended the revised ranges where necessary to obtain

final ranges for U(VI) and Np(V) in the deep brines (Castile and Salado) and Culebra brines (see Table 1).

Finally we used the experimentally obtained ranges for Th(IV) and the oxidation-state analogy to establish ranges for Pu(IV), U(IV), and Np(IV).

We attempted to use the same methods to establish experimentally obtained ranges for Am(III) (see Appendix C). Inspection of the sorption isotherms for the 6-week LANL sorption data, however, revealed that the K_ds are proportional to the final dissolved Am(III) concentration. (We did not observe significant trends such as this in the isotherms for U(VI), Th(IV), nor Np(V)). These trends suggest that sorption of Am by the container walls, precipitation of an Am-bearing solid phase, coprecipitation of Am by another phase, incomplete separation of the aqueous and the solid phases at the end of an experiment, or some combination of these processes occurred in the runs with Am(III). Triay carried out additional posttest analyses of the brines from some of her 6-week sorption experiments with Am(III) to determine, if possible, what caused these trends, and to redetermine these K_ds. However, she continued to obtain data that displayed trends similar to those described above, and thus cannot rule out the occurrence of processes other than sorption. Therefore, we recommend using the *experimentally obtained* ranges for Pu(V) (Appendix B) for Am(III) by assuming that the K_ds for Am(III) are greater than or equal to those for Pu(V). This assumption is reasonable in view of results such as those in Figure 5 of Canepa (1992). In this case, the Am(III) K_d obtained for the Yucca Mountain Project is about one order of magnitude higher than that obtained for Pu(V) under the same conditions. (We will cite additional examples of differences between the K_ds for Am(III) and Pu(V) in future reports and presentations.) We *have not* used the oxidation-state analogy to justify the use of Pu(V) data for Am(III); instead, this approach is based on *differences* in the behavior of these oxidation states. Furthermore, we recommend using the range for Am(III) for Pu(III) (Table 1); for this recommendation, we invoke the oxidation-state analogy.

Methods Used to Establish Probability Distributions of Matrix K_ds

M. S. Tierney, the PA Parameter Task Leader, provided guidance on establishing probability distributions of parameters for use in the PA calculations to support the CCA (see Tierney, 1996a; 1996b).

The RRP has studied the effects of several factors on sorption (see Description of Laboratory Studies Used to Determine Matrix K_ds, Predictions of Actinide Oxidation States in the Culebra, and Predictions of Brine Mixing in the Culebra above). Papenguth and Behl (1996) designed these studies to encompass the ranges of these factors expected in the Culebra. Therefore, the ranges of matrix K_ds established above correspond to the expected ranges of these factors in the Culebra. However, because of uncertainties about the extent to which deep (Castile and Salado) and Culebra brines will mix, there are uncertainties as to the

probability distributions of these factors (especially brine type, the partial pressure of CO_2, and the resulting pH) in the Culebra. Therefore, we *do not* recommend that PA use a Student t distribution based on the data included in these ranges, despite the fact that we included more than three data points for every range shown in Table 1.

Tierney (1996a) states that use of the uniform or log-uniform [probability] distribution "is appropriate when all that is known about a parameter is its range." Because we cannot specify probability distributions for the factors that affect sorption, we recommend that PA personnel use a uniform or a log-uniform distribution. Tierney (1996a) specifies use of a log-uniform distribution "when the range ... spans many orders of magnitude." Inspection of the ranges for deep and Culebra brines in Table 1 reveals that these ranges span 1.40 and 2.60 orders of magnitude (deep and Culebra brines, respectively) for Pu(III) and Am(III); 1.35 orders of magnitude (deep brines only) for Pu(IV), U(IV), Th(IV), and Np(IV); 3.00 orders of magnitude (deep brines only) for U(VI); and 2.65 and 2.30 orders of magnitude (deep and Culebra brines, respectively) for Np(V). (Each of these values is the common logarithm of the maximum value of each range divided by its minimum value. We could not calculate this parameter for Th(IV) and Culebra brines because we were unable to establish this range; see Appendix E below. We could not calculate this parameter for the range for U(VI) and Culebra brines because its minimum value is 0.) Because these ranges all span three orders of magnitude or less, we recommend that PA use a uniform distribution instead of a log-uniform distribution for all of them.

Methods Used for Final Selection of the Range of Matrix K_ds for Use in PA Calculations

We recommend that PA personnel use the range and probability distribution of matrix K_ds for deep (Castile and Salado) or Culebra brines that results in less retardation for each element or elemental oxidation state (see Predictions of Brine Mixing in the Culebra above). Because we have recommended that PA use a uniform distribution for *all* the ranges (see Methods Used to Establish Probability Distributions of Matrix K_ds above), the *average* K_d that PA will sample for all of its vectors is the mean of the maximum and minimum values of each range. Therefore, we compared the means of the ranges for deep and Culebra brines to determine which range results in less retardation for each element or elemental oxidation state. Inspection of the ranges in Table 1 reveals that the means are 260 and 2005 ml/g (deep and Culebra brines, respectively) for Pu(III) and Am(III); 10,450 ml/g (deep brines only) for Pu(IV), U(IV), Th(IV), and Np(IV); 15.015 and 35 ml/g (deep and Culebra brines, respectively) for U(VI); and 451 and 100.5 ml/g (deep and Culebra brines, respectively) for Np(V). (Each of these values is the sum of the maximum and the minimum values of each range divided by two; to facilitate this comparison, we *did not* round each result to one significant figure. We could not calculate this parameter for Th(IV) and Culebra brines because we could not establish this range; see Appendix E below.)

Therefore, we recommend that PA use a range of 20 to 500 ml/g (the range for deep brines) for Pu(III) and Am(III); a range of 900 to 20,000 ml/g (deep brines) for Pu(IV), U(IV), Th(IV), and Np(IV); a range of 0.03 to 30 ml/g (deep brines) for U(VI); and a range of 1 to 200 ml/g (Culebra brines) for Np(V). In Table 1, these ranges appear in bold font.

Because the ASTP has decided to specify the oxidation states of Pu, U, and Np by sampling the "oxstat" parameter (see Predictions of Actinide Oxidation States in the Culebra), the range and distribution for each specified oxidation state will constitute the range and distribution for each of these elements during a given vector.

REFERENCES

Canepa, J.A. 1992. *Proceedings of the DOE/Yucca Mountain Site Characterization Project Radionuclide Adsorption Workshop at Los Alamos National Laboratory, September 11-12, 1990.* LA-12325-C. Los Alamos, NM: Los Alamos National Laboratory.

Daveler, S.A., and T.J. Wolery. 1992. *EQPT, A Data File Preprocessor for the EQ3/6 Software Package: User's Guide and Related Documentation (Version 7.0).* UCRL-MA-110662 PT II. Livermore, CA: Lawrence Livermore National Laboratory.

Freeze, R.A., and J.A. Cherry. 1979. *Groundwater.* Englewood Cliffs, NJ: Prentice-Hall.

Garner, J. 1996. "Radioisotopes to Be Used in the 1996 CCA Calculations." Unpublished memorandum to C. T. Stockman, March 15, 1996. Albuquerque, NM: Sandia National Laboratories.

Molecke, M.A. 1983. *A Comparison of Brines Relevant to Nuclear Waste Experimentation.* SAND83-0516. Albuquerque, NM: Sandia National Laboratories.

Lindberg, R.D., and D.D. Runnells. 1984. "Ground Water Redox Reactions: An Analysis of Equilibrium State Applied to Eh Measurements and Geochemical Modeling," *Science.* Vol. 225, no. 4665, 925-927.

Molecke, M.A. 1983. *A Comparison of Brines Relevant to Nuclear Waste Experimentation.* SAND83-0516. Albuquerque, NM: Sandia National Laboratories.

Papenguth, H.W. and Y.K. Behl. 1996. *Test Plan for Evaluation of Dissolved Actinide Retardation at the Waste Isolation Pilot Plant.* TP 96-02. Albuquerque, NM: Sandia National Laboratories.

Popielak, R.S., R.L. Beauheim, S.R. Black, W.E. Coons, C.T. Ellingson and R.L. Olsen 1983. *Brine Reservoirs in the Castile Formation, Waste Isolation Pilot Plant Project, Southeastern New Mexico.* TME 3153. Carlsbad, NM: U.S. Department of Energy WIPP Project Office.

Ramsey, J. 1996. "Culebra Dissolved Actinide Parameter Request." Unpublished memorandum to E. J. Nowak, March 18, 1996. Albuquerque, NM: Sandia National Laboratories.

Sewards, T. 1991. *Characterization of Fracture Surfaces in Dolomite Rock, Culebra Dolomite Member, Rustler Formation.* SAND90-7019. Albuquerque, NM: Sandia National Laboratories.

Sewards, T., A. Brearly, R. Glenn, I.D.R. MacKinnon, and M.D. Siegel. 1992. *Nature and Genesis of Clay Minerals of the Rustler Formation in the Vicinity of the Waste Isolation Pilot Plant in Southeastern New Mexico.* SAND90-2569. Albuquerque, NM: Sandia National Laboratories.

Sewards, T., M.L. Williams, and K. Keil. 1991. "Mineralogy of the Culebra Dolomite," *Hydrogeochemical Studies of the Rustler Formation and Related Rocks in the Waste Isolation Pilot Plant Area, Southeastern New Mexico.* SAND88-0196. Eds. M.D. Siegel, S.J. Lambert, and K.L. Robinson. Albuquerque, NM: Sandia National Laboratories, 3-1 to 3-43.

Siegel, M.D., K.L. Robinson, and J. Myers. 1991. "Solute Relationships in Groundwaters from the Culebra Dolomite and Related Rocks in the Waste Isolation Pilot Plant Area, Southeastern New Mexico," *Hydrogeochemical Studies of the Rustler Formation and Related Rocks in the Waste Isolation Pilot Plant Area, Southeastern New Mexico.* SAND88-0196. Eds. M.D. Siegel, S.J. Lambert, and K.L. Robinson. Albuquerque, NM: Sandia National Laboratories, 6-1 to 6-35.

Tierney, M.S. 1996a. "Distributions." Unpublished memorandum to distribution, March 21, 1996. Albuquerque, NM: Sandia National Laboratories.

Tierney, M.S. 1996b "Development of Parameter Values Distribution Functions." Unpublished memorandum to distribution, April 16, 1996. Albuquerque, NM: Sandia National Laboratories.

WIPP Performance Assessment Department. 1992. *Preliminary Performance Assessment for the Waste Isolation Pilot Plant, December 1992. Volume 2: Technical Basis.* SAND92-0700/2. Albuquerque, NM: Sandia National Laboratories.

Wolery, T.J. 1992a. *EQ3/6, A Software Package for Geochemical Modeling of Aqueous Systems: Package Overview and Installation Guide (Version 7.0).* UCRL-MA-110662 PT I. Livermore, CA: Lawrence Livermore National Laboratory.

Wolery, T.J. 1992b. *EQ3NR, A Computer Program for Geochemical Aqueous Speciation-Solubility Calculations: Theoretical Manual, User's Guide, and Related Documentation (Version 7.0).* UCRL-MA-110662 PT III. Livermore, CA: Lawrence Livermore National Laboratory.

Wolery, T.J., and S.A. Daveler. 1992. *EQ6, A Computer Program for Reaction-Path Modeling of Aqueous Geochemical Systems: Theoretical Manual, User's Guide, and Related Documentation (Version 7.0).* UCRL-MA-110662 PT IV. Livermore, CA: Lawrence Livermore National Laboratory.

Table 1. Ranges of Matrix K_ds (ml/g) for Pu, Am, U, Th, and Np, and Dolomite-Rich Culebra Rcok. Ranges in bold font to be used by PA. Oxidation state of Pu, U, and Np to be specified by the value of "oxstat" parameter sampled to calculate dissolved actinide concentrations in WIPP disposal rooms. All probability distributions are uniform (see text). Table compiled by L. H. Brush on April 3, 1996, based on results of meeting held April 1 and 2, 1996. Table checked by Brush and Y. Behl on April 3, 1996. Table revised by Brush on April 6, 1996, based on memo by D. A. Lucero and G. O. Brown dated April 5, 1996. Table checked by Behl on April 8, 1996.

Oxidation State	Element				
	Pu	Am	U	Th	Np
VI	NA	NA	**0.03 to 30**[A, C]	NA	NA
			0 to 70[B, C]		
V	NA	NA	NA	NA	2 to 900;[A, C]
					1 to 200[B, C]
IV	900 to 20,000;[A, D]	NA	900 to 20,000;[A, E]	900 to 20,000;[A, C]	900 to 20,000;[A, G]
	NE		NE	NE	NE
III	20 to 500;[A, H]	20 to 500;[A, I]	NA	NA	NA
	10 to 4,000[B, H]	10 to 4,000[B, I]			

A: range for deep (Castile and Salado) brines only (see text).
B: range for Culebra brines only (see text).
C: experimentally obtained range (see text).
D: experimentally obtained range for Th(IV) applied to Pu(IV) by oxidation-state analogy.
E: experimentally obtained range for Th(IV) applied to U(IV) by oxidation-state analogy.
F: experimentally obtained range for Th(IV) and deep brines applied to Th(IV) and Culebra brines.
G: experimentally obtained range for Th(IV) applied to Np(IV) by oxidation-state analogy.
H: experimentally obtained range for Pu(V) applied to Pu(III) (see text).
I: experimentally obtained range for Pu(V) applied to Am(III) (see text).
NA: not applicable (element will not speciate in this oxidation state).
NE: not established for Culebra brines (see Appendix E).

APPENDIX A: MEETING TO ESTABLISH RANGES AND PROBABILITY DISTRIBUTIONS OF ACTINIDE K_ds FOR THE WIPP PA CALCULATIONS AND THE CCA

Invitation

March 25, 1996

Dear Colleague:

Attached is the agenda for the meeting to establish ranges and probability distributions of actinide K_ds for use in the long-term performance-assessment (PA) calculations to support the WIPP Compliance Certification Application (CCA). We will hold this meeting at the BDM Sandia Vista Building at 2301 Buena Vista SE in Albuquerque, NM, on Monday and Tuesday, April 1 and 2, 1996. Currently, we plan to meet in the Nuclear Waste Management Conference Room, the large conference room, all day Monday and Tuesday morning, and in Room 2105, a small conference room, on Tuesday afternoon. Because a key is required to enter the building in which the large conference room is located, I or someone else will meet you in the reception area of the Sandia Vista Building at 8:45 on Monday morning to take you to the large conference room if you do not have a key.

I view this as our main opportunity to reach consensus on the ranges and probability distributions of K_ds for Pu, Am U, Th, and Np that we will submit to the US DOE's Carlsbad Area Office for their use in meeting the requirements of the Consultation and Cooperation (C & C) Agreement with the State of New Mexico, and then to PA personnel for their calculations to support the CCA.

Because most of you presented most of your results at the Retardation Research Program Review Meeting in Carlsbad last month, I have scheduled only one presentation for next week's meeting, Predictions of Actinide Oxidation States in the Culebra by Harlan Stockman of Sandia. However, please bring viewgraphs updated to include as many of your new data as possible for use in our discussions. Because you are very busy, please do not feel obligated to spend a lot of time making nice viewgraphs.

Thank you very much in advance for taking time out of your busy schedule to participate in this meeting. I am looking forward to your input next week.

Best regards,

Larry Brush
WIPP Chemical & Disposal Room
Processes Department 6748

Distribution:

R. J. Lark, DOE/CAO
I. Triay, LANL
MS 0750 P. V. Brady (Org. 6118)
MS 0750 H. W. Stockman (Org. 6118)
MS 1320 E. J. Nowak (Org. 6831)
MS 1320 Y. Behl (Org. 6748)
MS 1320 G. O. Brown (Org. 6748)
MS 1320 K. G. Budge (Org. 6748)
MS 1320 R. V. Bynum (Org. 6831)
MS 1320 R. Holt (Org. 6748)
MS 1320 D. A. Lucero (Org. 6748)
MS 1320 H. W. Papenguth (Org. 6748)
MS 1320 W. G. Perkins (Org. 6748)
MS 1320 M. D. Siegel (Org. 6748)
MS 1328 M. S. Tierney (Org. 6741)
MS 1328 M. A. Martell (Org. 6749)
MS 1335 M. S. Y. Chu (Org. 6801)
MS 1337 W. D. Weart (Org. 6000)
MS 1341 J. T. Holmes (Org. 6748)
MS 1341 L. H. Brush (Org. 6748)
MS 1341 L. J. Storz (Org. 6748)
MS 1341 R. F. Weiner (Org. 6751)
MS 1395 L. E. Shephard (Org. 6800)
MS 1395 M. G. Marietta (Org. 6821)
MS 1330 SWCF (Org. 6352), WBS 1.1.10.3.1 (2)

Agenda

Monday and Tuesday, April 1 and 2, 1996
BDM Sandia Vista Building
2301 Buena Vista SE
Albuquerque, NM

Monday, April 1

9:00 - 9:30	Introduction	L. H. Brush, SNL
9:30 - 10:30	Predictions of Actinide Oxidation States in the Culebra	H. W. Stockman, SNL
10:30 - 10:45	Break	
10:45 - 11:45	Proposed Use of Ranges and Distributions of K_ds by PA	M. S. Tierney, SNL
11:45 - 13:00	Lunch	BDM Cafeteria
13:00 - 15:00	Discussion of Range and Distribution of K_ds for Pu(V)	All participants
15:00 - 15:15	Break	
15:15 - 17:15	Discussion of Range and Distribution of K_ds for Am(III) and Pu(III)	All participants

Tuesday, April 2

8:00 - 10:00	Discussion of Range and Distribution of K_ds for Th(IV), Pu(IV), and U(IV)	All participants
10:00 - 10:15	Break	
10:15 - 11:45	Discussion of Range and Distribution of K_ds for U(VI) and, if necessary, Pu(VI)	All participants
11:45 - 13:00	Lunch	BDM Cafeteria
13:00 - 13:30	Discussion of Range and Distribution of K_ds for U(VI) (continued)	All participants
13:30 - 13:45	Break	
13:45 - 15:45	Discussion of Range and Distribution of K_ds for Np(V)	All participants

Participants

Y. Behl, SciRes (SNL column transport study)
P. V. Brady, SNL (Principal Investigator for the SNL/LANL mechanistic sorption study)
L. H. Brush, SNL (Principal Investigator for the dissolved-actinide Retardation Research Program (RRP)
R. V. Bynum, SAIC (Actinide Source Term Program management)
C. Duffy, independent LANL contractor (LANL empirical sorption study)
K. M. Economy, Ecodynamics (PA Culebra transport calculations)
R. Holt, independent SNL contractor (characterization of clay minerals in the Culebra)
E. J. Nowak, SNL (Manager, WIPP Chemical & Disposal Room Processes Department 6748)
H. W. Papenguth, SNL (former Principal Investigator for the dissolved-actinide RRP)
W. G. Perkins, SNL (Retardation Research Program management)
M. D. Siegel, SNL (Principal Investigator for the Stanford mechanistic sorption study, brine mixing, and characterization of clay minerals in the Culebra)
H. W. Stockman, SNL (predictions of actinide oxidation states in the Culebra)
C. T. Stockman, SNL (predictions of actinide oxidation states in the Culebra)
M. S. Tierney, SNL (Task Leader for the PA database)
I. Triay, LANL (Group Leader, Chemical Science and Technology Group, and Principal Investigator for the LANL empirical sorption study)
R. F. Weiner, SNL (Actinide Source Term Program)

Observers

D. Hobart, Carlsbad Administrative and Technical Assistance Contractor (Actinide Source Term Program, Retardation Research Program)
R. J. Lark, US DOE Carlsbad Area Office

APPENDIX B: RANGES AND PROBABILITY DISTRIBUTIONS OF MATRIX K_ds FOR Pu(V) AND DOLOMITE-RICH CULEBRA ROCK

Based on a laboratory study carried out under expected WIPP conditions and previously published results obtained for applications other than the WIPP Project, ASTP personnel have predicted that Pu will speciate as Pu(III) or Pu(IV), but not as Pu(V) nor Pu(VI), in deep (Castile and Salado) brines in the repository. Furthermore, a modeling study of the effects of mixing deep and Culebra brines on the oxidation states of Pu, U, and Np in the Culebra showed that Culebra fluids are poorly poised (see Predictions of Actinide Oxidation States in the Culebra above). Therefore; Pu will not speciate as Pu(V) in the Culebra. However, we could not establish experimentally obtained ranges of matrix K_ds for Am(III) (see Methods Used to Establish Ranges of Matrix K_ds above and Appendix C below). Instead, we established experimentally obtained ranges for Pu(V) and used them for Am(III) and Pu(III) by assuming that the K_ds for Am(III) and Pu(III) are greater than or equal to those for Pu(V).

To establish the *initial* ranges for Pu(V) and the deep brines, we first considered *all* of the data from the 6-week empirical sorption experiments carried out with Brine A and ERDA-6 on the bench top (0.033% CO_2) by Triay and her group at LANL (see Methods Used to Establish Ranges of Matrix K_ds for the reasons for considering these data). These runs were: #6004, #6024, #6044, #6064, and #6084 (see Table B-1 below), and #6005, #6025, #6045, #6065, and #6085 (Table B-2). Next, we discarded the data from #6025, #6045, and #6065, the runs in which the difference between the activity of the ^{239}Pu in a standard and that in a control exceeded 3σ, where σ is the standard deviation (see Methods Used to Establish Ranges of Matrix K_ds.) Discarding the data from these three runs yielded an *initial* range of 22.7 ml/g (from #6004) to 459 ml/g (#6005) for Pu(V) and the deep brines.

To establish the *initial* ranges for Pu(V) and the Culebra brines, we first considered *all* of Triay's 6-week sorption data obtained with AISinR and H-17 on the bench top (0.033% CO_2) and in glove boxes with atmospheres containing 0.24 and 1.4% CO_2 (see Methods Used to Establish Ranges of Matrix K_ds). These were: #6006, #6026, #6046, #6066, #6086, #24006, #24026, #24046, #24066, #24086, #12006, #12026, #12046, #12066, and #12086 (Table B-3), and #6007, #6027, #6047, #6067, #6087, #24007, #24027, #24047, #24067, #24087, #12007, #12027, #12047, #12067, and #12087 (Table B-4). We then discarded the data from #6006, #24006, #24066, and #6007, the runs in which the difference between the activity of the ^{239}Pu in a standard and that in a control exceeded 3σ, to obtain the *initial* range of 9.61 ml/g (from #12007) to 3,620 ml/g (#12046) for Pu(V) and the Culebra brines.

Next, we compared these initial ranges with the data from the mechanistic sorption study by Brady and his colleagues at SNL and LANL. We used Brady's data to extend Triay's empirical sorption data for the deep brines to the basic conditions expected to result from the use of an MgO backfill in WIPP disposal rooms, *but not* to extend

Triay's data for the Culebra brines to basic conditions (see Methods Used to Establish Ranges of Matrix K_ds). Brady's data for 0.5 M NaCl, atmospheric CO_2, and the highest pH values under these conditions are (to three significant figures) 350 and 411 ml/g at a pH of 9.87 and 9.88, respectively (Table B-5). Because these values are *within* the initial range for Pu(V) and the deep brines (see above), and because we did not use this comparison to extend the initial range for Pu(V) and the Culebra brines to basic conditions, our *revised* ranges for Pu(V) remain 22.7 to 459 ml/g and 9.61 to 3,620 ml/g for the deep and Culebra brines, respectively.

We then compared both of these revised ranges with the data from the transport study with intact Culebra cores by Lucero and his colleagues at SNL. Lucero carried out his experiments under ambient atmospheric conditions; therefore, the CO_2 content of these experiments was probably similar to that in Triay's bench-top (0.033% CO_2) runs. Because Lucero *did not* observe breakthrough of Pu(V), it was only possible to determine a minimum K_d for this element. Lucero and his colleagues submitted their results on March 28, 1996, (see Table B-6), then revised them on April 5 and 16, 1996 (Tables B-7 and B-8, respectively). The minimum K_ds reported for experiments C-3, D3, and E-2 (Table B-8) *are consistent with the K_ds reported by Triay for Pu(V) and AlSinR in her experiments carried out on the bench top* (0.033% CO_2) (Table B-3). Because these values are consistent with the revised range for Pu(V) and the Culebra brines (see above), and because Lucero did not carry out any experiments with Pu(V) and the deep brines (Table B-8), our *final* ranges for Pu(V) remain 22.7 to 459 ml/g and 9.61 to 3,620 ml/g for the deep and Culebra brines, respectively. However, we rounded these ranges to 20 to 500 ml/g and 10 to 4,000 ml/g, respectively prior to inclusion in Table 1 above.

We recommend that PA personnel use a uniform probability distribution for both of these ranges (see Methods Used to Establish Probability Distributions of Matrix K_ds above).

Furthermore, we recommend that PA use the range of 20 to 500 ml/g (the range for deep brines) for Pu(V) because this range results in less retardation of this element than the range for Culebra brines (see Methods Used for Final Selection of the Range of Matrix K_ds for Use in PA Calculations above).

Finally, we recommend that PA use a range of 20 to 500 ml/g for Pu(III) and Am(III) (see Methods Used to Establish Ranges of Matrix K_ds and Appendix C).

Table B-1. Effects of Initial Radionuclide Concentration and P_{CO2} on Matrix K_ds for Pu(V), Dolomite-Rich Culebra Rock, and Brine A (LANL Empirical Sorption Study). Six-week sorption runs with VPX-25-8. No K_ds in this table excluded from ranges and distributions because of unacceptable differences between standards and controls. Data current as of April 3, 1996. Table compiled by L. H. Brush on March 23 and 30, 1996, based on information provided by LANL on March 19 and 26, 1996. Table checked by Brush and S. Boone on April 3, 1996. Table revised by Brush on June 7, 1996. Table checked by L. J. Storz on June 10, 1996.

Brine	Range of Initial ^{239}Pu Conc. (M)	K_d (ml/g), 0.033% CO_2	K_d (ml/g), 0.24% CO_2	K_d (ml/g), 1.4% CO_2	K_d (ml/g), 4.1% CO_2
Brine A	1.98×10^{-7} to 2.39×10^{-7}	22.7, #6004	23.7, #24004	31.9, #12004	28.3 #18004
Brine A	1.11×10^{-8} to 5.28×10^{-8}	54.9, #6024	261, #24024	38.5, #12024	35.9 #18024
Brine A	2.38×10^{-8} to 3.16×10^{-8}	28.0, #6044	34.6, #24044	43.9 #12044	39.4 #18044
Brine A	3.78×10^{-9} to 7.03×10^{-9}	27.2, #6064	30.5, #24064	65.0 #12064	32.1 #18064
Brine A	3.08×10^{-9} to 3.37×10^{-9}	28.6, #6084	30.5, #24084	31.2 #12084	30.3 #18084

Table B-2. Effects of Initial Radionuclide Concentration and P_{CO2} on Matrix K_ds for Pu(V), Dolomite-Rich Culebra Rock, and ERDA-6 (LANL Empirical Sorption Study). Six-week sorption runs with VPX-25-8. K_ds in bold font excluded from ranges and distributions because of unacceptable differences between standards and controls. Data current as of April 3, 1996. Table compiled by L. H. Brush on March 23 and 30, 1996, based on information provided by LANL on March 19 and 26, 1996. Table checked by Brush and S. Boone on April 3, 1996. Table revised by Brush on June 7, 1996. Table checked by L. J. Storz on June 10, 1996.

Brine	Range of Initial ^{239}Pu Conc. (M)	K_d (ml/g), 0.033% CO_2	K_d (ml/g), 0.24% CO_2	K_d (ml/g), 1.4% CO_2	K_d (ml/g), 4.1% CO_2
ERDA-6	1.45×10^{-9} to 6.01×10^{-8}	459, #6005	6,890, #24005	7,070, #12005	151 #18005
ERDA-6	3.88×10^{-10} to 1.24×10^{-8}	3,920, #6025	6,500, #24025	6,960 #12025	205 #18025
ERDA-6	2.36×10^{-10} to 6.35×10^{-9}	2,980, #6045	3,040, #24045	7,540 #12045	253 #18045
ERDA-6	1.59×10^{-10} to 1.67×10^{-9}	677, #6065	1,140, #24065	1,970 #12065	170 #18065
ERDA-6	3.29×10^{-11} to 1.20×10^{-10}	147, #6085	1,180, #24085	1,460 #12085	4,550 #18085

Table B-3. Effects of Initial Radionuclide Concentration and P_{CO2} on Matrix K_ds for Pu(V), Dolomite-Rich Culebra Rock, and AISinR (LANL Empirical Sorption Study). Six-week sorption runs with VPX-25-8. K_ds in bold font excluded from ranges and distributions because of unacceptable differences between standards and controls. Data current as of April 3, 1996. Table compiled by L. H. Brush on March 23 and 30, 1996, based on information provided by LANL on March 19 and 26, 1996. Table checked by Brush and S. Boone on April 3, 1996. Table revised by Brush on June 7, 1996. Table checked by L. J. Storz on June 10, 1996.

Brine	Range of Initial ^{239}Pu Conc. (M)	K_d (ml/g), 0.033% CO_2	K_d (ml/g), 0.24% CO_2	K_d (ml/g), 1.4% CO_2	K_d (ml/g), 4.1% CO_2
AISinR	1.76×10^{-9} to 9.71×10^{-8}	348, #6006	62.5, #24006	1,890, #12006	4,100 #18006
AISinR	4.22×10^{-10} to 3.91×10^{-8}	1,990, #6026	37.2, #24026	1,050 #12026	5,050, #18026
AISinR	1.91×10^{-10} to 1.85×10^{-8}	221, #6046	39.8, #24046	3,620 #12046	6,260 #18046
AISinR	1.20×10^{-10} to 3.18×10^{-9}	435, #6066	50.3, #24066	848 #12066	1,910 #18066
AISinR	8.43×10^{-11} to 1.93×10^{-9}	499, #6086	42.9, #24086	1,070, #12086	1,360 #18086

Table B-4. Effects of Initial Radionuclide Concentration and P_{CO2} on Matrix K_ds for Pu(V), Dolomite-Rich Culebra Rock, and H-17 (LANL Empirical Sorption Study). Six-week sorption runs with VPX-25-8. K_ds in bold font excluded from ranges and distributions because of unacceptable differences between standards and controls. Data current as of April 3, 1996. Table compiled by L. H. Brush on March 23 and 30, 1996, based on information provided by LANL on March 19 and 26, 1996. Table checked by Brush and S. Boone on April 3, 1996. Table revised by Brush on June 7, 1996. Table checked by L. J. Storz on June 10, 1996.

Brine	Range of Initial ^{239}Pu Conc. (M)	K_d (ml/g), 0.033% CO_2	K_d (ml/g), 0.24% CO_2	K_d (ml/g), 1.4% CO_2	K_d (ml/g), 4.1% CO_2
H-17	5.94×10^{-8} to 3.01×10^{-7}	157, #6007	89.5, #24007	9.61, #12007	26.7 #18007
H-17	4.55×10^{-9} to 7.16×10^{-8}	191, #6027	155, #24027	13.3 #12027	33.5 #18027
H-17	3.80×10^{-9} to 3.18×10^{-8}	332, #6047	183, #24047	14.3 #12047	36.6 #18047
H-17	9.35×10^{-10} to 5.48×10^{-9}	256, #6067	182, #24067	25.2 #12067	43.7 #18067
H-17	2.01×10^{-10} to 2.00×10^{-9}	235, #6087	637, #24087	93.9 #12087	45.8 #18087

Table B-5. Effects of pH and P_{CO2} on Matrix K_ds for Pu(V) and Pure Dolomite (SNL/LANL Mechanistic Sorption Study). Sorption runs with Norwegian dolomite and 0.5 M NaCl. Data current as of March 31, 1996. Table retyped by L. H. Brush on April 24, 1996. Table checked by Y. Behl on April 28, 1996.

pH (standard units	K_d (ml/g), atmospheric CO_2	K_d (ml/g), 0.5% CO_2	K_d (ml/g), 5% CO_2
9.88	410.9	NA	NA
9.87	349.56	NA	NA
8.42	0	NA	NA
6.7	-44.928	NA	NA
6.2	34.662	NA	NA
5.81	34.662	NA	NA
5.21	34.662	NA	NA
4.62	128.72	NA	NA
4.05	-113.15	NA	NA
3.51	-44.928	NA	NA
3.11	-310.23	NA	NA

NA: not applicable.

Table B-5. Effects of pH and P_{CO2} on Matrix K_ds for Pu(V) and Pure Dolomite (SNL/LANL Mechanistic Sorption Study) (continued).

pH (standard units	K_d (ml/g), atmospheric CO_2	K_d (ml/g), 0.5% CO_2	K_d (ml/g), 5% CO_2
6.9	NA	465.69	NA
8.49	NA	3711.1	NA
7.32	NA	1029.4	NA
7.19	NA	1162.5	NA
6.99	NA	968.83	NA
6.88	NA	418.41	NA
6.55	NA	319.12	NA
6.17	NA	570.38	NA
5.28	NA	199.2	NA
3.97	NA	99.265	NA
3.13	NA	99.265	NA

NA: not applicable.

Table B-5. Effects of pH and P_{CO2} on Matrix K_ds for Pu(V) and Pure Dolomite (SNL/LANL Mechanistic Sorption Study) (continued).

pH (standard units	K_d (ml/g), atmospheric CO_2	K_d (ml/g), 0.5% CO_2	K_d (ml/g), 5% CO_2
6.39	NA	NA	124.82
6.91	NA	NA	499.76
6.89	NA	NA	NR
6.8	NA	NA	499.76
6.75	NA	NA	520.02
6.84	NA	NA	371.73
6.49	NA	NA	423.82
6.07	NA	NA	222.63
5.76	NA	NA	147.77
4.91	NA	NA	22.561
3.62	NA	NA	124.82

NA: not applicable.
NR: not reported.

Table B-6. Minimum Values of R and K_d for Pu(V) in Intact Culebra Cores (SNL Column Transport Study). Data current as of March 26, 1996. Table compiled by L. H. Brush on March 30, 1996, based on memo by D. A. Lucero, G. O. Brown, and K. G. Budge dated March 28, 1996. Table checked by Brush on March 31, 1996.

Run #	Solid (core)	Brine	Flow rate (ml/ min)	Run Time (days)	Ef- fluent Vol. (L)	R_{min}	Poro- sity (%)	$K_{d,min}$ (ml/g)	Range (±ml/ g)
C-3	VPX- 28-6C	AIS.	0.1	211	30.45	5,200	3.7^{S}	84	NA
D-3	VPX- 25-8A	AIS.	0.1	118	17.02	1,140	$9.1,^{S}$ 5.3^{D}	46	NA
E-2	VPX- 27-7A	AIS.	0.1	61	8.83	405	$23,^{S}$ 15.7^{D}	40	NA

AIS: AISinR.
D: dual porosity assumed.
NA: not available yet.
S: single porosity assumed.

Table B-7. Minimum Values of R and K_d for Pu(V) in Intact Culebra Cores (SNL Column Transport Study). Data current as of March 26, 1996. Table compiled by L. H. Brush on March 30, 1996, based on memo by D. A. Lucero, G. O. Brown, and K. G. Budge dated March 28, 1996. Table checked by Brush on March 31, 1996. Table revised by Brush on April 6, 1996, based on memo by Lucero and Brown dated April 5, 1996. Table checked by Y Behl on April 8, 1996.

Run #	Solid (core)	Brine	Flow rate (ml/ min)	Run Time (days)	Ef- fluent Vol. (L)	R_{min}	Poro- sity (%)	$K_{d,\,min}$ (ml/g)	Range (±ml/ g)
C-3	VPX-28-6C	AIS.	0.1	211	30.45	5,200	3.7[S]	84	NA
D-3	VPX-25-8A	AIS.	0.1	118	17.02	1,140	9.1[S]	46	NA
E-2	VPX-27-7A	AIS.	0.1	61	8.83	405	23[S]	40	NA

AIS: AISinR.
NA: not available yet.
S: single porosity assumed.

Table B-8. Minimum Values of R and K_d for Pu(V) in Intact Culebra Cores (SNL Column Transport Study). Data current as of March 26, 1996. Table compiled by L. H. Brush on March 30, 1996, based on memo by D. A. Lucero, G. O. Brown, and K. G. Budge dated March 28, 1996. Table checked by Brush on March 31, 1996. Table revised by Brush on April 6, 1996, based on memo by Lucero and Brown dated April 5, 1996. Table checked by Y Behl on April 8, 1996. Table revised by Brush on April 17, 1996, based on memo by Brown dated April 16, 1996.

Run #	Solid (core)	Brine	Flow rate (ml/ min)	Run Time (days)	Ef- fluent Vol. (L)	R_{min}	Poro- sity (%)	$K_{d,\,min}$ (ml/g)	Range (±ml/ g)
C-3	VPX-28-6C	AIS.	0.1	211	30.45	5,200	3.7^S	84	NA
D-3	VPX-25-8A	AIS.	0.1	118	17.02	1,140	9.1^S	45	NA
E-2	VPX-27-7A	AIS.	0.1	61	8.83	405	23^S	40	NA

AIS: AISinR.
NA: not available yet.
S: single porosity assumed.

APPENDIX C: RANGES AND PROBABILITY DISTRIBUTIONS OF MATRIX K_ds FOR Am(III) AND DOLOMITE-RICH CULEBRA ROCK

For Am, only one oxidation state, Am(III), is possible in the Culebra (see Predictions of Actinide Oxidation States in the Culebra above). Therefore, we attempted to establish experimentally obtained ranges of matrix K_ds for Am(III), and use them and the oxidation-state analogy to establish ranges for Pu(III).

To establish the *initial* ranges for Am(III) and the deep brines, we first considered *all* of the data from the 6-week empirical sorption experiments carried out with Brine A and ERDA-6 on the bench top (0.033% CO_2) by Triay and her group at LANL (see Methods Used to Establish Ranges of Matrix K_ds above for the reasons for considering these data). These runs were: #6012, #6032, #6052, #6072, and #6092 (see Table C-1), and #6013, #6033, #6053, #6073, and #6093 (see Table C-2 below). We discarded the data from #6012, #6032, #6013, #6033, #6073, and #6093, the runs in which the difference between the activity of the ^{243}Am in a standard and that in a control exceeded 3σ, where σ is the standard deviation (see Methods Used to Establish Ranges of Matrix K_ds.) Even after discarding the results of these six runs, however, the defensibility of the remaining data is questionable because the K_ds retained for Brine A increase significantly as the final dissolved concentration of ^{243}Am increases. (We will include these isotherms in the parameter and analysis records packages for these K_ds. However, this trend is also apparent in Table C-1.) Furthermore, the isotherm obtained by plotting the quantity of radionuclide sorbed by the solid phase or phases versus the final dissolved radionuclide concentration does not appear to pass through the origin. The K_ds are also proportional to the final dissolved ^{243}Am concentration in the runs carried out in the glove box with an atmosphere containing 1.4% CO_2, and, based on the trends observed with *both* retained and discarded data, *appeared* to increase similarly in the runs conducted in the glove boxes with atmospheres containing 0.24 and 4.1% CO_2 (see Table C-1). Moreover, based on the trends observed with *both* retained and discarded data, these K_ds also *appear* proportional to the final dissolved ^{243}Am concentration at all four CO_2 concentrations in the runs with ERDA-6 (Table C-2). These trends suggest that sorption of Am by the container walls, precipitation of an Am-bearing solid phase, coprecipitation of Am by another phase, incomplete separation of the aqueous and the solid phases at the end of an experiment, or some combination of these processes occurred in the runs with Am(III). We thought we had eliminated reactions other than sorption by the rock in these experiments because: (1) LANL personnel had filtered the brines sequentially, with a minimum filter size of 0.2 μm, after these runs; (2) we had discarded results from the runs in which the difference between the activity of the radionuclide in the standard and that in the control exceeded 3σ before examining these data; (3) the final Am(III) concentrations in these runs were less than the solubilities predicted by FMT for these brines. Triay carried out additional posttest analyses of the brines from her 6-week sorption experiments with Am(III) with 0.033% CO_2 to determine, if possible, what caused these trends, and to redetermine these K_ds. She did not attempt any additional posttest analyses of the brines from experiments conducted in the glove boxes because

she had removed them from these glove boxes after the original runs, thus exposing them to conditions different from those during the runs. Triay first recounted the brines to determine if mistaken sample identification or improper data entry had caused the trends described above. She then refiltered, centrifuged, and/or ultracentrifuged the brines to remove any suspended particles, and recounted them. Finally, she recalculated the K_ds using the controls instead of the standards to specify the initial dissolved ^{243}Am concentration. Despite these efforts, the data continued to display trends similar to those described above.

The 6-week LANL sorption experiments carried out with Am(III) and the Culebra brines (AISinR and H-17) yielded the same trends described above for the deep brines (compare Tables C-3 and C-4 with Tables C-1 and C-2). Therefore, we could not use them to establish a range for Am(III).

We did not use the data from the mechanistic sorption study by Brady and his colleagues at SNL and LANL, nor the column transport study by Lucero and his colleagues at SNL to establish a range for Am(III) for several reasons. First, Brady had used pure Norwegian dolomite and pure NaCl solutions, not actual Culebra dolomite and synthetic Culebra fluids. (Although we used his data to *extend* the initial ranges established with Triay's empirical data to the basic conditions expected to result from the use of an MgO backfill in WIPP disposal rooms, we *did not* believe this would be defensible in the absence of *any* empirical data for actual Culebra dolomite and synthetic Culebra fluids.) Furthermore, Brady's data for Am(III) with atmospheric and 0.5% CO_2 (see Table C-6), the headspace concentrations corresponding to CO_2 partial pressures within the range that Siegel now considers likely for groundwaters in the Culebra off-site transport pathway (see Methods Used to Establish Ranges of Matrix K_ds), were all "high" above a pH of about 5 or 6. ("High" means that insufficient ^{243}Am remained in solution after these runs to determine a K_d). Moreover, although Brady *did* obtain data for Nd(III) with atmospheric and 0.5% CO_2 at neutral or nearly neutral values of pH (Table C-5), he also obtained them with pure Norwegian dolomite and pure NaCl solutions, not actual Culebra dolomite and synthetic Culebra fluids. Finally, because Lucero *did not* observe breakthrough of Am(III), it is only possible to determine minimum K_ds for this element (Tables C-7 through C-9). These minimum values are significantly lower than actual Am(III) K_ds typically obtained for applications other than the WIPP Project (see below).

Therefore, we recommend using the *experimentally obtained* ranges for Pu(V) (see Table 1 and Appendix B above) for Am(III) by assuming that the K_ds for Am(III) are greater than or equal to those for Pu(V). This assumption is reasonable in view of results such as those in Figure 5 of Canepa (1992). In this case, the Am(III) K_d obtained for the Yucca Mountain Project is about one order of magnitude higher than that obtained for Pu(V) under the same conditions. (We will cite additional examples of differences between the K_ds for Am(III) and Pu(V) in future reports and presentations.) We *have not* used the oxidation-state analogy to justify the use of Pu(V) data for Am(III); instead, this approach is based on *differences* in the behavior of these oxidation states. Furthermore, we recommend using the range for Am(III) for Pu(III); for this recommendation, we *have* used the oxidation-state analogy.

Canepa, J.A. 1992. *Proceedings of the DOE/Yucca Mountain Site Characterization Project Radionuclide Adsorption Workshop at Los Alamos National Laboratory, September 11-12, 1990.* LA-12325-C. Los Alamos, NM: Los Alamos National Laboratory.

Table C-1. Effects of Initial Radionuclide Concentration and P_{CO2} on Matrix K_ds for Am(III), Dolomite-Rich Culebra Rock, and Brine A (LANL Empirical Sorption Study). Six-week sorption runs with VPX-25-8. K_ds in bold font excluded from ranges and distributions because of unacceptable differences between standards and controls. Data current as of April 3, 1996. Table compiled by L. H. Brush on March 23 and 30, 1996, based on information provided by LANL on March 19 and 26, 1996. Table checked by Brush and S. Boone on April 3, 1996. Table revised by Brush on June 7, 1996. Table checked by L. J. Storz on June 10, 1996.

Brine	Range of Initial ^{243}Am Conc. (M)	K_d (ml/g), 0.033% CO_2	K_d (ml/g), 0.24% CO_2	K_d (ml/g), 1.4% CO_2	K_d (ml/g), 4.1% CO_2
Brine A	1.72×10^{-9} to 2.95×10^{-9}	965, #6012	1,040, #24012	1,320, #12012	1,260, #18012
Brine A	1.13×10^{-9} to 1.47×10^{-9}	927, #6032	1,120, #24032	1,140, #12032	1,070, #18032
Brine A	4.64×10^{-10} to 5.61×10^{-10}	509, #6052	521, #24052	553, #12052	597, #18052
Brine A	3.31×10^{-10} to 4.14×10^{-10}	330, #6072	356, #24072	392, #12072	346, #18072
Brine A	2.65×10^{-10} to 3.24×10^{-10}	67.9, #6092	76.6, #24092	86.8, #12092	77.8, #18092

Table C-2. Effects of Initial Radionuclide Concentration and P_{CO_2} on Matrix K_ds for Am(III), Dolomite-Rich Culebra Rock, and ERDA-6 (LANL Empirical Sorption Study). Six-week sorption runs with VPX-25-8. K_ds in bold font excluded from ranges and distributions because of unacceptable differences between standards and controls. Data current as of April 3, 1996. Table compiled by L. H. Brush on March 23 and 30, 1996, based on information provided by LANL on March 19 and 26, 1996. Table checked by Brush and S. Boone on April 3, 1996. Table revised by Brush on June 7, 1996. Table checked by L. J. Storz on June 10, 1996.

Brine	Range of Initial ^{243}Am Conc. (M)	K_d (ml/g), 0.033% CO_2	K_d (ml/g), 0.24% CO_2	K_d (ml/g), 1.4% CO_2	K_d (ml/g), 4.1% CO_2
ERDA-6	2.18×10^{-10} to 4.66×10^{-10}	5,620, #6013	9,590, #24013	10,800, #12013	5,230, #18013
ERDA-6	1.57×10^{-10} to 7.10×10^{-10}	5,100, #6033	4,760, #24033	8,110, #12033	2,080, #18033
ERDA-6	1.06×10^{-10} to 2.02×10^{-10}	1,650, #6053	1,610, #24053	2,010, #12053	1,210, #18053
ERDA-6	1.22×10^{-10} to 1.51×10^{-10}	978, #6073	877, #24073	832, #12073	754, #18073
ERDA-6	9.23×10^{-11} to 1.16×10^{-10}	211, #6093	272, #24093	249, #12093	258, #18093

Table C-3. Effects of Initial Radionuclide Concentration and P_{CO2} on Matrix K_ds for Am(III), Dolomite-Rich Culebra Rock, and ASIinR (LANL Empirical Sorption Study). Six-week sorption runs with VPX-25-8. K_ds in bold font! excluded from ranges and distributions because of unacceptable differences between standards and controls. Data current as of April 3, 1996. Table compiled by L. H. Brush on March 23 and 30, 1996, based on information provided by LANL on March 19 and 26, 1996. Table checked by Brush and S. Boone on April 3, 1996. Table revised by Brush on June 7, 1996. Table checked by L. J. Storz on June 10, 1996.

Brine	Range of Initial ^{243}Am Conc. (M)	K_d (ml/g), 0.033% CO_2	K_d (ml/g), 0.24% CO_2	K_d (ml/g), 1.4% CO_2	K_d (ml/g), 4.1% CO_2
AISinR	1.14×10^{-9} to 4.02×10^{-9}	**1,790, #6014**	**730, #24014**	**637, #12014**	**507, #18014**
AISinR	6.95×10^{-10} to 2.29×10^{-9}	**1,660, #6034**	**594, #24034**	**676, #12034**	**504, #18034**
AISinR	1.92×10^{-10} to 4.47×10^{-10}	934, #6054	760, #24054	437, #12054	436, #18054
AISinR	1.27×10^{-10} to 2.89×10^{-10}	653, #6074	640, #24074	344, #12074	334, #18074
AISinR	1.26×10^{-10} to 1.64×10^{-10}	190, #6094	145, #24094	133, #12094	156, #18094

Table C-4. Effects of Initial Radionuclide Concentration and P_{CO2} on Matrix K_ds for Am(III), Dolomite-Rich Culebra Rock, and H-17 (LANL Empirical Sorption Study). Six-week sorption runs with VPX-25-8. K_ds in bold font excluded from ranges and distributions because of unacceptable differences between standards and controls. Data current as of April 3, 1996. Table compiled by L. H. Brush on March 23 and 30, 1996, based on information provided by LANL on March 19 and 26, 1996. Table checked by Brush and S. Boone on April 3, 1996. Table revised by Brush on June 7, 1996. Table checked by L. J. Storz on June 10, 1996.

Brine	Range of Initial ^{243}Am Conc. (M)	K_d (ml/g), 0.033% CO_2	K_d (ml/g), 0.24% CO_2	K_d (ml/g), 1.4% CO_2	K_d (ml/g), 4.1% CO_2
H-17	6.35×10^{-10} to 1.69×10^{-9}	1,590, #6015	1,310, #24015	688, #12015	547, #18015
H-17	4.42×10^{-10} to 1.77×10^{-9}	1,140, #6035	1,120, #24035	622, #12035	484, #18035
H-17	2.27×10^{-10} to 3.60×10^{-10}	870, #6055	836, #24055	499, #12055	633, #18055
H-17	1.57×10^{-10} to 3.16×10^{-10}	826, #6075	626, #24075	418, #12075	383, #18075
H-17	1.43×10^{-10} to 3.36×10^{-10}	76.1, #6095	187, #24095	189, #12095	155, #18095

Table C-5. Effects of pH and P_{CO2} on Matrix K_ds for Nd(III) and Pure Dolomite (SNL/LANL Mechanistic Sorption Study). Sorption runs with Norwegian dolomite and 0.05 M NaCl. Data current as of March 31, 1996. Table retyped by L. H. Brush on April 24, 1996. Table checked by Y. Behl on April 28, 1996.

pH (standard units	K_d (ml/g), atmospheric CO_2	K_d (ml/g), 0.5% CO_2	K_d (ml/g), 5% CO_2
9.08	2864.3	NA	NA
8.41	1619.2	NA	NA
7.52	1225.2	NA	NA
6.72	1141.4	NA	NA
6.49	571.49	NA	NA
6.19	497.91	NA	NA
5.74	546.24	NA	NA
5.25	272.78	NA	NA
4.63	241.5	NA	NA
4.2	279.24	NA	NA
3.75	202.2	NA	NA
3.35	141.3	NA	NA

NA: not applicable.

Table C-5. Effects of pH and P_{CO2} on Matrix K_ds for Nd(III) and Pure Dolomite (SNL/LANL Mechanistic Sorption Study) (continued).

pH (standard units	K_d (ml/g), atmospheric CO_2	K_d (ml/g), 0.5% CO_2	K_d (ml/g), 5% CO_2
7.08	NA	538.93	NA
6.81	NA	403.05	NA
6.45	NA	261.86	NA
6.26	NA	386.81	NA
5.92	NA	149.45	NA
5.18	NA	84.721	NA
4.35	NA	55.485	NA
3.64	NA	51.358	NA

NA: not applicable.

Table C-5. Effects of pH and P_{CO2} on Matrix K_ds for Nd(III) and Pure Dolomite (SNL/LANL Mechanistic Sorption Study) (continued).

pH (standard units	K_d (ml/g), atmospheric CO_2	K_d (ml/g), 0.5% CO_2	K_d (ml/g), 5% CO_2
6.33	NA	NA	226.71
6.24	NA	NA	179.19
6.15	NA	NA	182.28
6.01	NA	NA	169.89
5.88	NA	NA	168.9
5.76	NA	NA	111.58
5.54	NA	NA	72.6
5.21	NA	NA	206.36
3.42	NA	NA	34.636

NA: not applicable.

Table C-6. Effects of pH and P_{CO2} on Matrix K_ds for Am(III) and Pure Dolomite (SNL/LANL Mechanistic Sorption Study). Sorption runs with Norwegian dolomite and 0.5 M NaCl. Data current as of March 31, 1996. Table retyped by L. H. Brush on April 24, 1996. Table checked by Y. Behl on April 28, 1996.

pH (standard units	K_d (ml/g), atmospheric CO_2	K_d (ml/g), 0.5% CO_2	K_d (ml/g), 5% CO_2
9.88	High	NA	NA
9.87	High	NA	NA
8.42	High	NA	NA
6.7	High	NA	NA
6.2	High	NA	NA
5.81	High	NA	NA
5.21	High	NA	NA
4.62	791.15	NA	NA
4.05	630.75	NA	NA
3.51	285.41	NA	NA
3.11	92.603	NA	NA

NA: not applicable.

Table C-6. Effects of pH and P_{CO2} on Matrix K_ds for Am(III) and Pure Dolomite (SNL/LANL Mechanistic Sorption Study) (continued).

pH (standard units	K_d (ml/g), atmospheric CO_2	K_d (ml/g), 0.5% CO_2	K_d (ml/g), 5% CO_2
6.9	NA	High	NA
8.49	NA	High	NA
7.32	NA	High	NA
7.19	NA	High	NA
6.99	NA	High	NA
6.88	NA	High	NA
6.55	NA	High	NA
6.17	NA	High	NA
5.28	NA	1130.9	NA
3.97	NA	65.441	NA
3.13	NA	158.09	NA

NA: not applicable.

Table C-6. Effects of pH and P_{CO2} on Matrix K_ds for Am(III) and Pure Dolomite (SNL/LANL Mechanistic Sorption Study) (continued).

pH (standard units	K_d (ml/g), atmospheric CO_2	K_d (ml/g), 0.5% CO_2	K_d (ml/g), 5% CO_2
6.39	NA	NA	High
6.91	NA	NA	High
6.89	NA	NA	High
6.8	NA	NA	High
6.75	NA	NA	High
6.84	NA	NA	High
6.49	NA	NA	High
6.07	NA	NA	High
5.76	NA	NA	1934.3
4.91	NA	NA	333.78
3.62	NA	NA	-10.908

NA: not applicable.

Table C-7 Minimum Values of R and K_d for Am(III) in Intact Culebra Cores (SNL Column Transport Study). Data current as of March 26, 1996. Table compiled by L. H. Brush on March 30, 1996, based on memo by D. A. Lucero, G. O. Brown, and K. G. Budge dated March 28, 1996. Table checked by Brush on March 31, 1996.

Run #	Solid (core)	Brine	Flow rate (ml/ min)	Run Time (days)	Ef- fluent Vol. (L)	R_{min}	Poro- sity (%)	$K_{d,\ min}$ (ml/g)	Range (±ml/ g)
C-3	VPX- 28-6C	AIS.	0.1	211	30.45	1,420	3.7[S]	11	NA
D-3	VPX- 25-8A	AIS.	0.1	118	17.02	350	9.1,[S] 5.3[D]	14	NA
E-2	VPX- 27-7A	AIS.	0.1	61	8.83	200	23,[S] 15.7[D]	20	NA

AIS: AISinR.
D: dual porosity assumed.
NA: not available yet.
S: single porosity assumed.

Table C-8. Minimum Values of R and K_d for Am(III) in Intact Culebra Cores (SNL Column Transport Study). Data current as of March 26, 1996. Table compiled by L. H. Brush on March 30, 1996, based on memo by D. A. Lucero, G. O. Brown, and K. G. Budge dated March 28, 1996. Table checked by Brush on March 31, 1996. Table revised by Brush on April 6, 1996, based on memo by Lucero and Brown dated April 5, 1996. Table checked by Y. Behl on April 8, 1996.

Run #	Solid (core)	Brine	Flow rate (ml/ min)	Run Time (days)	Ef- fluent Vol. (L)	R_{min}	Poro- sity (%)	$K_{d,\,min}$ (ml/g)	Range (±ml/ g)
C-3	VPX- 28-6C	AIS.	0.1	211	30.45	1,420	3.7^S	11	NA
D-3	VPX- 25-8A	AIS.	0.1	118	17.02	350	9.1^S	14	NA
E-2	VPX- 27-7A	AIS.	0.1	61	8.83	200	23^S	20	NA

AIS: AISinR.
NA: not available yet.
S: single porosity assumed.

Table C-9. Minimum Values of R and K_d for Am(III) in Intact Culebra Cores (SNL Column Transport Study). Data current as of March 26, 1996. Table compiled by L. H. Brush on March 30, 1996, based on memo by D. A. Lucero, G. O. Brown, and K. G. Budge dated March 28, 1996. Table checked by Brush on March 31, 1996. Table revised by Brush on April 6, 1996, based on memo by Lucero and Brown dated April 5, 1996. Table checked by Y. Behl on April 8, 1996. Table revised by Brush on April 17, 1996, based on memo by Brown dated April 16, 1996.

Run #	Solid (core)	Brine	Flow rate (ml/min)	Run Time (days)	Effluent Vol. (L)	R_{min}	Porosity (%)	$K_{d,min}$ (ml/g)	Range (±ml/g)
C-3	VPX-28-6C	AIS.	0.1	211	30.45	1,420	3.7^S	23	NA
D-3	VPX-25-8A	AIS.	0.1	118	17.02	350	9.1^S	14	NA
E-2	VPX-27-7A	AIS.	0.1	61	8.83	200	23^S	20	NA

AIS: AISinR.
NA: not available yet.
S: single porosity assumed.

APPENDIX D: RANGES AND PROBABILITY DISTRIBUTIONS OF MATRIX K_ds FOR U(VI) AND DOLOMITE-RICH CULEBRA ROCK

Based on experimental results, ASTP personnel have predicted that U will speciate as U(IV) or U(VI) in deep (Castile and Salado) brines in WIPP disposal rooms. Furthermore, a modeling study of the effects of mixing deep and Culebra brines on the oxidation states of Pu, U, and Np in the Culebra showed that Culebra fluids are poorly poised (see Predictions of Actinide Oxidation States in the Culebra above). Therefore; we established experimentally obtained ranges of matrix K_ds for U(VI) and used the experimentally obtained ranges for Th(IV) (see Appendix E below) and the oxidation-state analogy to establish ranges for U(IV) (and Np(IV)).

To establish the *initial* ranges for U(VI) and the deep brines, we first considered *all* of the data from the 6-week empirical sorption experiments carried out with Brine A and ERDA-6 on the bench top (0.033% CO_2) by Triay and her group at LANL (see Methods Used to Establish Ranges of Matrix K_ds above for the reasons for considering these data). These runs were: #6008, #6028, #6048, #6068, and #6088 (see Table D-1 below), and #6009, #6029, #6049, #6069, and #6089 (Table D-2). Next, we discarded the data from #6008, #6028, #6048, #6068, and #6009, the runs in which the difference between the activity of the ^{233}U in a standard and that in a control exceeded 3σ, where σ is the standard deviation (see Methods Used to Establish Ranges of Matrix K_ds). Discarding the data from these five runs yielded an *initial* range of 3.76 ml/g (from #6029) to 21.8 ml/g (#6088) for U(VI) and the deep brines.

To establish the *initial* ranges for U(VI) and the Culebra brines, we first considered *all* of Triay's 6-week sorption data obtained with AISinR and H-17 on the bench top (0.033% CO_2) and in glove boxes with atmospheres containing 0.24 and 1.4% CO_2 (see Methods Used to Establish Ranges of Matrix K_ds). These were: #6010, #6030, #6050, #6070, #6090, #24010, #24030, #24050, #24070, #24090, #12010, #12030, #12050, #12070, and #12090 (Table D-3), and #6011, #6031, #6051, #6071, #6091, #24011, #24031, #24051, #24071, #24091, #12011, #12031, #12051, #12071, and #12091 (Table D-4). We then discarded the data from #6010, #6050, #6070, #24010, #24030, #12010, #6011, #6031, #6051, #6071, #12011, and #12051, the runs in which the difference between the activity of the ^{233}U in a standard and that in a control exceeded 3σ, to obtain the *initial* range of -1.66 ml/g (from #12091) to 68.7 ml/g (#24091) for U(VI) and the Culebra brines. However, we set the lower limit of this range equal to 0 ml/g because there is no reason why a K_d could have a value less than 0.

Next, we compared these initial ranges with the data from the mechanistic sorption study by Brady and his colleagues at SNL and LANL. We used Brady's data to extend Triay's empirical sorption data for the deep brines to the basic conditions expected to result from the use of an MgO backfill in WIPP disposal rooms, *but not* to extend Triay's data for the Culebra brines to basic conditions (see Methods Used to Establish Ranges of Matrix K_ds). Brady's data for 0.5 M NaCl, atmospheric CO_2, and the highest

pH values under these conditions are (to three significant figures) 10.6 and 34.7 ml/g at a pH of 9.87 and 9.88, respectively (Table D-5). Because these values are *greater than the upper limit* of the initial range for U(VI) and the deep brines (see above), we extended this range to obtain a *revised* range for U(VI) and deep brines of 3.76 ml/g to 34.7 ml/g. Because we did not use this comparison to extend the initial range for U(VI) and the Culebra brines to basic conditions, this *revised* range remains 0 to 68.7 ml/g.

We then compared both of these revised ranges with the data from the transport study with intact Culebra cores by Lucero and his colleagues at SNL. Lucero carried out his experiments under ambient atmospheric conditions; therefore, the CO_2 content of these experiments was probably similar to that in the LANL bench-top (0.033% CO_2) runs. Lucero *did* observe breakthrough of U(VI) in his experiments. Therefore, it was possible to determine actual K_ds for this element. Lucero and his colleagues submitted their results on March 28, 1996, (see Table D-6), then revised them on April 5 and 16, 1996 (Tables D-7 and D-8, respectively). The K_d reported for Experiment C-7 with the deep brine ERDA-6 (Table D-8) *is less than the lower limit of the revised range of K_ds for U(VI) and the deep brines obtained from the empirical and mechanistic sorption studies* (see above). Therefore, we extended this range to obtain a *final* range for U(VI) and deep brines of 0.029 ml/g to 34.7 ml/g, and rounded it to 0.03 to 30 ml/g prior to inclusion in Table 1 above. Because Lucero's K_ds for U(VI) and the Culebra brine AISinR (B-3, B-6, C-2, D-5, and D-6 in Table D-8) are *within* the revised range for U(VI) and the Culebra brines (see above), our *final* range remains 0 to 68.7 ml/g, rounded to 0 to 70 ml/g for inclusion in Table 1.

We recommend that PA personnel use a uniform probability distribution for both of these ranges (see Methods Used to Establish Probability Distributions of Matrix K_ds above).

Finally, we recommend that PA use the range of 0.03 to 30 ml/g (the range for deep brines) for U(VI) because this range results in less retardation of this element than the range for Culebra brines (see Methods Used for Final Selection of the Range of Matrix K_ds for Use in PA Calculations above).

Table D-1. Effects of Initial Radionuclide Concentration and P_{CO2} on Matrix K_ds for U(VI), Dolomite-Rich Culebra Rock, and Brine A (LANL Empirical Sorption Study). Six-week sorption runs with VPX-25-8. K_ds in bold font excluded from ranges and distributions because of unacceptable differences between standards and controls. Data current as of April 3, 1996. Table compiled by L. H. Brush on March 23 and 30, 1996, based on information provided by LANL on March 19 and 26, 1996. Table checked by Brush and S. Boone on April 3, 1996. Table revised by Brush on June 7, 1996. Table checked by L. J. Storz on June 10, 1996.

Brine	Range of Initial ^{233}U Conc. (M)	K_d (ml/g), 0.033% CO_2	K_d (ml/g), 0.24% CO_2	K_d (ml/g), 1.4% CO_2	K_d (ml/g), 4.1% CO_2
Brine A	1.65×10^{-6} to 2.81×10^{-6}	**12.5**, #6008	**4.77**, #24008	**1.16**, #12008	0.709, #18008
Brine A	7.89×10^{-7} to 1.05×10^{-6}	**16.8**, #6028	2.86, #24028	1.21, #12028	2.67, #18028
Brine A	1.85×10^{-7} to 2.72×10^{-7}	**19.9**, #6048	5.23, #24048	1.47, #12048	2.46, #18048
Brine A	7.60×10^{-8} to 1.09×10^{-7}	**16.6**, #6068	6.81, #24068	0.933, #12068	2.30, #18068
Brine A	2.14×10^{-8} to 4.16×10^{-8}	21.8, #6088	4.70, #24088	-5.41, #12088	1.44, #18088

Table D-2. Effects of Initial Radionuclide Concentration and P_{CO2} on Matrix K_ds for U(VI), Dolomite-Rich Culebra Rock, and ERDA-6 (LANL Empirical Sorption Study). Six-week sorption runs with VPX-25-8. K_ds in bold font excluded from ranges and distributions because of unacceptable differences between standards and controls. Data current as of April 3, 1996. Table compiled by L. H. Brush on March 23 and 30, 1996, based on information provided by LANL on March 19 and 26, 1996. Table checked by Brush and S. Boone on April 3, 1996. Table revised by Brush on June 7, 1996. Table checked by L. J. Storz on June 10, 1996.

Brine	Range of Initial ^{233}U Conc. (M)	K_d (ml/g), 0.033% CO_2	K_d (ml/g), 0.24% CO_2	K_d (ml/g), 1.4% CO_2	K_d (ml/g), 4.1% CO_2
ERDA-6	2.62×10^{-6} to 2.99×10^{-6}	**0.542, #6009**	1.29, #24009	**4.13, #12009**	3.75, #18009
ERDA-6	8.61×10^{-7} to 9.87×10^{-7}	3.76, #6029	1.52, #24029	5.92, #12029	**3.17, #18029**
ERDA-6	2.14×10^{-7} to 2.56×10^{-7}	3.86, #6049	2.38, #24049	7.25, #12049	3.22, #18049
ERDA-6	8.40×10^{-8} to 9.28×10^{-8}	3.88, #6069	4.35, #24069	6.24, #12069	4.76, #18069
ERDA-6	2.31×10^{-8} to 2.87×10^{-8}	6.55, #6089	2.11, #24089	7.04, #12089	1.04, #18089

Table D-3. Effects of Initial Radionuclide Concentration and P_{CO2} on Matrix K_ds for U(VI), Dolomite-Rich Culebra Rock, and ASIinR (LANL Empirical Sorption Study). Six-week sorption runs with VPX-25-8. K_ds in bold font excluded from ranges and distributions because of unacceptable differences between standards and controls. Data current as of April 3, 1996. Table compiled by L. H. Brush on March 23 and 30, 1996, based on information provided by LANL on March 19 and 26, 1996. Table checked by Brush and S. Boone on April 3, 1996. Table revised by Brush on June 7, 1996. Table checked by L. J. Storz on June 10, 1996.

Brine	Range of Initial ^{233}U Conc. (M)	K_d (ml/g), 0.033% CO_2	K_d (ml/g), 0.24% CO_2	K_d (ml/g), 1.4% CO_2	K_d (ml/g), 4.1% CO_2
AISinR	2.86×10^{-6} to 3.04×10^{-6}	2.56, #6010	**0.351, #24010**	**0.550, #12010**	**1.67, #18010**
AISinR	9.57×10^{-7} to 1.06×10^{-6}	2.62, #6030	**2.69, #24030**	2.05, #12030	**0.756, #18030**
AISinR	2.63×10^{-7} to 2.87×10^{-7}	3.74, #6050	0.389, #24050	1.65, #12050	3.73, #18050
AISinR	8.22×10^{-8} to 9.50×10^{-8}	**4.02, #6070**	3.16, #24070	1.03, #12070	**0.341, #18070**
AISinR	2.60×10^{-8} to 2.79×10^{-8}	7.51, #6090	0.117, #24090	1.73, #12090	1.88, #18090

Table D-4. Effects of Initial Radionuclide Concentration and P_{CO2} on Matrix K_ds for U(VI), Dolomite-Rich Culebra Rock, and H-17 (LANL Empirical Sorption Study). Six-week sorption runs with VPX-25-8. K_ds in bold font excluded from ranges and distributions because of unacceptable differences between standards and controls. Data current as of April 3, 1996. Table compiled by L. H. Brush on March 23 and 30, 1996, based on information provided by LANL on March 19 and 26, 1996. Table checked by Brush and S. Boone on April 3, 1996. Table revised by Brush on June 7, 1996. Table checked by L. J. Storz on June 10, 1996.

Brine	Range of Initial ^{233}U Conc. (M)	K_d (ml/g), 0.033% CO_2	K_d (ml/g), 0.24% CO_2	K_d (ml/g), 1.4% CO_2	K_d (ml/g), 4.1% CO_2
H-17	2.76×10^{-6} to 2.97×10^{-6}	**3.63, #6011**	0.313, #24011	**-0.745, #12011**	-0.104, #18011
H-17	1.11×10^{-6} to 1.16×10^{-6}	**5.55, #6031**	1.30, #24031	0.157, #12031	0.530, #18031
H-17	2.72×10^{-7} to 2.92×10^{-7}	**6.97, #6051**	3.03, #24051	**-1.83, #12051**	2.26, #18051
H-17	8.73×10^{-8} to 9.86×10^{-8}	**5.12, #6071**	1.90, #24071	1.50, #12071	-1.22, #18071
H-17	6.89×10^{-9} to 2.83×10^{-8}	10.2, #6091	68.7, #24091	-1.66, #12091	2.96, #18091

Table D-5. Effects of pH and P_{CO2} on Matrix K_ds for U(VI) and Pure Dolomite (SNL/LANL Mechanistic Sorption Study). Sorption runs with Norwegian dolomite and 0.5 M NaCl. Data current as of March 31, 1996. Table retyped by L. H. Brush on April 24, 1996. Table checked by Y. Behl on April 28, 1996.

pH (standard units	K_d (ml/g), atmospheric CO_2	K_d (ml/g), 0.5% CO_2	K_d (ml/g), 5% CO_2
9.88	34.662	NA	NA
9.87	10.6	NA	NA
8.42	7691.2	NA	NA
6.7	4794.1	NA	NA
6.2	3345.6	NA	NA
5.81	5685.5	NA	NA
5.21	2476.5	NA	NA
4.62	2476.5	NA	NA
4.05	2621.3	NA	NA
3.51	2342.8	NA	NA
3.11	1897.1	NA	NA

NA: not applicable.

Table D-5. Effects of pH and P_{CO2} on Matrix K_ds for U(VI) and Pure Dolomite (SNL/LANL Mechanistic Sorption Study) (continued).

pH (standard units	K_d (ml/g), atmospheric CO_2	K_d (ml/g), 0.5% CO_2	K_d (ml/g), 5% CO_2
6.9	NA	775.74	NA
8.49	NA	-112.13	NA
7.32	NA	44.55	NA
7.19	NA	123.88	NA
6.99	NA	286.76	NA
6.88	NA	849.72	NA
6.55	NA	1114	NA
6.17	NA	455.52	NA
5.28	NA	1774.6	NA
3.97	NA	1611.4	NA
3.13	NA	4222.7	NA

NA: not applicable.

Table D-5. Effects of pH and P_{CO2} on Matrix K_ds for U(VI) and Pure Dolomite (SNL/LANL Mechanistic Sorption Study) (continued).

pH (standard units	K_d (ml/g), atmospheric CO_2	K_d (ml/g), 0.5% CO_2	K_d (ml/g), 5% CO_2
6.39	NA	NA	475.59
6.91	NA	NA	69.799
6.89	NA	NA	0
6.8	NA	NA	0
6.75	NA	NA	69.799
6.84	NA	NA	69.799
6.49	NA	NA	296.73
6.07	NA	NA	1517.2
5.76	NA	NA	2056.6
4.91	NA	NA	3075.4
3.62	NA	NA	1674.5

NA: not applicable.

Table D-6. Measured Values of R and Calculated Values of K_d for U(VI) in Intact Culebra Cores (SNL Column Transport Study). Values in bold font to be excluded from ranges and distributions because fits to elution data were inferior to those assuming single porosity and dual porosity with fracture retardation. Data current as of March 30, 1996. Table compiled by L. H. Brush on March 30, 1996, based on memo by D. A. Lucero, G. O. Brown, and K. G. Budge dated March 28, 1996. Table checked by Brush on March 31, 1996.

Run #	Solid (core)	Brine	Flow rate (ml/min)	Run Time (days)	Effluent Vol. (L)	R	Porosity (%)	K_d (ml/g)	Range (±ml/g)
B-3	VPX-26-11A	AIS.	0.1	NA	NA	3.4;[S] 1, 18.3;[N] 3.1, 5.2[DF]	9.8[S] 5.2[DN] 5.2[DF]	.084[S] 0.68[DN] .039[DF]	.022[S] .67[DN] 0.03[DF]
B-6	VPX-26-11A	AIS.	0.05	NA	NA	13.1;[S] 1, NA;[DN] NA, NA[DF]	4.8[S] NA[DN] NA[DF]	0.25[S] NA[DN] NA[DF]	0.07[S] NA[DN] NA[DF]
C-2	VPX-28-6C	AIS.	0.1	21	2	10.4;[S] 1, 260;[DN] 12.0, 0.6[DF]	5.7[S] 3.5[DN] 3.5[DF]	0.23[S] 3.9[DN] 0.17[DF]	0.08[S] 7[DN] 0.06[DF]
C-7	VPX-28-6C	ER-6	0.1	13	2	2.7;[S] 1, 0.6;[DN] 2.7, 0.76[DF]	3.9[S] 2.1[DN] 2.1[DF]	.029[S] .069[DN] .016[DF]	.022[S] 0.13[DN] .005[DF]

Table D-6. Measured Values of R and Calculated Values of K_d for U(VI) in Intact Culebra Cores (SNL Column Transport Study) (continued)

Run #	Solid (core)	Brine	Flow rate (ml/ min)	Run Time (days)	Ef- fluent Vol. (L)	R	Poro- sity (%)	K_d (ml/g)	Range (±ml/ g)
D-5	VPX-25-8A	AIS.	0.1	13	2	21;[S] 1, 184;[DN] NA, NA[DF]	17.3[S] 7.1[DN] 7.1[DF]	1.50[S] 5.6[DN] NA[DF]	0.38[S] 5.5[DN] NA[DF]
D-6	VPX-25-8A	AIS.	0.05	60	2	10.1;[S] 1, NA;[DN] 12.3, 71[DF]	15.5[S] 7.1[DN] 7.1[DF]	0.61[S] NA[DN] 0.35[DF]	0.15 NA[DN] 0.19[DF]

AIS: AISinR.
DF: dual porosity and fracture retardation assumed.
DN: dual porosity and no fracture retardation assumed.
ER.-6: ERDA-6.
NA: not available yet.
S: single porosity assumed.

Table D-7. Measured Values of R and Calculated Values of K_d for U(VI) in Intact Culebra Cores (SNL Column Transport Study). Data current as of March 30, 1996. Table compiled by L. H. Brush on March 30, 1996, based on memo by D. A. Lucero, G. O. Brown, and K. G. Budge dated March 28, 1996. Table checked by Brush on March 31, 1996. Table revised by Brush on April 6, 1996, based on memo by Lucero and Brown dated April 5, 1996. Table checked by Y. Behl on April 8, 1996.

Run #	Solid (core)	Brine	Flow rate (ml/min)	Run Time (days)	Effluent Vol. (L)	R	Porosity (%)	K_d (ml/g)	Range (±ml/g)
B-3	VPX-26-11A	AIS.	0.1	NA	NA	3.4[S]	9.8[S]	0.084[S]	NA[S]
B-6	VPX-26-11A	AIS.	0.05	NA	NA	13[S]	4.8[S]	0.25[S]	NA[S]
C-2	VPX-28-6C	AIS.	0.1	21	2	10.4[S]	5.7[S]	0.23[S]	NA[S]
C-7	VPX-28-6C	ER.-6	0.1	13	2	2.7[S]	3.9[S]	0.029[S]	NA[S]
D-5	VPX-25-8A	AIS.	0.1	13	2	21[S]	17.3[S]	1.5[S]	NA[S]
D-6	VPX-25-8A	AIS.	0.05	60	2	10[S]	15.5[S]	0.61[S]	NA[S]

AIS: AISinR.
ER.-6: ERDA-6.
NA: not available yet.
S: single porosity assumed.

Table D-8. Measured Values of R and Calculated Values of K_d for U(VI) in Intact Culebra Cores (SNL Column Transport Study). Data current as of March 30, 1996. Table compiled by L. H. Brush on March 30, 1996, based on memo by D. A. Lucero, G. O. Brown, and K. G. Budge dated March 28, 1996. Table checked by Brush on March 31, 1996. Table revised by Brush on April 6, 1996 based on memo by Lucero and Brown dated April 5, 1996. Table checked by Y. Behl on April 8, 1996. Table revised by Brush on April 17, 1996, based on memo by Brown dated April 16, 1996.

Run #	Solid (core)	Brine	Flow rate (ml/ min)	Run Time (days)	Ef- fluent Vol. (L)	R	Poro- sity (%)	K_d (ml/g)	Range (±ml/ g)
B-3	VPX-26-11A	AIS.	0.1	NA	NA	3.4[S]	9.8[S]	0.10[S]	NA[S]
B-6	VPX-26-11A	AIS.	0.05	NA	NA	13[S]	4.8[S]	0.25[S]	NA[S]
C-2	VPX-28-6C	AIS.	0.1	21	2	10.4[S]	5.7[S]	0.23[S]	NA[S]
C-7	VPX-28-6C	ER.-6	0.1	13	2	2.7[S]	3.9[S]	0.029[S]	NA[S]
D-5	VPX-25-8A	AIS.	0.1	13	2	21[S]	17.3[S]	1.5[S]	NA[S]
D-6	VPX-25-8A	AIS.	0.05	60	2	10[S]	15.5[S]	0.61[S]	NA[S]

AIS: AISinR.
ER.-6: ERDA-6.
NA: not available yet.
S: single porosity assumed.

APPENDIX E: RANGES AND PROBABILITY DISTRIBUTIONS OF MATRIX K_ds FOR Th(IV) AND DOLOMITE-RICH CULEBRA ROCK

For Th, only one oxidation state, Th(IV), is possible in the Culebra (see Predictions of Actinide Oxidation States in the Culebra above). Therefore, we established an experimentally obtained range of matrix K_ds for Th(VI), and used it and the oxidation-state analogy to establish ranges for Pu(IV), U(IV), and Np(IV).

To establish the *initial* ranges for Th(IV) and the deep brines, we first considered *all* of the data from the 6-week empirical sorption experiments carried out with Brine A and ERDA-6 on the bench top (0.033% CO_2) by Triay and her group at LANL (see Methods Used to Establish Ranges of Matrix K_ds above for the reasons for considering these data). These runs were: #7011A and #7011B (see Table E-1 below), and #7007A, #7007B, #7008A, #7008B, #7009A, #7009B, #7010A, and #7010B (Table E-2). Next, we discarded the data from #7011A and #7011B, the runs in which the difference between the activity of the ^{230}Th in a standard and that in a control exceeded 3σ, where σ is the standard deviation (see Methods Used to Establish Ranges of Matrix K_ds). Discarding the data from these two runs yielded an *initial* range of 864 ml/g (from #7010A) to 15,000 ml/g (#7008B) for Th(IV) and the deep brines.

For the *initial* ranges for Th(IV) and the Culebra brines, we first considered *all* of Triay's 6-week sorption data obtained with AISinR and H-17 on the bench top (0.033% CO_2) and in glove boxes with atmospheres containing 0.24 and 1.4% CO_2 (see Methods Used to Establish Ranges of Matrix K_ds). These were: #7012A, #7012B, #7054A, #7054B, #7026A, #7026B, #7040A, and #7040B (Table E-3), and #7013A, #7013B, #7055A, #7055B, #7027A, #7027B, #7041A, and #7041B (Table E-4). Unfortunately, we had to discard the data from *all* of these the runs because the difference between the activity of the ^{230}Th in a standard and that in a control exceeded 3σ. Therefore, we assumed that the *initial* range of 864 to 15,000 ml/g for Th(IV) and the deep brines does not differ significantly from that for Th(IV) and the Culebra brines.

Next, we attempted to compare these initial ranges with the data from the mechanistic sorption study by Brady and his colleagues at SNL and LANL. However, Brady *did not* obtain any usable results for Th because of one or more of the following reasons: (1) the walls of the containers used to prepare Th-bearing solutions sorbed essentially all of it prior to his experiments; (2) essentially all of the Th precipitated on the walls of these containers prior to his runs; (3) the walls of his apparatus sorbed essentially all of the Th during his runs; (4) essentially all of the Th precipitated on the dolomite and/or the apparatus during his runs. Therefore, our *revised* ranges for Th(IV) remained 864 to 15,000 ml/g for *both* the deep and Culebra brines.

We then compared the revised range with the data from the transport study with intact Culebra cores by Lucero and his colleagues at SNL. Lucero carried out his experiments under ambient atmospheric conditions; therefore, the CO_2 content of these

experiments was probably similar to that in the LANL bench-top (0.033% CO_2) runs. Because Lucero *did not* observe breakthrough of Th(IV), it was only possible to determine a minimum K_d for this element. Furthermore, the minimum K_ds calculated for Th are significantly lower than those calculated for Pu and Am, the other elements for which Lucero did not observe breakthrough (compare Tables B-8, C-9, and E-6), because: (1) the detection limit of γ-spectrometric analysis (one of the two methods used in this study) for ^{228}Th in the effluent is much higher than those for ^{241}Pu and ^{241}Am because of the low yield of the ^{228}Th γ emission; (2) although ^{228}Th emits α particles detectable by LSC (the other analytical method used in this study), its daughter products have interfering α emissions; (3) lowering the detection limit for ^{228}Th by observing the decay of its daughters, such as ^{224}Ra, was not possible because of interference by identical daughters produced by the decay of ^{232}U, which was used in all of the cores. Lucero and his colleagues submitted their results on March 28, 1996, (Table E-5), then revised them on April 5, 1996 (Table E-6). The minimum K_ds reported for experiments C-2, C-5, and D-2 (Table E-6) *are consistent with the revised range obtained from the empirical and mechanistic sorption studies* (see above). Therefore, our *final* range remains 864 to 15,000 ml/g, rounded to 900 to 20,000 ml/g prior to inclusion in Table 1 above.

We recommend that PA personnel use a uniform probability distribution for this range (see Methods Used to Establish Probability Distributions of Matrix K_ds above).

Finally, based on the oxidation-state analogy, we recommend that PA use a range of 900 to 20,000 ml/g for Pu(IV), U(IV), and Np(IV) (see Table 1).

Table E-1. Effects of Initial Radionuclide Concentration and P_{CO2} on Matrix K_ds for Th(IV), Dolomite-Rich Culebra Rock, and Brine A (LANL Empirical Sorption Study). Six -week sorption runs with VPX-25-8. K_ds in bold font excluded from ranges and distributions because of unacceptable differences between standards and controls. Data current as of April 3, 1996. Table compiled by L. H. Brush on March 30 and April 3, 1996, based on information provided by LANL on March 28 and April 1, 1996. Table checked by Brush and S. Boone on April 3, 1996.

Brine	Initial ^{230}Th Conc. (M)	K_d (ml/g), 0.033% CO_2	K_d (ml/g), 0.24% CO_2	K_d (ml/g), 1.4% CO_2	K_d (ml/g), 4.1% CO_2
Brine A	ND	ND	ND	ND	ND
Brine A	ND	ND	ND	ND	ND
Brine A	ND	ND	ND	ND	ND
Brine A	ND	ND	ND	ND	ND
Brine A	ND	ND	ND	ND	ND
Brine A	ND	ND	ND	ND	ND
Brine A	NA	313, #7011A	205, #7053A	338, #7025A	694, #7039A
Brine A	NA	250, #7011B	227, #7053B	352, #7025B	706, #7039B
Brine A	ND	ND	ND	ND	ND
Brine A	ND	ND	ND	ND	ND

NA: not available yet.
ND: not determined.

Table E-2. Effects of Initial Radionuclide Concentration and P_{CO2} on Matrix K_ds for Th(IV), Dolomite-Rich Culebra Rock, and ERDA-6 (LANL Empirical Sorption Study). Six-week sorption runs with VPX-25-8. K_ds in bold font excluded from ranges and distributions because of unacceptable differences between standards and controls. Data current as of April 3, 1996. Table compiled by L. H. Brush on March 30 and April 3, 1996, based on information provided by LANL on March 28 and April 1, 1996. Table checked by Brush and S. Boone on April 3, 1996.

Brine	Initial ^{230}Th Conc. (M)	K_d (ml/g), 0.033% CO_2	K_d (ml/g), 0.24% CO_2	K_d (ml/g), 1.4% CO_2	K_d (ml/g), 4.1% CO_2
ERDA-6	ND	ND	ND	ND	ND
ERDA-6	ND	ND	ND	ND	ND
ERDA-6	NA	5,340, #7007A	6,600, #7049A	12,900, #7021A	4,600, #7035A
ERDA-6	NA	5,270, #7007B	**8,950, #7049B**	15,900, #7021B	7,060, #7035B
ERDA-6	NA	6,650, #7008A	**8,720, #7050A**	8,670, #7022A	**7,340, #7036A**
ERDA-6	NA	15,000, #7008B	**6,450, #7050B**	7,780, #7022B	**9,620, #7036B**
ERDA-6	NA	2,180, #7009A	1,640, #7051A	14,100, #7023A	6,810, #7037A
ERDA-6	NA	2,820, #7009B	3,740, #7051B	7,270, #7023B	45,600, #7037B
ERDA-6	NA	864, #7010A	1,930, #7052A	High, #7024A	364, #7038A
ERDA-6	NA	1,300, #7010B	1,780, #7052B	1,130, #7024B	2,850, #7038B

NA: not available yet.
ND: not determined.

Table E-3. Effects of Initial Radionuclide Concentration and P_{CO2} on Matrix K_ds for Th(IV), Dolomite-Rich Culebra Rock, and AISinR (LANL Empirical Sorption Study). Six-week sorption runs with VPX-25-8. K_ds in bold font excluded from ranges and distributions because of unacceptable differences between standards and controls. Data current as of April 3, 1996. Table compiled by L. H. Brush on March 30 and April 3, 1996, based on information provided by LANL on March 28 and April 1, 1996. Table checked by Brush and S. Boone on April 3, 1996.

Brine	Initial ^{230}Th Conc. (M)	K_d (ml/g), 0.033% CO_2	K_d (ml/g), 0.24% CO_2	K_d (ml/g), 1.4% CO_2	K_d (ml/g), 4.1% CO_2
AISinR	ND	ND	ND	ND	ND
AISinR	ND	ND	ND	ND	ND
AISinR	ND	ND	ND	ND	ND
AISinR	ND	ND	ND	ND	ND
AISinR	ND	ND	ND	ND	ND
AISinR	ND	ND	ND	ND	ND
AISinR	NA	High, #7012A	10,800, #7054A	4,580, #7026A	57,100, #7040A
AISinR	NA	High, #7012B	16,900, #7054B	7,080, #7026B	High, #7040B
AISinR	ND	ND	ND	ND	ND
AISinR	ND	ND	ND	ND	ND

NA: not available yet.
ND: not determined.

Table E-4. Effects of Initial Radionuclide Concentration and P_{CO2} on Matrix K_ds for Th(IV), Dolomite-Rich Culebra Rock, and H-17 (LANL Empirical Sorption Study). Six-week sorption runs with VPX-25-8. K_ds in bold font excluded from ranges and distributions because of unacceptable differences between standards and controls. Data current as of April 3, 1996. Table compiled by L. H. Brush on March 30 and April 3, 1996, based on information provided by LANL on March 28 and April 1, 1996. Table checked by Brush and S. Boone on April 3, 1996.

Brine	Initial ^{230}Th Conc. (M)	K_d (ml/g), 0.033% CO_2	K_d (ml/g), 0.24% CO_2	K_d (ml/g), 1.4% CO_2	K_d (ml/g), 4.1% CO_2
H-17	ND	ND	ND	ND	ND
H-17	ND	ND	ND	ND	ND
H-17	ND	ND	ND	ND	ND
H-17	ND	ND	ND	ND	ND
H-17	ND	ND	ND	ND	ND
H-17	ND	ND	ND	ND	ND
H-17	NA	12,100, #7013A	7,580, #7055A	High, #7027A	14,500, #7041A
H-17	NA	High, #7013B	High, #7055B	23,700, #7027B	14,300, #7041B
H-17	ND	ND	ND	ND	ND
H-17	ND	ND	ND	ND	ND

NA: not available yet.
ND: not determined.

Table E-5. Minimum Values of R and K_d for Th(IV) in Intact Culebra Cores (SNL Column Transport Study). Data current as of March 26, 1996. Table compiled by L. H. Brush on March 30, 1996, based on memo by D. A. Lucero, G. O. Brown, and K. G. Budge dated March 28, 1996. Table checked by Brush on March 31, 1996.

Run #	Solid (core)	Brine	Flow rate (ml/min)	Run Time (days)	Effluent Vol. (L)	R_{min}	Porosity (%)	$K_{d,min}$ (ml/g)	Range (±ml/g)
C-2	VPX-28-6C	AIS.	0.1	237	34.15	35	5.7^{S}, 3.5^{D}	0.87	NA
C-5	VPX-28-6C	ER.-6	0.1	146	20.98	22	3.9^{S}, 2.3^{D}	0.36	NA
D-2	VPX-25-8A	AIS.	0.1	133	19.12	8.5	8.2^{S}, 5.5^{D}	0.25	NA

AIS: AISinR.
D: dual porosity assumed.
ER.-6: ERDA-6.
NA: not available yet.
S: single porosity assumed.

Table E-6. Minimum Values of R and K_d for Th(IV) in Intact Culebra Cores (SNL Column Transport Study). Data current as of March 26, 1996. Table compiled by L. H. Brush on March 30, 1996, based on memo by D. A. Lucero, G. O. Brown, and K. G. Budge dated March 28, 1996. Table checked by Brush on March 31, 1996. Table revised by Brush on April 6, 1996, based on memo by Lucero and Brown dated April 5, 1996. Table checked by Y. Behl on April 8, 1996.

Run #	Solid (core)	Brine	Flow rate (ml/ min)	Run Time (days)	Ef- fluent Vol. (L)	R_{min}	Poro- sity (%)	$K_{d,\ min}$ (ml/g)	Range (±ml/ g)
C-2	VPX-28-6C	AIS.	0.1	237	34.15	35	5.7^S	0.87	NA
C-5	VPX-28-6C	ER.-6	0.1	146	20.98	22	3.9^S	0.36	NA
D-2	VPX-25-8A	AIS.	0.1	133	19.12	8.5	8.2^S	0.25	NA

AIS: AISinR.
ER.-6: ERDA-6.
NA: not available yet.
S: single porosity assumed.

APPENDIX F: RANGES AND PROBABILITY DISTRIBUTIONS OF MATRIX K_ds FOR Np(V) AND DOLOMITE-RICH CULEBRA ROCK

Based on experimental results, ASTP personnel have predicted that Np will speciate as Np(IV) or Np(V), but not as Np(VI), in deep (Castile and Salado) brines in WIPP disposal rooms. Furthermore, a modeling study of the effects of mixing deep and Culebra brines on the oxidation states of Pu, U, and Np in the Culebra showed that Culebra fluids are poorly poised (see Predictions of Actinide Oxidation States in the Culebra above). Therefore; we established experimentally obtained ranges of matrix K_ds for Np(V) and used the experimentally obtained ranges for Th(IV) (see Appendix E above) and the oxidation-state analogy to establish ranges for Np(IV) (and U(IV)).

For the *initial* ranges for Np(V) and the deep brines, we first considered *all* of the data from the 6-week empirical sorption experiments carried out with Brine A and ERDA-6 on the bench top (0.033% CO_2) by Triay and her group at LANL (see Methods Used to Establish Ranges of Matrix K_ds above for the reasons for considering these data). These runs were: #6020, #6040, #6060, and #6080 (see Table F-1 below), and #6021, #6041, #6061, #6081 (Table F-2). Next, we discarded the data from #6040, #6021, and #6041, the runs in which the difference between the activity of the ^{237}Np in a standard and that in a control exceeded 3σ, where σ is the standard deviation (see Methods Used to Establish Ranges of Matrix K_ds). Discarding the data from these three runs yielded an *initial* range of 8.64 ml/g (from #6020) to 47.7 ml/g (#6061) for Np(V) and the deep brines.

For the *initial* ranges for Np(V) and the Culebra brines, we first considered *all* of Triay's 6-week sorption data obtained with AISinR and H-17 on the bench top (0.033% CO_2) and in glove boxes with atmospheres containing 0.24 and 1.4% CO_2 (see Methods Used to Establish Ranges of Matrix K_ds). These were: #6022, #6042, #6062, #6082 #24022, #24042 #24062, #24082, #12022, #12042, #12062, and #12082 (Table F-3), and #6023, #6043, #6063, #6083, #24023, #24043, #24063, #24083, #12023, #12043, #12063, and #12083 (Table F-4). We then discarded the data from #24042 and #24082, the runs in which the difference between the activity of the ^{237}Np in a standard and that in a control exceeded 3σ, to obtain the *initial* range of 2.09 ml/g (from #12022) to 163 ml/g (#6042) for Np(V) and the Culebra brines.

Next, we compared these initial ranges with the data from the mechanistic sorption study by Brady and his colleagues at SNL and LANL. We used Brady's data to extend Triay's empirical sorption data for the deep brines to the basic conditions expected to result from the use of an MgO backfill in WIPP disposal rooms, *but not* to extend Triay's data for the Culebra brines to basic conditions (see Methods Used to Establish Ranges of Matrix K_ds). Brady's data for 0.5 M NaCl, atmospheric CO_2, and the highest pH values under these conditions are (to three significant figures) 892 and 938 ml/g at a pH of 9.87 and 9.88, respectively (Table F-5). Because these values are *greater than the upper limit* of the initial range for Np(V) and the deep brines (see above), we extended

this range to obtain a *revised* range for Np(V) and deep brines of 8.64 to 938 ml/g. Because we did not use this comparison to extend the initial range for Np(V) and the Culebra brines to basic conditions, this *revised* range remains 2.09 to 163 ml/g.

We then compared both of these revised ranges with the data from the transport study with intact Culebra cores by Lucero and his colleagues at SNL. Lucero carried out his experiments under ambient atmospheric conditions; therefore, the CO_2 content of these experiments was probably similar to that in the LANL bench-top (0.033% CO_2) runs. Lucero *did* observe breakthrough of Np(V) in his experiments. Therefore, it was possible to determine actual K_ds for this element. Lucero and his colleagues submitted their results on March 28, 1996, (see Table F-6), then revised them on April 5, 1996 (Table F-7). The K_d reported for Experiment C-7 with the deep brine ERDA-6 (Table F7) *is less than the lower limit of the revised range of K_ds for Np(V) and the deep brines obtained from the empirical and mechanistic sorption experiments* (see above). Therefore, we extended this range to obtain a *final* range for Np(V) and deep brines of 2.0 to 938 ml/g, and rounded it to 2 to 900 ml/g prior to inclusion in Table 1 above. Because Lucero's K_ds for Np(V) and the Culebra brine AISinR (C-6, D-2, and D4 in Table F-7), *are also less than the lower limit of the revised range for Np(V) and the Culebra brines obtained from the sorption studies* (see above), we extended this range to obtain a *final* range of 1.0 to 163 ml/g, rounded to 1 to 200 ml/g (Table 1).

We recommend that PA personnel use a uniform probability distribution for both of these ranges (see Methods Used to Establish Probability Distributions of Matrix K_ds above).

Furthermore, we recommend that PA use the range of 1 to 200 ml/g (the range for Culebra brines) for Np(V) because this range results in less retardation of this element than the range for deep brines (see Methods Used for Final Selection of the Range of Matrix K_ds for Use in PA Calculations above).

Table F-1. Effects of Initial Radionuclide Concentration and P_{CO2} on Matrix K_ds for Np(V), Dolomite-Rich Culebra Rock, and Brine A (LANL Empirical Sorption Study). Six-week sorption runs with VPX-25-8. K_ds in bold font excluded from ranges and distributions because of unacceptable differences between standards and controls. Data current as of April 3, 1996. Table compiled by L. H. Brush on March 23 and 30, 1996, based on information provided by LANL on March 19 and 26, 1996. Table checked by Brush and S. Boone on April 3, 1996. Table revised by Brush on June 7, 1996. Table checked by L. J. Storz on June 10, 1996.

Brine	Range of Initial ^{237}Np Conc. (M)	K_d (ml/g), 0.033% CO_2	K_d (ml/g), 0.24% CO_2	K_d (ml/g), 1.4% CO_2	K_d (ml/g), 4.1% CO_2
Brine A	ND	ND	ND	ND	ND
Brine A	6.80×10^{-7} to 9.26×10^{-6}	8.64, #6020	5.05, #24020	224, #12020	380, #18020
Brine A	3.86×10^{-6} to 4.52×10^{-6}	**16.1, #6040**	**31.9, #24040**	11.8, #12040	8.91, #18040
Brine A	6.09×10^{-7} to 6.56×10^{-7}	20.3, #6060	150, #24060	21.3, #12060	21.9, #18060
Brine A	2.16×10^{-7} to 2.58×10^{-7}	37.5, #6080	32.5, #24080	36.7, #12080	27.0, 18080

ND: not determined.

Table F-2. Effects of Initial Radionuclide Concentration and P_{CO2} on Matrix K_ds for Np(V), Dolomite-Rich Culebra Rock, and ERDA-6 (LANL Empirical Sorption Study). Six-week sorption runs with VPX-25-8. K_ds in bold font excluded from ranges and distributions because of unacceptable differences between standards and controls. Data current as of April 3, 1996. Table compiled by L. H. Brush on March 23 and 30, 1996, based on information provided by LANL on March 19 and 26, 1996. Table checked by Brush and S. Boone on April 3, 1996. Table revised by Brush on June 7, 1996. Table checked by L. J. Storz on June 10, 1996.

Brine	Range of Initial ^{237}Np Conc. (M)	K_d (ml/g), 0.033% CO_2	K_d (ml/g), 0.24% CO_2	K_d (ml/g), 1.4% CO_2	K_d (ml/g), 4.1% CO_2
ERDA-6	ND	ND	ND	ND	ND
ERDA-6	4.43×10^{-7} to 9.85×10^{-7}	**218**, #6021	**241**, #24021	562, #12021	**508**, #18021
ERDA-6	4.81×10^{-7} to 1.46×10^{-6}	**55.2**, #6041	**181**, #24041	153, #12041	**117**, #18041
ERDA-6	1.70×10^{-7} to 5.58×10^{-7}	47.7, #6061	280, #24061	163, #12061	29.9, #18061
ERDA-6	8.59×10^{-9} to 2.78×10^{-7}	31.7, #6081	14,000, #24081	High! #12081	High! #18081

ND: not determined.

Table F-3. Effects of Initial Radionuclide Concentration and P_{CO2} on Matrix K_ds for Np(V), Dolomite-Rich Culebra Rock, and AISinR (LANL Empirical Sorption Study). Six-week sorption runs with VPX-25-8. K_ds in bold font excluded from ranges and distributions because of unacceptable differences between standards and controls. Data current as of April 3, 1996. Table compiled by L. H. Brush on March 23 and 30, 1996, based on information provided by LANL on March 19 and 26, 1996. Table checked by Brush and S. Boone on April 3, 1996. Table revised by Brush on June 7, 1996. Table checked by L. J. Storz on June 10, 1996.

Brine	Range of Initial ^{237}Np Conc. (M)	K_d (ml/g), 0.033% CO_2	K_d (ml/g), 0.24% CO_2	K_d (ml/g), 1.4% CO_2	K_d (ml/g), 4.1% CO_2
AISinR	ND	ND	ND	ND	ND
AISinR	7.62×10^{-6} to 8.72×10^{-6}	5.12, #6022	3.70, #24022	2.09, #12022	2.19, #18022
AISinR	6.06×10^{-7} to 4.53×10^{-6}	163, #6042	**11.9**, #24042	2.35, #12042	2.23, #18042
AISinR	5.26×10^{-7} to 8.08×10^{-7}	20.4, #6062	9.64, #24062	4.06, #12062	4.83, #18062
AISinR	2.39×10^{-7} to 3.81×10^{-7}	32.9, #6082	46.7, #24082	9.89, #12082	10.4, #18082

ND: not determined.

Table F-4. Effects of Initial Radionuclide Concentration and P_{CO2} on Matrix K_ds for Np(V), Dolomite-Rich Culebra Rock, and H-17 (LANL Empirical Sorption Study). Six-week sorption runs with VPX-25-8. No K_ds in this table excluded from ranges and distributions because of unacceptable differences between standards and controls. Data current as of April 3, 1996. Table compiled by L. H. Brush on March 23 and 30, 1996, based on information provided by LANL on March 19 and 26, 1996. Table checked by Brush and S. Boone on April 3, 1996. Table revised by Brush on June 7, 1996. Table checked by L. J. Storz on June 10, 1996.

Brine	Range of Initial ^{237}Np Conc. (M)	K_d (ml/g), 0.033% CO_2	K_d (ml/g), 0.24% CO_2	K_d (ml/g), 1.4% CO_2	K_d (ml/g), 4.1% CO_2
H-17	ND	ND	ND	ND	ND
H-17	2.88×10^{-7} to 9.88×10^{-6}	52.4, #6023	19.0, #24023	2.96, #12023	1.40, #18023
H-17	3.30×10^{-6} to 4.93×10^{-6}	15.8, #6043	13.3, #24043	3.23, #12043	2.37, #18043
H-17	3.44×10^{-7} to 8.87×10^{-7}	40.1, #6063	25.8, #24063	47.1, #12063	4.61, #18063
H-17	2.16×10^{-7} to 8.19×10^{-6}	44.2, #6083	8.02, #24083	3.79, #12083	6.60, #18083

ND: not determined.

Table F-5. Effects of pH and P_{CO2} on Matrix K_ds for Np(V) and Pure Dolomite (SNL/LANL Mechanistic Sorption Study). Sorption runs with Norwegian dolomite and 0.5 M NaCl. Data current as of March 31, 1996. Table retyped by L. H. Brush on April 24, 1996. Table checked by Y. Behl on April 28, 1996.

pH (standard units	K_d (ml/g), atmospheric CO_2	K_d (ml/g), 0.5% CO_2	K_d (ml/g), 5% CO_2
9.88	938.1	NA	NA
9.87	891.95	NA	NA
8.42	324.37	NA	NA
6.7	59.493	NA	NA
6.2	59.493	NA	NA
5.81	-6.7249	NA	NA
5.21	59.493	NA	NA
4.62	59.493	NA	NA
4.05	59.493	NA	NA
3.51	59.493	NA	NA
3.11	-6.7249	NA	NA

NA: not applicable.

Table F-5. Effects of pH and P_{CO_2} on Matrix K_ds for Np(V) and Pure Dolomite (SNL/LANL Mechanistic Sorption Study) (continued).

pH (standard units	K_d (ml/g), atmospheric CO_2	K_d (ml/g), 0.5% CO_2	K_d (ml/g), 5% CO_2
6.9	NA	82.353	NA
8.49	NA	623.53	NA
7.32	NA	352.94	NA
7.19	NA	248.87	NA
6.99	NA	248.87	NA
6.88	NA	159.66	NA
6.55	NA	82.353	NA
6.17	NA	159.66	NA
5.28	NA	82.353	NA
3.97	NA	82.353	NA
3.13	NA	159.66	NA

NA: not applicable.

Table F-5. Effects of pH and P_{CO2} on Matrix K_ds for Np(V) and Pure Dolomite (SNL/LANL Mechanistic Sorption Study) (continued).

pH (standard units	K_d (ml/g), atmospheric CO_2	K_d (ml/g), 0.5% CO_2	K_d (ml/g), 5% CO_2
6.39	NA	NA	-56.83
6.91	NA	NA	100.36
6.89	NA	NA	0
6.8	NA	NA	100.36
6.75	NA	NA	100.36
6.84	NA	NA	100.36
6.49	NA	NA	100.36
6.07	NA	NA	15.721
5.76	NA	NA	15.721
4.91	NA	NA	100.36
3.62	NA	NA	15.721

NA: not applicable.

Table F-6. Measured Values of R and Calculated Values of K_d for Np(V) in Intact Culebra Cores (SNL Column Transport Study). Values in bold font to be excluded from ranges and distributions because fits to elution data were inferior to those assuming single porosity and dual porosity with fracture retardation. Data current as of March 30, 1996. Table compiled by L. H. Brush on March 30, 1996, based on memo by D. A. Lucero, G. O. Brown, and K. G. Budge dated March 28, 1996. Table checked by Brush on March 31, 1996.

Run #	Solid (core)	Brine	Flow rate (ml/min)	Run Time (days)	Effluent Vol. (L)	R	Porosity	K_d (ml/g)	Range (±ml/g)
C-5	VPX-28-6C	ER.-6	0.1	13	2	30.8;[S] 1, 166;[DN] 7.0, 103[DF]	3.9[S] 2.3[DN] 2.3[DF]	0.51[S] 1.65[DN] 0.06[DF]	0.29[S] 1.0[DN] 0.03[DF]
C-6	VPX-28-6C	AIS.	0.1	13	2	58.5;[S] 1, 301;[DN] 22, 158[DF]	4.5[S] 1.85[DN] 1.85[DF]	1.12[S] 2.4[DN] .169[DF]	0.26[S] 1.4[DN] .048[DF]
C-7	VPX-28-6C	ER.-6	0.1	13	2	119;[S] 1, 910;[DN] 169, 0[DF]	3.9[S] 2.1[DN] 2.1[DF]	2.0[S] 8.3[DN] 1.53[DF]	0.8[S] 11.9[DN] 38[DF]
D-2	VPX-25-8A	AIS.	0.1	12	2	47;[S] 1, 1670;[N] 6.6, NA[DF]	8.2[S] 5.5[DN] 5.5[DF]	1.64[S] 40[DN] NA[DF]	0.58[S] 6[DN] NA[DF]

Table F-6. Measured Values of R and Calculated Values of K_d for Np(V) in Intact Culebra Cores (SNL Column Transport Study) (continued).

Run #	Solid (core)	Brine	Flow rate (ml/ min)	Run Time (days)	Ef-fluent Vol. (L)	R	Poro-sity	K_d (ml/g)	Range (±ml/ g)
D-4	VPX-25-8A	AIS.	0.1	13	2	39;[S] 1, 340;[DN] 17.5, 154[DF]	10.0[S]	1.65[S]	0.22[S]
							4.8[DN]	7.1[DN]	4.2[DN]
							4.8[DF]	0.34[DF]	0.07[DF]

AIS: AISinR.
DF: dual porosity and fracture retardation assumed.
DN: dual porosity and no fracture retardation assumed.
ER.-6: ERDA-6.
NA: not available yet.
S: single porosity assumed.

Table F-7. Measured Values of R and Calculated Values of K_d for Np(V) in Intact Culebra Cores (SNL Column Transport Study). Data current as of March 30, 1996. Table compiled by L. H. Brush on March 30, 1996, based on memo by D. A. Lucero, G. O. Brown, and K. G. Budge dated March 28, 1996. Table checked by Brush on March 31, 1996. Table revised by Brush on April 6, 1996, based on memo by Lucero and Brown dated April 5, 1996. Table checked by Y. Behl on April 8, 1996.

Run #	Solid (core)	Brine	Flow rate (ml/min)	Run Time (days)	Effluent Vol. (L)	R	Porosity	K_d (ml/g)	Range (±ml/g)
C-6	VPX-28-6C	AIS.	0.1	13	2	59^S	4.5^S	1.1^S	NA
C-7	VPX-28-6C	ER.-6	0.1	13	2	120^S	3.9^S	2.0^S	NA
D-2	VPX-25-8A	AIS.	0.1	12	2	47^S	8.2^S	1.6^S	NA
D-4	VPX-25-8A	AIS.	0.1	13	2	39^S	10.0^S	1.6^S	NA

AIS: AISinR.
ER.-6: ERDA-6.
NA: not available yet.
S: single porosity assumed.

APPENDIX G: EFFECTS OF ORGANIC LIGANDS ON RANGES AND PROBABILITY DISTRIBUTIONS OF MATRIX K_ds FOR Pu(V), Am(III), U(VI), Th(IV), Np(V), AND DOLOMITE-RICH CULEBRA ROCK

Triay and her group at LANL carried out two sets of experiments on the effects of four organic ligands (acetate, citrate, ethylenediaminetetraacetic acid or EDTA, and lactate) on the K_ds for dissolved Pu(V), Am(III), U(VI), Th(IV), and Np(V) under conditions expected in the Culebra. Brush (1990) concluded that these and six other organic and two inorganic ligands could affect the solubilities of the actinide elements in TRU waste. Therefore, he estimated the concentrations of these 12 ligands in three quantities of brine that could resaturate WIPP disposal rooms after filling and sealing. Since 1990, the ASTP has reduced the number of organic ligands of concern from twelve to four (acetate, citrate, EDTA, and oxalate). Triay carried out experiments with acetate, citrate, EDTA, and lactate because the ASTP had not eliminated lactate from consideration yet, and because Triay concluded that oxalate would be extremely insoluble given the dissolved Ca concentrations expected in WIPP brines. Triay conducted the first set of runs with ERDA-6 and H17, and acetate, citrate, EDTA, and lactate all present at concentrations as close as possible to the "minimum" and "maximum" concentrations estimated by Brush (1990) (see Table G-1 below). Soon after Triay started their preliminary experiments, Weiner (1996) used the quantities of acetate, citrate, EDTA, and oxalate in TRU waste estimated by Drez (1996) to predict the concentrations of these organic ligands in brines in the repository (Table G-1).

Tables G-2, G-3, G-4, G-5, and G-6 give the results of the preliminary experiments with ERDA-6 and H-17, and Pu(V), Am(III), U(VI), Th(IV), and Np(V), respectively. At low concentrations, acetate, citrate, EDTA, and lactate have little or no effect on the K_ds for these elements (compare the results for "low-concentration organics" to those for "none," the runs without any organic ligands present.) In fact, for Pu(V) and ERDA-6 in contact with ambient atmospheric or (about 0.033%) CO_2; Am(III), ERDA-6, and 0.033% CO_2; and U(VI), ERDA-6, and 0.033% CO_2, low concentrations of these organic ligands actually *increase* the K_ds relative to those obtained without any organic ligands. However, at high concentrations, these organic ligands significantly *decrease* the K_ds for all of these elements. Note that the low and the high concentrations of acetate, citrate, and EDTA used in these preliminary runs bracket the predicted concentrations of these organic ligands (Table G-1).

Triay used ERDA-6 and H-17, which contain 19 and 74.1 mM Mg, respectively, for this set of experiments. However, ASTP personnel have predicted the effects of acetate, citrate, EDTA, and oxalate on the solubilities of the actinide elements by assuming that all of these organic ligands will dissolve in intergranular Salado brine as it accumulates in WIPP disposal rooms. Novak (1996) used FMT to predict that the Mg concentration in SPC brine (Brine A modified by omitting minor and trace constituents, and used by the ASTP to simulate Salado brine in several experimental and modeling studies) will be 454 mM after equilibration with halite, anhydrite, the actinide elements and the organic ligands in TRU waste, and an MgO backfill. This Mg concentration is significantly higher than that of ERDA-6 before or after equilibration with this backfill (19 and 48 mM, respectively) and significantly higher than that of H-17 (74.1 mM). Because we hoped that competition among Mg and Pu, Am, U, Th, and Np for the binding sites on these organic ligands

would mitigate the effects of these organics on the K_ds for these elements, Triay carried out an additional set of experiments with acetate, citrate, EDTA, and lactate at low, intermediate, and high concentrations (see Table G-1) and with Brine A modified to simulate the composition of Salado brine after equilibration with an MgO backfill.

Table G-7 shows the results of these experiments. Low concentrations of organics significantly decreased the K_ds for Th relative to those obtained without any organics, but had much less effect on the K_ds for the other elements. Intermediate concentrations of organics significantly decreased the K_ds for all of the elements except U(VI). High concentrations significantly decreased the K_ds for all five of these elements.

However, we *have not* revised the ranges and probability distributions of K_ds for Pu, Am, U, Th , and Np shown in Table 1 (see above) because large quantities of other metals (see below) will be present to form complexes with these organic ligands, thus preventing them from forming complexes with the actinide elements and decreasing the K_ds for the actinides in the Culebra. (These other metals will also prevent these organic ligands from increasing the solubilities of the actinide elements in WIPP disposal rooms.) These other metals include Fe, large quantities which will be present in WIPP disposal rooms in steel waste containers (drums and boxes) and as steels, stainless steels, and other Fe-base materials in the waste; Mg,, large quantities of which will be emplaced in the repository as an MgO backfill to remove microbially produced CO_2 (but will be present as $MgCO_3$ and/or $Mg(OH)_2$, and magnesium oxychloride after reaction with CO_2 and/or brine); and Cr, Mn, Ni, Pb, and V, which will be present in lesser but still sufficient quantities in steel drums and boxes, and in steels, stainless steels, and other Fe-base alloys in the waste, and in other waste constituents. Preliminary modeling of the equilibria among dissolved and solid-phase Pu and Am, Fe, Mg, and Ni, and EDTA imply that, under the conditions expected in WIPP disposal rooms, Ni would form complexes with 99.8% of the EDTA expected to be present in the repository, thus preventing it from complexing significant quantities of Pu and Am. A detailed description of these calculations, and any additional modeling or laboratory studies of these competitive equilibria, will appear elsewhere.

REFERENCES

Brush, L.H. 1990. *Test Plan for Laboratory and Modeling Studies of Repository and Radionuclide Chemistry for the Waste Isolation Pilot Plant.* SAND90-0266. Albuquerque, NM: Sandia National Laboratories.

Drez, P.E. 1996. "Final Preliminary Estimates of Complexing Agents in TRU Solidified Waste Forms Scheduled for Disposal in WIPP." Unpublished memorandum to J. Harvill, March 20, 1996. Albuquerque, NM: Drez Environmental Associates.

Novak, C.F., and R.C. Moore. 1996. "Estimates of Dissolved Concentrations for +III, +IV, +V, and +VI Actinides in a Salado and a Castile Brine under Anticipated Repository Conditions." Unpublished memorandum to M. D. Siegel, March 28, 1996. Albuquerque, NM: Sandia National Laboratories.

Weiner, R. 1996. "Dissolved Ligand Concentrations." Unpublished memorandum to C. F. Novak, March 27, 1996. Albuquerque, NM: Sandia National Laboratories.

Table G-1. Concentrations of Organic Ligands in Experiments with ERDA-6, H-17, and Modified Brine A, and Predicted Concentrations of Organic Ligands in Brines in WIPP Disposal Rooms. Table compiled by L. H. Brush on May 10, 1996, based on information provided by LANL on April 25, 1996. Table checked by L. J. Storz on May 17, 1996.

Organic Ligand	Low Conc. (ERDA-6 and H-17) (mM)	High Conc. (ERDA-6 and H-17) (mM)	Low Conc. (Modified Brine A) (mM)	Intermediate Conc. (Modified Brine A) (mM)	High Conc. (Modified Brine A) (mM)	Predicted Conc. in WIPP (mM)
Acetate	0.195 (ERDA-6)	19.5172 (ERDA-6)	0.489	4.89	48.9	1.062
	0.195 (H-17)	19.5172 (H-17)				
Citrate	0.0340 (ERDA-6)	3.4002 (ERDA-6)	0.03417	0.3417	3.417	0.465
	0.0340 (H-17	3.4002 (H-17				
EDTA	0.000146 (ERDA-6)	0.0146 (ERDA-6)	0.00011	0.0011	0.011	0.00416
	0.000146 (H-17)	0.0146 (H-17)				
Lactate	0.00761 (ERDA-6)	0.7610 (ERDA-6)	0.02088	0.2088	2.088	Not predicted
	0.00796 (H-17)	0.7956 (H-17)				
Oxalate	NU	NU	NU	NU	NU	7.404

NU: Not used because LANL expected Ca-oxalate to precipitate from these brines at very low oxalate concentrations.

Table G-2. Effects of Brine, Organic Ligands, and P_{CO2} on Matrix K_ds for Pu(V) and Dolomite-Rich Culebra Rock (LANL Empirical Sorption Study). One-week sorption runs with H-19, B-4, Box 7. K_ds in bold font excluded from ranges and distributions because of unacceptable differences between standards and controls. Still counting new controls for underlined samples. Data current as of May 30, 1996. Table compiled by L. H. Brush on May 16, 1996, based on information provided by LANL on May 15, 1996. Table checked by L. J. Storz on May 16 and 17, 1996. Table revised by Brush on May 31 and June 1, 1996, based on information provided by LANL on May 30 and 31, 1996. Table checked by L. J. Storz on June 10, 1996.

Brine	Additive	K_d, (ml/g), 0.033% CO_2	K_d (ml/g), 4.1% CO_2
ERDA-6	None	157, #JRF O-131	217, #JRF O-181
ERDA-6	None	158, #JRF O-132	223, #JRF O-182
ERDA-6	Avg. without organics	158	220
ERDA-6	Low-conc. organics	787, #JRF O-139	171, #JRF O-189
ERDA-6	Low-conc. organics	142, #JRF O-140	184, #JRF O-190
ERDA-6	Avg. w. low-conc. org.	464	178
ERDA-6	High-conc. organics	6.44, #JRF O-137	10.3, #JRF O-187
ERDA-6	High-conc. organics	7.48, #JRF O-138	9.10, #JRF O-188
ERDA-6	Avg. w. high-conc. org.	6.96	9.70

Table G-2. Effects of Brine, Organic Ligands, and P_{CO2} on Matrix K_ds for Pu(V) and Dolomite-Rich Culebra Rock (LANL Empirical Sorption Study) (continued).

Brine	Additive	K_d (ml/g), 0.033% CO_2	K_d (ml/g), 4.1% CO_2
H-17	None	18.4, #JRF O-31	8.51, #JRF O-81
H-17	None	19.8, #JRF O-32	9.19, #JRF O-82
H-17	Avg. without organics	19.1	8.85
H-17	Low-conc. organics	9.50, #JRF O-39	4.45, #JRF O-89
H-17	Low-conc. organics	17.0, #JRF O-40	7.73, #JRF O-90
H-17	Avg. w. low-conc. org.	13.2	6.14
H-17	High-conc. organics	1.39, #JRF O-37	0.315, #JRF O-87
H-17	High-conc. organics	0.934, #JRF O-38	0.515, #JRF O-88
H-17	Avg. w. high-conc. org.	1.16	0.415

Table G-3. Effects of Brine, Organic Ligands, and P_{CO2} on Matrix K_ds for Am(III) and Dolomite-Rich Culebra Rock (LANL Empirical Sorption Study). One-week sorption runs with H-19, B-4, Box 7. K_ds in bold font excluded from ranges and distributions because of unacceptable differences between standards and controls. Still counting new controls for underlined samples. Data current as of May 30, 1996. Table compiled by L. H. Brush on May 16, 1996, based on information provided by LANL on May 15, 1996. Table checked by L. J. Storz on May 16 and 17, 1996. Table revised by Brush on May 31 and June 1, 1996, based on information provided by LANL on May 30 and 31, 1996. Table checked by L. J. Storz on June 10, 1996.

Brine	Additive	K_d, (ml/g), 0.033% CO_2	K_d, (ml/g), 4.1% CO_2
ERDA-6	None	199, #JRF O-141	2.890, #JRF O-191
ERDA-6	None	1,220, #JRF O-142	2.160, #JRF O-192
ERDA-6	Avg. without organics	710	2.520
ERDA-6	Low-conc. organics	1,390 #JRF O-161	1,680, #JRF O-199
ERDA-6	Low-conc. organics	1,470, #JRF O-171	1,880, #JRF O-200
ERDA-6	Avg. w. low-conc. org.	1,430	1,780
ERDA-6	High-conc. organics	**10.6, #JRF O-147**	7.40, #JRF O-197
ERDA-6	High-conc. organics	**7.84, #JRF O-151**	5.05, #JRF O-198
ERDA-6	Avg. w. high-conc. org.	**9.22**	6.22

Table G-3. Effects of Brine, Organic Ligands, and P_{CO2} on Matrix K_ds for Am(III) and Dolomite-Rich Culebra Rock (LANL Empirical Sorption Study) (continued).

Brine	Additive	K_d (ml/g), 0.033% CO_2	K_d (ml/g), 4.1% CO_2
H-17	None	533, #JRF O-41	379, #JRF O-91
H-17	None	549, #JRF O-42	391, #JRF O-92
H-17	Avg. without organics	541	385
H-17	Low-conc. organics	503, #JRF O-49	311, #JRF O-99
H-17	Low-conc. organics	497, #JRF O-50	299, #JRF O-100
H-17	Avg. w. low-conc. org.	500	305
H-17	High-conc. organics	7.79, #JRF O-47	3.58, #JRF O-97
H-17	High-conc. organics	7.37, #JRF O-48	3.75, #JRF O-98
H-17	Avg. w. high-conc. org.	7.58	3.66

Table G-4. Effects of Brine, Organic Ligands, and P_{CO2} on Matrix K_ds for U(VI) and Dolomite-Rich Culebra Rock (LANL Empirical Sorption Study). One-week sorption runs with H19, B-4, Box 7. K_ds in bold font excluded from ranges and distributions because of unacceptable differences between standards and controls. Still counting new controls for underlined samples. Negative K_ds set to 0.00 before determining the mean. Data current as of May 30, 1996. Table compiled by L. H. Brush on May 16, 1996, based on information provided by LANL on May 15, 1996. Table checked by L. J. Storz on May 16 and 17, 1996. Table revised by Brush on May 31 and June 1, 1996, based on information provided by LANL on May 30 and 31, 1996. Table checked by L. J. Storz on June 10, 1996.

Brine	Additive	K_d, (ml/g), 0.033% CO_2	K_d, (ml/g), 4.1% CO_2
ERDA-6	None	-0.148, #JRF O-111	-0.296, #JRF O-159
ERDA-6	None	0.220, #JRF O-112	0.275, #JRF O-160
ERDA-6	Avg. without organics	0.110	0.138
ERDA-6	Low-conc. organics	1.83, #JRF O-119	-0.0367, #JRF O-168
ERDA-6	Low-conc. organics	-0.371, #JRF O-120	-0.933, #JRF O-169
ERDA-6	Avg. w. low-conc. org.	0.915	0.00
ERDA-6	High-conc. organics	-0.631, #JRF O-117	-0.475 #JRF O-166
ERDA-6	High-conc. organics	-0.638, #JRF O-118	-0.948, #JRF O-167
ERDA-6	Avg. w. high-conc. org.	0.000	0.00

Table G-4. Effects of Brine, Organic Ligands, and P_{CO2} on Matrix K_ds for U(VI) and Dolomite-Rich Culebra Rock (LANL Empirical Sorption Study) (continued).

Brine	Additive	K_d (ml/g), 0.033% CO_2	K_d (ml/g), 4.1% CO_2
H-17	None	-2.11, #JRF O-11	-1.69, #JRF O-61
H-17	None	-1.79, #JRF O-12	-0.323, #JRF O-62
H-17	Avg. without organics	0.00	0.00
H-17	Low-conc. organics	-1.27, #JRF O-19	-0.601, #JRF O-69
H-17	Low-conc. organics	-1.67, #JRF O-20	-1.44, #JRF O-70
H-17	Avg. w. low-conc. org.	0.00	0.00
H-17	High-conc. organics	-1.77, #JRF O-17	-1.81, #JRF O-67
H-17	High-conc. organics	-1.51, #JRF O-18	-1.67, #JRF O-68
H-17	Avg. w. high-conc. org.	0.00	0.00

Table G-5. Effects of Brine, Organic Ligands, and P_{CO2} on Matrix K_ds for Th(IV) and Dolomite-Rich Culebra Rock (LANL Empirical Sorption Study). One-week sorption runs with H-19, B-4, Box 7. K_ds in bold font excluded from ranges and distributions because of unacceptable differences between standards and controls. Still counting new controls for underlined samples. Data current as of May 30, 1996. Table compiled by L. H. Brush on May 16, 1996, based on information provided by LANL on May 16, 1996. Table checked by L. J. Storz on May 16 and 17, 1996. Table revised by Brush on May 31 and June 1, 1996, based on information provided by LANL on May 30 and 31, 1996. Table checked by L. J. Storz on June 10, 1996.

Brine	Additive	K_d, (ml/g), 0.033% CO_2	K_d, (ml/g), 4.1% CO_2
ERDA-6	None	120, #JRF O-101	153, #JRF O-148
ERDA-6	None	98.6, #JRF O-102	169, #JRF O-149
ERDA-6	Avg. without organics	109	161
ERDA-6	Low-conc. organics	101, #JRF O-109	157, #JRF O-157
ERDA-6	Low-conc. organics	99.9, #JRF O-110	166, #JRF O-158
ERDA-6	Avg. w. low-conc. org.	100	162
ERDA-6	High-conc. organics	30.0, #JRF O-107	55.0, #JRF O-155
ERDA-6	High-conc. organics	32.8, #JRF O-108	63.2, #JRF O-156
ERDA-6	Avg. w. high-conc. org.	31.4	59.1

Table G-5. Effects of Brine, Organic Ligands, and P_{CO2} on Matrix K_ds for Th(IV) and Dolomite-Rich Culebra Rock (LANL Empirical Sorption Study) (continued).

Brine	Additive	K_d (ml/g), 0.033% CO_2	K_d (ml/g), 4.1% CO_2
H-17	None	15.0, #JRF O-1	12.0, #JRF O-51
H-17	None	16.6, #JRF O-2	11.3, #JRF O-52
H-17	Avg. without organics	15.8	11.6
H-17	Low-conc. organics	13.8, #JRF O-9	9.72, #JRF O-59
H-17	Low-conc. organics	14.4, #JRF O-10	9.20, #JRF O-60
H-17	Avg. w. low-conc. org.	14.1	9.46
H-17	High-conc. organics	5.72, #JRF O-7	0.874, #JRF O-57
H-17	High-conc. organics	8.04, #JRF O-8	1.06, #JRF O-58
H-17	Avg. w. high-conc. org.	6.88	0.967

Table G-6. Effects of Brine, Organic Ligands, and P_{CO2} on Matrix K_ds for Np(V) and Dolomite-Rich Culebra Rock (LANL Empirical Sorption Study). One-week sorption runs with H-19, B-4, Box 7. K_ds in bold font excluded from ranges and distributions because of unacceptable differences between standards and controls. Still counting new controls for underlined samples. Data current as of May 30, 1996. Table compiled by L. H. Brush on May 16, 1996, based on information provided by LANL on May 15, 1996. Table checked by L. J. Storz on May 16 and 17, 1996. Table revised by Brush on May 31 and June 1, 1996, based on information provided by LANL on May 30 and 31, 1996. Table checked by L. J. Storz on June 10, 1996.

Brine	Additive	K_d, (ml/g), 0.033% CO_2	K_d, (ml/g), 4.1% CO_2
ERDA-6	None	96.5, #JRF O-121	136. #JRF O-170
ERDA-6	None	87.6, #JRF O-122	148. #JRF O-172
ERDA-6	Avg. without organics	92.0	142
ERDA-6	Low-conc. organics	83.6. #JRF O-129	175. #JRF O-179
ERDA-6	Low-conc. organics	79.1. #JRF O-130	147. #JRF O-180
ERDA-6	Avg. w. low-conc. org.	81.4	161
ERDA-6	High-conc. organics	63.9. #JRF O-127	131. #JRF O-177
ERDA-6	High-conc. organics	63.3. #JRF O-128	113. #JRF O-178
ERDA-6	Avg. w. high-conc. org.	63.6	122

Table G-6. Effects of Brine, Organic Ligands, and P_{CO2} on Matrix K_ds for Np(V) and Dolomite-Culebra Rock (LANL Empirical Sorption Study) (continued).

Brine	Additive	K_d (ml/g), 0.033% CO_2	K_d (ml/g), 4.1% CO_2
H-17	None	5.17, #JRF O-21	0.905, #JRF O-71
H-17	None	4.37, #JRF O-22	1.06, #JRF O-72
H-17	Avg. without organics	4.77	0.983
H-17	Low-conc. organics	4.86, #JRF O-29	1.33, #JRF O-79
H-17	Low-conc. organics	4.44, #JRF O-30	0.694, #JRF O-80
H-17	Avg. w. low-conc. org.	4.65	1.01
H-17	High-conc. organics	1.45, #JRF O-27	-0.236, #JRF O-77
H-17	High-conc. organics	1.67, #JRF O-28	-0.433, #JRF O-78
H-17	Avg. w. high-conc. org.	1.56	0.00

Table G-7. Effects of Organic Ligands on Matrix K_ds (ml/g) for Pu(V), Am(III), U(VI), Th(IV), and Np(V), Dolomite-Rich Culebra Rock, and Modified Brine A (LANL Empirical Sorption Study). One-week sorption runs with H-19, B-4, Box 7. K_ds in bold font excluded from ranges and distributions because of unacceptable differences between standards and controls. Data current as of May 30, 1996. Table compiled by L. H. Brush on May 16, 1996, based on information provided by LANL on May 15, 1996. Table checked by L. J. Storz on May 16, 1996. Table revised by Brush on May 31, 1996, based on information provided by LANL on May 30, 1996. Table checked by L. J. Storz on June 10, 1996.

	Element and Oxidation State				
Additive	Pu(V)	Am(III)	U(VI)	Th(IV)	Np(V)
None	8.73, #JRF-233	528, #JRF-243	19.3, #JRF-213	11,300, #JRF-203	22.7, #JRF-223
None	10.1, #JRF-234	501, #JRF-244	19.1, #JRF-214	10,700, #JRF-204	17.1, #JRF-224
Avg. without organics	9.42	514	19.2	11,000	19.9
Low-conc. organics	7.69, #JRF-239	355, #JRF-249	12.4, #JRF-219	1.70, #JRF-209	11.9, #JRF-229
Low-conc. organics	8.84, #JRF-240	325, #JRF-250	17.2, #JRF-220	6.47, #JRF-210	10.5, #JRF-230
Avg. w. low-conc. organics	8.26	340	14.8	4.08	11.2
Intermed.-conc. organics	5.03, #JRF-237	67.6, #JRF-247	16.6, #JRF-217	1.05, #JRF-207	6.25, #JRF-227
Intermed.-conc. organics	5.06, #JRF-238	36.7, #JRF-248	16.8, #JRF-218	6.29, #JRF-208	5.89, #JRF-228
Avg. w. inter.-conc. org.	5.04	52.2	16.7	3.67	6.07

Table G-7. Effects of Organic Ligands on Matrix K_ds (ml/g) for Pu(V), Am(III), U(VI), Th(IV), and Np(V), Dolomite-Rich Culebra Rock, and Modified Brine A (LANL Empirical Sorption Study) (continued).

	Element and Oxidation State				
Additive	Pu(V)	Am(III)	U(VI)	Th(IV)	Np(V)
High-conc. organics	2.55, #JRF-235	2.34, #JRF-245	10.1, #JRF-215	0.469, #JRF-205	1.93, #JRF-225
High-conc. organics	2.22, #JRF-236	2.05, #JRF-246	8.01, #JRF-216	0.467, #JRF-206	2.49, #JRF-226
Avg. w. high-conc. org.	2.38	2.20	9.06	0.468	2.21

Sandia National Laboratories

P. O. Box 5800
Albuquerque, New Mexico 87185-1320

Managed by Sandia Corporation
a Lockheed Martin Company

WBS: 1.1.10.3.4

date: 9 June, 1997

to: D. Lucero MS-1320 (6832)

Malcolm Siegel for CC Craft

INFORMATION ONLY

from: C. C. Craft, M. D. Siegel, MS-1320 (6832)

subject: Additional calculations of solubility-limited concentrations of actinides for injection spikes used in WIPP core column experiments at Sandia National Laboratories

Summary

Calculations have been previously carried out to evaluate the possibility that precipitation of neptunium, americium, or thorium had occurred in either the VPX series or ERDA-6 WIPP core column experiments at Sandia National Laboratories (Siegel, 1996a). This memo summarizes a second round of solubility calculations using the most recent, QA-approved version of the FMT code (version 2.3, "FMT_PA97.EXE") on the VAX Alpha machines. The calculations corroborate the conclusions of the previous calculations: it is likely that the initial concentrations of Am in VPX-28 water exceeded the solubility of $AmOHCO_3$ solid. Initial concentrations of Np and Th in the columns in ERDA-6 and VPX-28 were below the solubility limits of their respective stable solids. The calculations also suggest that the compositions of the solutions used in the core column experiments were slightly different than those measured in the field. The calculations suggest that under atmospheric conditions, the recipes used to mix the brines correspond to solutions that would be supersaturated with respect to calcite. However, it is unlikely that these compositional differences will affect the solubilities of the actinides significantly.

Method of Calculation

The recipes corresponding to salts used in synthesis of the brine simulants are shown in Table 1a. The data tables supplied by you are attached as Appendix A. The recipes used for the VPX-28 and ERDA-6 brines may be supersaturated with respect to dolomite under atmospheric conditions; therefore, the solubilities both with and without dolomite equilibrium were calculated. In cases where

dolomite in the mass balance and mass action calculations was not included, magnesite was also omitted. In FMT calculations, constant CO_2 partial pressure is represented by a condition in which excess "solid" CO_2 with a specific dimensionless chemical potential is present. For atmospheric pCO_2 the appropriate value of -167.151 is input for the CO_2 solid in the thermodynamic database (CHEMDAT file) called by the code. Details of the method of calculations for each water are given below.

In these calculations, the most recent version of the FMT database file (FMT_970407.CHEMDAT) was used after modifications to include constant CO_2 fugacity and excess radionuclide solids as described below. (Note that the identification of "active " solids is found in the CHEMDAT files and may not always agree with the comments in the INGUESS files).

When the above assumptions concerning CO_2 fugacity and stable solids are used in FMT calculations, the calculated equilibrium composition differ slightly from the salt recipes used to initially define the solutions. These differences are due to calculated precipitation or dissolution that changes the amount of calcium and carbonate in solution. The compositions of the final "stable" solutions according to the FMT calculations are compared to the field "or targeted" compositions in Table 1b.

Castile Waters: ERDA-6

The calculations were carried out in 4 steps:

1) BATCH calculation of brine speciation with the "nMOLES, nEXACT" flag and a fixed total CO_2 in the absence of radionuclides. The assumed salt concentrations for ERDA-6 are listed in Appendix A and are converted to molar concentrations in the attached Excel file SOLDAT2.xls (sheet "recipe"). (The calculated molar concentrations also can be found in the *.inguess files for each system). This calculation produces a produces an FMT *.for88 file.
2) A series of calculations wascarried out next to correct for the fact that although the initial input values were molar concentrations, FMT accepts them as if they were molal concentrations. To correct for this, the *.for88 file was renamed to *.inguess, and a series of BATCH calculations were carried out with the "MOLES, EXACT" flag. In these calculations, the H_2O value was adjusted downward in the *.inguess file until the molar concentration value for Cl^- in the FMT.OUT file was equivalent to that found in Table 1b.
3) Calculation of brine speciation at fixed partial pressure of CO_2 in the absence of radionuclides (this is accomplished by renaming the FMT *.for88 file to a *.inguess file and specifying 10 moles of solid CO_2 in the file; this produces a second *.for88 file from a BATCH run.
4) Calculation of brine speciation at fixed partial pressure of CO_2 with an excess amount of radioelement. This is accomplished by renaming the *.for88 file to a *.inguess file, and specifying the concentrations of the solids $Am(OH)_3$, NpO_2OH and $ThO_2(am)$ to be 1 molar in a BATCH run.

The sums of the molar concentrations of the aqueous radionuclide species are reported as the solubility-limited radioelement concentrations in Table 2. The stable solid and the calculated pmH values in equilibrium with atmospheric CO_2 are also listed.

Culebra waters VPX-28

Calculations for VPX-28 were carried out in a different way:

1. A BATCH run for pure water was used to create a *.for88 file.
2. The *for88 files were renamed *.inguess files and these files were edited by specifying the molar amounts of salts listed in Table 1a above.
3. Further BATCH runs were made using the "MOLES,EXACT" flag, in which the H_2O was again adjusted to convert molarity to molality, but this time, the molar Br^- concentration in Table 1a was used as a reference.
4. The next two steps were the same as steps 3 and 4 in the calculations for ERDA-6 brine:

- Calculation of brine speciation at fixed partial pressure of CO_2 in the absence of radionuclides (this is accomplished by renaming the FMT *.for88 file to a *.inguess file and specifying 10 moles of solid CO_2 in the file; this produces a second *.for88 file from a BATCH run.
- Calculation of brine speciation at fixed partial pressure of CO_2 with an excess amount of radioelement (accomplished by renaming the *.for88 file to a *.inguess file, specifying the concentrations of the solids $Am(OH)_3$, NpO_2OH and ThO_2(am) to be 1 molar in a BATCH run.)

Results and Discussion

Solubility-limiting concentrations of radionuclides in VPX-28 and ERDA-6 brines

The results of the calculations are summarized in Table 2. Output (and input) files for the BATCH runs are included on a disk that was submitted with this document to the WIPP Central Files. The 10 subdirectory names found there reflect the brines (ERDA-6 or VPX-28), the actinides (Am, Th, or Np), and the chemical conditions (dolomite present or absent) considered. Each subdirectory contains: 1) a ccc.com file which names the VAX files used in the calculation for that system, 2) a ccc.in file which describes the initial system in terms of total element concentrations, 3) a ccc.ing (inguess file) file which describes the input for the final radionuclide speciation calculation; 4) a ccc.for file which contains the tabulated results in the *.for88 file format, and 5) a ccc.out file which contains the results in the *.out format. For more description of the output file format, please refer to the Users Guide for the FMT code (Novak and Babb, 1995). The file SOLDAT2.xls tabulates the detailed speciation for each of the 10 systems examined. These Excel workbook sheets were prepared by importing text from the ccc.out files from each subdirectory on the diskette.

The calculations corroborate the conclusions of previous calculations: it is likely that the initial concentrations of Am in VPX-28 water exceeded the solubility of $AmOHCO_3$ solid. Initial concentrations of Np and Th in the columns in ERDA-6 and VPX-28 were below the solubility limits of their respective stable solids.

Uncertainty in brine compositions

Several sources of error in our predictions of solubilities are related to the solution compositions assumed in the calculations. Foremost among these is the lack of reliable measurements of the in-situ pmH or f_{CO2} in the core column experiments. The results of the calculations of the solubilities and the pmH presented in this memo are valid only for systems in which equilibrium is established between atmospheric CO_2 and CO_2 in the pore water. Secondly, as mentioned above, these calculations suggest that the compositions of the solutions used in the core column experiments were slightly different than those measured in the field. It is likely that under atmospheric conditions, the recipes used to mix the brines correspond to solutions that would not be in equilibrium with calcite. In the case of ERDA-6 water, the calculations predict that some CO_2 is lost from the solution during equilibration with the atmosphere. Finally, the "trial and error" procedure described above that was used to convert molarity to molality in these calculations may introduce some error into the results.

As noted above, the compositions of the final "stable" solutions according to the FMT calculations are compared to the field or "targeted" compositions in Table 1b. The differences in compositions are consistent with observations that the compositions of the brines as measured by ICP differed from those predicted from the salt recipe used to prepare the brines (J. Kelly, personal communication), suggesting that some precipitation from VPX-28 may have occurred in the laboratory. The differences are within the observed uncertainty in ICP measurements for brines and similar to the compositional differences among the VPX series brines sampled in the Air Intake Shaft (Table 3, Lucero et al., 1995). It is unlikely that these compositional differences will affect the solubilities of the actinides significantly. However, these calculations do indicate that the composition and stability of brines used in any future diffusion or column experiments should be examined after they have been pre-equilibrated with crushed dolomite.

This memo was reviewed by R. Moore.

References:

Lucero, D. A., F. Geldbard, Y. K. Behl and J. A. Romero, 1995. *Test Plan for Laboratory Column Experiments for Radionuclide Adsorption Studies of the Culebra Dolomite Member of the Rustler Formation at the WIPP Site, TP 95-03,* Sandia National Laboratories, Albuquerque, NM.

Novak, C. F. and Babb, S. C., 1995. *FMT Chemical Aqueous Solubility Calculations: User Guide and Reference Manual, Version 2.0,* Draft WIPP Document, December 27, 1995, Sandia National Laboratories, Albuquerque, NM.

Siegel, M. D., *Initial Calculations of Solubility-Limited Concentrations and Saturation States of Radioelement Solids for Injection Spikes Used in WIPP Core Column Experiments at Sandia National Laboratories,* memo to L. Brush, July 1, 1996

Enclosures

Table 1. Brine compositions assumed for solubility calculations
- a. Brine recipes in terms of salts
- b. Compositions of the final "stable" solutions according to the FMT calculations compared to the field or "targeted" compositions

Table 2. Solubility-limited concentrations (molarity) for column experiments

Appendix A. Copies of salt recipes supplied by Dan Lucero
Appendix B. List of files found on diskette included in records package.

Distribution w/enc and diskettes.
SWCF-A: WBS 1.1.10.3.4; TD:QA: Core Column Tests: Actinide Solubilities

Distribution w/enc and w/o diskettes.
MS-1320 G. W. Perkins 6831

Distribution w/o enc.
MS-1320 E. J. Nowak 6831
MS-1341 J. T. Holmes 6832
MS-1341 S. Miller 6811

Table 1a. Brine recipes in terms of salts

Compound	ERDA-6 (g/L)	VPX-28 (g/L)	Molecular Weight (g)
NaCl	261.64	29.34	58.44
Na_2SO_4	23.70	7.910	142.04
$Na_2B_4O_7 \bullet 10H_2O$	6.00	0	381.39
NaBr	1.13	0.02794	102.91
KCl	7.23	0	74.55
$MoCl_2 \bullet 6H_2O$	3.86	0	203.3
$CaCl_2 \bullet 2H_2O$	1.762	3.063	146.98
$NaHCO_3$	1.34	0.08392	84.007
$MgSO_4$	0	2.094	120.38
$Na_2B_4O_7$	0	0.1275	201.22
K_2SO_4	0	0.7063	174.27

Table 1b. Compositions of the "stable" solutions according to the FMT calculations compared to the field or "target" compositions (g/L)

Element	VPX-28 "FMT stable"*	VPX-28 "target"	ERDA-6 "FMT stable"*	ERDA-6 "target"
Na	14.176	14.161	114.3504	111.942
Cl	19.261	19.277	167.9309	164.360
SO4	7.654	7.410	16.37965	16.028
K	0.317	0.317	3.869851	3.792
Br	0.022	0.022	0.897122	0.877
C	0.007	0.012	0.018612	0.192
Mg	0.478	0.423	0.471137	0.462
Ca	0.786	0.835	0.049798	0.480
pH	7.87	8.09	8.17	6.17

*no dolomite or magnesite precipitation

Table 2. Solubility-limited concentrations (molarity) for column experiments; $\log pCO_2 = -3.5$

Brine	Element	total tracer concentration (Molar)	Without dolomite equilibrium		With dolomite equilibrium		Solid Phase
			calculated pmH*	solubility	calculated pmH*	solubility	
VPX-28	Am	3.38E-07	7.73	6.46E-09	7.64	9.63E-09	$AmOHCO_3$
ERDA-6/10	Np	6.48E-10	8.71	4.17E-07	8.23	9.51E-07	$KNpO_2CO_3(s)$
VPX-28	Np	4.21E-10	7.72	7.84E-06	7.64	1.10E-05	$KNpO_2CO_3(s)$
ERDA-6/10	Th	2.82E-10	8.72	3.98E-07	8.23	1.21E-07	ThO_2 (amorphous)
VPX-28	Th	2.67E-8	7.73	1.90E-07	7.64	1.57E-07	ThO_2 (amorphous)

* rounded to 3 significant figures.

Appendix A. Copies of salt recipes supplied by Dan Lucero

ERDA-6 BRINE

Two Liter Batch Preparation

1. Addition of Components:

Lot. No.	Salt	Lot No. (500g)	Mass (g)/2L	(10L) Desired wt (g)	Actual wt (g)
751450	$NaCl$ *	947724	523.28	2,616.4	2,616.4001
751628	Na_2SO_4 *		47.40	237	237.0004
51183	$Na_2B_4O_7 \cdot 10H_2O$		12.00	60	60.0000
25252	$NaHCO_3$		2.68	13.4	13.4001
53458	$NaBr$ *		2.26	11.3	11.2999
130280	KCl *		14.46	72.3	72.3000
942062	$MgCl_2 \cdot 6H_2O$		7.72	38.6	38.6016
941925	$CaCl_2$ (anh) $\cdot 2H_2O$		~~2.66~~ 3.5235	17.6175	17.6182

2. pH Adjustment: Adjust pH using 10% HCl to pH 6.17, measured with a combination glass electrode.

3. Filtration: Filter solution through a medium glass frit filter.

4. Notes:

Add about 500 mL of deionized water to a 2 L volumetric flask. Using a magnetic stirrer, allow each component to dissolve before adding next. Keep flask stoppered between additions. No heating is necessary.

Dilute to 2 L after pH adjustment.

* Chemical is dried in a 110°C oven overnight

Lori R. Montano 10/30 10/31/95 10/31/95

ERDA-6 BRINE

Two Liter Batch Preparation

1. Addition of Components:

Lot. No.	Salt	Lot No. (500g)	Mass (g)/2L	Desired wt (g) (10L)	Actual wt (g)
751450	$NaCl$*	947724	523.28	2,616.4	2,616.4001
751628	Na_2SO_4*		47.40	237	237.0004
51183	$Na_2B_4O_7 \cdot 10H_2O$		12.00	60	60.0000
25252	$NaHCO_3$		2.68	13.4	13.4001
53458	$NaBr$*		2.26	11.3	11.2999
30280	KCl*		14.46	72.3	72.3000
42062	$MgCl_2 \cdot 6H_2O$		7.72	38.6	38.6016
141925	$CaCl_2$ (~~anh~~)$\cdot 2H_2O$		~~2.66~~ 3.5235	17.6175	17.6182

2. pH Adjustment: Adjust pH using 10% HCl to pH 6.17, measured with a combination glass electrode.

3. Filtration: Filter solution through a medium glass frit filter.

4. Notes:

Add about 500 mL of deionized water to a 2 L volumetric flask. Using a magnetic stirrer, allow each component to dissolve before adding next. Keep flask stoppered between additions. No heating is necessary.

Dilute to 2 L after pH adjustment.

* Chemical is dried in a 110°C oven overnight

Lori R. Montano 10/30 10/31/95 10/31/95

Appendix B. List of directories and files found on diskette included in records package.

This diskette contains input and out files for FMT calculations of solubility of Am, Np and Th solids in VPX-28 and ERDA6 brines. Each subdirectory at the lowest level contains input files: (cc.com, ccc.in, ccc.ing) and output files (ccc.f88 or .ccc.out files).

Directories:

e6Npdno
e6Npdol
e6Thdno
e6Thdol
Vpamdno
Vpamdol
VpNpdno
VpNpdol
VpThdno
VpThdol

Files:
soldat2.xls

Sandia National Laboratories

Albuquerque, New Mexico 87185

date: February 3, 1997

to: George Perkins, 6832, MS1320

from: Dan Lucero, 6832, MS1320

INFORMATION ONLY

subject: Memo of Record for Column Effluent Times

Test	Start/End	Cum Time	Time (sec)	Tracer	Flowrate
C-3	Start 7/10/95			Am, Pu	0.1 ml/min
*	End 4/9/96	269 days	2.3e07 s		0.1 ml/min
**	Restart 6/4/96				0.05 ml/min
In Process	2/4/97	241 days	2.1e07 s		0.05 ml/min
D-3	Start 9/28/95			Am, Pu	0.1 ml/min
	End 1/30/96	125 days	1.1e07 s		
D-6	Start 1/30/96				0.05 ml/min
	End 3/19/96	48 days	4.1e06 s		
	Start 3/19/96				0.1 ml/min
*	End 4/9/96	21 days	1.8e06 s		
**	Restart 6/4/96				0.05 ml/min
In Process	2/4/97	241 days	2.1e07 s		
E-2	Start 1/16/96			Am, Pu	0.1 ml/min
	End 4/9/96	83 days	7.2e06 s		
	Restart 6/4/96				0.05 ml/min
Post Test	End 7/15/96	41 days	3.5e06 s		

* Test suspended per memo from L. Brush

** Test restarted per verbal instructions from J. Nowak

cc: Glen Brown, OSU
John Holmes, 6832, MS1341
SWCF-A:1.1.10.3.4,1.1.5.1.5:Effluent memo of record;QA;

WP08760

Sandia National Laboratories

Albuquerque, New Mexico 87185

date 13 August 1993

to Fred Gelbard, 6119

from Stephen Yeh
Stephen Yeh, 6119

INFORMATION ONLY

subject: Revised Viscosity Measurements of Culebra Brines

Enclosed is my revised report titled "Determination of the Viscosity of Synthetic Culebra Brines in the Temperature Range of 20°C to 30°C." The revision results in only a very small change to the viscosities.

Copy to:
6115 R. Beauheim
6115 S. Webb
6119 D. Lucero
6119 H. Papenguth
6119 K. Robinson
6119 J.A. Romero
6119 File 3.2
6303 SWCF/WBS 1.1.5.1.5 RWC/SOW SYC 9/1/93

DETERMINATION OF THE VISCOSITY OF SYNTHETIC CULEBRA BRINES IN THE TEMPERATURE RANGE OF 20°C TO 30°C

Stephen Yeh
Department 6119
Sandia National Laboratories
Revised August 1993

ABSTRACT

Experimentally determined values for two synthetic Culebra brines (one based on the composition of VPX26E brine, one based on average compositions of VPX26A, -B, -C, -D, and -E brines -- see Appendix for Analytical Report on brine compositions) show that the viscosity of the brines are very close to predetermined values for a sodium chloride solution of comparable concentration (about 4% salinity). In a temperature range of 20°C to 30°C, the values vary from 1.079 cP ± 0.0027 cP to 0.8610 cP ± .0037 cP for synthetic Culebra brine 1 and 1.106 cP ± 0.0035 cP to 0.8857 cP ± 0.0009 cP for synthetic Culebra brine 2.

INTRODUCTION

The viscosity of synthetic Culebra brine 1 (mixed 2/15/93) was determined experimentally at two degree (Celsius) increments on 6/14-16/93. The composition of "synthetic Culebra brine 1" -- see Table 5 -- used an old, incorrect recipe based on VPX26E brine composition; a new recipe based on the average compositions of VPX26A, -B, -C, -D, and -E was developed and tested as "synthetic Culebra brine 2". The viscosity of synthetic Culebra brine 2 (mixed 5/3/93) was also determined at two degree increments on 6/28-30/93. New calibrated Cannon-Fenske viscometers (No. U383/50 for brine 1 and No. U513/50 for brine 2) were used in conjunction with a Jupiter Viscosity Timer Model 821 and a PolyScience 730 Immersion Circulator constant temperature bath. Deionized Ultra Filtered water from Fisher Scientific Co. was used for checking the viscosity. The calibration certificates for applicable instruments and a list of equipment and manufacturers are given in the Appendices.

EXPERIMENT

The viscometer is initially rinsed with deionized water by filling the bulb with about 6.7 or 6.8 mL of liquid (depending on charge volume specified by manufacturer) and drawing it through and up into the capillary a few times. The water is then poured out and a fresh charge of deionized water is added. The viscometer is inserted vertically in the self-aligning holder in the constant temperature bath (initially set at 20°C) and left for about ten

minutes to allow the liquid inside to equilibrate. The temperature in the bath is monitored by a calibrated thermocouple. (See Appendix for calibration certificate).

To check the viscometer, the meniscus of the water is allowed to flow freely past two marked points. Light timers that are activated by the refraction change as the meniscus passes the sensor are mounted across the markings. The elapsed, or efflux, time is recorded. To convert the efflux time to viscosity in centipoise, it is multiplied by the viscometer constant (supplied and verified by the manufacturer -- constants are given for 40°C and 100°C and are extrapolated for the desired temperatures) and then multiplied by the density of the liquid being tested. In the case of the deionized water check, the densities at varying temperatures were taken from the Handbook of Chemistry and Physics (Weast, 1990, page F-4). About five runs are made and recorded.

If the determined viscosity values for the deionized water agree within a couple percent of the tabulated viscosities (from Weast, 1990, page F-40) then the brine can now be tested. The same rinsing procedure used with deionized water is used with brine (i.e. 6.7 or 6.8 mL drawn in, rinsed, poured out and refilled). Again the viscometer is allowed to reach testing temperature and then flow times are recorded. Ten runs are made at each temperature.

Following the brine test-runs, deionized water is used again (same procedure for rinsing, etc.) and values compared to previous values to check for large discrepancies or errors such as brine precipitation and blockage of the viscometer capillary. Again, about five time values are recorded. Once assured there are no significant discrepancies, the water bath is raised two degrees Centigrade, and the above procedure is repeated.

Brine densities are recorded at various temperatures (about 20°C to 30°C) using a Mettler Portable Density/Specific Gravity Meter model DA-110. The meter is checked with deionized water and densities verified to be accurate to three decimal places.

RESULTS

Table 1 shows a summary of the data for brine 1. Table 2 shows a summary of the data for brine 2. Given are averages of the individual times and temperatures (not reprinted here), one standard deviation, two standard deviations, densities, number of points or readings, and calculated viscosities and errors.

Errors refer only to the viscosity calculations and were calculated as follows: For the deionized water checks, percent error is relative to tabulated book values from the Handbook of Chemistry and Physics. For the standard deviations, errors reflect what percent of the average viscosity the deviation is (i.e. deviation divided by average viscosity multiplied by 100% = error). Temperature standard deviations indicate temperature fluctuations or error over time, not actual thermocouple calibration error.

Tables 3 and 4 briefly summarize the determined viscosities

and densities and their respective temperatures for brines 1 and 2.

Table 5 gives the composition of synthetic Culebra brine 1 followed by the composition of synthetic Culebra brine 2.

Five graphs follow. The first four graphs show how the viscosity (Figures 1 and 3) and density (Figures 2 and 4) of synthetic Culebra brine 1 and 2 vary with temperature. In Figures 1 and 3, error bars are included for temperature and viscosity and indicate two standard deviations (about 95% confidence). Again, temperature error bars indicate fluctuations over time, not thermocouple error. The thermocouple error (see Appendix A) is about +0.1°C, which means the measured temperatures are about 0.1°C too high. This results in an error in the viscosity calculations of less than one-half of one percent (for example, viscosities read off of Figure 1 may be 0.004 cP too high). For the densities in Figures 2 and 4, since measurements were not repeated for a given temperature, (constant temperature is too hard to keep without fluctuation) there are no error bars, but estimated density error is about 0.001 g/mL or about 0.1%. (Note: This was not added into the error calculation for viscosity). The equation for the line fits were derived using the method of least squares (Fred Gelbard wrote a program in Fortran that was used for this purpose).

The fifth graph shows the viscosity trends of both of the Culebra brines on the same scale for comparison.

DISCUSSION

The graphs for the viscosity of Culebra brine show a general decreasing trend. The values also agree with published salinity viscosities (see Reference 1).

The errors calculated for the experimental viscosities of the brines were mostly less than 0.5% and show experimental consistency. Taking into account thermocouple (calibration) error and density error adds only about 0.5% at the most to the viscosity values. Viscosity errors were slightly lower for synthetic Culebra brine 2 than for brine 1. This may be because the temperature fluctuated less during testing of brine 2 (which may or may not be due to the meter that was hooked up to the thermocouple.) But water viscosity errors seemed slightly higher for synthetic Culebra brine 2 than brine 1 (which may have been due to the different viscometers used). The deionized water viscosities differed from published values by no more than 2.9% for all tests. Even if one takes into account that the times increase slightly for progressing runs at the same temperature (i.e. pre-check times versus post-check times), and therefore probably for the whole test, the error remains near or under 3%.

The density measurements were harder to take because the meter drifted during measurements. The drift was probably due to the brine changing temperature when introduced into the meter. Also, the meter's thermometer was too inaccurate (it usually did not change much, if at all), so the same thermocouple as for the water bath was used. Density values in Tables 1 and 2 for the brines

were extrapolated from the line fit equations. One should note that comparing published values for the viscosity of a 4% salinity solution (Reference 1) to the brine viscosities show evidence that saline solution viscosities may be applicable to brines.

Comparing the viscosities for synthetic Culebra brine 1 to synthetic culebra brine 2 show that the brine 2 values are consistently 0.02 cP or more higher than the brine 1 values; that is, the curves in Figures 1 and 3 are very nearly parallel. Comparing brine compositions shows that there are about three more grams of $CaCl_2*2H_2O$ in brine 2 as compared to brine 1. That extra amount of salt is approximately a 5.9% increase in the salinity of brine 2 over brine 1. It seems that even a seemingly minor change like that is noticeable in the experimental data (though not proportionally 5.9% higher; the data shows that brine 2 is 2.7% more viscous than brine 1 on average) and suggests that brine viscosities are sensitive to such small changes in concentration.

CONCLUSION

The experimental procedure for determining the viscosity of brine seems to be very consistent and relatively simple. The accuracy of the results is limited only by the accuracy of the thermocouple (small at about 0.1°C), time variations in the constant temperature water bath (which appeared minimal at about 0.1°C and could also include the thermocouple error), and possible clogging in the viscometer due to precipitation of brine or particulates. Though no visible problems were noted, sometimes the efflux times for the water checks dropped over time (i.e. after maybe five or more flow measurements). This may indicate that the viscometer is cleaning itself out slowly when it has water soaking in it; but, times do not change by more than about one second. Possible considerations regarding this may include more water checks.

The synthetic Culebra brine viscosities seem to follow closely the viscosities of a comparable percent by weight sodium chloride solution.

Possible future measurements include determining viscosities for actual Salado brine which is much more concentrated than Culebra brine. Synthetic Salado brines may also be tested. Those data can also be compared to saline viscosity data.

TABLE 1

C=calib. const.
Viscosity=pCt: p=density (g/mL) C=0.0042462 to 0.0042493 (cSt/s) t=time (s)

Approximate tempurature:			Temp(C)	Time(s)	Visc.(cP)	%error
20 degrees (C)	pre-check	Average:	20.17	239.9	1.018	1.6
	6pts	Std.Dev.:	0.26	0.59	0.0025	0.25
	p=.9982	2 Std. Dev.:	0.52	1.18	0.005	0.5
	Brine test	Average:	20.26	248.5	1.079	
	10pts	Std.Dev.:	0.14	0.31	0.0013	0.13
	p=1.0220	2 Std. Dev.:	0.28	0.62	0.0027	0.25
	post-check	Average:	20.03	240.2	1.019	1.7
	5pts	Std.Dev.:	0.03	0.19	0.0008	0.08
	p=.9982	2 Std. Dev.:	0.06	0.38	0.0016	0.16
22 degrees (C)	pre-check	Average:				
	0pts	Std.Dev.:	no	data	taken	here
	p=.9978	2 Std. Dev.:				
	Brine test	Average:	22.03	238.2	1.033	
	10pts	Std.Dev.:	0.05	0.15	0.0006	0.06
	p=1.0204	2 Std. Dev.:	0.1	0.3	0.0013	0.13
	post-check	Average:	22.02	229.5	0.9729	1.9
	5pts	Std.Dev.:	0.03	0.08	0.0003	0.03
	p=.9978	2 Std. Dev.:	0.06	0.16	0.0007	0.07
24 degrees (C)	pre-check	Average:	24.02	217.7	0.9223	1.2
	5pts	Std.Dev.:	0.03	0.09	0.0004	0.04
	p=.9973	2 Std. Dev.:	0.06	0.18	0.0008	0.09
	Brine test	Average:	24.03	227.5	0.9044	
	10pts	Std.Dev.:	0.03	0.45	0.0019	0.19
	p=1.0186	2 Std. Dev.:	0.06	0.9	0.0039	0.4
	post-check	Average:	24.1	218.7	0.9266	1.7
	3pts	Std.Dev.:	0	0	0	0
	p=.9973	2 Std. Dev.:	0	0	0	0

TABLE 1
(cont'd)

Approximate tempurature:			Temp(C)	Time(s)	Visc.(cP)	%error
26 degrees (C)	pre-check	Average:	25.98	209.3	0.8861	1.8
	5pts	Std.Dev.:	0.03	0.26	0.0011	0.12
	p=.9968	2 Std. Dev.:	0.06	0.52	0.0022	0.25
	Brine test	Average:	26	217.9	0.9411	
	10pts	Std.Dev.:	0	0.31	0.0013	0.14
	p=1.0169	2 Std. Dev.:	0	0.62	0.0027	0.29
	post-check	Average:	26	210.4	0.8908	2.3
	5pts	Std.Dev.:	0	0.05	0.0002	0.02
	p=.9968	2 Std. Dev.:	0	0.1	0.0004	0.04
28 degrees (C)	pre-check	Average:	27.95	201.3	0.8516	2.3
	5pts	Std.Dev.:	0	0.09	0.0004	0.05
	p=.9962	2 Std. Dev.:	0	0.18	0.0008	0.09
	Brine test	Average:	28	208.6	0.8993	
	10pts	Std.Dev.:	0.06	0.27	0.0012	0.13
	p=1.0151	2 Std. Dev.:	0.12	0.54	0.0023	0.26
	post-check	Average:	27.95	200	0.8461	1.6
	5pts	Std.Dev.:	0	0.52	0.0022	0.26
	p=.9962	2 Std. Dev.:	0	1.04	0.0044	0.52
30 degrees (C)	pre-check	Average:	29.95	191.3	0.8187	1.4
	5pts	Std.Dev.:	0	0.04	0.0002	0.02
	p=.9956	2 Std. Dev.:	0	0.08	0.0003	0.04
	Brine test	Average:	29.95	200.1	0.861	
	10pts	Std.Dev.:	0	0.43	0.0018	0.21
	p=1.0133	2 Std. Dev.:	0	0.86	0.0037	0.43
	post-check	Average:	30	192	0.8117	1.8
	5pts	Std.Dev.:	0.04	0.08	0.0003	0.04
	p=.9956	2 Std. Dev.:	0.08	0.16	0.0007	0.09

TABLE 2

C=calib. const.
Viscosity=pCt: p=density (g/mL) C=0.0039950 to 0.0039980 (cSt/s) t=time (s)

Approximate tempurature:			Temp(C)	Time(s)	Visc.(cP)	%error
20 degrees (C)	pre-check	Average:	20	254.5	1.016	1.4
	6pts	Std.Dev.:	0	0.12	0.0005	0.05
	p=.9982	2 Std. Dev.:	0	0.24	0.001	0.09
	Brine test	Average:	20.01	268.2	1.106	
	10pts	Std.Dev.:	0.04	0.42	0.0017	0.15
	p=1.0315	2 Std. Dev.:	0.08	0.84	0.0035	0.32
	post-check	Average:	20.05	255.5	1.02	1.8
	5pts	Std.Dev.:	0.05	0.25	0.001	0.1
	p=.9982	2 Std. Dev.:	0.1	0.5	0.002	0.2
22 degrees (C)	pre-check	Average:	22.03	244.4	0.9748	2.1
	5pts	Std.Dev.:	0.04	0.19	0.0007	0.07
	p=.9978	2 Std. Dev.:	0.09	0.38	0.0015	0.15
	Brine test	Average:	22.02	256.4	1.055	
	10pts	Std.Dev.:	0.03	0.18	0.0007	0.07
	p=1.0295	2 Std. Dev.:	0.07	0.35	0.0014	0.13
	post-check	Average:	22.04	244.3	0.9744	2.1
	5pts	Std.Dev.:	0.04	0.27	0.0011	0.11
	p=.9978	2 Std. Dev.:	0.08	0.54	0.0022	0.22
24 degrees (C)	pre-check	Average:	24	234.5	0.9341	2.6
	5pts	Std.Dev.:	0	0	0	0
	p=.9973	2 Std. Dev.:	0	0	0	0
	Brine test	Average:	24	246	1.01	
	10pts	Std.Dev.:	0	0.07	0.0003	0.03
	p=1.0276	2 Std. Dev.:	0	0.13	0.0006	0.06
	post-check	Average:	24	233.6	0.93	2.1
	3pts	Std.Dev.:	0	0.11	0.0004	0.05
	p=.9973	2 Std. Dev.:	0	0.22	0.0009	0.09

TABLE 2
(cont'd)

Approximate tempurature:			Temp(C)	Time(s)	Visc.(cP)	%error
26 degrees (C)	pre-check	Average:	26	223.9	0.8919	2.5
	5pts	Std.Dev.:	0	0.07	0.0003	0.03
	p=.9968	2 Std. Dev.:	0	0.14	0.0006	0.07
	Brine test	Average:	26	235.3	0.9644	
	9pts	Std.Dev.:	0.02	0.09	0.0004	0.04
	p=1.0256	2 Std. Dev.:	0.05	0.18	0.0007	0.07
	post-check	Average:	25.99	223.5	0.8903	2.3
	5pts	Std.Dev.:	0.02	0	0	0
	p=.9968	2 Std. Dev.:	0.04	0	0	0
28 degrees (C)	pre-check	Average:	28.01	214.2	0.8526	2.4
	5pts	Std.Dev.:	0.02	0.09	0.0004	0.05
	p=.9962	2 Std. Dev.:	0.04	0.18	0.0007	0.08
	Brine test	Average:	28	227.3	0.9297	
	10pts	Std.Dev.:	0	0.05	0.0002	0.02
	p=1.0237	2 Std. Dev.:	0	0.1	0.0004	0.04
	post-check	Average:	28	215.2	0.8566	2.9
	5pts	Std.Dev.:	0	0.08	0.0003	0.04
	p=.9962	2 Std. Dev.:	0	0.17	0.0007	0.08
30 degrees (C)	pre-check	Average:	30	204.9	0.815	2.2
	5pts	Std.Dev.:	0	0.15	0.0006	0.07
	p=.9956	2 Std. Dev.:	0	0.3	0.0012	0.15
	Brine test	Average:	30.02	217	0.8857	
	10pts	Std.Dev.:	0.05	0.11	0.0004	0.05
	p=1.0217	2 Std. Dev.:	0.1	0.21	0.0009	0.1
	post-check	Average:	30.02	205.6	0.8178	2.5
	10pts	Std.Dev.:	0.05	0.31	0.0012	0.15
	p=.9956	2 Std. Dev.:	0.11	0.62	0.0025	0.3

TABLE 3

DATA SUMMARY
PROPERTIES OF SYNTHETIC CULEBRA BRINE 1

Computed (From Measured) Values:

Temperature (°C)	Viscosity (cP)
20.26	1.079
22.03	1.033
24.03	0.9844
26.00	0.9411
28.00	0.8993
29.95	0.8610

Measured Values:

	Temperature (°C)	Density (g/mL)
In order taken:	21.1	1.0207
	22.5	1.0196
	23.7	1.0187
	24.2	1.0181
	26.5	1.0160
	27.5	1.0153
	31.7	1.0115
	29.5	1.0140
	28.5	1.0148
	27.5	1.0159
	26.8	1.0164
	26.3	1.0172
	25.2	1.0183
	24.8	1.0184
	24.4	1.0190
	24.0	1.0192
	23.7	1.0194
	23.0	1.0198
	22.6	1.0202
	21.3	1.0210
	20.1	1.0220
	19.4	1.0228
	20.0	1.0220
	20.5	1.0210
	21.9	1.0206
	29.6	1.0130
	30.0	1.0130
	29.0	1.0138
	28.2	1.0142
	25.7	1.0168
	25.0	1.0175

TABLE 4

DATA SUMMARY
PROPERTIES OF SYNTHETIC CULEBRA BRINE 2

Computed (From Measured) Values:

Temperature (°C)	Viscosity (cP)
20.01	1.106
22.02	1.055
24.00	1.010
26.00	0.9644
28.00	0.9297
30.02	0.8857

Measured Values:

	Temperature (°C)	Density (g/mL)
In order taken:	21.5	1.0298
	22.1	1.0292
	23.3	1.0281
	25.0	1.0265
	26.8	1.0250
	27.5	1.0240
	28.1	1.0237
	28.7	1.0230
	29.8	1.0223
	30.5	1.0212
	30.0	1.0220
	29.2	1.0233
	28.6	1.0233
	28.1	1.0235
	27.8	1.0239
	27.3	1.0244
	26.4	1.0256
	26.0	1.0258
	25.7	1.0261
	25.2	1.0269
	24.7	1.0275
	24.3	1.0277
	23.9	1.0280
	23.6	1.0285
	22.5	1.0296
	22.1	1.0299
	21.6	1.0300
	21.0	1.0303
	19.9	1.0312
	20.3	1.0310
	23.0	1.0282
	29.5	1.0212
	28.6	1.0222
	28.0	1.0228
	20.7	1.0308

TABLE 5

COMPOSITION OF SYNTHETIC CULEBRA BRINE 1

Compound	Quantity (g/L)
$NaHCO_3$	0.0839
$CaCl_2*2H_2O$	0.01563
$MgSO_4$	2.054
K_2SO_4	0.742
Na_2SO_4	7.615
NaCl	29.20
$Na_2B_4O_7$	0.1256

pH = 8.11

COMPOSITION OF SYNTHETIC CULEBRA BRINE 2

Compound	Quantity (g/L)
$NaHCO_3$	0.08492
$CaCl_2*2H_2O$	3.052
$MgSO_4$	2.074
K_2SO_4	0.742
Na_2SO_4	7.615
NaCl	29.20
$Na_2B_4O_7$	0.1223
NaBr	0.0291

pH = 7.67

Figure 1

VISCOSITY (cP) vs. TEMPERATURE (C)

Synthetic Culebra Brine 1

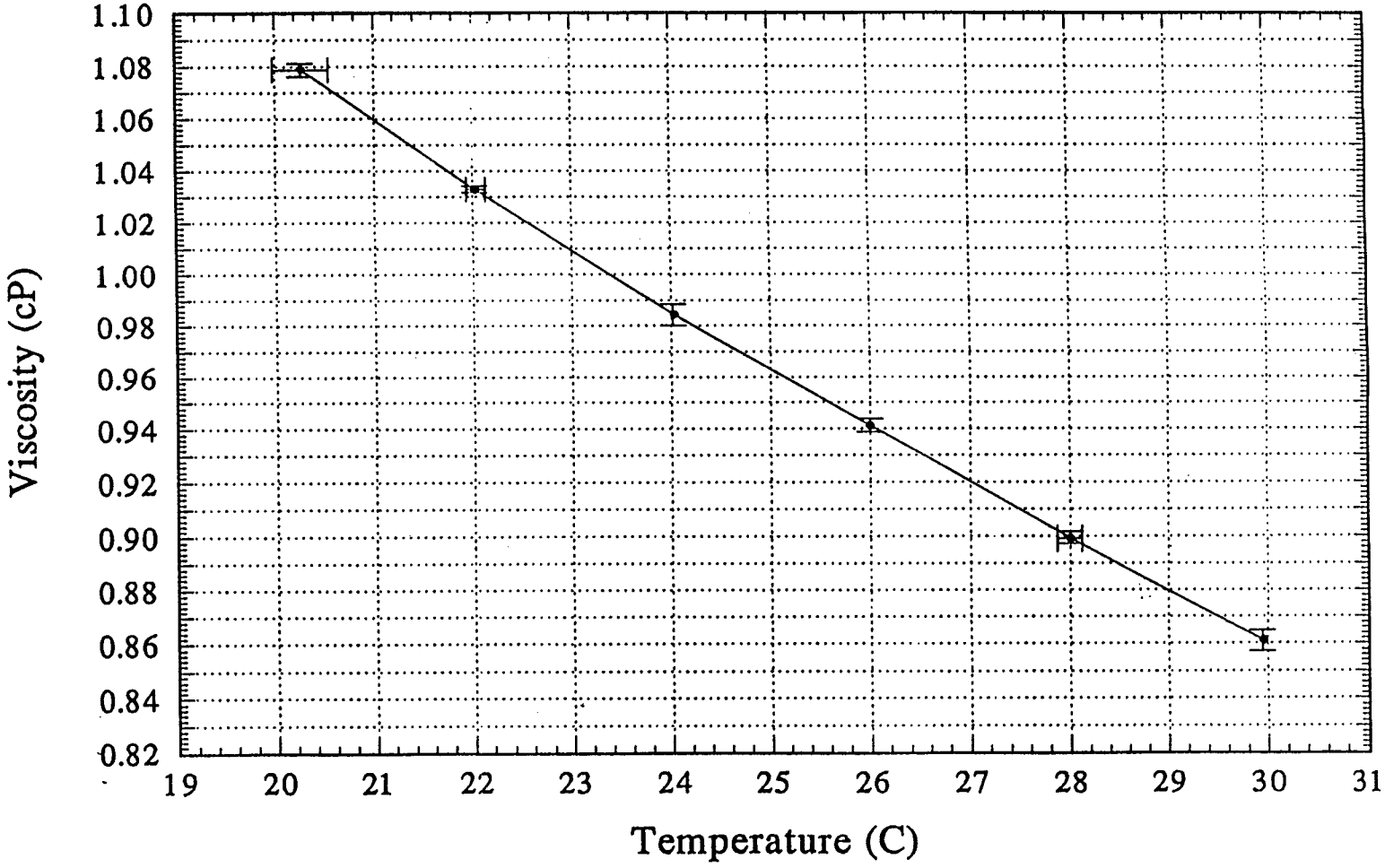

Figure 2

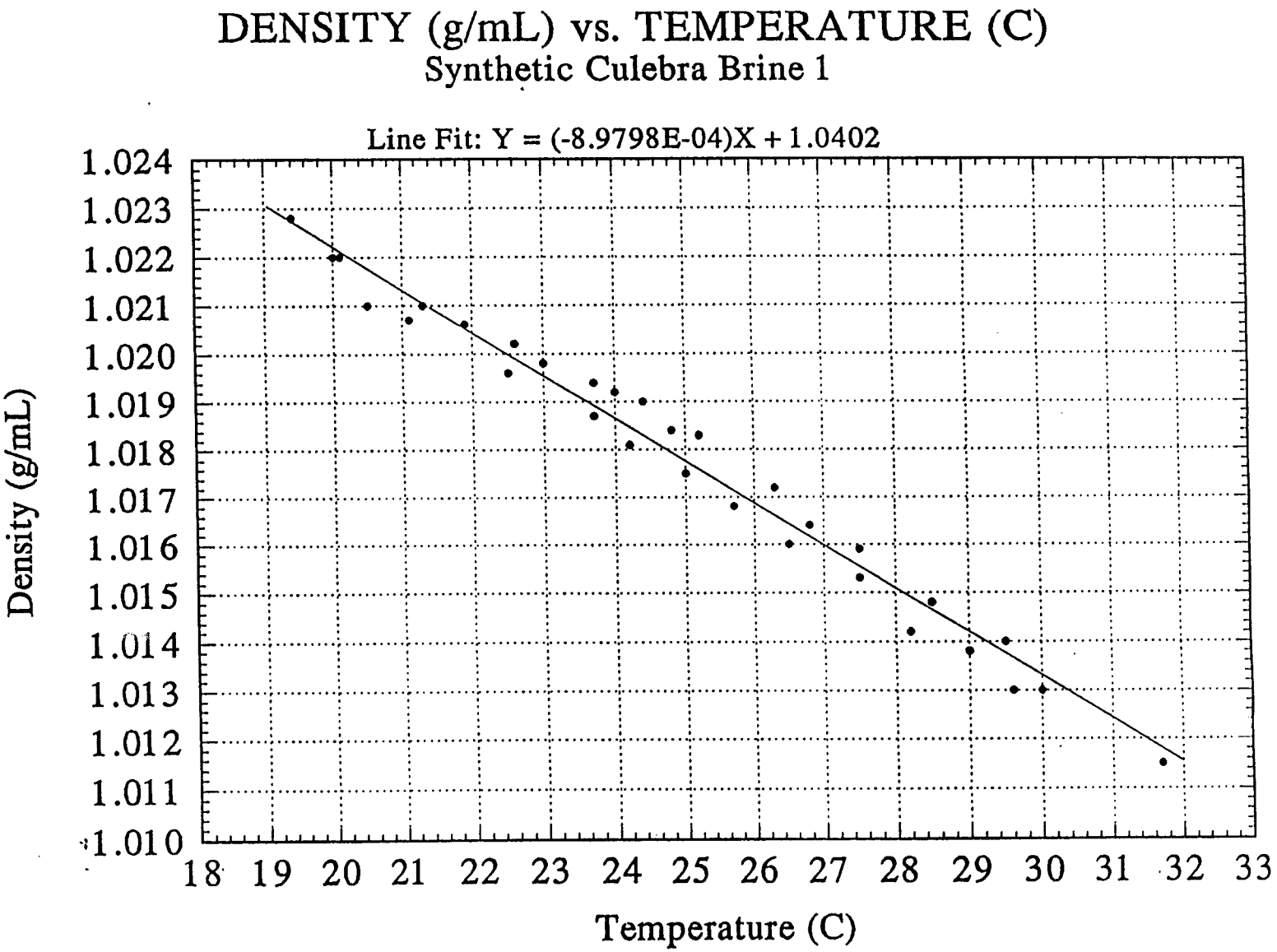
DENSITY (g/mL) vs. TEMPERATURE (C)
Synthetic Culebra Brine 1
Line Fit: Y = (-8.9798E-04)X + 1.0402
Density (g/mL)
1.024
1.023
1.022
1.021
1.020
1.019
1.018
1.017
1.016
1.015
1.014
1.013
1.012
1.011
1.010
18 19 20 21 22 23 24 25 26 27 28 29 30 31 32 33
Temperature (C)

Figure 3

VISCOSITY (cP) vs. TEMPERATURE (C)

Synthetic Culebra Brine 2

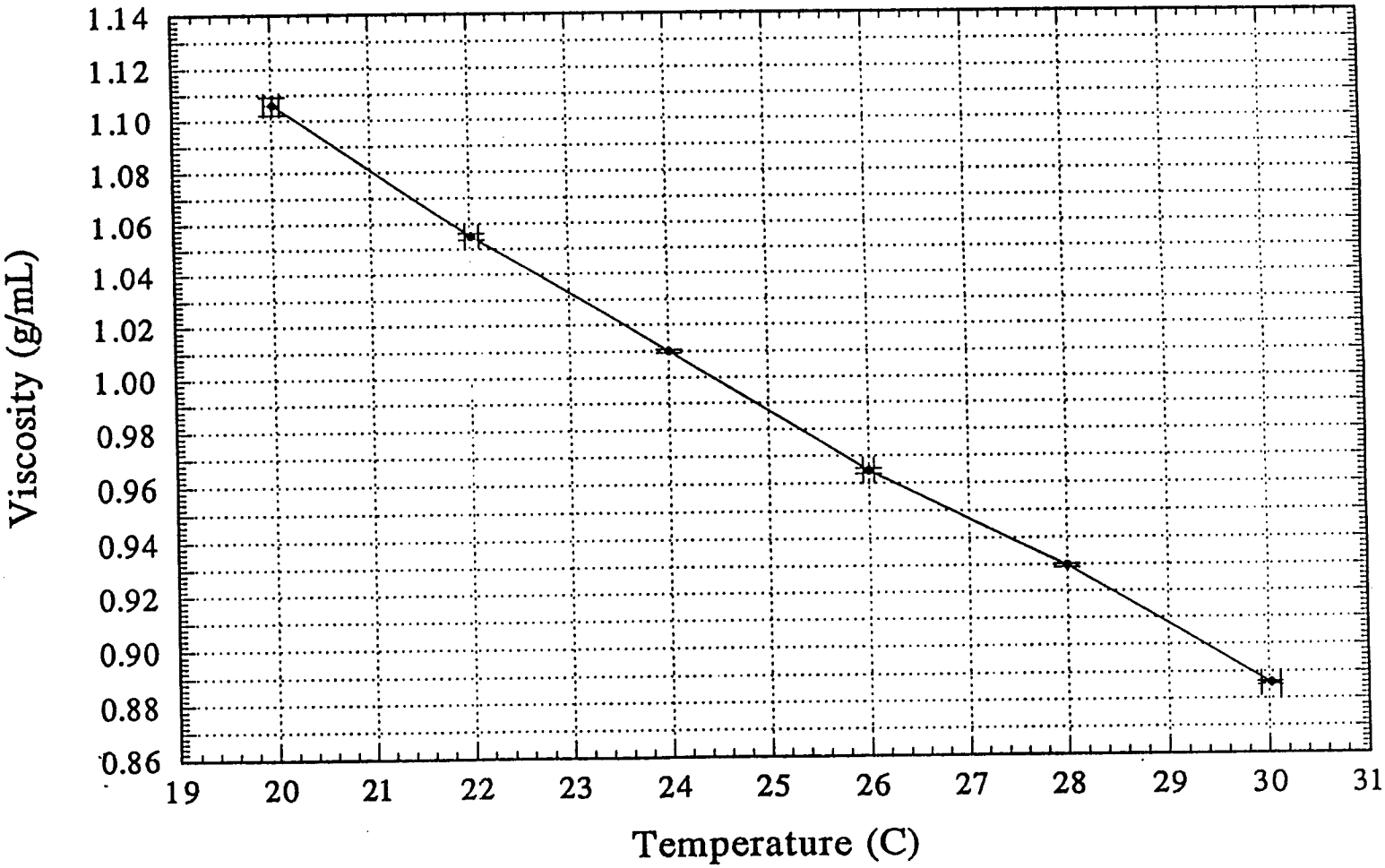

Figure 4

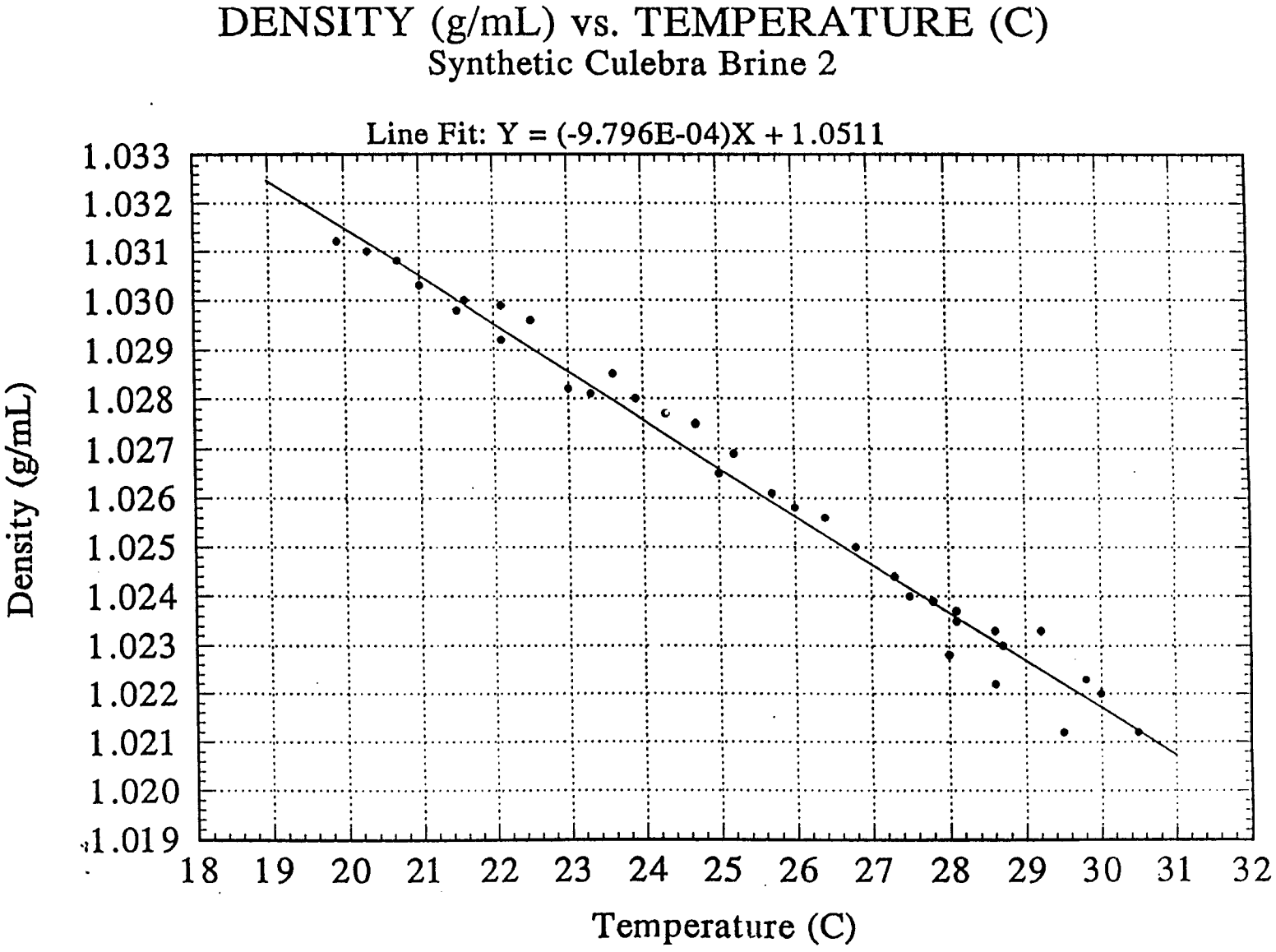
DENSITY (g/mL) vs. TEMPERATURE (C)
Synthetic Culebra Brine 2
Line Fit: Y = (-9.796E-04)X + 1.0511
Density (g/mL)
1.033
1.032
1.031
1.030
1.029
1.028
1.027
1.026
1.025
1.024
1.023
1.022
1.021
1.020
1.019
18 19 20 21 22 23 24 25 26 27 28 29 30 31 32
Temperature (C)

Figure 5

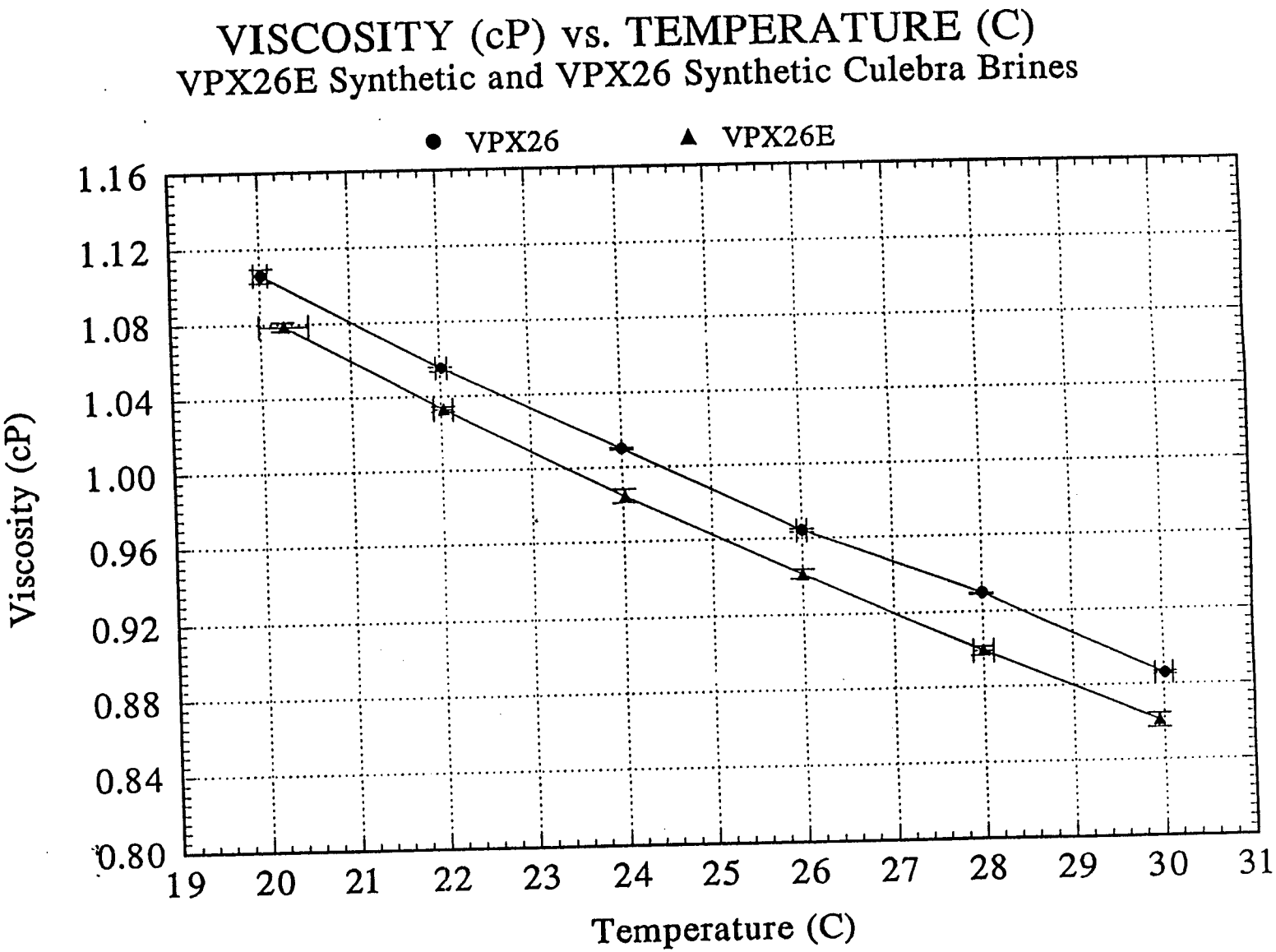
VISCOSITY (cP) vs. TEMPERATURE (C)
VPX26E Synthetic and VPX26 Synthetic Culebra Brines
VPX26
VPX26E
Viscosity (cP)
1.16
1.12
1.08
1.04
1.00
0.96
0.92
0.88
0.84
0.80
19
20
21
22
23
24
25
26
27
28
29
30
31
Temperature (C)

APPENDIX A

CERTIFICATES OF CALIBRATION

Certificate of Calibration

Viscometer No. 50 U513

CANNON-FENSKE ROUTINE TYPE POR TRANSPARENT LIQUIDS

(Standard Test ASTM D 445, IP 71 and ISO 3104)

Constant at 40°C 0.003992 mm^2/s^2, (cSt/s)

Constant at 100°C 0.003974 mm^2/s^2, (cSt/s)

The viscometer constant at other temperatures can be obtained by interpolation or extrapolation. To obtain kinematic viscosity in mm^2/s(cSt) multiply the efflux time in seconds by the viscometer constant. To obtain viscosity in mPa·s (cP) multiply the kinematic viscosity in mm^2/s(cSt) by the density in grams per milliliter.

The above constants assume a value for the coefficient of thermal expansion typical to that for mineral oil, and that the viscometer was filled with test sample at room temperature. If the filling temperature T_F is substantially different than room temperature, the viscometer constant at test temperature T_T is C_o (1 - B [T_T - T_F]). The values of C_o and B shown below are based on a coefficient of thermal expansion typical to that for a mineral oil.

Kinematic viscosities of the standards used in calibrating were established in Master Viscometers as described in Ind. Eng. Chem. Anal. Ed. 16,708(1944), ASTM D 2162, and the Journal of Research of the National Bureau of Standards, Vol. 52, No. 3, March 1954, Research Pa[illegible]479.

Kinematic viscosities are based on the value for water adopted by the National Institute for Standards and Technology and The American Society for Testing Materials July 1, 1953. The kinematic viscosity basis is 1.0038 mm^2/s(cSt) for water at 20°C (ITS-90). The gravitational constant, g, is 980.1 cm/sec^2 at the Cannon Instrument Company. The gravitational constant varies up to 0.1% in the United States. To make this small correction in the viscometer constant, multiply the above viscometer constant by the factor [g(at your laboratory) /980.1]. The calibration data below are traceable to the National Institute for Standards and Technology. Temperature measurement traceable to NIST (Test No. 246089).

CALIBRATION DATA AT 40°C

Viscosity Standard	Kinematic Viscosity mm^2/s, (cSt)	Efflux Time Seconds	Constant mm^2/s^2, (cSt/s)
9203	1.0084	252.66	0.003991
9204	2.045	512.09	0.003993

Average = 0.003992

C_o = 0.003998

B = 76 x 10^{-6}/°C

Room Temp. (approx.) 21 °C.

Charge (approx.) 6.8 ml.

Driving fluid head (approx.) 9.4 cm.

Working diameter of lower reservoir 3.0 cm.

Constant at 100° C. is 0.46 % lower than the constant at 40° C.

Calibrated by VSM 366008 on 29-Oct-92 under supervision of

R. E. Manning, Ph.D., P.E.
W. A. Lloyd, Ph.D., P.E.
M. R. Hoover, Ph.D.
M. K. Gerfin, C.Q.E.
Cannon Instrument Co.
State College, PA 16804, USA

Please note: This calibration remains valid for 10 years unless (1) the viscometer has been damaged or (2) materials which chemically attack borosilicate glass (e.g., hydrofluoric acid or highly alkaline solutions) have been used. Nonetheless, it is recommended that the calibration be verified with kinematic viscosity standards periodically, if a change in calibration is indicated, carefully examine all sources of error, including especially temperature measurement since most apparent changes in calibration of the viscometer are due to errors in temperature measurement.

Test No.: 366008 - 11

The S.I. unit of kinematic viscosity is 1 meter squared per second, and is equal to 10^4 stokes. The S.I. unit of viscosity is 1 pascal second, and is equal to 10 poises. One centistokes is equal to one millimeter squared per second.

991

Certificate of Calibration

Viscometer No. 50 U383

CANNON-FENSKE ROUTINE TYPE FOR TRANSPARENT LIQUIDS

(Standard Test ASTM D 445, IP 71 and ISO 3104)

Constant at 40°C 0.004243 mm^2/s^2, (cSt/s)

Constant at 100°C 0.004224 mm^2/s^2, (cSt/s)

The viscometer constant at other temperatures can be obtained by interpolation or extrapolation. To obtain kinematic viscosity in mm^2/s(cSt) multiply the efflux time in seconds by the viscometer constant. To obtain viscosity in mPa·s (cP) multiply the kinematic viscosity in mm^2/s(cSt) by the density in grams per milliliter.

The above constants assume a value for the coefficient of thermal expansion typical to that for mineral oil, and that the viscometer was filled with test sample at room temperature. If the filling temperature T_F is substantially different than room temperature, the viscometer constant at test temperature T_T is C_o (1 - B [T_T - T_F]). The values of C_o and B shown below are based on a coefficient of thermal expansion typical to that for a mineral oil.

Kinematic viscosities of the standards used in calibrating were established in Master Viscometers as described in Ind. Eng. Chem. Anal. Ed. 16,708(1944), ASTM D 2162, and the Journal of Research of the National Bureau of Standards, Vol. 52, No. 3, March 1954, Research Paper 2479.

Kinematic viscosities are based on the value for water adopted by the National Institute for Standards and Technology and The American Society for Testing Materials July 1, 1953. The kinematic viscosity basis is 1.0038 mm^2/s(cSt) for water at 20°C (ITS-90). The gravitational constant, g, is 980.1 cm/sec^2 at the Cannon Instrument Company. The gravitational constant varies up to 0.1% in the United States. To make this small correction in the viscometer constant, multiply the above viscometer constant by the factor [g(at your laboratory) /980.1]. The calibration data below are traceable to the National Institute for Standards and Technology. Temperature measurement traceable to NIST (Test No. 246089).

CALIBRATION DATA AT 40°C

Viscosity Standard	Kinematic Viscosity mm^2/s, (cSt)	Efflux Time Seconds	Constant mm^2/s^2, (cSt/s)
9203	1.0086	237.72	0.004243
9204	2.045	481.89	0.004244

Average = 0.004243

C_o = 0.004249

B = 76 x 10^{-6}/°C

Room Temp. (approx.) 22 °C.

Charge (approx.) 6.7 ml.

Driving fluid head (approx.) 9.2 cm.

Working diameter of lower reservoir 3.0 cm.

Constant at 100° C. is 0.46 % lower than the constant at 40° C.

Calibrated by MAG 371036 on 12-May-92 under supervision of R E Manning

R. E. Manning, Ph.D., P.E.
W. A. Lloyd, Ph.D., P.E.
M. R. Hoover, Ph.D.
M. K. Gerfin, C.Q.E.
Cannon Instrument Co.
State College, PA 16804, USA

Please note: This calibration remains valid for 10 years unless (1) the viscometer has been damaged or (2) materials which chemically attack borosilicate glass (e.g., hydrofluoric acid or highly alkaline solutions) have been used. Nonetheless, it is recommended that the calibration be verified with kinematic viscosity standards periodically; if a change in calibration is indicated, carefully examine all sources of error, including especially temperature measurement since most apparent changes in calibration of the viscometer are due to errors in temperature measurement.

Test No.: 371036 - 2

The S.I. unit of kinematic viscosity is 1 meter squared per second, and is equal to 10^4 stokes. The S.I. unit of viscosity is 1 pascal second, and is equal to 10 poises. One centistokes is equal to one millimeter squared per second.

991

Standards Laboratory Certificate

Sandia National Laboratories
Albuquerque, New Mexico 87185

File No. 4522

THERMOCOUPLE TYPE
OMEGA
Model No. 6" Probe
Serial No. 92321-1

Submitted by: 6119

Certified: November 16, 1992
Expires: November 16, 1993

Tests performed between the temperatures of -40 to 100 deg C show this thermocouple to be in agreement within +/- 1 deg C of the values published in IPTS-68.

Under normal use conditions it is probable this thermocouple will remain within the above accuracies for the certification interval.

Metrologist: J. J. LaMarr, 2414

Georgia Brown for

Certified by: J. M. Simons, 2414

TLC29:JJL
1/30/92

SERIAL #	MV READING	TEMPERATURE	DELTA	Δ °C
STD 257		-39.980 °C		
~~STD 100~~	0.0001	-0.019 C	0.000	
NON	-1.5312	-40.127 C	-40.109	
NON	-1.5304	-40.103 C	-40.084	
NON	-1.5301	-40.094 C	-40.076	
NON	-1.5303	-40.100 C	-40.081	
NON	-1.5307	-40.111 C	-40.092	
NON	-1.5314	-40.130 C	-40.111	
NON	-1.5320	-40.146 C	-40.128	
NON	-1.5322	-40.152 C	-40.133	
NON	-1.5226	-39.890 C	-39.871	
NON	-1.5240	-39.928 C	-39.910	
NON	-1.5261	-39.986 C	-39.967	
NON	-1.5250	-39.955 C	-39.937	
NON	-1.5223	-39.882 C	-39.863	
NON	-1.5295	-40.078 C	-40.059	
NON	-1.5283	-39.854 C	-39.836	
NON	-1.5285	-39.887 C	-39.869	
NON	-1.5295	-40.078 C	-40.059	
NON	-1.5319	-40.119 C	-40.100	
NON	-1.5331	-40.176 C	-40.158	
3201	-1.5343	-40.209 C	-40.190	-.229 ←
3202	-1.5345	-40.214 C	-40.196	-.234
3203	-1.5252	-39.961 C	-39.942	.019
3204	-1.5247	-39.947 C	-39.929	.033

SERIAL #	MV READING	TEMPERATURE	DELTA	Δ °C
STD 257		23.520 °C		
~~STD 100~~	0.0001	0.019 C	0.000	
NON	0.9361	23.417 C	23.398	
NON	0.9361	23.417 C	23.398	
NON	0.9361	23.417 C	23.398	
NON	0.9357	23.412 C	23.393	
NON	0.9340	23.350 C	23.332	
NON	0.9364	23.424 C	23.406	
NON	0.9360	23.414 C	23.396	
NON	0.9361	23.417 C	23.398	
NON	0.9367	23.432 C	23.413	
NON	0.9371	23.442 C	23.423	
NON	0.9372	23.446 C	23.428	
NON	0.9364	23.424 C	23.406	
NON	0.9365	23.427 C	23.408	
NON	0.9361	23.417 C	23.398	
NON	0.9361	23.417 C	23.398	
NON	0.9377	23.456 C	23.437	
NON	0.9382	23.467 C	23.448	
NON	0.9388	23.483 C	23.465	
NON	0.9387	23.481 C	23.462	
3201	0.9418	23.558 C	23.539	.038 ←
3202	0.9440	23.612 C	23.593	.092
3203	0.9441	23.614 C	23.595	.094
3204	0.9435	23.607 C	23.588	.087

SERIAL #	MV READING	TEMPERATURE	DELTA	Δ °C
STD 257		64.801 °C		
~~STD 400~~	0.0001	0.019 C	0.000	
NON	2.6406	64.945 C	64.927	
NON	2.6398	64.926 C	64.907	
NON	2.6399	64.928 C	64.910	
NON	2.6397	64.924 C	64.905	
NON	2.6399	64.928 C	64.910	
NON	2.6416	64.969 C	64.951	
NON	2.6398	64.926 C	64.907	
NON	2.6408	64.950 C	64.932	
NON	2.6342	64.791 C	64.772	
NON	2.6363	64.842 C	64.823	
NON	2.6408	64.950 C	64.932	
NON	2.6405	64.943 C	64.924	
NON	2.6394	64.916 C	64.898	
NON	2.6416	64.969 C	64.951	
NON	2.6413	64.962 C	64.944	
NON	2.6406	64.945 C	64.927	
NON	2.6413	64.962 C	64.944	
NON	2.6432	65.008 C	64.989	
NON	2.6441	65.030 C	65.011	
3201	2.6508	65.191 C	65.173	.390 ←
3202	2.6520	65.220 C	65.202	.419
3203	2.6500	65.172 C	65.153	.371
3204	2.6494	65.157 C	65.138	.356

SERIAL #	MV READING	TEMPERATURE	DELTA	Δ °C
STD 257		-18.593 °C		
~~STD 400~~	0.0005	0.093 C	0.000	
NON	-0.7300	-18.762 C	-18.854	
NON	-0.7290	-18.735 C	-18.828	
NON	-0.7286	-18.725 C	-18.81[illegible]	
NON	-0.7292	-18.741 C	[illegible]	
NON	-0.7306	-18.762 C	[illegible]	
NON	-0.7311	[illegible]	[illegible]	
NON	-0.7301	-18.7[illegible]	[illegible]	
[illegible]	[illegible]	-18.781	[illegible]	
[illegible]	[illegible]	-18.8[illegible]	[illegible]	
[illegible]	[illegible]	-18.7[illegible]	[illegible]	
[illegible]	[illegible]	-18.7[illegible]	[illegible]	
[illegible]	[illegible]	-18.602	[illegible]	
[illegible]	[illegible]	-18.56[illegible]	[illegible]	
[illegible]	[illegible]	-18.73[illegible]	[illegible]	
NON	-0.7252	-18.577 C	[illegible]	
[illegible]	[illegible]	[illegible]	[illegible]	
[illegible]	-0.7272	-18.702 C	[illegible]	
NON	-0.7297	-18.75[illegible]	[illegible]	
NON	-0.7308	-18.751	[illegible]	
[illegible]	[illegible]	-18.811	[illegible]	-.218 ←
3202	-0.7300	-18.767 C	[illegible]	-.176
[illegible]	-0.7261	-18.660	[illegible]	-.067
[illegible]	[illegible]	-18.611	[illegible]	-.022

SERIAL #	MV READING	TEMPERATURE	DELTA	Δ °C
STD 257		98.445		
~~STD 100~~	[illegible]	[illegible]	[illegible]	
NON	[illegible]	[illegible]	[illegible]	
NON	[illegible]	[illegible]	[illegible]	
NON	[illegible]	[illegible]	[illegible]	
NON	[illegible]	[illegible]	[illegible]	
NON	[illegible]	[illegible]	[illegible]	
NON	4.0513	98.933	[illegible]	
NON	4.0484	98.867	[illegible]	
NON	4.0503	98.913	[illegible]	
NON	4.0554	[illegible]	[illegible]	
NON	4.0426	[illegible]	[illegible]	
NON	[illegible]	[illegible]	[illegible]	
NON	[illegible]	[illegible]	[illegible]	
NON	[illegible]	[illegible]	[illegible]	
NON	[illegible]	[illegible]	[illegible]	
NON	[illegible]	[illegible]	[illegible]	
NON	[illegible]	[illegible]	[illegible]	
NON	[illegible]	[illegible]	[illegible]	
NON	[illegible]	[illegible]	[illegible]	
3201	4.0616	99.186		.741 ←
3202	4.0629	99.218		.773
3203	4.0594	99.133		.688
3204	4.0594	99.133		.688

Standards Laboratory Certificate

Sandia National Laboratories
Albuquerque, New Mexico 87185

THERMOCOUPLE TYPE
OMEGA
Model No. 6" PROBE
Serial No. 92321-1

File No. 4522

Submitted by: 6119

Certified: August 12, 1993
Expires: August 12, 1994

Tests performed between the temperatures of -40 to 100 deg C show this thermocouple to be in agreement within +/- 1 deg C of the values published in IPTS-68.

Under normal use conditions it is probable this thermocouple will remain within the above accuracies for the certification interval.

Metrologist: J. J. LaMarr, 4344

Certified by: J. M. Simons, 4344

TLC29:JJL
7/8/93

6" Type K TC   92321-1   74522
8/12/93

Std Ω	°C		Test mV	°C
27.5885	19.981		.8008	20.07
27.7686	21.760		.8724	21.84
27.8643	22.705		.9094	22.76
28.3910	27.913		1.1230	28.03
29.0656	34.596		1.3964	34.74
29.1028	34.965		1.4117	35.12

CERTIFICATE

APPENDIX B

BRINE COMPOSITION ANALYSES

ANALYTICAL REPORT

TO: FRED GELBARD

PROJECT: 6S0007000

DATE: 15-APR-92

REQUISITION: 7070

VOLUME I OF IV

PREPARED BY:

CHEM-NUCLEAR GEOTECH ANALYTICAL LABORATORY
2597 B 3/4 ROAD
P.O. BOX 14000
GRAND JUNCTION, COLORADO 81502-5504
(303-248-6165) D-152

ANALYTICAL RESULTS

CUSTOMER ID: VPX 26 A
TICKET ID:

REQUESTOR: FRED GELBARD
SAMPLE MATRIX: BRINE
REQUISITION: 7070

DATE: 16-APR-92
LAB ID: 195510

PROJECT NUMBER: 6S0007000
DATE RECEIVED: 25-FEB-92
DATE COLLECTED: 12-DEC-91

ANALYSIS REQUESTED	RESULTS	RESULTS	RESULTS	UNITS	RPD	METHOD OF ANALYSIS
Silver	<0.1			MG/L		AS-5 R04
Aluminum	<0.05			MG/L		AS-2 R05
Boron	25.8	25.3		MG/L	2.	AS-5 R04
Bromide	22.2	22.9		MG/L	-3.	D-3 R08
Calcium	847	815		MG/L	4.	AS-5 R04
Cadmium	<0.05			MG/L		AS-6 R03
Chloride	19300	19300		MG/L	0.	D-3 R08
Chromium	<0.1			MG/L		AS-5 R04
Copper	<0.25			MG/L		AS-5 R04
Fluoride	1.5	1.6		MG/L	-6.	D-3 R08
Iron	<0.50			MG/L		AS-5 R04
Iodide	0.08	0.08		MG/L	0.	D-3 R08
Potassium	331	340		MG/L	-3.	AS-1 R04
Lithium	0.336	0.339		MG/L	-1.	AS-6 R03
Magnesium	424	410		MG/L	3.	AS-5 R04
Manganese	0.19	0.18	0.16	MG/L	9.	AS-5 R04
Molybdenum	<0.5			MG/L		AS-5 R04
Sodium	13900	13600		MG/L	2.	AS-5 R04
Ammonium	<0.10			MG/L		F-6 R05
Nitrate	<0.2	<0.2		MG/L		D-3 R08
Lead	<0.03			MG/L		AS-6 R03
pH	7.63	7.70			-1.	H-4 R03
Phosphate	0.1	0.1		MG/L	0.	F-4 R05
Antimony	<0.6			MG/L		AS-5 R04
Specific Gravity	1.03	1.03		G/CC	0.	K-4 R01
Silica	9.19	9.86		MG/L	-7.	AS-5 R04
Sulfate	7300	7190		MG/L	2.	D-3 R08
Strontium	9.58	10.0		MG/L	-4.	AS-5 R04
Total Dissolved Solids	44000	45000		MG/L	-2.	K-3 R04
Titanium	<1			MG/L		AS-5 R04
Total Inorganic Carbon	13.3	13.0		MG/L	2.	K-5 R03
Uranium	<0.05			MG/L		AS-6 R03
Vanadium	<0.5			MG/L		AS-5 R04
Zinc	<0.2			MG/L		AS-5 R04

(SECTION I)

CUSTOMER ID: VPX 26 B
TICKET ID:

REQUESTOR: FRED GELBARD
SAMPLE MATRIX: BRINE
REQUISITION: 7070

ANALYTICAL RESULTS

DATE: 16-APR-92
LAB ID: 195511

PROJECT NUMBER: 6S0007000
DATE RECEIVED: 25-FEB-92
DATE COLLECTED: 15-DEC-91

ANALYSIS REQUESTED	RESULTS	RESULTS	RESULTS	UNITS	RPD	METHOD OF ANALYSIS
Silver	<0.1			MG/L		AS-5 R04
Aluminum	<0.05			MG/L		AS-2 R05
Boron	26.2	25.2		MG/L	4.	AS-5 R04
Bromide	22.2	22.8		MG/L	-3.	D-3 R08
Calcium	846	820		MG/L	3.	AS-5 R04
Cadmium	<0.05			MG/L		AS-6 R03
Chloride	19200	19400		MG/L	-1.	D-3 R08
Chromium	<0.1			MG/L		AS-5 R04
Copper	<0.25			MG/L		AS-5 R04
Fluoride	1.5	1.6		MG/L	6.	D-3 R08
Iron	<0.50			MG/L		AS-5 R04
Iodide	0.07	0.08		MG/L	-13.	D-3 R08
Potassium	341	333		MG/L	2.	AS-1 R04
Lithium	0.329	0.342		MG/L	-4.	AS-6 R03
Magnesium	430	411		MG/L	5.	AS-5 R04
Manganese	0.25	0.23		MG/L	8.	AS-5 R04
Molybdenum	<0.5			MG/L		AS-5 R04
Sodium	13900	13500		MG/L	3.	AS-5 R04
Ammonium	<0.10			MG/L		F-6 R05
Nitrate	<0.2	<0.2		MG/L		D-3 R08
Lead	<0.03			MG/L		AS-6 R03
pH	7.59	7.69			-1.	H-4 R03
Phosphate	<0.1			MG/L		F-4 R05
Antimony	<0.6			MG/L		AS-5 R04
Specific Gravity	1.03	1.03		G/CC	0.	K-4 R01
Silica	8.76	9.57		MG/L	-9.	AS-5 R04
Sulfate	7310	7210		MG/L	1.	D-3 R08
Strontium	9.66	10.0		MG/L	-3.	AS-5 R04
Total Dissolved Solids	44000	45000		MG/L	-2.	K-3 R04
Titanium	<1			MG/L		AS-5 R04
Total Inorganic Carbon	12.0	12.0		MG/L	0.	K-5 R03
Uranium	<0.05			MG/L		AS-6 R03
Vanadium	<0.5			MG/L		AS-5 R04
Zinc	<0.2			MG/L		AS-5 R04

(SECTION I)

ANALYTICAL RESULTS

CUSTOMER ID: VPX 26 C
TICKET ID:

REQUESTOR: FRED GELBARD
SAMPLE MATRIX: BRINE
REQUISITION: 7070

DATE: 16-APR-92
LAB ID: 195512

PROJECT NUMBER: 680007000
DATE RECEIVED: 25-FEB-92
DATE COLLECTED: 16-DEC-91

ANALYSIS REQUESTED	RESULTS	RESULTS	RESULTS	UNITS	RPD	METHOD OF ANALYSIS
Silver	<0.1			MG/L		AS-5 R04
Aluminum	<0.05			MG/L		AS-2 R05
Boron	25.6	27.5	26.2	MG/L	4.	AS-5 R04
Bromide	22.3	22.7		MG/L	-2.	D-3 R08
Calcium	845	818		MG/L	3.	AS-5 R04
Cadmium	<0.05			MG/L		AS-6 R03
Chloride	19300	19300		MG/L	0.	D-3 R08
Chromium	<0.1			MG/L		AS-5 R04
Copper	<0.25			MG/L		AS-5 R04
Fluoride	1.6	1.6		MG/L	0.	D-3 R08
Iron	<0.50			MG/L		AS-5 R04
Iodide	0.09	0.09		MG/L	0.	D-3 R08
Potassium	310	331	329	MG/L	4.	AS-1 R04
Lithium	0.325	0.348		MG/L	-7.	AS-6 R03
Magnesium	426	412		MG/L	3.	AS-5 R04
Manganese	<0.15			MG/L		AS-5 R04
Molybdenum	<0.5			MG/L		AS-5 R04
Sodium	14000	13600		MG/L	3.	AS-5 R04
Ammonium	<0.10			MG/L		F-6 R05
Nitrate	<0.2	<0.2		MG/L		D-3 R08
Lead	<0.03			MG/L		AS-6 R03
pH	7.56	7.63			-1.	H-4 R03
Phosphate	<0.1			MG/L		F-4 R05
Antimony	<0.6			MG/L		AS-5 R04
Specific Gravity	1.03	1.03		G/CC	0.	K-4 R01
Silica	9.59	10.1	10.4	MG/L	4.	AS-5 R04
Sulfate	7320	7210		MG/L	2.	D-3 R08
Strontium	9.61	9.81		MG/L	-2.	AS-5 R04
Total Dissolved Solids	44000	44000		MG/L	0.	K-3 R04
Titanium	<1			MG/L		AS-5 R04
Total Inorganic Carbon	11.8	11.5		MG/L	3.	K-5 R03
Uranium	<0.05			MG/L		AS-6 R03
Vanadium	<0.5			MG/L		AS-5 R04
Zinc	<0.2			MG/L		AS-5 R04

(SECTION I)

ANALYTICAL RESULTS

CUSTOMER ID: VPX 26 D
TICKET ID:

REQUESTOR: FRED GELBARD
SAMPLE MATRIX: BRINE
REQUISITION: 7070

DATE: 16-APR-92
LAB ID: 195513

PROJECT NUMBER: 680007000
DATE RECEIVED: 25-FEB-92
DATE COLLECTED: 16-DEC-91

ANALYSIS REQUESTED	RESULTS	RESULTS	RESULTS	UNITS	RPD	METHOD OF ANALYSIS
Silver	<0.1	<0.1		MG/L		AS-5 R04
Aluminum	<0.05			MG/L		AS-2 R05
Boron	26.4	26.7		MG/L	-1.	AS-5 R04
Bromide	22.8	22.9		MG/L	0.	D-3 R08
Calcium	857	823		MG/L	4.	AS-5 R04
Cadmium	<0.05			MG/L		AS-6 R03
Chloride	19400	19500		MG/L	-1.	D-3 R08
Chromium	<0.1	<0.1		MG/L		AS-5 R04
Copper	<0.25			MG/L		AS-5 R04
Fluoride	1.5	1.6		MG/L	-6.	D-3 R08
Iron	<0.50			MG/L		AS-5 R04
Iodide	0.09	0.09		MG/L	0.	D-3 R08
Potassium	323	335	351	MG/L	4.	AS-1 R04
Lithium	0.327	0.35		MG/L	-7.	AS-6 R03
Magnesium	433	418		MG/L	4.	AS-5 R04
Manganese	<0.15			MG/L		AS-5 R04
Molybdenum	<0.5	<0.5		MG/L		AS-5 R04
Sodium	13900	13700		MG/L	1.	AS-5 R04
Ammonium	<0.10			MG/L		F-6 R05
Nitrate	<0.2	<0.2		MG/L		D-3 R08
Lead	<0.03			MG/L		AS-6 R03
pH	7.53	7.58			-1.	H-4 R03
Phosphate	<0.1			MG/L		F-4 R05
Antimony	<0.6			MG/L		AS-5 R04
Specific Gravity	1.03	1.03		G/CC	0.	K-4 R01
Silica	9.30	9.95	10.1	MG/L	4.	AS-5 R04
Sulfate	7330	7200		MG/L	2.	D-3 R08
Strontium	9.72	9.89		MG/L	-2.	AS-5 R04
Total Dissolved Solids	46000	44000		MG/L	4.	K-3 R04
Titanium	<1			MG/L		AS-5 R04
Total Inorganic Carbon	12.1	11.8		MG/L	3.	K-5 R03
Uranium	<0.05			MG/L		AS-6 R03
Vanadium	<0.5			MG/L		AS-5 R04
Zinc	<0.2			MG/L		AS-5 R04

(SECTION I)

ANALYTICAL RESULTS

CUSTOMER ID: VPX 26 E
TICKET ID:

REQUESTOR: FRED GELBARD
SAMPLE MATRIX: BRINE
REQUISITION: 7070

DATE: 16-APR-92
LAB ID: 195514

PROJECT NUMBER: 680007000
DATE RECEIVED: 25-FEB-92
DATE COLLECTED: 16-DEC-91

ANALYSIS REQUESTED	RESULTS	RESULTS	RESULTS	UNITS	RPD	METHOD OF ANALYSIS
Silver	<0.1			MG/L		AS-5 R04
Aluminum	<0.05			MG/L		AS-2 R05
Boron	26.4	27.6		MG/L	-4.	AS-5 R04
Bromide	22.2	22.7		MG/L	-2.	D-3 R08
Calcium	838	815		MG/L	3.	AS-5 R04
Cadmium	<0.05			MG/L		AS-6 R03
Chloride	19000	19300		MG/L	-2.	D-3 R08
Chromium	<0.1			MG/L		AS-5 R04
Copper	<0.25			MG/L		AS-5 R04
Fluoride	1.6	1.6		MG/L	0.	D-3 R08
Iron	<0.50			MG/L		AS-5 R04
Iodide	0.08	0.08		MG/L	0.	D-3 R08
Potassium	327	344		MG/L	-5.	AS-1 R04
Lithium	0.326	0.341		MG/L	-4.	AS-6 R03
Magnesium	421	409		MG/L	3.	AS-5 R04
Manganese	<0.15			MG/L		AS-5 R04
Molybdenum	<0.5			MG/L		AS-5 R04
Sodium	14100	13500	14000	MG/L	2.	AS-5 R04
Ammonium	<0.10			MG/L		F-6 R05
Nitrate	<0.2	<0.2		MG/L		D-3 R08
Lead	<0.03			MG/L		AS-6 R03
pH	7.45	7.55			-1.	H-4 R03
Phosphate	<0.1			MG/L		F-4 R05
Antimony	<0.6			MG/L		AS-5 R04
Specific Gravity	1.03	1.03		G/CC	0.	K-4 R01
Silica	9.42	9.80	10.3	MG/L	4.	AS-5 R04
Sulfate	7290	7170		MG/L	2.	D-3 R08
Strontium	9.54	9.73		MG/L	-2.	AS-5 R04
Total Dissolved Solids	44000	44000		MG/L	0.	K-3 R04
Titanium	<1			MG/L		AS-5 R04
Total Inorganic Carbon	12.0	11.9		MG/L	1.	K-5 R03
Uranium	<0.05			MG/L		AS-6 R03
Vanadium	<0.5			MG/L		AS-5 R04
Zinc	<0.2			MG/L		AS-5 R04

(SECTION I)

APPENDIX C

LIST OF EQUIPMENT AND MANUFACTURERS

PolyScience 730 Immersion Circulator
Serial # 926370
PolyScience
P.O. Box 48312
Niles, IL 60648
(708) 965-0611

Jupiter Viscosity Timer Model 821
Serial # J 2033-1
Jupiter Instrument Company
407 Commerce Way A15
Jupiter, FL 33458
(407) 743-8486

Mettler Portable Density/Specific Gravity Meter DA-110
Mfg. No. NJA31791
Mettler Instrument Corporation
Box 71
Hightstown, NJ 08520
(609) 488-3000

Cannon-Fenske Routine Viscometer
Viscometer No. U383 size 50
Viscometer No. U513 size 50
Cannon Instrument Company
P.O. Box 16
State College, PA 16804

Deionized Ultra Filtered Water
Lot No. 923068
Fisher Scientific Company
Fairlawn, NJ 07410
(201) 796-7100

REFERENCES

Earlougher, Robert C. Jr. 1977. Advances In Well Test Analysis. 2nd edition. Society of Petroleum Engineers of AIME, New York. Page 241.

Analytical Report. Volume I of IV. Chem-Nuclear Geotech Analytical Laboratory, Grand Junction, CO. 1992. Section 1.

Weast, Robert C. 1989. Handbook of Chemistry and Physics. 70th edition (1989-1990). Boca Raton, Florida: CRC Press, Inc.

WP08761

Sandia National Laboratories

Albuquerque, New Mexico 87185

date 13 August 1993

to Fred Gelbard, 6119

INFORMATION ONLY

from: Stephen Yeh
Stephen Yeh, 6119

subject: Viscosity Measurements of Salado Brines

Enclosed is my report on the viscosities of three Salado brines.

Copy to:
6115 R. Beauheim
6115 S. Webb
6119 D. Lucero
6119 H. Papenguth
6119 K. Robinson
6119 J.A. Romero
6119 File 3.2
6303 SWCF/WBS 1.1.5.1.5 LUC/SOW 9.9C 9/1/93

DETERMINATION OF THE VISCOSITY OF SALADO BRINES IN THE TEMPERATURE RANGE OF 20°C TO 35°C

Stephen Yeh
Department 6119
Sandia National Laboratories
August 1993

ABSTRACT

Experimentally determined values for three Salado brines (field brines L4P51 and QPBO2D, and synthetic brine SB-139-B) were measured in a temperature range of 20°C to 35°C. The viscosity values decrease with temperature from 2.572 cP ± 0.0075 cP to 1.619 cP ± .005 cP.

INTRODUCTION

The viscosity of QPBO2D Salado brine (bottled 8/16/90) was determined experimentally at two degree (Celsius) increments on 7/12-16/93. The viscosity of SB-139-B synthetic Salado brine (mixed 6/18/93) was determined on 7/19-22/93 for six temperatures: 20, 26, 27, 28, 29, and 35 degrees Celsius. The viscosity of L4P51 Salado brine (bottle date 7/22/93) was also determined for the above six temperatures on 7/26-29/93. New calibrated Cannon-Fenske viscometers (No. U736/50 for QPBO2D, No. U677/50 for SB-139-B, and No. U667/50 for L4P51) were used in conjunction with a Jupiter Viscosity Timer Model 821 and a PolyScience 730 Immersion Circulator constant temperature bath. Deionized Ultra Filtered water from Fisher Scientific Co. was used for checking the viscosity. The calibration certificates for applicable instruments and a list of equipment and manufacturers are given in the Appendices.

EXPERIMENT

The viscometer is initially rinsed with deionized water by filling the bulb with about 7.0 mL of liquid (depending on charge volume specified by manufacturer) and drawing it through and up into the capillary a few times. The water is then poured out and a fresh charge of deionized water is added. The viscometer is inserted vertically in the self-aligning holder in the constant temperature bath (initially set at 20°C) and left for about ten minutes to allow the liquid inside to equilibrate. The temperature in the bath is monitored by a calibrated thermocouple. (See Appendix for calibration certificate).

To check the viscometer, the meniscus of the water is allowed to flow freely past two marked points. Light timers that are activated by the refraction change as the meniscus passes the

sensor are mounted across the markings. The elapsed, or efflux, time is recorded. To convert the efflux time to viscosity in centipoise, it is multiplied by the viscometer constant (supplied and verified by the manufacturer -- viscometer constants are given for 40°C and 100°C and are extrapolated to the desired testing temperatures) and then multiplied by the density of the liquid being tested. In the case of the deionized water check, the densities at varying temperatures were taken from the Handbook of Chemistry and Physics (Weast, 1990, page F-4). About five runs are made and recorded at each temperature.

If the determined viscosity values for deionized water agree within a couple percent of the tabulated viscosities (from Weast, 1990, page F-40) then the brine can now be tested. The same rinsing procedure used with deionized water is used with brine (i.e. about 1-4 mL drawn in, rinsed, poured out and refilled). Again the viscometer is allowed to reach testing temperature and then flow times are recorded. Ten runs are made at each temperature.

Following the brine test-runs, deionized water is used again (same procedure for rinsing, etc.) and values compared to previous values to check for large discrepancies or errors such as brine precipitation and blockage of the viscometer capillary. Again, about five time values are recorded. Once assured there are no significant discrepancies, the water bath is raised to the next desirable temperature, and the above procedure is repeated.

Brine densities are recorded at various temperatures (about 20°C to 35°C) using a Mettler Portable Density/Specific Gravity Meter model DA-110. The meter is checked with deionized water and densities verified to be accurate to three decimal places.

RESULTS

Tables 1, 2, and 3 show summaries of the data for the QPBO2D, SB-139-B, and L4P51 brines respectively. Given are averages of the individual times and temperatures (not reprinted here), one standard deviation, two standard deviations, densities, number of points or readings, and calculated viscosities and errors.

Errors refer only to the viscosity calculations and were calculated as follows: For the deionized water checks, percent error is relative to tabulated book values from the Handbook of Chemistry and Physics. For the standard deviations, errors reflect what percent of the average viscosity the deviation is (i.e. deviation divided by average viscosity multiplied by 100% = error). Temperature standard deviations indicate temperature fluctuations or error over time, not actual thermocouple calibration error.

Tables 4, 5, and 6 briefly summarize the determined viscosities and densities and their respective temperatures for the three brines.

Table 7 gives the composition of the synthetic Salado brine.

Following are seven graphs. The graphs for the viscosity and density of Salado brines show a general decreasing trend with

increasing temperature. The first six graphs show how the density (Figures 1, 3, and 5) and viscosity (Figures 2, 4, and 6) of QPBO2D, SB-139-B, and L4P51 vary with temperature. In Figures 2, 4, and 6, error bars are included for temperature and viscosity and indicate two standard deviations (about 95% confidence). Again, temperature error bars indicate fluctuations over time, not thermocouple error. The thermocouple error (see Appendix A) is about +0.1°C, which means the measured temperatures are about 0.1°C too high. This results in an error in the viscosity calculations of less than one-half of one percent (for example, viscosities read off of Figure 1 may be 0.004 cP too high). For the densities in Figures 1, 3, and 5, since measurements were not repeated for a given temperature, (constant temperature is too hard to keep without fluctuation) there are no error bars, but estimated density error is about 0.001 to 0.005 g/mL or about 0.1 to 0.5%. (Note: This was not added into the error calculation for viscosity). The equation for the line fits were derived using the method of least squares. The seventh graph shows the viscosity trends of all three Salado brines on the same scale for comparison.

DISCUSSION

The errors calculated for the experimental viscosities of the brines were mostly less than 0.5% and show experimental consistency. Taking into account thermocouple (calibration) error and density error adds only about 0.5% at most to the viscosity values. The deionized water viscosities differed from published values by no more than 2.4% for all tests. Even if one takes into account that the times increase slightly for progressing runs at the same temperature (i.e. pre-check times versus post-check times), and therefore probably for the whole test, the error remains near or under 3%.

The density measurements were harder to take because the meter drifted during measurements. The drift was probably due to the brine changing temperature when introduced into the meter. Also, the meter's thermometer was too inaccurate (it usually did not change much, if at all), so the same thermocouple as for the water bath was used. Density values in Tables 1, 2, and 3 for the brines were extrapolated from the line fit equations.

Comparing the viscosities for the different brines show that L4P51 values are consistently 0.05 cP to 0.10 cP higher than the QPBO2D values. The QPBO2D values in turn are consistently about 0.15 cP higher than the SB-139-B values. All this is to say the curves for the three Salado brines are very nearly parallel (as seen in Figure 7). This would suggest that the QPBO2D and L4P51 brines may be more concentrated in solutes than SB-139-B (which has lower viscosities). This could be because SB-139-B is a synthetic and therefore probably not as saturated as a natural brine. From previous viscosity experiments with Culebra brines, it seems that even a seemingly minor change in concentration is noticeable in the experimental data; the actual data show that a 5.9% increase in

salt or solute results in an average increase of 2.7% in the viscosity. This suggests that brine viscosities are sensitive to such small changes in concentration.

CONCLUSION

The experimental procedure for determining the viscosity of brine seems to be very consistent and relatively simple. The accuracy of the results is limited only by the accuracy of the thermocouple (small at about 0.1°C), time variations in the constant temperature water bath (which appeared minimal at about 0.1°C and could also include the thermocouple error), and possible clogging in the viscometer due to precipitation of brine or particulates. Though no visible problems were noted, sometimes the efflux times for the water checks dropped over time (i.e. after maybe five or more flow measurements). This may indicate that the viscometer is cleaning itself out slowly when it has water soaking in it; but, times do not change by more than about one or two seconds. Possible considerations regarding this may include more water checks.

The Salado brine viscosities seem like they would be similar to viscosities of a comparable percent by weight sodium chloride solution but there are no available saline solution data available for comparison.

TABLE 1

C=calib. const.
Viscosity=pCt: p=density (g/mL) C=0.0040328 to 0.0040373 (cSt/s) t=time (s)

Approximate tempurature:			Temp(C)	Time(s)	Visc.(cP)	%error
20 degrees (C)	pre-check	Average:	19.99	251.5	1.014	1.2
	6pts	Std.Dev.:	0.04	0.23	0.0009	0.09
	p=.9982	2 Std. Dev.:	0.08	0.46	0.0019	0.19
	Brine test	Average:	20.07	508.5	2.473	
	10pts	Std.Dev.:	0.05	0.62	0.003	0.12
	p=1.2046	2 Std. Dev.:	0.1	1.24	0.006	0.24
	post-check	Average:	20.02	252.2	1.016	1.4
	5pts	Std.Dev.:	0.04	0.19	0.0008	0.08
	p=.9982	2 Std. Dev.:	0.09	0.39	0.0016	0.16
22 degrees (C)	pre-check	Average:	22.05	240	0.9666	1.2
	5pts	Std.Dev.:	0.04	0.23	0.0009	0.09
	p=.9978	2 Std. Dev.:	0.07	0.46	0.0019	0.2
	Brine test	Average:	22.05	485.6	2.355	
	10pts	Std.Dev.:	0.02	0.67	0.0032	0.14
	p=1.2017	2 Std. Dev.:	0.05	1.35	0.0065	0.28
	post-check	Average:	22.05	240.2	0.9674	1.3
	5pts	Std.Dev.:	0.04	0.09	0.0004	0.04
	p=.9978	2 Std. Dev.:	0.07	0.18	0.0007	0.07
24 degrees (C)	pre-check	Average:	24.01	229.5	0.9237	1.4
	5pts	Std.Dev.:	0.04	0.04	0.0002	0.02
	p=.9973	2 Std. Dev.:	0.08	0.09	0.0004	0.04
	Brine test	Average:	24.04	463.5	2.243	
	11pts	Std.Dev.:	0.02	0.45	0.0022	0.1
	p=1.1988	2 Std. Dev.:	0.04	0.9	0.0044	0.2
	post-check	Average:	24.03	229.6	0.9241	1.4
	5pts	Std.Dev.:	0.03	0.4	0.0016	0.17
	p=.9973	2 Std. Dev.:	0.05	0.8	0.0032	0.35

TABLE 1
(cont'd)

Approximate tempurature:			Temp(C)	Time(s)	Visc.(cP)	%error
26 degrees (C)	pre-check	Average:	26.04	217.9	0.8765	0.6
	5pts	Std.Dev.:	0.04	0.15	0.0006	0.07
	p=.9968	2 Std. Dev.:	0.08	0.3	0.0012	0.14
	Brine test	Average:	26.02	439.4	2.12	
	10pts	Std.Dev.:	0.03	0.15	0.0007	0.03
	p=1.1959	2 Std. Dev.:	0.05	0.3	0.0014	0.07
	post-check	Average:	25.97	219.6	0.8833	1.5
	5pts	Std.Dev.:	0.03	0.35	0.0014	0.16
	p=.9968	2 Std. Dev.:	0.05	0.7	0.0028	0.32
28 degrees (C)	pre-check	Average:	27.97	210.3	0.8453	1.5
	5pts	Std.Dev.:	0.03	0.04	0.0002	0.02
	p=.9962	2 Std. Dev.:	0.05	0.09	0.0004	0.05
	Brine test	Average:	28.01	422.4	2.033	
	10pts	Std.Dev.:	0.02	0.08	0.0004	0.02
	p=1.1930	2 Std. Dev.:	0.04	0.16	0.0008	0.04
	post-check	Average:	28.01	210.9	0.8477	1.8
	5pts	Std.Dev.:	0.07	0.15	0.0006	0.07
	p=.9962	2 Std. Dev.:	0.15	0.3	0.0012	0.14
30 degrees (C)	pre-check	Average:	29.94	202.3	0.8125	1.9
	6pts	Std.Dev.:	0.04	0.13	0.0005	0.06
	p=.9956	2 Std. Dev.:	0.08	0.25	0.001	0.12
	Brine test	Average:	30.02	404.9	1.944	
	10pts	Std.Dev.:	0.06	0.5	0.0024	0.12
	p=1.1900	2 Std. Dev.:	0.13	1	0.0048	0.25
	post-check	Average:	29.95	202.8	0.8145	2.1
	5pts	Std.Dev.:	0	0.08	0.0003	0.04
	p=.9956	2 Std. Dev.:	0	0.17	0.0007	0.09

TABLE 1
(cont'd)

Approximate tempurature:			Temp(C)	Time(s)	Visc.(cP)	%error
32 degrees (C)	pre-check	Average:	32.01	194.3	0.7798	2
	5pts	Std.Dev.:	0.02	0.09	0.0004	0.05
	p=.9950	2 Std. Dev.:	0.04	0.18	0.0007	0.09
	Brine test	Average:	32.01	389.4	1.865	
	12pts	Std.Dev.:	0.05	3.28	0.0157	0.84
	p=1.1871	2 Std. Dev.:	0.09	6.56	0.0314	1.7
	post-check	Average:	32	194.7	0.7814	2.2
	5pts	Std.Dev.:	0.04	0.26	0.001	0.13
	p=.9950	2 Std. Dev.:	0.07	0.52	0.0021	0.27
34 degrees (C)	pre-check	Average:	33.99	186	0.7459	1.6
	7pts	Std.Dev.:	0.05	0.3	0.0012	0.16
	p=.9944	2 Std. Dev.:	0.1	0.6	0.0024	0.32
	Brine test	Average:	34.04	370.9	1.771	
	10pts	Std.Dev.:	0.02	0.3	0.0015	0.08
	p=1.1841	2 Std. Dev.:	0.04	0.6	0.0029	0.16
	post-check	Average:	33.97	187.1	0.7503	2.2
	5pts	Std.Dev.:	0.04	0.2	0.0008	0.11
	p=.9944	2 Std. Dev.:	0.09	0.4	0.0016	0.21

TABLE 2

C=calib. const.
Viscosity=pCt: p=density (g/mL) C=0.0041808 to 0.0041860 (cSt/s) t=time (s)

Approximate tempurature:			Temp(C)	Time(s)	Visc.(cP)	%error
20 degrees (C)	pre-check	Average:	20.04	243.8	1.019	1.7
	5pts	Std.Dev.:	0.02	0.09	0.0004	0.04
	p=.9982	2 Std. Dev.:	0.04	0.18	0.0008	0.08
	Brine test	Average:	20.05	458.5	2.301	
	11pts	Std.Dev.:	0.04	0.51	0.0025	0.11
	p=1.1988	2 Std. Dev.:	0.08	1.02	0.0051	0.22
	post-check	Average:	20.07	244.7	1.022	2
	5pts	Std.Dev.:	0.04	0.33	0.0014	0.14
	p=.9982	2 Std. Dev.:	0.09	0.67	0.0028	0.27
26 degrees (C)	pre-check	Average:	26.03	211	0.88	1.1
	6pts	Std.Dev.:	0.03	0.15	0.0006	0.07
	p=.9968	2 Std. Dev.:	0.05	0.29	0.0012	0.14
	Brine test	Average:	26.04	400	1.991	
	11pts	Std.Dev.:	0.04	0.38	0.0019	0.1
	p=1.1897	2 Std. Dev.:	0.08	0.76	0.0038	0.19
	post-check	Average:	25.99	211.5	0.8821	1.3
	5pts	Std.Dev.:	0.02	0.11	0.0005	0.06
	p=.9968	2 Std. Dev.:	0.04	0.22	0.0009	0.1
27 degrees (C)	pre-check	Average:	27	207.8	0.8664	1.8
	5pts	Std.Dev.:	0.04	0.23	0.001	0.12
	p=.9965	2 Std. Dev.:	0.07	0.46	0.0019	0.22
	Brine test	Average:	27	392.7	1.952	
	10pts	Std.Dev.:	0.02	0.37	0.0018	0.09
	p=1.1883	2 Std. Dev.:	0.05	0.75	0.0037	0.19
	post-check	Average:	26.96	208.9	0.871	2.3
	5pts	Std.Dev.:	0.02	0.14	0.0006	0.07
	p=.9965	2 Std. Dev.:	0.04	0.28	0.0012	0.14

TABLE 2
(cont'd)

Approximate tempurature:			Temp(C)	Time(s)	Visc.(cP)	%error
28 degrees (C)	pre-check	Average:	27.95	204.6	0.8526	2.4
	5pts	Std.Dev.:	0	0.08	0.0003	0.04
	p=.9962	2 Std. Dev.:	0	0.17	0.0007	0.08
	Brine test	Average:	27.96	382.4	1.899	
	10pts	Std.Dev.:	0.02	0.44	0.0022	0.12
	p=1.1868	2 Std. Dev.:	0.04	0.88	0.0044	0.23
	post-check	Average:	27.95	203.3	0.8472	1.7
	5pts	Std.Dev.:	0	0.04	0.0002	0.02
	p=.9962	2 Std. Dev.:	0	0.09	0.0004	0.05
29 degrees (C)	pre-check	Average:	28.98	198.8	0.8282	1.6
	5pts	Std.Dev.:	0.03	0.09	0.0004	0.05
	p=.9959	2 Std. Dev.:	0.05	0.18	0.0007	0.08
	Brine test	Average:	29.04	373.4	1.851	
	10pts	Std.Dev.:	0.02	0.48	0.0023	0.12
	p=1.1852	2 Std. Dev.:	0.05	0.95	0.0047	0.25
	post-check	Average:	29	198.5	0.8269	1.5
	5pts	Std.Dev.:	0	0.09	0.0004	0.05
	p=.9959	2 Std. Dev.:	0	0.18	0.0007	0.08
35 degrees (C)	pre-check	Average:	34.99	175.9	0.731	1.6
	6pts	Std.Dev.:	0.02	0.09	0.0004	0.05
	p=.9940	2 Std. Dev.:	0.04	0.18	0.0007	0.1
	Brine test	Average:	35.01	329.3	1.619	
	10pts	Std.Dev.:	0.03	0.09	0.0025	0.15
	p=1.1761	2 Std. Dev.:	0.06	0.18	0.005	0.31
	post-check	Average:	34.99	176.8	0.7347	2.1
	5pts	Std.Dev.:	0.02	0.16	0.0007	0.1
	p=.9940	2 Std. Dev.:	0.04	0.33	0.0014	0.19

TABLE 3

C=calib. const.
Viscosity=pCt: p=density (g/mL) C=0.0039857 to 0.0039907 (cSt/s) t=time (s)

Approximate tempurature:			Temp(C)	Time(s)	Visc.(cP)	%error
20 degrees (C)	pre-check 5pts p=.9982	Average:	20.04	254.6	1.014	1.2
		Std.Dev.:	0.02	0.08	0.0003	0.03
		2 Std. Dev.:	0.04	0.17	0.0006	0.06
	Brine test 10pts p=1.2230	Average:	20.01	527	2.572	
		Std.Dev.:	0.02	0.77	0.0038	0.15
		2 Std. Dev.:	0.04	1.54	0.0075	0.29
	post-check 5pts p=.9982	Average:	20.03	255.4	1.017	1.5
		Std.Dev.:	0.03	0.09	0.0004	0.04
		2 Std. Dev.:	0.05	0.18	0.0007	0.07
26 degrees (C)	pre-check 6pts p=.9968	Average:	25.99	220.1	0.8751	0.53
		Std.Dev.:	0.02	0	0	0
		2 Std. Dev.:	0.04	0	0	0
	Brine test 10pts p=1.2127	Average:	26.04	452.1	2.187	
		Std.Dev.:	0.02	0.26	0.0013	0.06
		2 Std. Dev.:	0.05	0.52	0.0025	0.11
	post-check 5pts p=.9968	Average:	25.99	221.2	0.8795	1
		Std.Dev.:	0.04	0.26	0.001	0.11
		2 Std. Dev.:	0.08	0.52	0.002	0.23
27 degrees (C)	pre-check 5pts p=.9965	Average:	26.94	216.5	0.8604	1.1
		Std.Dev.:	0.02	0	0	0
		2 Std. Dev.:	0.04	0	0	0
	Brine test 10pts p=1.2110	Average:	26.98	441.3	2.131	
		Std.Dev.:	0.03	0.69	0.0033	0.15
		2 Std. Dev.:	0.05	1.37	0.0066	0.31
	post-check 5pts p=.9965	Average:	27	215.9	0.8581	0.8
		Std.Dev.:	0	0.23	0.0009	0.1
		2 Std. Dev.:	0	0.47	0.0019	0.22

TABLE 3
(cont'd)

Approximate tempurature:			Temp(C)	Time(s)	Visc.(cP)	%error
28 degrees (C)	pre-check	Average:	27.94	211.1	0.8387	0.72
	5pts	Std.Dev.:	0.04	0.04	0.0002	0.02
	p=.9962	2 Std. Dev.:	0.08	0.09	0.0003	0.04
	Brine test	Average:	28	430.7	2.077	
	10pts	Std.Dev.:	0.02	0.82	0.004	0.19
	p=1.2093	2 Std. Dev.:	0.03	1.64	0.0079	0.38
	post-check	Average:	28.02	212.2	0.843	1.2
	5pts	Std.Dev.:	0.03	0.09	0.0004	0.05
	p=.9962	2 Std. Dev.:	0.05	0.18	0.0007	0.08
29 degrees (C)	pre-check	Average:	28.97	207.8	0.8257	1.3
	5pts	Std.Dev.:	0.04	0.11	0.0004	0.05
	p=.9959	2 Std. Dev.:	0.09	0.22	0.0009	0.11
	Brine test	Average:	28.99	421.9	2.033	
	10pts	Std.Dev.:	0.03	0.65	0.0032	0.16
	p=1.2075	2 Std. Dev.:	0.07	1.3	0.0063	0.31
	post-check	Average:	29.01	207.9	0.8261	1.4
	5pts	Std.Dev.:	0.02	0.11	0.0004	0.05
	p=.9959	2 Std. Dev.:	0.04	0.23	0.0009	0.11
35 degrees (C)	pre-check	Average:	34.95	183.9	0.7286	1.3
	5pts	Std.Dev.:	0	0.05	0.0002	0.03
	p=.9940	2 Std. Dev.:	0	0.11	0.0004	0.05
	Brine test	Average:	34.95	371.9	1.775	
	10pts	Std.Dev.:	0	0.06	0.0003	0.02
	p=1.1973	2 Std. Dev.:	0	0.13	0.0006	0.03
	post-check	Average:	34.95	184.7	0.7317	1.7
	5pts	Std.Dev.:	0	0.05	0.0002	0.03
	p=.9940	2 Std. Dev.:	0	0.11	0.0004	0.05

TABLE 4

DATA SUMMARY
PROPERTIES OF QPBO2D SALADO BRINE

Computed (From Measured) Values:

Temperature (°C)	Viscosity (cP)
20.07	2.473
22.05	2.355
24.04	2.243
26.02	2.120
28.01	2.033
30.02	1.944
32.01	1.865
34.04	1.770

Measured Values:

	Temperature (°C)	Density (g/mL)
In order taken:	18.8	1.2090
	19.9	1.2060
	20.3	1.2040
	22.5	1.1993
	24.6	1.1957
	27.4	1.1930
	28.7	1.1910
	30.3	1.1890
	31.0	1.1880
	32.0	1.1869
	34.4	1.1850
	33.1	1.1857
	32.7	1.1864
	31.9	1.1875
	31.3	1.1885
	30.5	1.1901
	29.7	1.1917
	28.0	1.1930
	26.9	1.1932

TABLE 5

DATA SUMMARY
PROPERTIES OF SB-139-B SYNTHETIC SALADO BRINE

Computed (From Measured) Values:

Temperature (°C)	Viscosity (cP)
20.05	2.301
26.04	1.991
27.00	1.952
27.96	1.899
29.04	1.851
35.01	1.619

Measured Values:

	Temperature (°C)	Density (g/mL)
In order taken:	18.6	1.2020
	19.5	1.1999
	20.2	1.1982
	20.5	1.1975
	21.2	1.1963
	21.8	1.1959
	22.9	1.1946
	23.5	1.1937
	24.4	1.1922
	26.0	1.1910
	26.8	1.1895
	29.6	1.1865
	27.0	1.1875
	28.7	1.1856
	27.7	1.1880
	29.4	1.1860
	30.0	1.1830
	31.7	1.1802
	33.4	1.1803
	35.0	1.1771
	34.2	1.1782
	31.0	1.1825
	29.0	1.1855
	28.0	1.1864
	27.3	1.1871
	24.7	1.1913
	23.8	1.1921
	25.5	1.1899
	22.8	1.1932
	21.4	1.1942
	30.5	1.1837
	28.6	1.1850
	32.5	1.1805

TABLE 6

DATA SUMMARY
PROPERTIES OF L4P51 SALADO BRINE

Computed (From Measured) Values:

Temperature (°C)	Viscosity (cP)
20.01	2.572
26.02	2.187
26.98	2.131
28.00	2.077
28.99	2.033
34.95	1.775

Measured Values:

	Temperature (°C)	Density (g/mL)
In order taken:	22.2	1.2238
	23.0	1.2165
	23.8	1.2135
	26.1	1.2110
	28.2	1.2088
	30.2	1.2064
	31.5	1.2050
	34.5	1.2022
	34.5	1.2011
	32.3	1.2022
	30.8	1.2040
	29.0	1.2065
	26.9	1.2083
	26.3	1.2099
	25.4	1.2110
	25.1	1.2109
	24.6	1.2125
	24.0	1.2132
	23.5	1.2134
	20.9	1.2250
	17.9	1.2290
	18.8	1.2285
	21.2	1.2248

TABLE 7

COMPOSITION OF SB-139-B SYNTHETIC SALADO BRINE

Compound	Quantity (g/L)
$NaHCO_3$	*
$CaCl_2*2H_2O$	1.2790
$MgSO_4$	19.9259
$MgCl_2*6H_2O$	130.6083
KCl	32.3960
NaCl	203.1150
$Na_2B_4O_7$	7.0018
NaBr	1.8745

* Did not have appropriate equipment to accurately meausure out 0.00013 g of a salt.

pH = 6.15

Figure 1

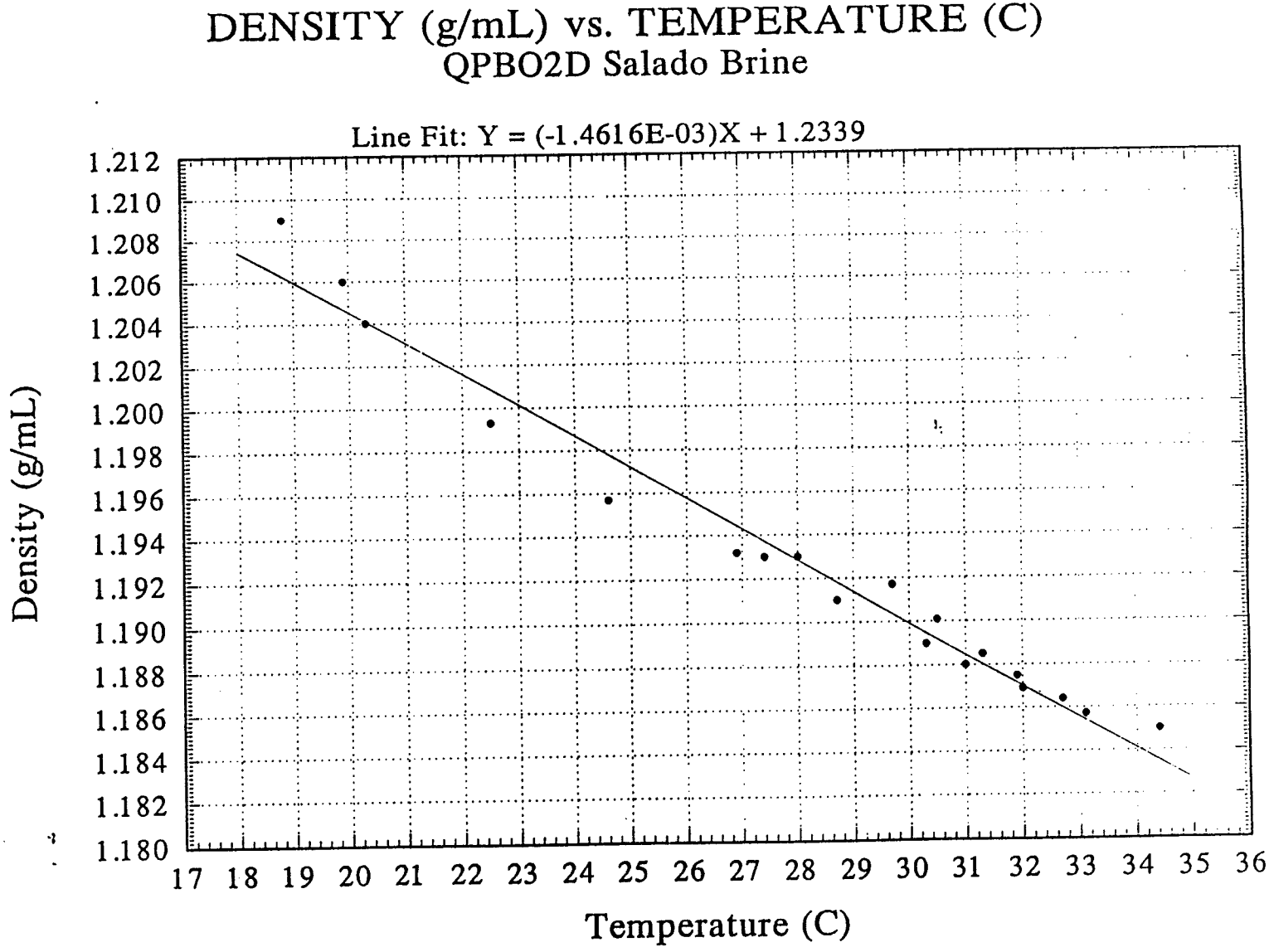
DENSITY (g/mL) vs. TEMPERATURE (C)
QPBO2D Salado Brine
Line Fit: Y = (-1.4616E-03)X + 1.2339
Density (g/mL)
1.212
1.210
1.208
1.206
1.204
1.202
1.200
1.198
1.196
1.194
1.192
1.190
1.188
1.186
1.184
1.182
1.180
17 18 19 20 21 22 23 24 25 26 27 28 29 30 31 32 33 34 35 36
Temperature (C)

Figure 2

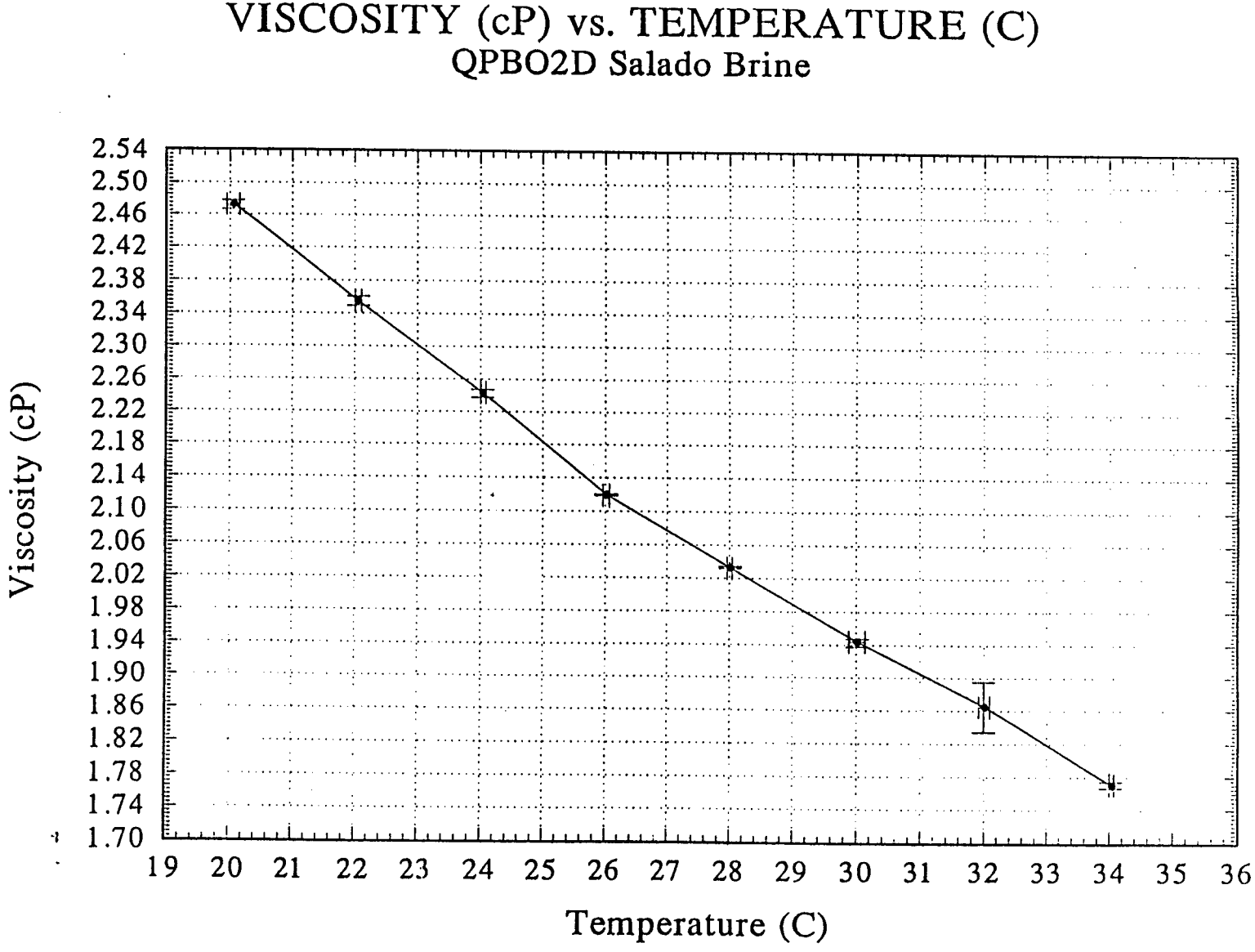
VISCOSITY (cP) vs. TEMPERATURE (C)
QPBO2D Salado Brine
Viscosity (cP)
2.54
2.50
2.46
2.42
2.38
2.34
2.30
2.26
2.22
2.18
2.14
2.10
2.06
2.02
1.98
1.94
1.90
1.86
1.82
1.78
1.74
1.70
19 20 21 22 23 24 25 26 27 28 29 30 31 32 33 34 35 36
Temperature (C)

Figure 3

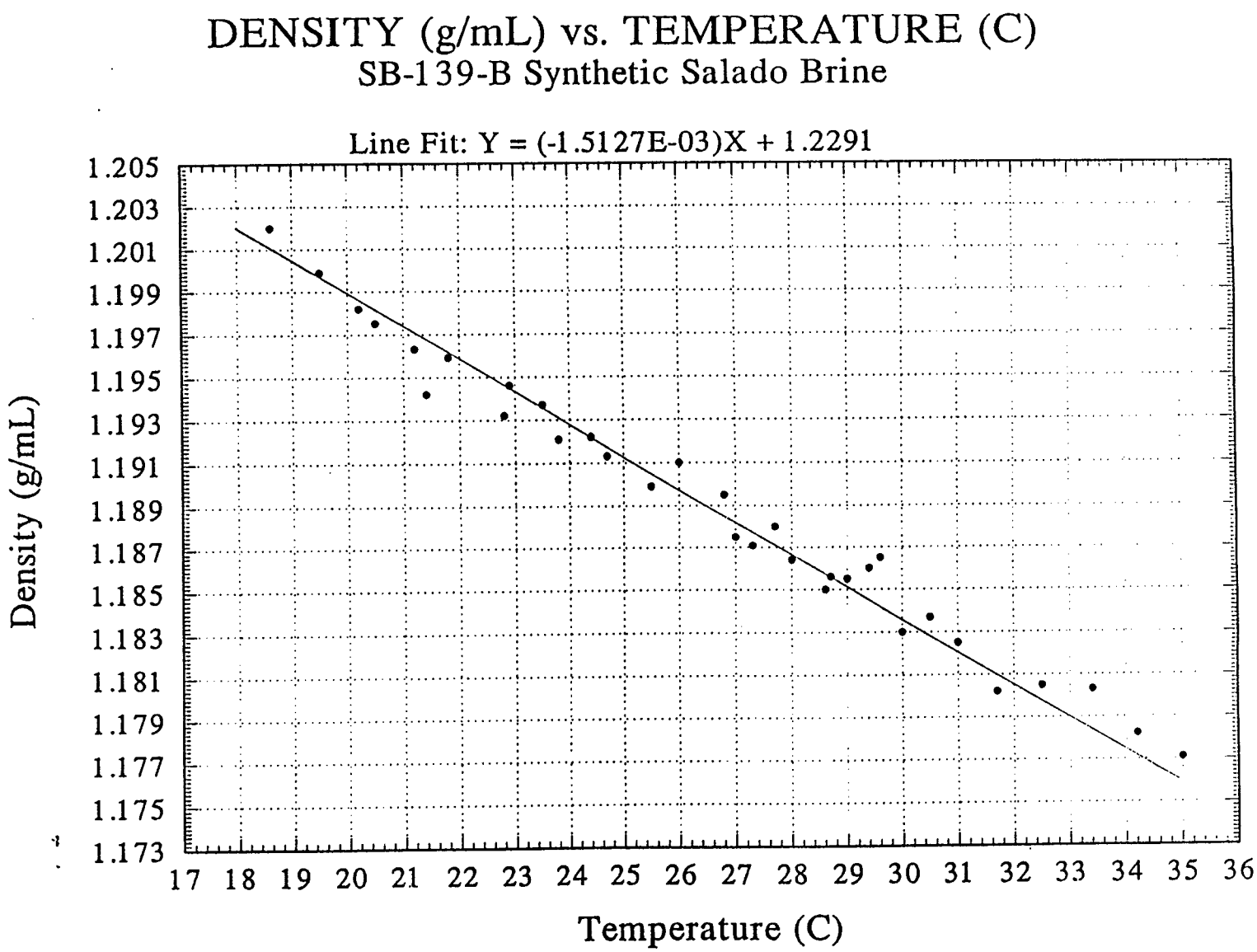
DENSITY (g/mL) vs. TEMPERATURE (C)
SB-139-B Synthetic Salado Brine
Line Fit: Y = (-1.5127E-03)X + 1.2291
Density (g/mL)
1.205
1.203
1.201
1.199
1.197
1.195
1.193
1.191
1.189
1.187
1.185
1.183
1.181
1.179
1.177
1.175
1.173
17 18 19 20 21 22 23 24 25 26 27 28 29 30 31 32 33 34 35 36
Temperature (C)

Figure 4

VISCOSITY (cP) vs. TEMPERATURE (C)

SB-139-B Synthetic Salado Brine

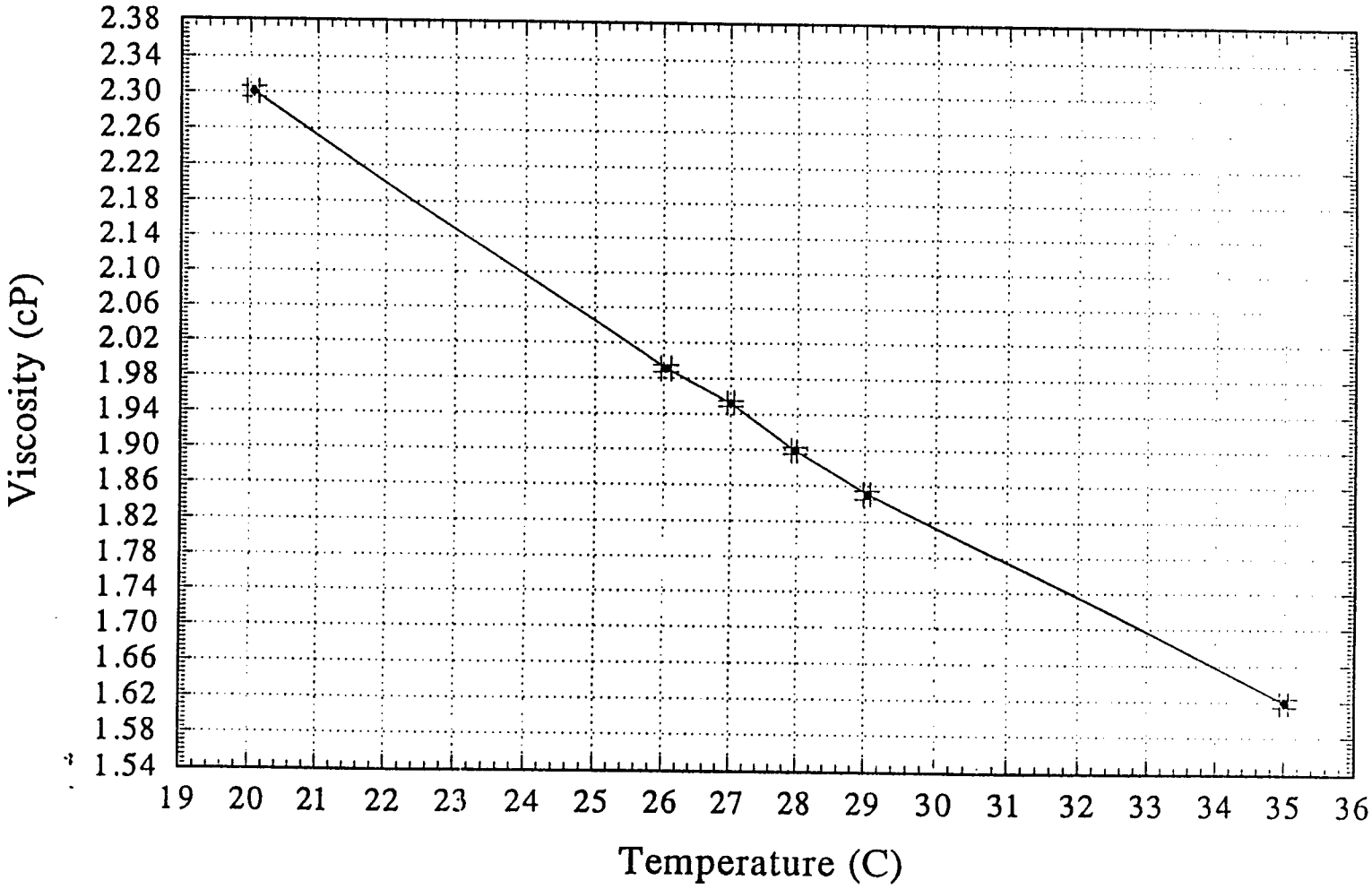

Figure 5

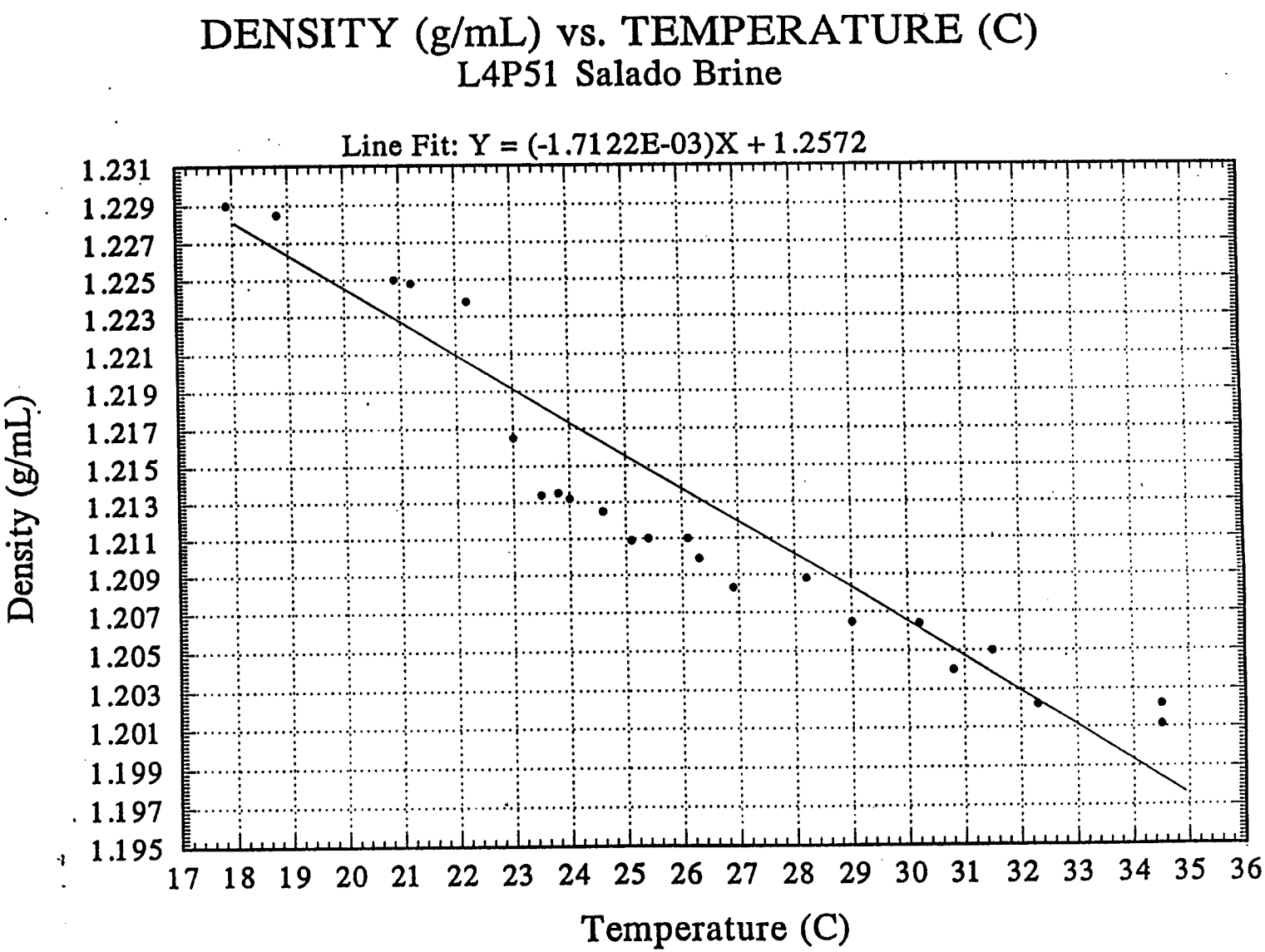
DENSITY (g/mL) vs. TEMPERATURE (C)
L4P51 Salado Brine
Line Fit: Y = (-1.7122E-03)X + 1.2572
Density (g/mL)
1.231
1.229
1.227
1.225
1.223
1.221
1.219
1.217
1.215
1.213
1.211
1.209
1.207
1.205
1.203
1.201
1.199
1.197
1.195
17 18 19 20 21 22 23 24 25 26 27 28 29 30 31 32 33 34 35 36
Temperature (C)

Figure 6

VISCOSITY (cP) vs. TEMPERATURE (C)

L4P51 Salado Brine

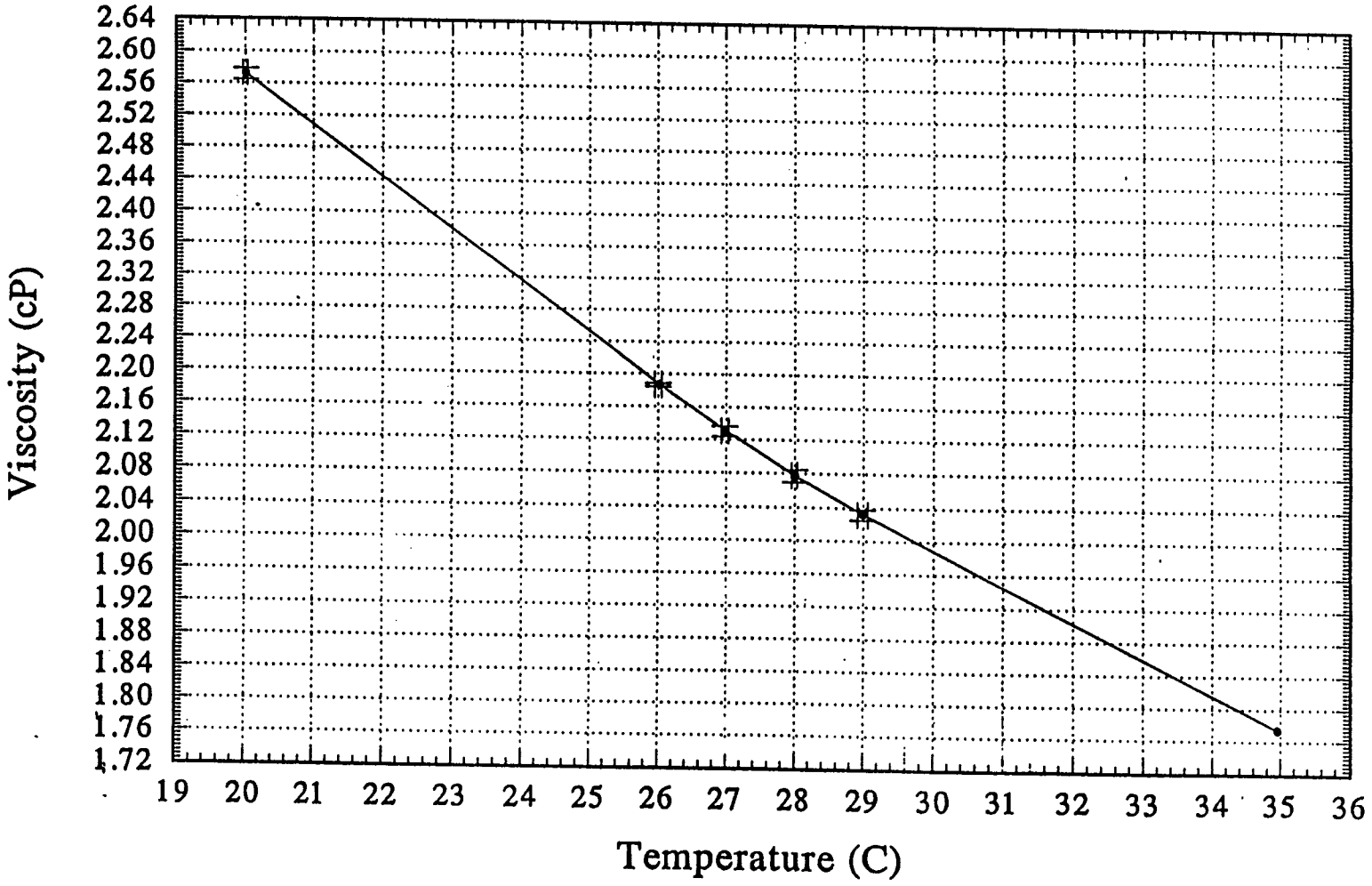

Figure 7

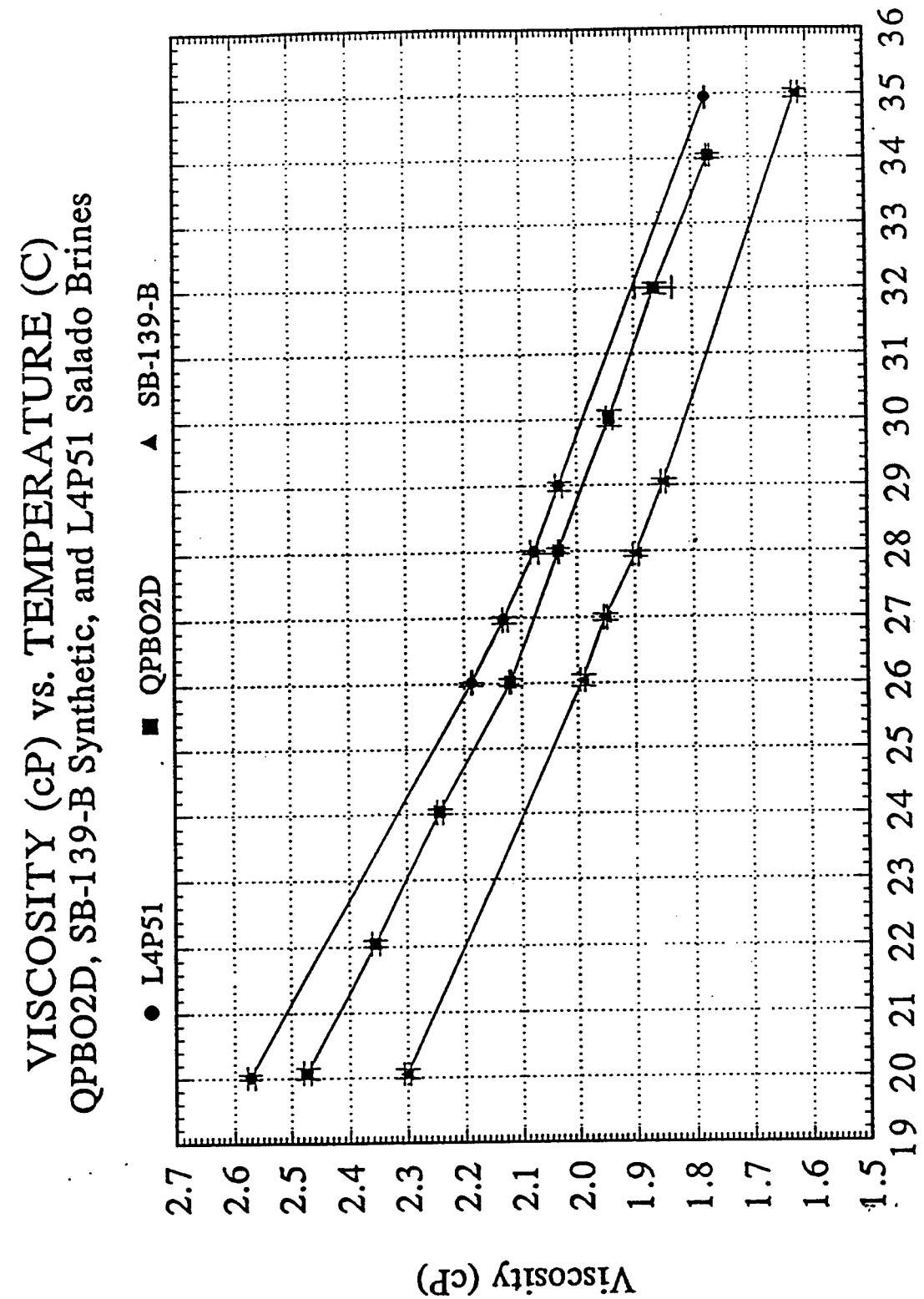
VISCOSITY (cP) vs. TEMPERATURE (C)
QPBO2D, SB-139-B Synthetic, and L4P51 Salado Brines
● L4P51
■ QPBO2D
▲ SB-139-B
Viscosity (cP)
2.7
2.6
2.5
2.4
2.3
2.2
2.1
2.0
1.9
1.8
1.7
1.6
1.5
19 20 21 22 23 24 25 26 27 28 29 30 31 32 33 34 35 36
Temperature (C)

APPENDIX A

CERTIFICATES OF CALIBRATION

Temp °C	Constant (cSt/s
20	.00403 75
22	.00403 64
24	.00403 58
26	.00403 52
28	.00403 46
30	.00403 40
32	.00403 34
34	.00403 28

SG 7/24

Certificate of Calibration

Viscometer No. 50 U736

CANNON-FENSKE ROUTINE TYPE FOR TRANSPARENT LIQUIDS

(Standard Test ASTM D 445, IP 71 and ISO 3104)

Constant at 40°C $0.004031\ mm^2/s^2$, (cSt/s)

Constant at 100°C $0.004012\ mm^2/s^2$, (cSt/s)

The viscometer constant at other temperatures can be obtained by interpolation or extrapolation. To obtain kinematic viscosity in mm^2/s(cSt) multiply the efflux time in seconds by the viscometer constant. To obtain viscosity in mPa·s (cP) multiply the kinematic viscosity in mm^2/s(cSt) by the density in grams per milliliter.

The above constants assume a value for the coefficient of thermal expansion typical to that for mineral oil, and that the viscometer was filled with test sample at room temperature. If the filling temperature T_F is substantially different than room temperature, the viscometer constant at test temperature T_T is C_o (1 - B [T_T - T_F]). The values of C_o and B shown below are based on a coefficient of thermal expansion typical to that for a mineral oil.

Kinematic viscosities of the standards used in calibrating were established in Master Viscometers as described in Ind. Eng. Chem. Anal. Ed. 16,708(1944), ASTM D 2162, and the Journal of Research of the National Bureau of Standards, Vol. 52, No. 3, March 1954, Research Paper 2479.

Kinematic viscosities are based on the value for water adopted by the National Institute for Standards and Technology and The American Society for Testing Materials July 1, 1953. The kinematic viscosity basis is 1.0038 mm^2/s(cSt) for water at 20°C (ITS-90). The gravitational constant, g, is 980.1 cm/sec^2 at the Cannon Instrument Company. The gravitational constant varies up to 0.1% in the United States. To make this small correction in the viscometer constant, multiply the above viscometer constant by the factor [g(at your laboratory) /980.1]. The calibration data below are traceable to the National Institute for Standards and Technology. Temperature measurement traceable to NIST (Test No. 246089).

CALIBRATION DATA AT 40°C

Viscosity Standard	Kinematic Viscosity mm^2/s, (cSt)	Efflux Time Seconds	Constant mm^2/s^2, (cSt/s)
9303	1.0079	250.20	0.004028
9304	2.047	507.58	0.004033

Room Temp. (approx.) 19 °C. Average = 0.004031

Charge (approx.) 6.9 ml. C_o = 0.004037

Driving fluid head (approx.) 9.2 cm. B = 78 $x\ 10^{-6}$/°C

Working diameter of lower reservoir 3.0 cm.

Constant at 100° C. is 0.47 % lower than the constant at 40° C.

Calibrated by VSM 368048 on 08-Mar-93 under supervision of

R. E. Manning, Ph.D., P.E.
W. A. Lloyd, Ph.D., P.E.
M. R. Hoover, Ph.D.
M. K. Gerfin, C.Q.E.
Cannon Instrument Co.
State College, PA 16804, USA

Please note: This calibration remains valid for 10 years unless (1) the viscometer has been damaged or (2) materials which chemically attack borosilicate glass (e.g., hydrofluoric acid or highly alkaline solutions) have been used. Nonetheless, it is recommended that the calibration be verified with kinematic viscosity standards periodically; if a change in calibration is indicated, carefully examine all sources of error, including especially temperature measurement since most apparent changes in calibration of the viscometer are due to errors in temperature measurement.

Test No.: 368048 - 5

The S.I. unit of kinematic viscosity is 1 meter squared per second, and is equal to 10^4 stokes. The S.I. unit of viscosity is 1 pascal second, and is equal to 10 poises. One centistokes is equal to one millimeter squared per second.

Temp °C	Constant
20	.003967
26	.003967
27	.003953
28	.003950
29	.003977
35	.003957

54.7/26

Certificate of Calibration

Viscometer No. 50 U667

CANNON-FENSKE ROUTINE TYPE FOR TRANSPARENT LIQUIDS

(Standard Test ASTM D 445, IP 71 and ISO 3104)

Constant at 40°C	0.003984 mm^2/s^2, (cSt/s)
Constant at 100°C	0.003964 mm^2/s^2, (cSt/s)

The viscometer constant at other temperatures can be obtained by interpolation or extrapolation. To obtain kinematic viscosity in mm^2/s(cSt) multiply the efflux time in seconds by the viscometer constant. To obtain viscosity in mPa·s (cP) multiply the kinematic viscosity in mm^2/s(cSt) by the density in grams per milliliter.

The above constants assume a value for the coefficient of thermal expansion typical to that for mineral oil, and that the viscometer was filled with test sample at room temperature. If the filling temperature T_F is substantially different than room temperature, the viscometer constant at test temperature T_T is C_o (1 - B [T_T - T_F]). The values of C_o and B shown below are based on a coefficient of thermal expansion typical to that for a mineral oil.

Kinematic viscosities of the standards used in calibrating were established in Master Viscometers as described in Ind. Eng. Chem. Anal. Ed. 16,708(1944), ASTM D 2162, and the Journal of Research of the National Bureau of Standards, Vol. 52, No. 3, March 1954, Research Paper 2479.

Kinematic viscosities are based on the value for water adopted by the National Institute for Standards and Technology and The American Society for Testing Materials July 1, 1953. The kinematic viscosity basis is 1.0038 mm^2/s(cSt) for water at 20°C (ITS-90). The gravitational constant, g, is 980.1 cm/sec^2 at the Cannon Instrument Company. The gravitational constant varies up to 0.1% in the United States. To make this small correction in the viscometer constant, multiply the above viscometer constant by the factor [g(at your laboratory) /980.1]. The calibration data below are traceable to the National Institute for Standards and Technology. Temperature measurement traceable to NIST (Test No. 246089).

CALIBRATION DATA AT 40°C

Viscosity Standard	Kinematic Viscosity mm^2/s, (cSt)	Efflux Time Seconds	Constant mm^2/s^2, (cSt/s)
9303	1.0079	253.08	0.003983
9304	2.047	513.62	0.003985

Room Temp. (approx.) 22 °C. Average = 0.003984

Charge (approx.) 7.0 ml. C_o = 0.003990

Driving fluid head (approx.) 9.0 cm. B = 81 x 10^{-6}/°C

Working diameter of lower reservoir 3.0 cm.

Constant at 100° C. is 0.49 % lower than the constant at 40° C.

Calibrated by VSM 368036 on 23-Feb-93 under supervision of

R. E. Manning, Ph.D., P.E.
W. A. Lloyd, Ph.D., P.E.
M. R. Hoover, Ph.D.
M. K. Gerfin, C.Q.E.
Cannon Instrument Co.
State College, PA 16804, USA

Please note: This calibration remains valid for 10 years unless (1) the viscometer has been damaged or (2) materials which chemically attack borosilicate glass (e.g., hydrofluoric acid or highly alkaline solutions) have been used. Nonetheless, it is recommended that the calibration be verified with kinematic viscosity standards periodically; if a change in calibration is indicated, carefully examine all sources of error, including especially temperature measurement since most apparent changes in calibration of the viscometer are due to errors in temperature measurement.

Test No.: 368036 - 9

The S.I. unit of kinematic viscosity is 1 meter squared per second, and is equal to 10^4 stokes. The S.I. unit of viscosity is 1 pascal second, and is equal to 10 poises. One centistokes is equal to one millimeter squared per second. 991

Temp °C	Constant (cSt/s)
20	.0041866
26	.0041839
27	.0041836
28	.0041832
29	.0041833
35	.0041808

SJ. 7/22/93

Certificate of Calibration

Viscometer No. 50 U677

CANNON-FENSKE ROUTINE TYPE FOR TRANSPARENT LIQUIDS

(Standard Test ASTM D 445, IP 71 and ISO 3104)

Constant at 40°C 0.004179 mm^2/s^2, (cSt/s)

Constant at 100°C 0.004158 mm^2/s^2, (cSt/s)

The viscometer constant at other temperatures can be obtained by interpolation or extrapolation. To obtain kinematic viscosity in mm^2/s(cSt) multiply the efflux time in seconds by the viscometer constant. To obtain viscosity in mPa·s (cP) multiply the kinematic viscosity in mm^2/s(cSt) by the density in grams per milliliter.

The above constants assume a value for the coefficient of thermal expansion typical to that for mineral oil, and that the viscometer was filled with test sample at room temperature. If the filling temperature T_F is substantially different than room temperature, the viscometer constant at test temperature T_T is C_o (1 - B [T_T - T_F]). The values of C_o and B shown below are based on a coefficient of thermal expansion typical to that for a mineral oil.

Kinematic viscosities of the standards used in calibrating were established in Master Viscometers as described in Ind. Eng. Chem. Anal. Ed. 16,708(1944), ASTM D 2162, and the Journal of Research of the National Bureau of Standards, Vol. 52, No. 3, March 1954, Research Paper 2479.

Kinematic viscosities are based on the value for water adopted by the National Institute for Standards and Technology and The American Society for Testing Materials July 1, 1953. The kinematic viscosity basis is 1.0038 mm^2/s(cSt) for water at 20°C (ITS-90). The gravitational constant, g, is 980.1 cm/sec^2 at the Cannon Instrument Company. The gravitational constant varies up to 0.1% in the United States. To make this small correction in the viscometer constant, multiply the above viscometer constant by the factor [g(at your laboratory) /980.1]. The calibration data below are traceable to the National Institute for Standards and Technology. Temperature measurement traceable to NIST (Test No. 246089).

CALIBRATION DATA AT 40°C

Viscosity Standard	Kinematic Viscosity mm^2/s, (cSt)	Efflux Time Seconds	Constant mm^2/s^2, (cSt/s)
9303	1.0079	241.28	0.004177
9304	2.047	489.68	0.004180

Room Temp. (approx.) 22 °C. Average = 0.004179

Charge (approx.) 7.2 ml. C_o = 0.004185

Driving fluid head (approx.) 9.0 cm. B = 83 x 10^{-6}/°C

Working diameter of lower reservoir 3.0 cm.

Constant at 100° C. is 0.50 % lower than the constant at 40° C.

Calibrated by VSM 368038 on 23-Feb-93 under supervision of

Please note: This calibration remains valid for 10 years unless (1) the viscometer has been damaged or (2) materials which chemically attack borosilicate glass (e.g., hydrofluoric acid or highly alkaline solutions) have been used. Nonetheless, it is recommended that the calibration be verified with kinematic viscosity standards periodically; if a change in calibration is indicated, carefully examine all sources of error, including especially temperature measurement since most apparent changes in calibration of the viscometer are due to errors in temperature measurement.

R. E. Manning, Ph.D., P.E.
W. A. Lloyd, Ph.D., P.E.
M. R. Hoover, Ph.D.
M. K. Gerfin, C.Q.E.
Cannon Instrument Co.
State College, PA 16804, USA

Test No.: 368038 - 7

The S.I. unit of kinematic viscosity is 1 meter squared per second, and is equal to 10^4 stokes. The S.I. unit of viscosity is 1 pascal second, and is equal to 10 poises. One centistokes is equal to one millimeter squared per second.

991

Standards Laboratory Certificate

Sandia National Laboratories
Albuquerque, New Mexico 87185

File No. 4522

THERMOCOUPLE TYPE
OMEGA
Model No. 6" Probe
Serial No. 92321-1

Submitted by: 6119

Certified: November 16, 1992
Expires: November 16, 1993

Tests performed between the temperatures of -40 to 100 deg C show this thermocouple to be in agreement within +/- 1 deg C of the values published in IPTS-68.

Under normal use conditions it is probable this thermocouple will remain within the above accuracies for the certification interval.

Metrologist: J. J. LaMarr, 2414

Georgia Brown for
Certified by: J. M. Simons, 2414

TLC29:JJL
1/30/92

SERIAL #	MV READING	TEMPERATURE	DELTA	Δ °C
STD 257		-39.980 °C		
~~STD 400~~	-0.0001	-0.019 C	0.000	
NON	-1.5313	-40.127 C	-40.109	
NON	-1.5304	-40.103 C	-40.084	
NON	-1.5301	-40.094 C	-40.076	
NON	-1.5303	-40.100 C	-40.081	
NON	-1.5307	-40.111 C	-40.092	
NON	-1.5314	-40.130 C	-40.111	
NON	-1.5320	-40.146 C	-40.128	
NON	-1.5322	-40.152 C	-40.133	
NON	-1.5226	-39.890 C	-39.871	
NON	-1.5240	-39.928 C	-39.910	
NON	-1.5261	-39.986 C	-39.967	
NON	-1.5250	-39.955 C	-39.937	
NON	-1.5223	-39.882 C	-39.863	
NON	-1.5295	-40.078 C	-40.059	
NON	-1.5213	-39.854 C	-39.836	
NON	-1.5225	-39.887 C	-39.869	
NON	-1.5295	-40.078 C	-40.059	
NON	-1.5319	-40.119 C	-40.100	
NON	-1.5331	-40.176 C	-40.158	
3201	-1.5343	-40.209 C	-40.190	-.229 ←
3202	-1.5345	-40.214 C	-40.196	-.234
3203	-1.5252	-39.961 C	-39.942	.019
3204	-1.5247	-39.947 C	-39.928	.033

SERIAL #	MV READING	TEMPERATURE	DELTA	Δ °C
STD 257		23.520 °C		
~~STD 400~~	0.0001	0.019 C	0.000	
NON	0.9361	23.417 C	23.398	
NON	0.9361	23.417 C	23.398	
NON	0.9361	23.417 C	23.398	
NON	0.9359	23.412 C	23.393	
NON	0.9340	23.360 C	23.341	
NON	0.9364	23.424 C	23.406	
NON	0.9360	23.414 C	23.395	
NON	0.9361	23.417 C	23.398	
NON	0.9357	23.407 C	23.388	
NON	0.9351	23.392 C	23.373	
NON	0.9373	23.446 C	23.427	
NON	0.9364	23.424 C	23.405	
NON	0.9355	23.401 C	23.382	
NON	0.9352	23.393 C	23.374	
NON	0.9361	23.417 C	23.398	
NON	0.9357	23.406 C	23.387	
NON	0.9382	23.469 C	23.450	
NON	0.9388	23.483 C	23.465	
NON	0.9387	23.481 C	23.462	
3201	0.9418	23.558 C	23.539	.038 ←
3202	0.9440	23.612 C	23.593	.092
3203	0.9441	23.614 C	23.595	.094
3204	0.9438	23.607 C	23.588	.087

SERIAL #	MV READING	TEMPERATURE	DELTA	Δ °C
STD 257		64.801 °C		
~~STD. 400~~	0.0001	0.019 C	0.000	
NON	2.6406	64.945 C	64.927	
NON	2.6398	64.926 C	64.907	
NON	2.6399	64.928 C	64.910	
NON	2.6397	64.924 C	64.905	
NON	2.6399	64.928 C	64.910	
NON	2.6416	64.969 C	64.951	
NON	2.6398	64.926 C	64.907	
NON	2.6408	64.950 C	64.932	
NON	2.6342	64.791 C	64.772	
NON	2.6363	64.842 C	64.823	
NON	2.6408	64.950 C	64.932	
NON	2.6405	64.943 C	64.924	
NON	2.6394	64.916 C	64.898	
NON	2.6416	64.969 C	64.951	
NON	2.6413	64.962 C	64.944	
NON	2.6406	64.945 C	64.927	
NON	2.6413	64.962 C	64.944	
NON	2.6432	65.008 C	64.989	
NON	2.6441	65.030 C	65.011	
3201	2.6508	65.191 C	65.173	.390 ←
3202	2.6520	65.220 C	65.202	.419
3203	2.6500	65.172 C	65.153	.371
3204	2.6494	65.157 C	65.139	.356

SERIAL #	MV READING	TEMPERATURE	DELTA	Δ °C
STD 257		-18.593 °C		
~~STD. 400~~	0.0005	0.093 C	0.000	
NON	-0.7300	-18.762 C	-18.854	
NON	-0.7290	-18.735 C	-18.828	
NON	0.7286	-18.725 C	-18.818	
NON	-0.7292	-18.741 C	-18.834	
NON	0.7300	-18.762 C	-18.851	
NON	0.7311	[illegible]	-18.884	
NON	-0.7302	-18.747	[illegible]	
[illegible]	[illegible]	[illegible]	[illegible]	
[illegible]	[illegible]	[illegible]	[illegible]	
[illegible]	[illegible]	-18.707	[illegible]	
[illegible]	[illegible]	[illegible]	[illegible]	
[illegible]	0.7239	-18.602	[illegible]	
[illegible]	[illegible]	-18.56	[illegible]	
[illegible]	[illegible]	18.76	[illegible]	
NON	0.7288	18.577	[illegible]	
[illegible]	[illegible]	[illegible]	[illegible]	
[illegible]	0.7270	-18.702 C	[illegible]	
NON	0.7297	-18.754	[illegible]	
NON	0.7306	-18.752	[illegible]	
3201	[illegible]	-18.811 C	[illegible]	-.218 ←
3202	0.7300	-18.769 C	[illegible]	-.176
3203	-0.7261	-18.660 C	[illegible]	-.067
[illegible]	0.7244	-18.611 C	[illegible]	-.022

6" Type K TC 92321-1 T4522
8/12/93

Std mV	°C	Test mV	°C
27.5885	19.981	.8008	20.07
27.7686	21.760	.8729	21.84
27.8647	22.705	.9094	22.76
28.3910	27.913	1.1230	28.03
29.0650	34.596	1.3564	34.74
29.1028	34.965	1.4117	35.12

CERTIFICATE

APPENDIX B

LIST OF EQUIPMENT AND MANUFACTURERS

PolyScience 730 Immersion Circulator
Serial # 926370
PolyScience
P.O. Box 48312
Niles, IL 60648
(708) 965-0611

Jupiter Viscosity Timer Model 821
Serial # J 2033-1
Jupiter Instrument Company
407 Commerce Way A15
Jupiter, FL 33458
(407) 743-8486

Mettler Portable Density/Specific Gravity Meter DA-110
Mfg. No. NJA31791
Mettler Instrument Corporation
Box 71
Hightstown, NJ 08520
(609) 488-3000

Cannon-Fenske Routine Viscometer
Viscometer No. U736 size 50
Viscometer No. U677 size 50
Viscometer No. U667 size 50
Cannon Instrument Company
P.O. Box 16
State College, PA 16804

Deionized Ultra Filtered Water
Lot No. 923068
Fisher Scientific Company
Fairlawn, NJ 07410
(201) 796-7100

REFERENCES

Earlougher, Robert C. Jr. 1977. Advances In Well Test Analysis. 2nd edition. Society of Petroleum Engineers of AIME, New York. Page 241.

Analytical Report. Volume I of IV. Chem-Nuclear Geotech Analytical Laboratory, Grand Junction, CO. 1992. Section 1.

Weast, Robert C. 1989. Handbook of Chemistry and Physics. 70th edition (1989-1990). Boca Raton, Florida: CRC Press, Inc.

Report Number (14) SAND--97-1763

Publ. Date (11) 199804

Sponsor Code (18) DOE/DP, XF

UC Category (19) UC-721, DOE/ER